# CLASSIFYING PHYSICAL ACTIVITIES FROM ACCELEROMETRY DATA RECORDED FROM HEALTHY, ELDERLY AND NEUROLOGICAL SUBJECTS

Anthony F. Dalton

B.Eng, MSc. F.E.,

Doctor of Philosophy Degree

December 2012


# CLASSIFYING PHYSICAL ACTIVITIES FROM ACCELEROMETRY DATA RECORDED FROM HEALTHY, ELDERLY AND NEUROLOGICAL SUBJECTS

Anthony F. Dalton B.Eng, MSc. F.E.,

A Thesis Submitted for

Doctor of Philosophy Degree

Work Carried Out at

Bioelectronics Research Cluster,
National Centre for Biomedical
Engineering Science,
National University of Ireland Galway, Ireland

Spaulding Rehabilitation Hospital,
Department of Physical Medicine
& Rehabilitation,
Harvard Medical School, Boston, MA, USA

Supervisor

Professor Gearóid Ó Laighin

Submitted to the National University of Ireland Galway, December 2012

# ABSTRACT

By 2050 two billion people will be aged 60 or older representing 22% of the global population. As this skew in the population distribution develops the nature of elderly health care provision will need to evolve. This dissertation investigates the practical application of accelerometer based sensors as inexpensive tools to monitor various physical activities and neuro-degenerative disorders.

Four distinct studies were conducted. The first and second study investigated the ability of supervised learning algorithms to classify various physical activities. Specifically, several classifiers were trained on time-domain and frequency-domain features derived from accelerometry data gathered from healthy and elderly populations in a laboratory and home environment, respectively. The primary findings were that a correctly parameterized supervised classifier could achieve high sensitivity and specificity in activity recognition without the need for user specific training data while only employing sensors affixed to the wrist, arm and chest. In the third study conducted a body sensor network to detect motor patterns of epileptic seizures was developed. A template matching algorithm based on accelerometry data was successfully designed to monitor seizure occurrence outside the laboratory setting. Finally, the fourth study conducted investigated the capacity of an accelerometer based sensor affixed to the upper chest to detect gait and balance impairments in pre-symptomatic and symptomatic Huntington's disease subjects. The primary motivations were the known limitations of commonly used ordinal based clinical tests and the considerable expense of laboratory-based walkways and other quantitative systems currently employed to monitor Huntington's disease. By analyzing spatio-temporal gait parameters derived from the accelerometry data Hunington's disease progression was identified.

These studies demonstrate the practical application and indicate the significant potential of accelerometer based sensors as inexpensive tools to monitor various physical activities and neuro-degenerative disorders.

# ACKNOWLEDGMENTS

I wish to sincerely thank my supervisor, Prof. Gearóid Ó Laighin. At all times he demonstrated patience, guidance and insight and without whom this work could not have been completed.

I also wish to sincerely thank Prof. Paolo Bonato who presented me with life changing opportunities and to whom I am extremely grateful.

A special thanks to my friends and colleagues who through their encouragement and insight helped shape this work.

Finally, and most importantly, I thank my parents, Rita and Frank Dalton. Their endless sacrifices are the foundations of this work.

“I am the wisest man alive, for I know one thing, and that is that I know nothing.”

- *Plato*

“The soul takes nothing with her to the next world but her education and her culture. At the beginning of the journey to the next world, one's education and culture can either provide the greatest assistance, or else act as the greatest burden, to the person who has just died”

- *Plato*

“While the miser is merely a capitalist gone mad, the capitalist is a rational miser.”

- *Karl Marx*

“But I, being poor, have only my dreams; I have spread my dreams under your feet; Tread softly because you tread on my dreams."

- *W.B. Yeats*

# TABLE OF CONTENTS

# List of Figures

# LIST OF TABLES

# CHAPTER I

# INTRODUCTION

## *1.1 Introduction & Motivation*

The world's elderly population is dramatically increasing. The estimated change in the total size of the world's older population (65 and over) from July 2007 to July 2008 was 10.4 million people, or approximately 867,000 per month. The growth rate of the 80-and-over population was 4.3% compared to 1.2% for the entire population. Furthermore, by 2018 it is projected that older people will outnumber children for the first time in history. Finally, a majority of developed countries are expected to have a median age of 45 years or greater by 2040, an increase of 22% over current levels [1]

A rather easy but generally incorrect conclusion drawn from these statistics is that such remarkable shifts in population demographics will dramatically increase health care expenses. In support of such arguments are observations such that the older population in the United States required 36% of healthcare expenditure but only constituted 30% of the population in 2002 with average spending for this portion of the population three times that of the working population [2]. However, more detailed and recent research analyzing healthcare spending in OECD countries from 1970 through 2002 found that population ageing accounted for only 0.5% of a total increase of 3.7% in healthcare costs [3]. Interestingly, it was found that healthcare spending increased rapidly in the final years before death regardless of the age bracket of the individual.

Even though strong causality may not exist between an increasing older population and significantly rising healthcare costs it is clear that a shift in healthcare provision and personnel will be required to address this demographic divergence. In a survey of healthcare professionals conducted across the United States, the United Kingdom, Germany and India, care in the home was selected as the second most important area for healthcare investment behind increased funding for hospitals and clinics [4]. Furthermore, there is a strong desire among the elderly to remain within the home [5]. However, a significant portion of this long-term home healthcare is currently provided by unpaid individuals with over 6 million unpaid carers estimated in the United Kingdom in 2009 [6]. As the median population age trends upwards this situation will swiftly become impractical and unmanageable.

Such a dramatic shift in the age distribution of the world's population and a predicted future demand for a change in health care provision has seen a concentration of published work on the development of telemonitoring and home healthcare.

## *1.2 Research Methodology*

Within this thesis we focus on the subset of research dedicated to home healthcare provided through wearable kinematic sensors. Our research investigated the practical application of accelerometer based sensors as tools to monitor various physical activities and neuro-degenerative disorders.

The foundation of our work began with an investigation of physical activity monitoring using base-level and meta-level learning classifiers. Although this was an area which had previously received considerable published attention it was felt that systematic research with a large sample size had not yet been conducted and several important questions remained unanswered. Specifically, using 25 healthy subjects wearing 5 accelerometer based sensors as they completed a range of physical activities we aimed to address the following questions; compare base-level and meta-level classifiers, analyze the redundancy of time-domain and frequency domain features, define the optimal length of the data segmentation window, investigate the redundancy of sensor placement and, importantly, compare subject dependant versus subject independent training data. Our core findings from this study were that subject independent data were found to outperform subject dependent data indicating that high recognition rates can be achieved without the need for prior user specific training and the dominance of the wrist and ankle sensors which provide several options for embedding sensors in wearable electronics.

Our second layer of research was motivated by and expanded upon our initial study. Specifically, our original observations were based on a homogeneous dataset of healthy subjects in a controlled laboratory setting. We thus conducted a second study in a home environment with 5 elderly subjects again wearing 5 accelerometer based sensors as they completed a range of physical activities. A wireless body sensor network was developed to allow the sensors to communicate with a mobile device.

Encouragingly, from this study it was also found that the most accurate classifier did not require subject specific training and a high level of accuracy could be maintained using sensors attached at the mid-sternum, wrist and ankle.

Within this research we also wished to investigate the applicability of accelerometer based sensors for monitoring various neurodegenerative disorders. Driven primarily by an aging population, neurodegenerative disorders account for an ever increasing proportion of morbidity and mortality in the developed world [7]. The prevalence of Parkinson's disease [8], Huntington's disease [9] and Epilepsy [10] have all been found to increase with age.

We conducted a third study to develop a body sensor network to detect motor patterns of epileptic seizures. Specifically, several accelerometer based sensors were attached to 5 subjects undergoing medication titration. Throughout the course of the study subjects completed a range of predefined physical activities and were simultaneously monitored for seizure occurrence using EEG and video data. Using these data as the gold standard, an offline template matching algorithm was designed with the accelerometer data to distinguish seizure activity from other similar physical activities. A proof of concept body sensor network employing the accelerometer based sensors and an internet tablet was then designed and tested in a laboratory setting. From a dataset of 21 seizure events the sensitivity of our template matching algorithm was found to be 0.91 and specificity of 0.84 with a battery lifetime of 10.5 hours.

A fourth and final study was designed to analyze gait and balance in presymptomatic and symptomatic Huntington's disease subjects. Specifically, 34 subjects in various stages of disease progression wore an accelerometer based sensor as they completed a range of clinically approved gait and balance tests in a laboratory environment. A known algorithm was employed to derive gait parameters from the raw accelerometer data and a computerized walkway was used as the gold standard. Strong agreement was found between the sensor and the walkway and furthermore, the sensor was capable of distinguishing between subjects in various stages of disease progression.

## *1.3 Thesis Structure*

*Chapter Two*

This chapter begins with a theoretical overview of the accelerometer sensor utilized throughout this thesis, its calibration and various signal analysis. This is proceeded by a detailed background discussion of each of the four studies conducted. For each study a thorough review of relevant literature and description of the hardware, software and algorithms employed is given.

*Chapter Three*

This chapter presents the first study conducted in this body of work, a comparison of base-level and meta-level classifiers for physical activity recognition using accelerometry. This chapter has been published in the IEEE Journal of Biomedical & Health Informatics [11].

*Chapter Four*

This chapter presents a study conducted on physical activity identification using meta-level classifiers and accelerometer based sensors with an elderly population in a home environment. This chapter is under review by Medical Engineering & Physics.

*Chapter Five*

This chapter presents the first of the studies conducted on neurological subjects, the development of a body sensor network to detect motor patterns of epileptic seizures. This chapter has been published in IEEE Transactions on Biomedical Engineering [12].

*Chapter Six*

Chapter six presents the final study conducted in this thesis, an analysis of gait and balance through a single triaxial accelerometer in presymptomatic and symptomatic Huntington's disease. This chapter has been published in Gait & Posture [13].

*Summary, Conclusion & Future Work*

The final chapter discusses the primary observations and conclusions of this thesis and presents several potential avenues for future research.

### *References*


[1] Kinsella, K., & He, W. (2009). 'Census Bureau, International Population Reports. An Aging World: 2008', [Online]. Available: www.census.gov/p95-09-1.pdf (Accessed: May 2012)

[2] Stanton, M. W., & Rutherford, M. K. (2006). 'The high concentration of US health care expenditures', *US Department of Health & Human Services: Agency for Healthcare Research and Quality*, pp. 6-16.

[3] White, C. (2007). 'Health care spending growth: How different is the United States from the rest of the OECD?', *Health Affairs*, vol. 26(1), pp. 154-161.

[4] Wyke, A. (2009). 'Fixing Healthcare Professionals Perspective' *Economist Intelligence Unit*

[5] Age Concern England, (2012) 'The age agenda 2008: public policy and older people', *London, Age Concern England*.

[6] Carers UK, (2009). 'Policy Briefing: Facts about carers', *Carers UK*, London.

[7] Skovronsky, D. M., Lee, V. M. Y., & Trojanowski, J. Q. (2006). 'Neurodegenerative diseases: new concepts of pathogenesis and their therapeutic implications', *Annual Review of Pathology-mechanisms of Disease*, vol. 1, pp. 151-170.

[8] Dorsey, E, Constantinescu, R., Thompson, J, Biglan, K. M., Holloway, R. G., Kieburtz, K., & Tanner, C. M. (2007). 'Projected number of people with Parkinson disease in the most populous nations, 2005 through 2030', *Neurology*, vol. 68(5), pp. 384-386.

[9] Myers, R. H. (2004). 'Huntington's disease genetics', *NeuroRx*, vol. 1(2), pp. 255-262.

[10] Forsgren, L., Beghi, E., & Sillanpää, M. (2005). 'The epidemiology of epilepsy in Europe–a systematic review', *European Journal of Neurology*, vol. 12(4), pp. 245-253.

[11] Dalton, A., & ÓLaighin, G. (2012). 'Comparing supervised learning techniques on the task of physical activity recognition', *IEEE Journal of Biomedical & Health Informatics,* vol. 17, pp. 46-52

[12] Dalton, A., Patel, S., Chowdhury, A., Welsh, M., Pang, T., Schachter, S., ÓLaighin, G., & Bonato, P. (2012). 'Development of a body sensor network to detect motor patterns of epileptic seizures', *IEEE Transactions on Biomedical Engineering*, vol. 59 (11), pp. 3204-3211.

[13] Dalton, A., Khalil, H., Busse, M., Rosser, A., van Deursen, R., & ÓLaighin, G. (2012). 'Analysis of gait and balance through a single triaxial accelerometer in presymptomatic and symptomatic Huntington's disease', *Gait & Posture*, vol. 37(1), pp. 49-54.

# CHAPTER II
# BACKGROUND INFORMATION & REVIEW OF RELEVANT LITERATURE

## *2.1 Chapter Overview*

In this chapter we will discuss the background of each study conducted during this body of research. The motivations and primary objectives will be highlighted, followed by a review of relevant literature, a brief description of the hardware and software employed and an overview of the various algorithms investigated. Prior to this we will provide an introduction to the core sensor employed in this thesis.

### *2.1.1 The Accelerometer*

The underlying concept of the accelerometer is a damped mass on a spring. Imagine a spring affixed to a casing at one end and to a mass at the other. The spring currently exerts no force on the mass. If we accelerate the entire structure then the spring will expand in the opposite direction expending a force equivalent to that required to accelerate the mass. Piezoresistive accelerometers employ silicon resistors whose electrical resistance changes in response to an applied acceleration [1]. These sensors are usually constructed from a surface micro-machined polysilicon structure built over a silicon wafer. The structure is suspended with polysilicon springs over the surface of the wafer and deflect with acceleration forces. The piezoresistive sensor can be connected in a Wheatstone bridge configuration to produce a voltage proportional to the amplitude of the acceleration of the mass within the sensor [1]. Alternatively, piezoelectric accelerometers contain a piezoelectric element with a seismic mass which causes the piezoelectric element to bend when the sensor is accelerated. This reaction induces a displacement charge built up on one side of the sensor which produces a variable output voltage signal that is proportional to the applied acceleration [1]. A third approach to accelerometer construction is a differential capacitor with central plates attached to a moving mass and fixed external plates. When an acceleration is applied the capacitor will become unbalanced and an output wave with an amplitude proportional to the applied acceleration will be generated [1]. Differentiable capacitor based accelerometers are favored within the research community for activity and movement analysis as they are sensitive to constant acceleration such as that induced by gravity therefore facilitating the calibration of the sensor by rotation within the gravitational field. Within our research we used an accelerometer developed by Freescale® electronics, Fig. 2.1 [2].

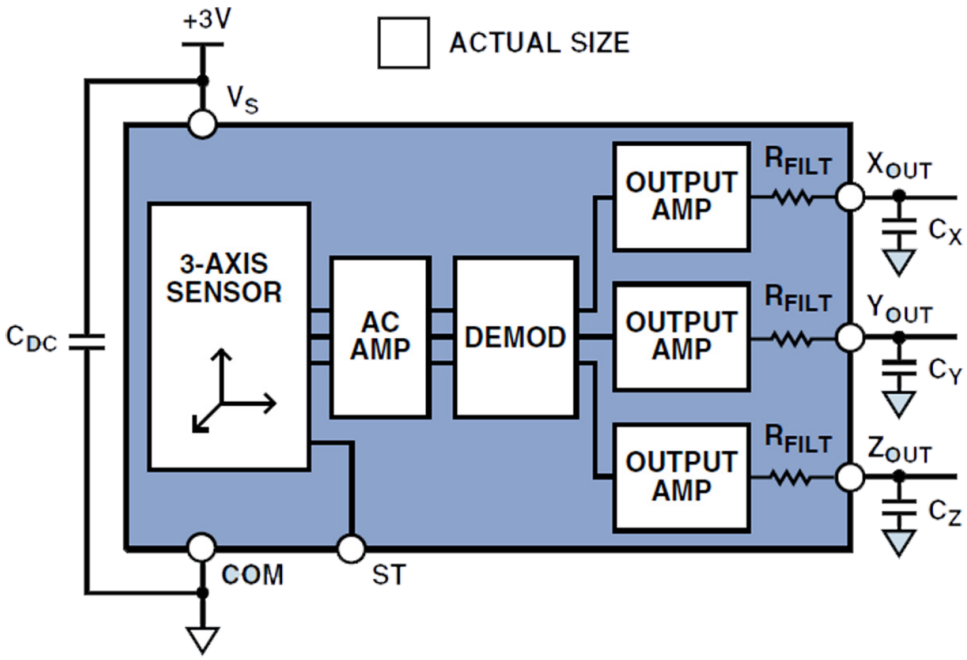


Fig. 2.1 Freescale MMA7260QT accelerometer block diagram

### *2.1.2 Calibration, Placement and Signal Decomposition*

Employing accelerometers to monitor static and dynamic physical activities requires several practical considerations, specifically; a sensor which monitors the appropriate frequency range for human motion, efficient calibration and finally, effective decomposition of the accelerometer signal.

Cappozzo et al [3] found that accelerations measured at the lower back range from -0.3g (9.81 $m/s^2$) to 0.8g and remain below 5Hz during walking in males. Bhattacarya et al [4] found that maximum acceleration measured at the ankle whilst running to be less than 18Hz in a dataset of 8 males. Aminian et al [5-6] found accelerations measured at the lower back and ankle during treadmill walking in a dataset of 6 young adults did not exceed 16Hz. Bouten et al [7] summarized the requirements stating that devices capable of operating in a range of $\pm$6g and a frequency of 0-20Hz are required. The device [2] used through this research adheres to these requirements.

Accelerometer data can be considered as a combination of three components; acceleration due to body movement, acceleration due to gravity and noise [1]. A static accelerometer in a gravitational field will register an output according to Equation 2.1

$$Aceeleration = g * cos(\Theta) \quad (2.1)$$

where $g = 9.81 m/s^2$ is the acceleration due to gravity and $\Theta$ is the angle between the gravitational vector and the sensitive axis of the accelerometer. Fig. 2.2 demonstrates the behaviour of an accelerometer at rest and in motion. The gravitational component of the signal can range from $+1g$ when the accelerometer's sensitive axis is parallel to the gravitational vector, to $-1g$ when the sensitive axis is antiparallel to the gravitational vector. However, a significant issue is the nonlinearity of the gravitational component. With reference to Fig. 2.3, the cosine curve is steepest near 90° where the output registers $0g$ and flattens out near 0° and 180° where the output registers $\pm 1g$. As can be seen by the slope of the cosine curve (-sine) when the sensitive axis of the accelerometer is in line with the gravitational vector, small changes in orientation have little effect on the signal output. When the sensitive axis is perpendicular to the gravitational vector small changes in orientation induce significant signal adjustments.

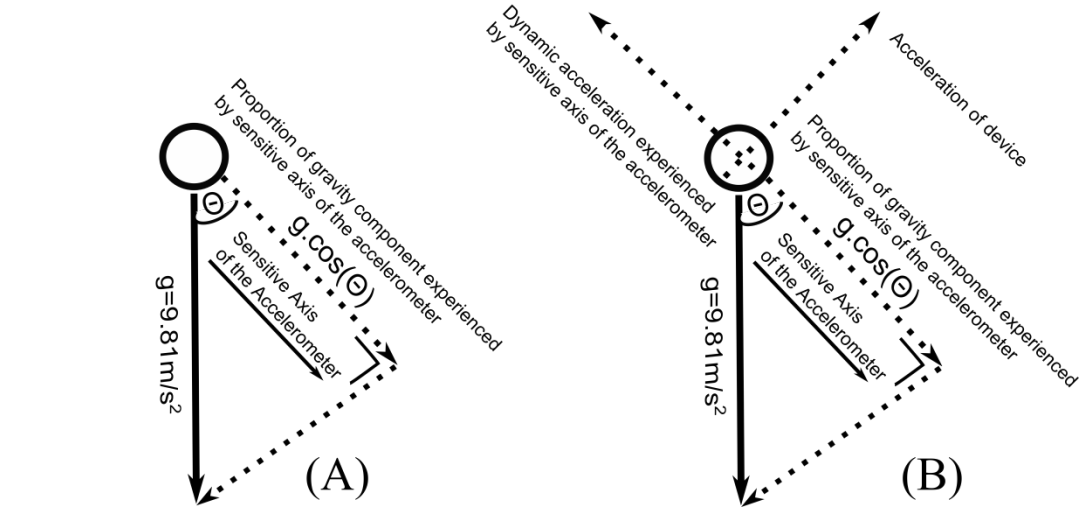


Fig. 2.2 Displays acceleration experienced during (a) static and (b) dynamic conditions

By employing two or more sensitive axes these issues can be largely addressed. Since the acceleration detected by a single axis is proportional to the cosine of the angle of inclination, the sensitivity of the second orthogonal axis will be proportional to the sine of the angle; as the sensitivity of one axis decreases the sensitivity of the other increases.

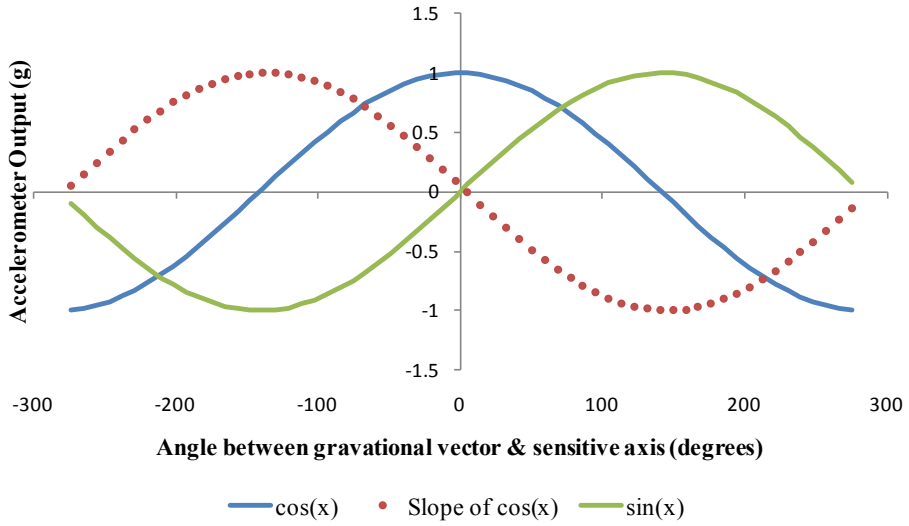


Fig. 2.3 Plot of the cosine curve and its first derivative

Accurate and reliable calibration of an accelerometer is a further important consideration. A simple rotational procedure can be adopted to find the offset and sensitivity of the device and adjust the raw accelerometer readings accordingly [8]. The sensitive axis is initially held in a steady state, parallel to the gravitational vector and a recording is taken, $V_{+1g}$. The device is then rotated until it is antiparallel to the gravitational vector and a second reading is taken, $V_{-1g}$. Note, we do not take these measurements with the sensitive axis perpendicular to the gravitational vector due to the nonlinearity issues previously discussed. By employing Equations 2.2 the accelerometer can be calibrated and the process is repeated for each sensitive axis.

$$Sensitivity = \frac{V_{+1g} - V_{-1g}}{2} \quad Offset = \frac{V_{+1g} + V_{-1g}}{2} \tag{2.2}$$

$$Accel_{Calib} = \frac{Accel_{raw} - Offset}{Sensitivity}$$

If an accelerometer undergoes a translation without rotation only a response due to body movement will be registered. Performing a translation while rotating the device will produce responses due to both gravity and body further compounded by noise. Therefore the spectrum of acceleration due to body movement, acceleration due to gravity and noise overlap and they cannot be perfectly decomposed. However, some simplifying assumptions can reduce the complexity of the problem. With an accelerometer affixed to the body we can assume that any change in acceleration means

that a subject must be moving, as postural orientation (acceleration due to gravity) cannot change without a nonzero acceleration due to body movement. Furthermore, we can assume that the change in acceleration due to body movement is much greater than the change in acceleration due to postural orientation and thus body acceleration generally occurs at higher frequencies than acceleration due to gravity. An estimation of the acceleration due to body movement can be found by employing a high pass filter of the raw accelerometer data. An estimation of acceleration due to gravity can then be made by removing the acceleration due to body movement from the raw data. Similarly, a low pass filter can be employed to initially find an estimation of acceleration due to gravity and in-turn an estimation of acceleration due to body movement.

Mathie et al [1] conducted a comprehensive analysis of accelerometer signal decomposition. The authors investigated the impulse and step responses of a host of filters including elliptical, bessel, butterworth, remez, chebyshev, kaiser and FIR filters. They rated each filter on the amount of acceleration due to body movement present in the estimated acceleration to gravity component and the magnitude of ringing in the filtered signal. The highest performance was achieved by a high pass 3$^{rd}$ order elliptical filter. We performed similar analysis and also found superior results with an elliptical filter and therefore we employed this filter throughout our work. Fig 2.4 presents accelerometer data for a range of tasks recorded during this research.

Finally, in theory, since acceleration is the first derivative of velocity and the second derivative of displacement, a double integration technique can be employed to derive these parameters from the raw data. However, it has been well noted that in practice such techniques lead to significant measurement error [1]. The primary issue is the d.c. offset embedded within the accelerometer signal from the gravitational component and as previously noted it is not plausible to completely decompose the raw data. Double integration over short time periods is plausible however, the error increases with the square of time [1]. Due to this inherit error, we only calculated displacement in one subsection of our work, pelvic displacement during the gait cycle over short periods of time. We employed cumulative trapezoidal numerical integration [1] and several filters to reduce the measurement error. Please see Appendix C for more information.

**Fig. 2.4: Accelerometer Data**

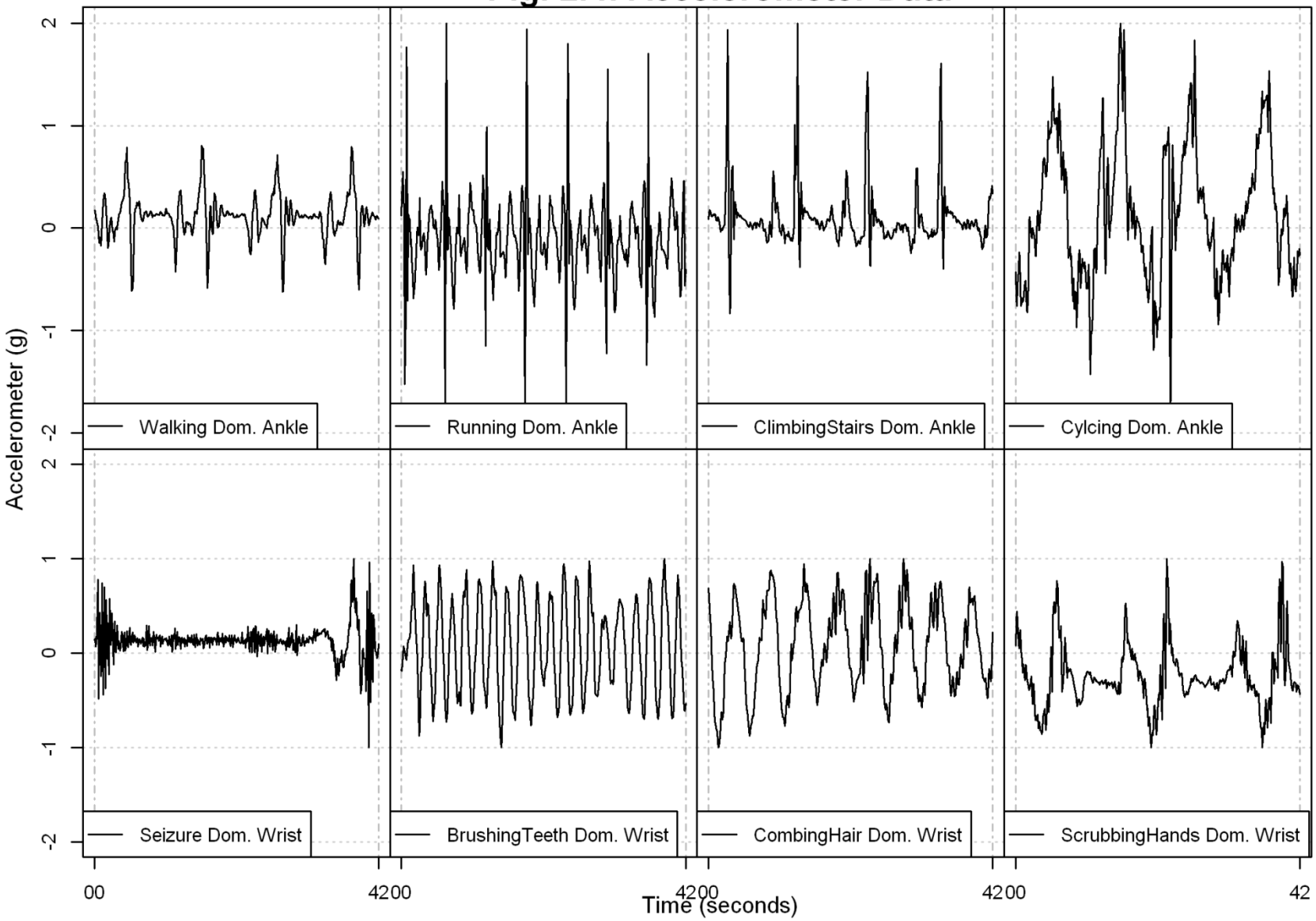

## 2.2 *Physical Activity Recognition: Supervised Learning Classifiers*

In the proceeding section we discuss the background of the first study conducted in this thesis, a comparison of supervised learning algorithms trained from triaxial accelerometry data on the task of physical activity recognition. The journal paper arising from this work is presented in Chapter 3. To provide context and background the motivations and primary objectives behind this section of the thesis are initially presented. This is followed by a review of the relevant literature, a brief description of the hardware and software employed and an overview of the algorithms investigated.

### *2.2.1 Motivation & Objective*

Over the last several years there has been a growing interest in the application of machine learning tools and kinematic sensors towards the problem of activity recognition. However, as detailed in the next section, the literature review for this segment of research revealed that the published work was fragmented and disjointed with a significant number of studies publishing work on small sample sizes. Therefore, it was decided to conduct a more comprehensive study by attaching 5 accelerometer based sensors to 25 healthy subjects as they completed several physical activities. Several key objectives were defined; 1. Perform a brute force comparison of the most popular machine learning classifiers, 2. Analyze the redundancy of time-domain and frequency domain features, 3. Compare user-specific and user-independent training sets and 4. Investigate whether the window size by which data are segmented or the location of sensor attachment affects classifier accuracy.

### *2.2.2 Review of Relevant Literature*

Physical activity recognition through kinematic based sensors is not a new concept. Table 2.1 presents a summary of some of the published work in this area. The majority of these studies share a common methodology similar to that adopted in our research; specifically; kinematic sensor(s) are attached to one or more subjects as they perform several physical activities. The raw data are then transformed into time-domain, frequency domain or time-frequency domain feature sets. These feature sets are then subdivided into training and test data, usually in a 70% / 30% split. A phase of feature

reduction, selection and extraction is then conducted on the training data set along with classifier fine tuning through parameter optimization. Finally, these optimized parameters and classifiers are tested on the independent test dataset to gauge a true measure of the classification error. It is also quite popular to repeat this process a number of times by randomly selecting different segments of your dataset to represent training and testing folds in a technique know has n-fold cross validation [11-12]. Fig 2.5 presents a conceptual overview of this process. In general the published work differs on the numbers of subjects studied, the range of activities performed, the type of features calculated and the classifiers compared.

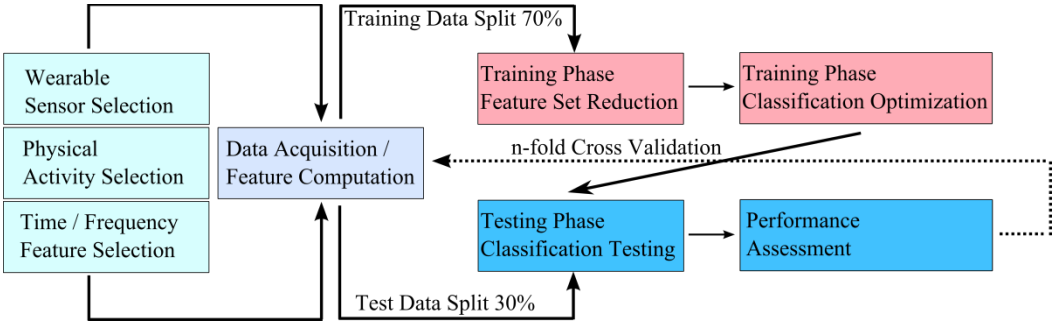


Fig. 2.5 Conceptual scheme of activity classification

Bao et al [14] conducted one of the broadest studies in this field. Five accelerometer based sensors were attached to 20 subjects as they performed 20 self-annotated activities and these data were used to compare several base-level classifies with the C4.5 [15] decision tree classifier achieving the highest accuracy. An interesting finding from their work was that several activities required user specific training data and, in general, classifier accuracy was higher when user specific training data were employed. However, these particular findings were based on a considerably smaller subset of subjects and Bao et al notes that the accuracy of these preliminary results is limited by the low-number of subjects involved in this part of their study. To date few other publications have investigated such a combination of concepts with a significantly large sample size. Kwapisz et al [16] investigated 29 subjects carrying an accelerometer enabled mobile phone inserted in the front pocket while they completed 6 activities and achieved 92% accuracy with the multilayer perceptron [17] algorithm. Paraschiv-Ionescu et al [18] attached three sensors to 21 subjects and monitored three activities. Using a wavelet coefficients decision tree an average accuracy of 98% was achieved.

Maekawa et al [19] investigated a diverse set of 15 activities with several different sensors including accelerometers, microphones, speakers and a compass achieving an accuracy of 85% with a decision tree classifier. Parkka et al [20] adopted a similar approach by testing a host of sensors attached to 16 subjects as they completed a range of activities with decision tress again performing strongly. Pirttikangas et al [21] attached four accelerometer based sensors to 13 subjects as they completed a range of activities and found Multilayer Perceptron [16] outperformed the k-Nearest Neighbors [22] classifier. Fahrenberg et al [23] attached four single axis accelerometers to 26 subjects and used the raw accelerometer data with discriminant analysis to distinguish 7 unique activities with an accuracy of 91%. The same authors continued this work with a new dataset of 24 subjects and a slightly extended list of activities classified by an $L_1$-norm similarity score with similar results [24]. Mathie et al [25] employed a single waist mounted accelerometer to 26 subjects and detected several static activities with DC / AC threshold analysis with high accuracy. Using similar threshold analysis Lee et al [26] investigated running and walking up / down stairs with a single sensor attached to the back with strong results. Najafi et al & Sekine et al [27-30] employed wavelet and fractal analysis on accelerometry and gyroscopic data with 20 or more subjects to detect several static activities and walking. Hernen et al [31] investigated an Artificial Neural Network trained on data from two accelerometers attached to the lower back and ankle of 20 subjects in an effort to classify running at various speeds with strong results. Lakany et al [32] employed the MacReflex system and a Kohonen self-organizing map [12] to detect walking at various speeds with 35 subjects achieving 85% accuracy. Wang et al [33] applied empirical mode decomposition with 52 subjects to detect walking up / down stairs with 96% accuracy. Ibrahim et al [34] employed a single waist mounted accelerometer and a Gaussian Mixture model on a dataset of 50 subjects achieving an accuracy of 86% in detecting 5 distinct gait patterns. Finally, in a return to Bao et al's original dataset, Mannini et al [13] investigated the applicability of Hidden Markov Models [12] and found they compared favorably with other machine learning algorithms.

In comparison to these larger scale datasets a significant number of studies have been preliminary in nature with smaller sample sizes. Ravi et al [35] recruited 2 subjects

who performed 8 activities with a sensor mounted at the waist and investigated a significant range of classifiers with Plurality Voting achieving 90% accuracy. Maurer et al [36] also investigated a large range of classifiers with a sample of 6 subjects wearing an accelerometer based wrist sensor with decision trees outperforming simple Bayesian classifiers. Olguin et al [37] investigated Hidden Markov Models with 6 sensors attached to the right wrist, left hip and chest with 3 subjects for 8 activities achieving 92% accuracy. Khan et al [38] built a hierarchical recognizer on data from a single chest mounted accelerometer attached to 6 subjects across a large range of activities achieving 99% accuracy. Mantyari et al [39] built an Artificial Neural Network on data from 2 accelerometers attached to either hip of 6 subjects as they walked up / down stairs achieving an accuracy of 90%. Altun et al [40] investigated several classifiers on a dataset of 8 subjects wearing 5 inertial measurement units (accelerometers, gyroscopes and magnetometers) while they completed a list of 19 different activities and found Bayesian classifiers outperformed their peers. Other researchers investigated threshold based algorithms. Hynes et al [41] applied an average magnitude difference function to a cohort of 10 elderly subjects to identify activity level using a commercial accelerometer enabled handset achieving high accuracy. Veltink et al [42] attached 1 dimensional accelerometers to the sternum and thigh of 6 subjects as they performed various static and dynamic activities. Similarly, Bussmann et al [43]-[44] investigated binary trees and threshold methods achieving between 81%-88% accuracy. Ní Scanaill et al [45] developed a threshold based technique to monitor static and dynamic activities achieving 90% accuracy. Lyons et al [46] employed an accelerometer as an inclinometer and developed a threshold based algorithm to distinguish static from dynamic activities with 91% accuracy. Finally, Karantonis et al [47] also employed a binary tree to detect static and dynamic activities from 6 subjects using a waist mounted accelerometer with 90% accuracy.

As can be seen a considerable body of work has been amassed on the application of kinematic sensors towards the problem of activity recognition however, we felt the findings from published work were fragmented and disjointed and a study combining many of the insights from previous work was warranted.

**Table 2.1 A summary of studies applying supervised / unsupervised classifiers for activity recognition**

| Author<br># Subjs / Study Lgth<br>Fs (Hz)/Wind Size | Activities | Feature Set | Placement /<br>Sensor Type | 'Best' Classifiers (%) | |
|---|---|---|---|---|---|
| Allen [48] (2006)<br>6 / ~700 minutes<br>45 / 32 samples | Standing, sitting, lying, stand-to-sit, sit-to-stand, stand-to-lie, lie-to-stand, walking | FFT coeffs, signal magnitude area, shifted delta coeffs | Waist / ADXL210 accelerometer | Heuristic Algorithm | 71.10 |
| | | | | Gaussian Model | 91.30 |
| Altun [40] (2010)<br>8<br>25 / 125 samples | Lying, sitting, standing, walking, running, treadmill, cycling, basketball, up / down stairs | 4 central moments, autocorrelation, max, min, Fourier Transform | Chest, arms & legs / Accelerometer, gyro & Magnetometer | SVM | 98.60 |
| | | | | Bayesian | 99.10 |
| | | | | DTW | 98.50 |
| | | | | kNN | 98.20 |
| Aminian [5] (1999)<br>5 | Lying, sitting, standing and locomotion | Median,<br>standard deviation | Chest & thigh /<br>2 1-D accelerometers | Threshold | 89.30 |
| Aminian [6] (2001)<br>9 Hlthy, 11 elderly | Various walking conditions | Wavelet analysis | Shank & feet / Gyro & footswitches | Strong discrimination between groups | |
| Baek [49] (2004)<br>1 / ~ 1 day | Standing, sitting, lying supine, walking, running, up / down stairs | Short Fast Fourier Transform (SFFT) analysis | Waist /<br>3-D accelerometers | Threshold | 97.50 |
| Bao [14] (2004)<br>20 / ~40 hours<br>76.25 / 512 Samples | Sitting, walking, running cycling, vacuuming, folding laundry, computer work, up / down stairs | Mean, energy, entropy, pairwise axis-correlation | Hip, wrist, upper arm, ankle, thigh / 3-D accelerometer | C4.5 | 84.26 |
| | | | | kNN | 82.70 |
| | | | | Naïve Bayes | 52.35 |
| Barralon [50] (2005)<br>1 / ~ 1 day | Walking and postural changes | Angle of inclination, FFT, video analysis | Armpit | Walking | 76.00 |
| | | | | Postures | 80.00 |
| Barralon [51] (2006)<br>20 / ~ 1 day | Various walking periods | STFT, DWT & CWTs | Armpit | DWT Sensitivity | 78.50 |
| | | | | DWT Specificity | 67.60 |
| Betker [52] (2006)<br>16 / ~ 1 day | Estimation of COM | Inclination Angle, MSE | Trunk & limb /<br>2-D accelerometer | Neural Network | 90.30 |
| | | | | Fuzzy Netork | 89.20 |
| | | | | Gaussian Model | 90.40 |
| Bharatula [53] (2005)<br>3 / ~ 1 day | Design choices in a multi-sensor system, 4 activities | 9 time domain & 4 frequency domain features | Wrist / 3-D accelerometer, light | C4.5 | 86.00 |
| | | | | BayesNet | 81.00 |
| | | | | NaivesBayes | 76.00 |

| Author<br># Subjs / Study Lgth<br>Fs (Hz)/Wind Size | Activities | Feature Set | Placement /<br>Sensor Type | 'Best' Classifiers (%) | |
|---|---|---|---|---|---|
| Bonnet [54] (2007)<br>1 / ~ 1 day | Sit-to-stand transition | Chest inclination | Upper Back /<br>Magnetometer | Unknown | |
| Bouten [7] (1997)<br>13 / ~1 day | Sitting, standing, walking<br>Benchmark: Respiration chamber | Mean, standard deviation,<br>Fast Fourier Transform | Waist, lower back | $IMA_{tot}$ | r=0.77 |
| | | | | $EE_{act}$ | r=0.89 |
| Boyle [55] (2005)<br>NA | Design of a remote monitoring system, transmission, power and size | NA | Chest, thigh, waist,<br>Accel, magne., gyro,<br>ECG | NA | |
| Bussmann [43] (2001)<br>UNKW | Various activities & walking conditions | Angular signal, motility,<br>Fast Fourier Transform | 1-D & 2-D<br>accelerometer | Binary Tree | 81.00 |
| Bussmann [44] (1998)<br>3 / ~1 day | Range of static vs. dynamic activities | Angular signal, motility,<br>Fast Fourier Transform | Thighs & sternum | Threshold<br>spontaneous | 88.00 |
| | | | | Threshold<br>standard | 96.00 |
| Coley [56] (2005)<br>10 Hlthy, 10 Eldly | Up / down stairs | Wavelet coefficients<br>Decision Tree | Shank / Gyroscope | Sensitivity | 95.00 |
| | | | | Specificity | 94.00 |
| Culhane [57] (2004)<br>5 stroke / 24h | Sitting, standing, lying, posture transition | Means, std deviation,<br>best estimate analysis | Chest & thigh /<br>2-D accelerometer | Visual detection | |
| Ermes [58] (2008)<br>12 / 68 hours<br>20 / 120 samples | Sitting, standing, lying, walking, nordic walking, running, cycling, rowing, playing football | 4 central moments,<br>percentiles, spectral<br>spread, signal power | Hip, wrist /<br>Garmin eTrex GPS<br>ADXL202<br>accelerometer | Custom Dec. Tree | 83.00 |
| | | | | Neural Network | 87.00 |
| | | | | Hybrid Model | 89.00 |
| Fahrenberg [23]<br>(1997)<br>26 students | Sitting, standing, lying supine, sitting & talking, using PC, walking, up / down stairs, cycling | Raw accelerometer signal | Sternum, wrist, thigh,<br>lower leg, heart rate /<br>1-D accelerometer | Discriminant<br>Analysis | 91.00 |
| Forester [24] (1999)<br>24 | Sitting, standing, lying supine, sitting & talking, using PC, walking, up / down stairs, cycling | Fast Fourier Transform<br>Analysis | Sternum, wrist, thigh,<br>lower leg, Heart-Rate<br>/ 1-D accelerometer | Similarity<br>Assessment<br>through $L_1$ Norm. | 95.80 |

| Author<br># Subjs / Study Lgth<br>Fs (Hz)/Wind Size | Activities | Feature Set | Placement /<br>Sensor Type | 'Best' Classifiers (%) | |
|---|---|---|---|---|---|
| Hendlman [60] (2000)<br>25 | Calculation of energy expenditure during golfing. window washing, vacuuming, lawn mowing, gardening | MEE and accelerometer count | Yamax Digiwalker, a CSA and a Tritrac accelerometer. | CSA | r: 0.59 |
| | | | | Trit rac | r: 0.62 |
| Herren [61] (1999)<br>20 | Running at various speeds and inclines | Neural Network | Lower back and ankle / 3-D accelerometer | Speed MSE | 0.12 |
| | | | | Incline MSE | 0.14 |
| Hester [62] (2006)<br>6 stroke / ~ 1 day | Range of activities | Dominant freq comps, cross-corr, auto-cov | Wrist, ankle, walking stick / Accel. & gyro | Threshold Sensitivity | 95.00 |
| | | | | Threshold Specificity | 95.00 |
| Huynh [63] (2005)<br>2 / 200 minutes<br>512 / 128-2048 | Walking, standing, jogging, skipping, hopping, riding bus | Mean, variance, entropy, axis-corr., FFT coeffs | Shoulder (RucksStrap) / 3-D accelerometer | For each activity individual feature / window length chosen | |
| Huynh [64] (2006)<br>1 / 18.7 minutes<br>92 / 50 Samples | Sitting, standing, walking, up / down stairs, shaking hands, writing on whiteboard, typing | Mean, variance | 12 body locations / ADXL311JE accelerometer | Naïve Bayes | 73.50 |
| | | | | Eigenspaces | 71.30 |
| | | | | SVM & EignSpaces | 88.30 |
| Karantnis [47] (2006)<br>6 / ~1 day | Sitting, standing waking, running, sit-to-stand | Magnitude, tilt Angle, Fast Fourier Transform | Waist /<br>3-D accelerometer | Binary Tree | 90.80 |
| Kern [65] (2003)<br>1 / 18.7 mins<br>92 Hz / 50 samples | Sitting, standing, walking, shaking hands, writing, typing, up / down stairs | Running mean & variance | Knee, wrist, elbow, ankle, hip, shoulder / 12 2-D accelerometer | Naïve Bayes | 85.00 |
| Khan [38] (2010)<br>6 Healthy / 21 hours<br>20 Hz / 64 samples | Lying, sitting, standing, lie-to-stand, stand-to-lie, lie-to-sit, sit-to-lie, sit-to-stand, stand-to-sit, walk-to-stand, stand-to-walk, up / down stairs | State recognition using first two moments. A LDA taking AR model built on SMA and Tilt Angle | Chest / Accelerometer (Witilt 2.5) | Auto Regressive (AR) | 72.00 |
| | | | | AR, SMA | 81.50 |
| | | | | AR,SMA,TA | 99.00 |

| Author<br># Subjs / Study Lgth<br>Fs (Hz)/Wind Size | Activities | Feature Set | Placement /<br>Sensor Type | 'Best' Classifiers (%) | |
|---|---|---|---|---|---|
| Krause [66] (2003)<br>2 / 240 hours | Walking, driving, eating, fitness, sleeping. | Kohonen Self Organizing Map, k-Means clustering on FFT | SenseWear armband, 2 accels, galvanic skin response, skin temperature | Distinct clusters were indentified in each case | |
| Kwapisz [16] (2010)<br>29 / 12.5 hrs<br>20 / 200 samples | Walking, jogging, up / down stairs, sitting, standing | Mean, standard deviation, skewness | Cell Phone pocket / 3-D accelerometer | C4.5 | 85.10 |
| | | | | Logistic Reg | 78.10 |
| | | | | MultiLayer Perc | 91.70 |
| | | | | Straw Man | 37.20 |
| Lakany [32] (2000)<br>35 | Various walking speeds | Wavelet coeffs & Kohonen Self Org. Map | MacReflex System | Threshold | 85.00 |
| Lee [67] (2002)<br>8 | Sitting, standing, walking | Raw data, std dev, compass derivative | Waist, Leg / 2-D accel, gyro, compass | Threshold | 92.20 |
| Lee [26] (2003)<br>24 / ~ 1 Day | Stand, sit, lie supine & prone, walking, running, up/down stairs | DC / AC threshold analysis | Back / 3-D accelerometer | Threshold | 95.10 |
| Lester [68] (2005)<br>2 / 12 hours<br>550 / 4 samples | Sitting, standing, walking, jogging, up /down stairs, up/down elevator, cycling, driving | Mean, variance, integrals, entropy, filer coeffs, FFT coeffs | Shoulder / multi-modal sensor board | Naïve Bayes | 68.50 |
| | | | | Decision Stumps | 91.00 |
| | | | | HMM & Dec Stumps | 95.00 |
| Lester [69] (2006)<br>12 / 6 hours<br>550 / 4 samples | Sitting, standing, walking, up /down stairs, riding elevator up/down, brushing teeth | Mean, variance, integrals, entropy, filer coeffs, FFT coeffs | Shoulder / multi-modal sensor board | Static Classifier | 71.99 |
| | | | | HMM Classifier | 81.68 |
| Liu [70] (2006)<br>19 | Defined new walking parameters: responding time for inclination medio-laterial Rhythmicity | Threshold algorithm | Lower Back / 2-D accelerometer | RTI Recall | 100 |
| | | | | RTI Precision | 50.00 |
| Lo [71] (2005)<br>1 | Design of a body sensor network | On board FFT | ECG, SpO2, 3-D accelerometer | Visual Inspection | |

| Author<br># Subjs / Study Lgth<br>Fs (Hz)/Wind Size | Activities | Feature Set | Placement /<br>Sensor Type | 'Best' Classifiers (%) | |
|---|---|---|---|---|---|
| Lukowicz [72] (2002)<br>1 | Various scenarios: walking in a building, cooking in a kitchen | Numerous features | WearNET / 10 various sensors | Visual Inspection | |
| Lyons [46]<br>1 / Repeated | Sitting, lying, standing, moving | Raw data and inclination angle | Sternum & upper thigh | Threshold Sit | 93.00 |
| | | | | Threshold Stand | 95.00 |
| | | | | Threshold Lie: | 84.00 |
| Maekawa [19] (2010)<br>15 / ~50 hrs<br>PDA Annotation | Brush teeth, cook pasta, feed fish, listen music, make cocoa, coffee, juice, tea, take medicine, vacuum, wash dishes plants. | Visual, sound, Fast Fourier Transform | Wrist / accelerometer Camera, microph, compass, illuminometer | AdaBoost+HMM | 80.00 |
| | | | | C4.5+HMM | 85.00 |
| Mannini [13] (2010)<br>(Bao's dataset)<br>13 / ~40 hours<br>76.25 / 512 Samples | Sitting, lying, standing, walking, up / down stairs, running, cycling | Mean, energy, entropy, pairwise axis-correlation | Hip, wrist, upper arm, ankle, thigh / ADXL210 acceleromter | Nearest Mean | 98.50 |
| | | | | k-Nearest neighbors | 98.30 |
| | | | | Hiden Markov Model | 98.40 |
| | | | | Neural Networks | 96.10 |
| Mantyari [39] (2001)<br>6 / 256 Hz | Waking, up / down stairs | PCA. ICA analysis, wavelet Coefficients | Left / Right Hip 3-D accelerometer | Neural Networks | 83.00 |
| Mathie [25] (2003)<br>26 / ~ 1 Day | Sit-to-stand, lying, sitting, standing | DC / AC threshold analysis | Waist / 3-D accelerometer | Threshold Transitions | 95.10 |
| | | | | Threshold Lie / Walk | 90.00 |
| Maurer [36] (2006)<br>6 / ~300 minutes<br>50 / 300 Samples | Sitting, standing, walking, up / down stairs, running | 4 central moments, cumulative histogram, ZCR, Percentiles(5-95) | Wrist / ADXL202 accel. Light sensor | C4.5 | 88.06 |
| | | | | Naïve Bayes | < C4.5 |
| | | | | kNN | < C4.5 |
| Najafi [29] (2000)<br>11 / ~1 day | Sitting, standing, lying, walking | Wavelet Coefficients | Chest / Gyroscope | Threshold | > 90.00 |
| Najafi [30] (2003)<br>44 | Stand-to-sit and sit-to-stand transitions | Wavelet Coefficients | Chest / Gyroscope | Threshold | > 90.00 |

| Author<br># Subjs / Study Lgth<br>Fs (Hz)/Wind Size | Activities | Feature Set | Placement /<br>Sensor Type | 'Best' Classifiers (%) | |
|---|---|---|---|---|---|
| NiScannaill [45]<br>1 | Sitting, standing, lying, walking | Means, threshold, SMS capable | Trunk & thigh / 2D accelerometer | Threshold | 90.00 |
| Noury [73] (2004)<br>5 / ~ 1 day | Walking and postural transitions | Fast Fourier Transform analysis | Thigh, wrist, chest, ankle / accelerometer and magnetometer | Visual detection | |
| Olguin [74] (2002)<br>3 / ~36 minutes<br>50 / 1 sample | Sitting, standing, crawling lying, walking, running, squatting, , hand movements while standing | Mean, variance | Right wrist,<br>left hip, chest /<br>MITes | HMM 1 Sensor | 65.86 |
| | | | | HMM 2 Sensors | 87.24 |
| | | | | HMM 3 Sensors | 92.13 |
| Paraschiv-Ionescu [18] (2004)<br>21 / 61 hours | Sitting, standing, lying and walking | Wavelet coefficients<br>Decision Tree | Chest, waist, ankle / accelerometers & gyroscopes | Sitting | 98.20 |
| | | | | Standing | 98.00 |
| | | | | Lying | 97.40 |
| | | | | Walking | 92.40 |
| Park [74] (2006)<br>1 | A dance performance | Threshold | The Eco System / 2D Accelerometers | Visual Inspection | |
| Parkka [20] (2006)<br>16 / 31h<br>200 / 800 Samples | Lying, sitting / standing, walking, running, rowing, nordic walking, cycling | 4 central moments, percentiles, spectral spread, signal power | Wrist, chest, back, forehead, finger / Several kinematic sensors | Auto Dec. Tree | 86.00 |
| | | | | Cust DecTree | 82.00 |
| | | | | Art Neural Net | 82.00 |
| Pirttikngas [21] (2006)<br>13 / ~240 minutes<br>20 / 10 samples | Standing, sitting, lying drinking, brushing teeth, up /down stairs, cycling, typing, running | Mean, standard deviation., ZCR, pairwise axis-corr., mean heart rate | Right thigh, both wrists, necklace / ADXL210 accel. | kNN | 90.61 |
| | | | | Multilayer Perceptron | 92.89 |
| Randell [75] (2000)<br>10 | Walking, running, sitting, standing , up / down stairs | RMS velocity | Pocket /<br>3-D accelerometer | ANN | 95.00 |
| Ravi [35] (2005)<br>2 / Unknown<br>50 / 256 Samples | Standing, walking, running, up / down stairs, sit-ups, vacuuming, brushing teeth | Mean, energy, std deviation, pairwise axis-correlation | Waist /<br>CDXL04M3 accelerometer | Plurality Voting | 90.61 |
| | | | | Naïve Bayes | 89.96 |
| | | | | SVM | 68.78 |

| Author<br># Subjs / Study Lgth<br>Fs (Hz)/Wind Size | Activities | Feature Set | Placement /<br>Sensor Type | 'Best' Classifiers (%) | |
|---|---|---|---|---|---|
| Salarian [76] (2005)<br>10 PD 10 Hlthy | Lying, sitting, standing, eating, writing, talking, walking, brushing teeth, combing hair, up / down stairs | Angular velocity, Linear Regression Model | Trunk, Shank /<br>3-D accelerometer & gyroscope | Transitions | 95.44 |
| | | | | Walking | 97.00 |
| Sekine [27] (2002)<br>23 | Walking & standing | Wavelet coefficients,<br>Fractal Dimensions | Waist /<br>3-D accelerometer | Threshold | 96.80 |
| Sekine [28] (2000)<br>20 / 256 Hz | Walking, up / down stairs | Wavelet coefficients | Waist /<br>3-D accelerometer | Threshold | 98.80 |
| Song [77] (2005)<br>6 / UNKW | Up / down stairs, walking, standing, sitting | Wavelet coefficients | Thigh /<br>2-D accelerometer | kNN | 86.60 |
| Tamura [78] (1995)<br>10 / ~1 day | Detect activity levels | Frequency components | Waist, wrist, ankle /<br>1-D accelerometer | Threshold | UNKW |
| Tapia [79] (2006)<br>1 / several weeks | Numerous ADLs and iADLs | Wavelet coefficients<br>Decision tree | Body / 12 various sensors | NA | |
| Veltink [42] (1993)<br>5 | Standing, sitting, lying, moving | DC Comp, standard deviation | Sternum & Thigh /<br>1-D Accelerometer | Threshold | UNKW |
| Veltink [80] (1996)<br>10 / ~1 day | Standing, sitting, lying, walking, upstairs, descending downstairs, cycling | DC Comp, standard deviation | Sternum & Thigh /<br>1-D Accelerometer | Threshold | 80.00 |
| Wang [33] (2008)<br>52 | Walking, up / down stairs | 20 stat features from empirical mode decomp | Waist / 3-D accelerometer | GMM | 96.02 |
| Yoshida [81] (2000)<br>3 / ~1 day | Lying supine, lie left-side, lie right-side, sitting, standing, walking, running, transitions | Integrated outputs for I minute resolution | Centre of abdomen /<br>1-D Accelerometer | Visual detection | |

SVM: Support Vector Machine, DTW: Dynamic Time Warping, kNN: k-Nearest Neighbor, FFT: Fast Fourier Transform, SMA: Signal Magnitude Area, PCA; Principal Component Analysis, ICA: Independent Component Analysis, ZCR: Zero Crossing Rate.

### *2.2.3 Hardware / Software*

#### *2.2.3.1 Witilt Sensor*

A considerable amount of time was spent investigating various sensors and their likely placement on the subject. In the end it was decided to employ a commercially available wireless accelerometer, the Witilt sensor [82], Fig 2.6. The Witilt sensor employs a Mitsumi Bluetooth Class 1 Module [83], a Freescale MMA7260Q triaxial accelerometer [2] and a PIC16LF88 microcontroller [84]. Unique enclosures measuring 90mm x 50mm x 20mm were built to accommodate the sensor and a 1250mAh lithium-ion battery. To reprogram the sensors an ICSP connection was used. Data were sampled at a frequency of 135Hz and at a range of +/- 6g ($m/s^2$).

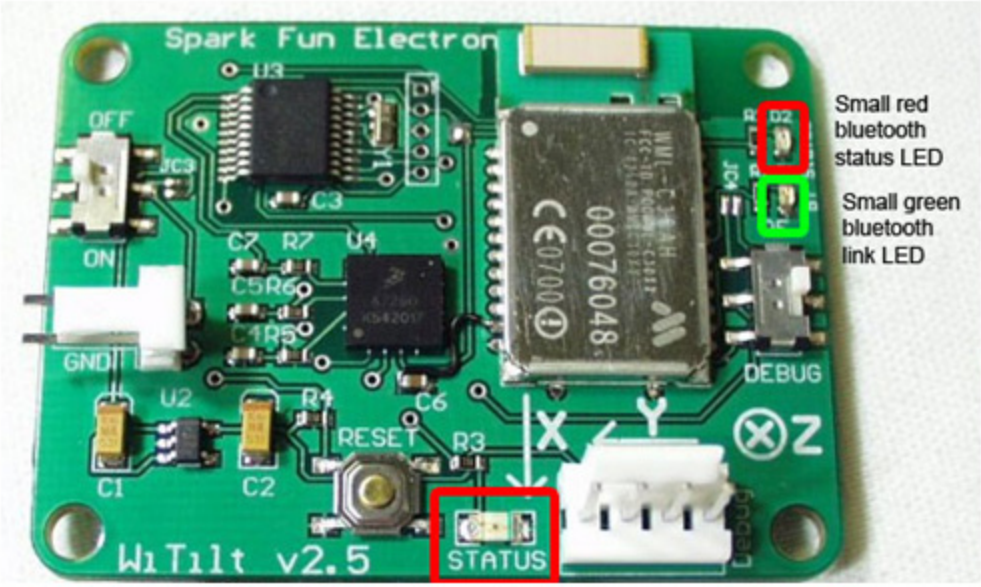


Fig. 2.6: The Witilt sensor

#### *2.2.3.2 MFC and The WEKA Environmen*

The lifecycle of the data during the study can be seen in Fig. 2.7. Initially, a program to communicate with the kinematic sensors over Bluetooth through virtual com ports was written in C++ using Microsoft Foundation Classes (MFC) [85]. This program synchronized, logged and parsed the data. During the development of this program we investigated both the Microsoft Bluetooth Stack [86] and the Widcomm Bluetooth Stack [87] for compatibility, throughput and reliability with the Microsoft Bluetooth Stack the clear winner. A second issue encountered during this stage of development was the

necessity to generate a stable multithreaded program. As there were five sensors each simultaneously requesting access to the Bluetooth pipe, deadlock safe programming was an important feature of the design. Once the data was gathered and parsed the next stage in the lifecycle was the generation of feature sets for the classifiers to digest. This task was accomplished using the Matlab® [88] environment where a second GUI, Fig. 2.8, was developed to accommodate smooth and easy interaction with the large dataset. To perform classifier comparison the Java based open source suite of machine learning algorithms from the University of Waikato, Waikato Environment for Knowledge Analysis (WEKA) [11], was employed. Fig. 2.9 presents an example use case scenario of the explorer environment within WEKA.

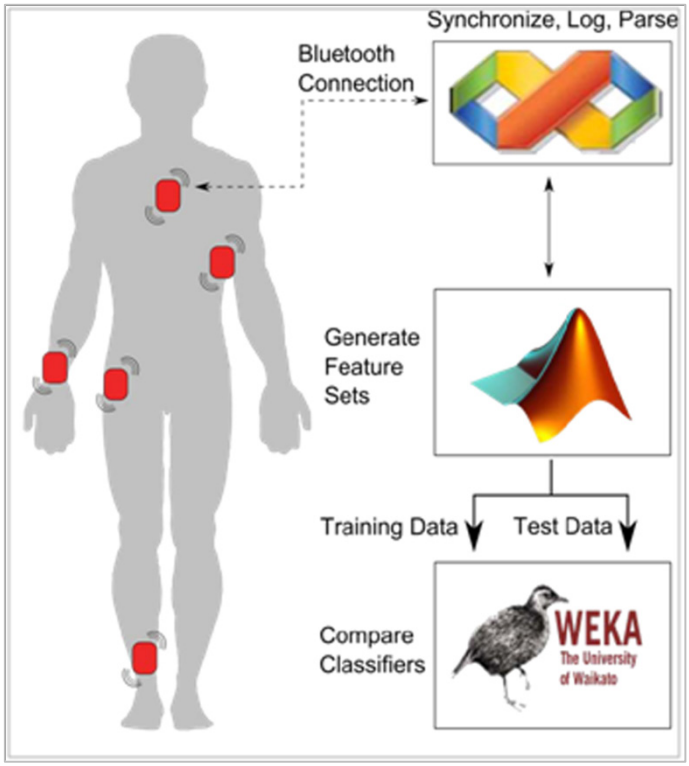


Fig. 2.7. The life cycle of data in the study

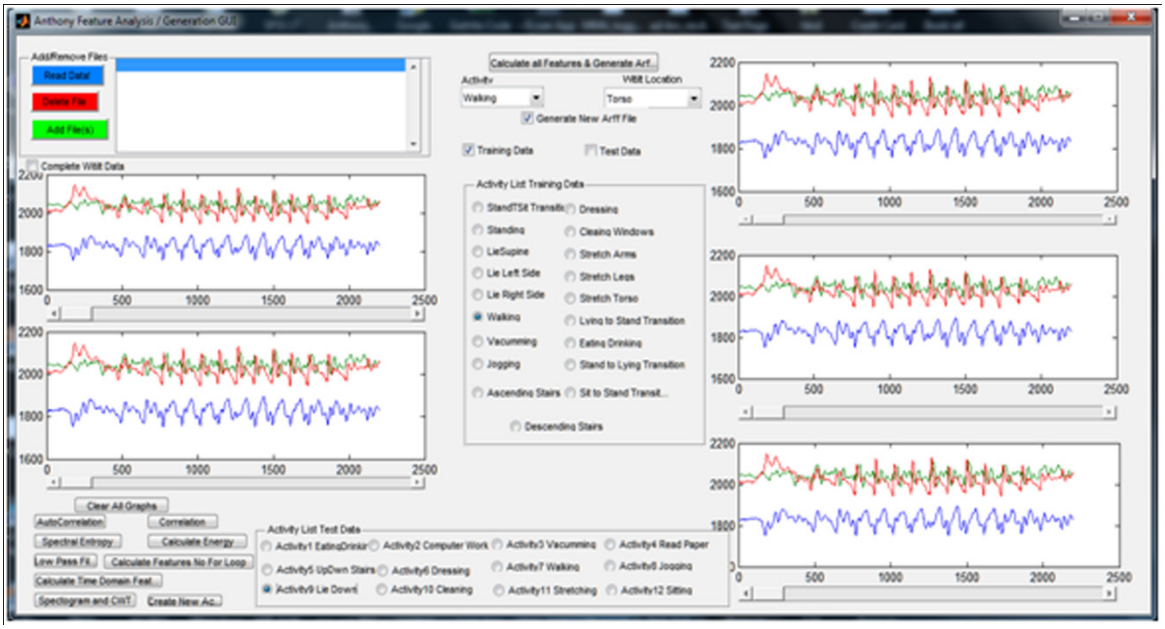


Fig. 2.8: The custom built Matlab feature generation GUI

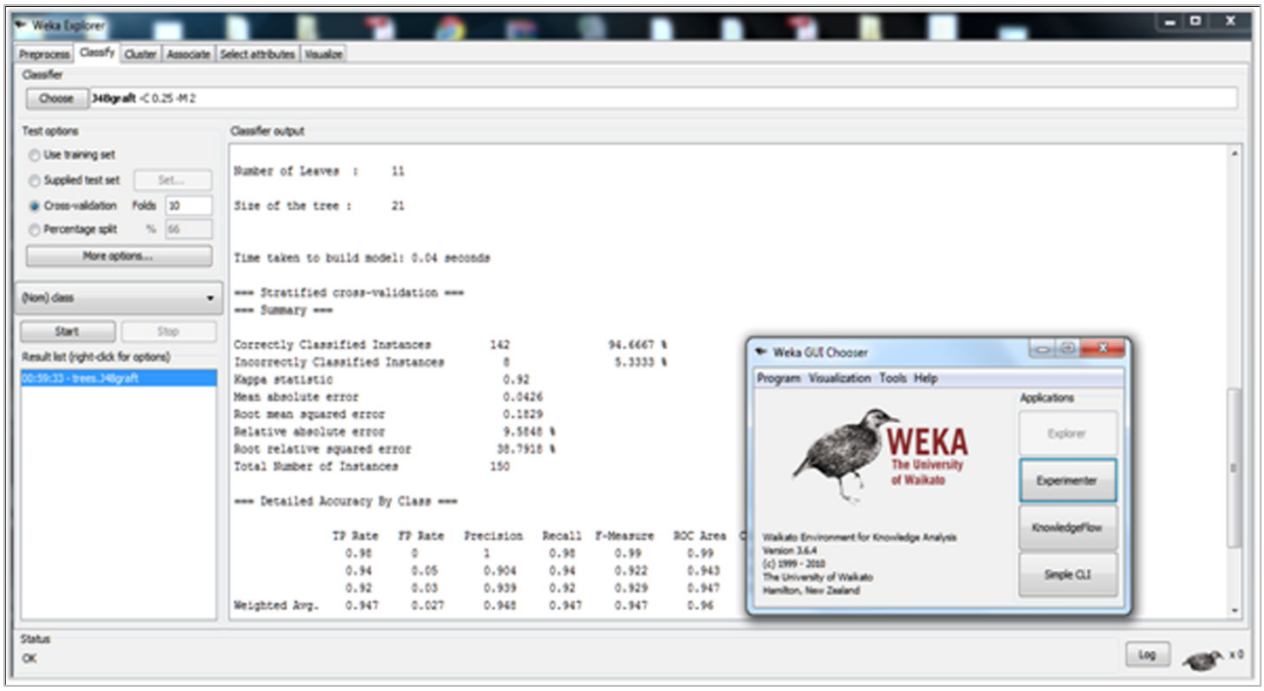


Fig. 2.9: The WEKA explorer environment

### *2.2.4 Supervised Learning Algorithms*

The algorithms developed in the field of machine learning broadly fall into one of two categories; supervised and unsupervised learning [11-12], [89-90]. In the case of supervised learning, several training examples with identified classes are initially fed to the algorithm. From this training data the algorithm infers a classification function. The nature of this function is dependent on the choice of classifier implied. The accuracy of the classification function is then evaluated with separate test data. Specifically, the true classes of the test data are withheld from the classifier and the classifier decision function is used to define sensitivity and specificity [11]. The second classification category is that of unsupervised learning. The primary difference between the two techniques is that unsupervised learning employs unlabeled training data with the objective of data reduction or data clustering [12].

In the context of this study we focused primarily on supervised learning. We considered a host of classifiers including Decision Trees [15], Bayesian networks [92], Nearest-Neighbours [93], Rules based [94], Support Vector Machines [90] and Neural Networks [17] which collectively can be categorized as base-level classifiers. However, the sensitivity and specificity of a classifier can, in general, be improved by the combination of these low level classifiers into higher meta-level classifiers [11] which we also investigated. The proceeding section provides an overview of each classifier. For a full review of these classifiers we refer the interested reader to [11-12], [89].

To aid in the description of the base-level models a brief example of each classifier applied to a classic machine learning dataset will be given. The renowned *iris* dataset [95] consists of 150 samples labeled as one of three iris flowers; iris setosa, iris versicolor and iris virginica. The dataset contains four features; sepal length (cm), sepal width (cm), petal length (cm) and petal width (cm). These examples were produced using the R statistical language [96] and the corresponding code can be found in Appendix B. Although we employed the more flexible WEKA environment we believe the included R code provides a more intuitive practical introduction to the classifiers. An example of the meta-level classifiers is withheld until the end of this section where a discussion of the bias-variance trade-off in classifier construction is given.

#### *2.2.4.1 Decision Tree's: C4.5 Graft*

The core of decision tree algorithms lies in the top-down induction approach developed at the University of Sydney in the early 1990's [11]. Essentially, the construction of a decision tree can be defined recursively. A specific feature is placed at the root node with a branch generated for each possible feature value which generates data subsets. The process is performed recursively for each subset and each feature until a class label is reached. The choice of which attribute to split on is based on a metric known as the information or gain ratio. Conceptually this measurement can be viewed as the amount of information gained by making the decision at this node. Several key issues such as numeric datasets and tree pruning must be considered.

Decision trees were originally designed for use with nominal datasets [11], [15]. Thankfully, a simple adjustment to the classical algorithm allows for adaption to numeric data. Essentially, each numeric feature is ranked based on classes and several binary switches are used to define new daughter nodes. A second key question is that of tree pruning. Although decision trees constructed by the top-down induction method perform well on training data they have a tendency to over-fit and generalize poorly to new test data. This problem is addressed by pruning the tree structure with two core methods; subtree replacement and subtree raising [11]. The decision tree algorithm employed in our study, C4.5 [15], employs subtree raising. This method essentially collapses down segments of the tree based on statistical factors derived from the training dataset. C4.5 is the open source version of the commercial C5.0 algorithm and the WEKA environment implementation of C4.5 is known as J48. One final important factor to consider is the complexity of decision tree induction defined in Equation 2.3

$$0\big(mnlog(n)\big) + 0\left(n\big(log(n)\big)^2\right) \tag{2.3}$$

where $n$ is the number of classes and $m$ the number of features.

Fig. 2.10 demonstrates a simple decision tree to classify the iris dataset. Within and along each node we can see which feature was used to split on and the confidence of this decision. The iris dataset lends itself naturally to a decision tree classifier and a 98% accuracy level is achieved on the test dataset. The R code can be found in Appendix B.

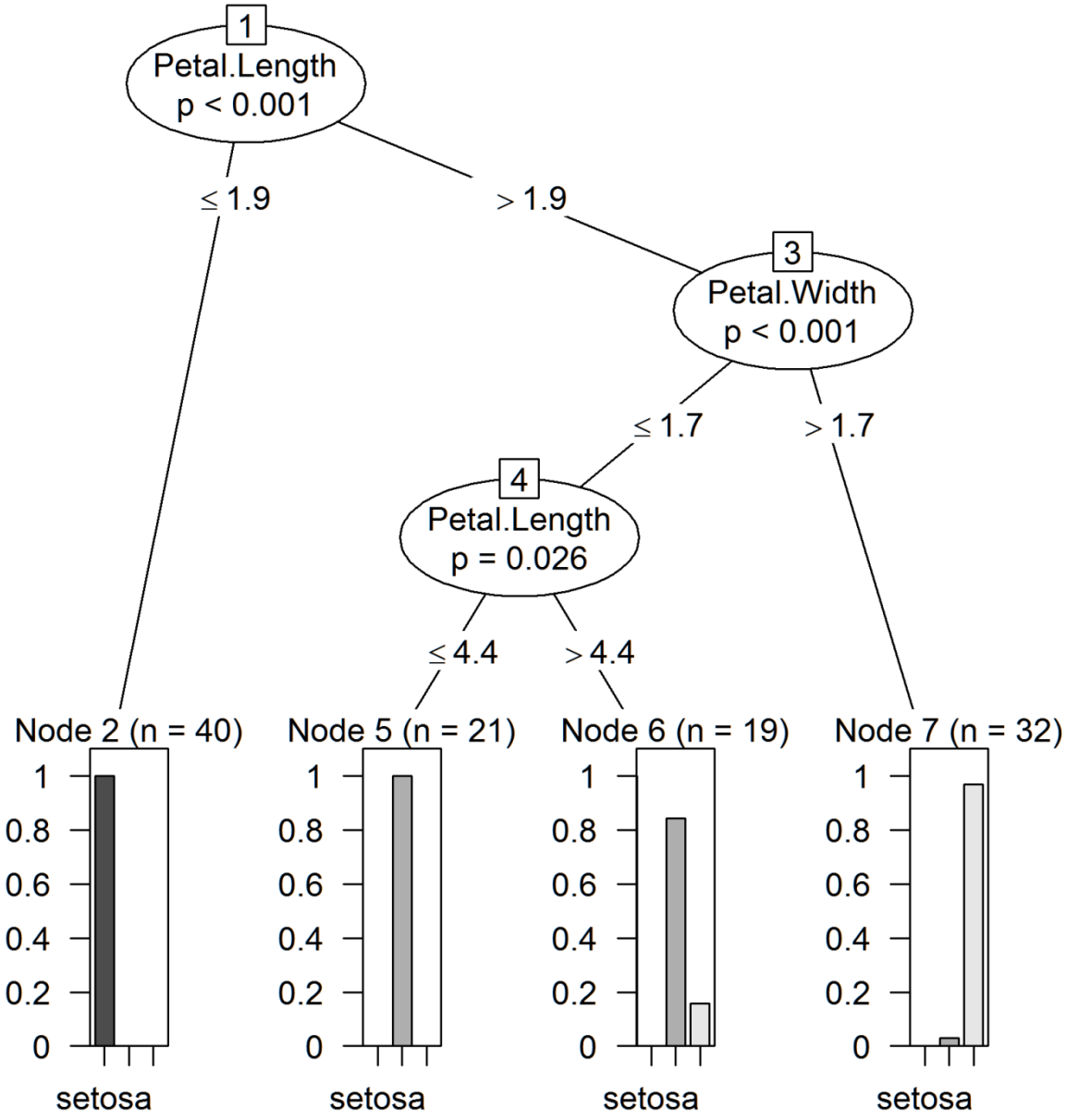


Fig. 2.10: A C4.5 decision tree built on the iris dataset

#### *2.2.4.2 Bayesian Networks: Naïve Bayes & BayesNET*

A simple and perhaps naive approach to building classifiers is to assume all features make equally important and independent contributions to the decision function [97]. This concept underpins a group of classifiers known as Bayesian networks. The classical Bayes rule of conditional probability states that given a hypothesis $H$ and evidence $E$ that bears on that hypothesis then in Equation 2.4

$$Pr[H/E] = \frac{Pr[E/H]Pr[H]}{Pr[E]} \tag{2.4}$$

The simplest Bayesian classifier, Naïve Bayes, updates the prior probabilities established from the training data with the new information supplied by the test data to choose a class label [11]. Unfortunately, this algorithm suffers from some severe assumptions. Firstly, the assumption of equal importance and independence makes the algorithm prone to datasets with redundant features; factors which add no value to the decision function [97]. A second key issue is the assumption of normally distributed numeric features. Although the normal distribution has some well known and useful properties it is an unfortunate fact of life that most datasets are simply not normally distributed. To further investigate the power of this assumption we employed kernel density estimation with Naïve Bayes and thus did not implicitly assume a particular distribution. We also investigated a second Bayesian classifier in our research. BayesNET is a slightly more sophisticated Bayesian classifier which internally employs the tree augmented Naïve Bayes (TAN) search algorithm [92].

Every Bayesian classifier requires some method of searching through the feature space. The simplest and most inefficient approach is to greedily search all possibilities. The alternative TAN algorithm is highly efficient in finding the set of features that maximizes the classifiers accuracy based on computing the network's maximum weighted spanning tree [11]. Although the Bayesian classifiers suffer from some heavy assumptions they tend to perform surprisingly well in practice [11].

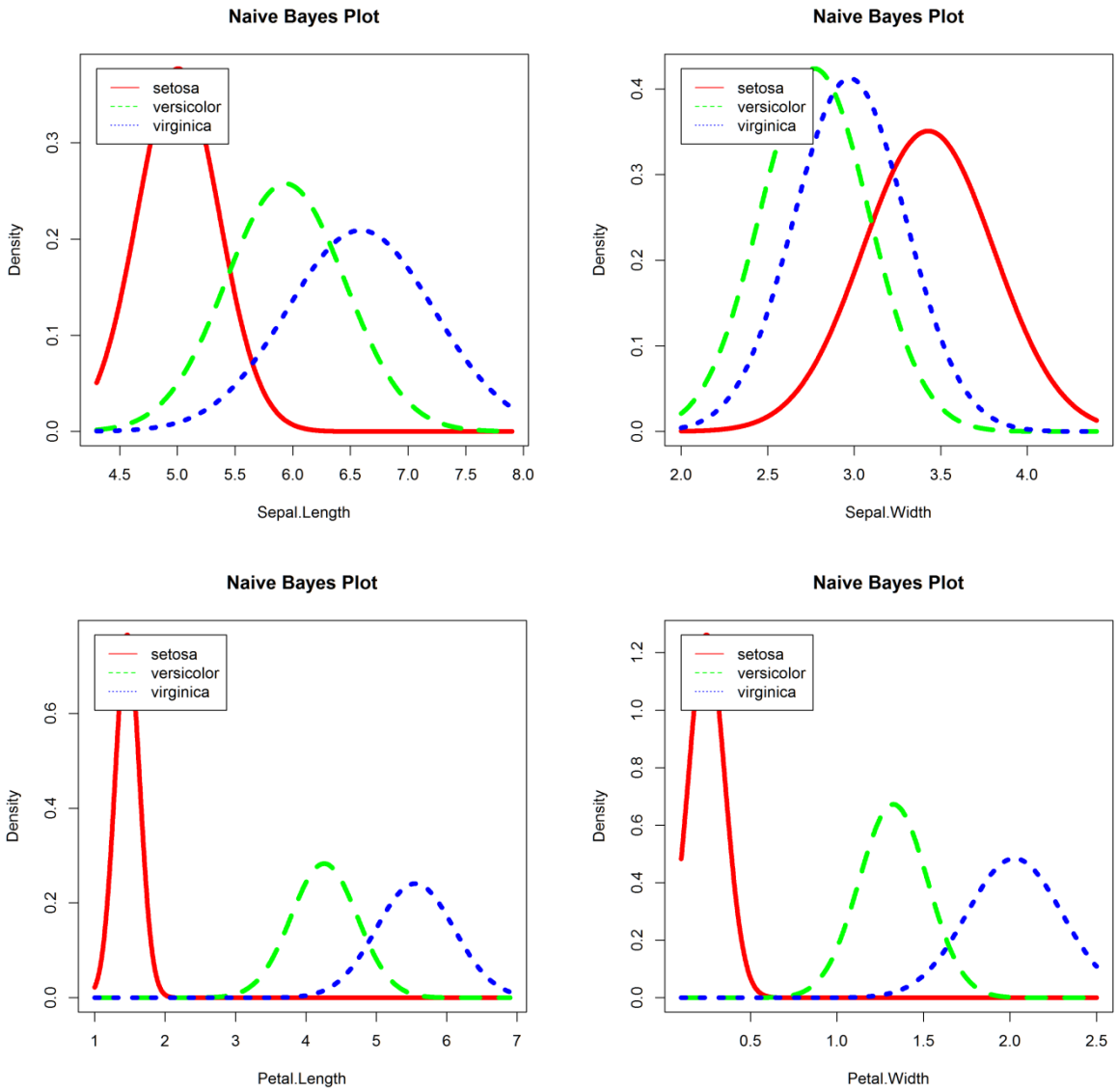


Fig. 2.11: Marginal Distributions of the Iris dataset employed by Naïve Bayes

It is difficult to provide a graphical representation of the Bayesian algorithm at work. Rather Fig. 2.11 presents the marginal probabilities, conditional on each of the four features (sepal length, sepal width, petal length and petal width), employed by a Naïve Bayes classifier as it attempts to classify the iris dataset. As noted this classifier is deceptively powerful and it matches the C4.5 decision tree in prediction accuracy on the iris test dataset. The code to reproduce this example can be found in the Appendix B.

### *2.2.4.3* Nearest-Neighbour Lazy Classifiers: IB1, IBK, KSTAR

Nearest neighbour classifiers can be categorized as instance-based learners or slightly more derogatorily as lazy classifiers [11], [93], [98]. Essentially these algorithms store the training examples and perform no real work until classification time. A new test data-point is processed by finding the training data point closest as measured by some predefined distance metric and assigning this training data point's class to the new data. A slightly more sophisticated approach is to employ multiple neighbours and a simple majority voting scheme to determine the appropriate class label. This is known as K-nearest neighbours (IBK) with K=1 known as IB1 [99].

The choice of distance metric is the key decision when utilizing these classifiers. The classical Euclidean represents the distance between a class with feature values $a_1^{(1)}, a_2^{(1)} \ldots a_k^{(1)}$ and a class with feature values $a_1^{(2)}, a_2^{(2)} \ldots a_k^{(2)}$ defined in Equation 2.5

$$\sqrt{\left(a_1^{(1)} - a_1^{(2)}\right)^2 + \left(a_2^{(1)} - a_2^{(2)}\right)^2 + \cdots + \left(a_k^{(1)} - a_k^{(2)}\right)^2} \qquad (2.5)$$

The simplicity of this metric might be considered a drawback of the algorithm and therefore we also investigated the KSTAR algorithm which incorporates a generalized distance function based on statistical properties of the training data set [11].

A significant advantage of instance based algorithms is that new data points can be added to the training test set at any time. However, there also exits some severe disadvantages. The implementation is severely slow with the time taken to make a single prediction proportional to the number of features. However, this problem can be partially addressed with techniques such as k-D and ball trees [99]. Another disadvantage is the algorithm can be easily corrupted by noisy datasets. The IBK implementation addresses this issue to some extent.

Fig. 2.12 presents the IBK algorithm applied to the iris dataset for k = 3. It is important to note that the iris dataset is multivariate and thus to produce a meaningful plot we most scale down to two dimensions. By analyzing Fig. 2.12 we can see that iris setosa can be easily separated however, there exists considerable overlap between iris versicolor and iris virginica with several misclassified labels.

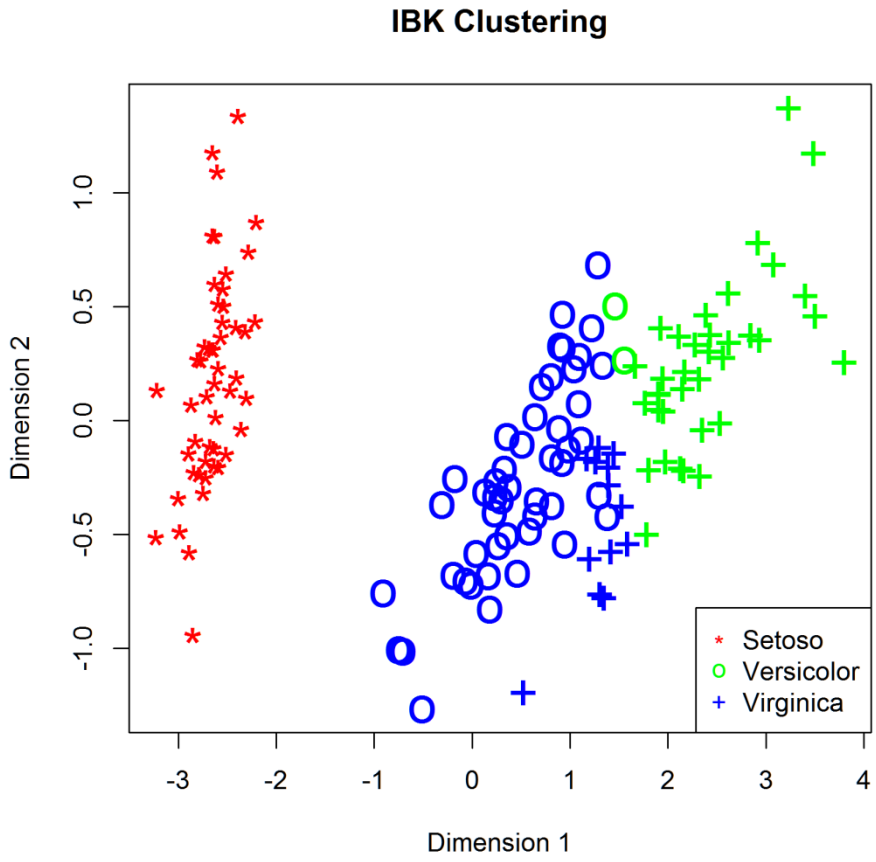


Fig. 2.12: IBK with k=3 applied to the Iris dataset

#### *2.2.4.4 Rule Based: JRIP*

An alternative approach to the divide-and-conquer technique adopted by decision tree algorithms is the separate-and-conquer methodology adopted by rule-generating algorithms [11], [100]. This technique takes each class label in turn and searches for a way to cover all relevant examples of the class in the training set while simultaneously excluding all examples not in that class. This approach is also called a covering algorithm as each rule covers a specific subset class label. The difference between decision trees and rules is subtle; covering algorithms function by adding tests to the current rule under construction with the objective of creating a rule with maximum accuracy whereas decision trees operate by adding tests to the tree under construction with the objective of maximizing the separation among the classes [11].

Unfortunately, rule generated algorithms are also subject to the problem of over-fitting, especially in noisy datasets. Therefore, a robust method of measuring the worth of generated rules is required. The standard technique is to evaluate their error rate on an independent dataset. Specifically, the traditional training set is divided into two segments; a growing set and a pruning set. A rule is formed on data from the growing set. Then a unique test case is deleted from the rule and the accuracy of this new truncated rule is evaluated on the pruning set. This process is repeated until the original rule cannot be improved upon anymore. Finally, the whole process is repeated for each class label in the dataset effectively generating one best rule for each class label. This pruning concept is called incremental reduced error pruning [101]. A slight modification to this algorithm whereby a global optimization on the final rule set is performed leads to the algorithm implemented in this study; RIPPER: repeated incremental pruning to produce error reduction [101]. A clear danger is that important structural information may be lost in the arbitrary splitting of data into growing and pruning sets. This problem can be slightly addressed by re-splitting the respective datasets on each fold.

The output from the JRIP classifier is simply a set of rules and it is difficult to visualize the classifier in action. It would be misleading to present the rules in a tree-like format and thus the rules produced from running the classifier on the iris dataset with example code is available in Appendix B.

#### *2.2.4.5 Support Vector Machine*

Support Vector Machines (SVMs) essentially address a binary classification problem. The primary objective is, dependent on the dimensionality of the problem, to find a line, plane or hyperplane which *best* separates a given labeled dataset [90]. The two cornerstones of SVMs are the concept of employing the dot product as a similarity score and the use of the perceptron as a learning mechanism. It was during the course of this study that we realized the unique learning potential of SVMs and thus decided to devote an entire second study to an investigation of this powerful algorithm. Therefore, a thorough description of the theoretical background of this technique is reserved until section 2.3 of this chapter.

#### *2.2.4.6 Neural Networks (Multilayer Perceptron)*

SVMs and Neural Networks are related through the concept of a perceptron, affectionately known as the grandfather of Neural Networks. Specifically, if a classification problem can be separated perfectly into two groups using a hyperplane it is said to be linearly separable [90]. If such a hyperplane exists it is easily found through the perceptron learning rule. Within a perceptron, an aggregation function sums *n* weighted input signals, $\mathrm{x}_1, \cdots, \mathrm{x}_\mathrm{n}$, with weights $\mathrm{w}_1, \cdots, \mathrm{w}_\mathrm{n}$ with a bias, $b$, of constant weight $-1$. The output of this aggregation function is in turn passed to a transfer function which assigns a $\pm 1$ label dependent on the sign of the input. Specifically, a perceptron represents a decision function shown in Equation 2.6

$$\bar{f}(x) = sgn\left(\left[\sum_{k=1}^{n} w_k x_k\right] - b\right) = sgn(\overline{\mathrm{w}} \cdot \bar{\mathrm{x}} - \mathrm{b}) \tag{2.6}$$

In the perceptron learning algorithm a greedy search heuristic adjusts $\overline{\mathrm{w}}$ and b through rotation and translation of the separating plane until a suitable decision surface is found [90]. A perceptron can be conceptually perceived as an artificial neuron similar to that of the human brain. When the brain undertakes a complicated task such as image recognition it does so by decomposing the task into numerous subtasks each handled by an individual neuron. A Neural Network can be perceived as a network of multilayered interconnected perceptrons [11].

The two primary issues with multilayer perceptron based Neural Networks are learning the structure of the network and learning the weights between each perceptron [90]. The latter issue is addressed with a technique known as backpropagation. This technique employs an optimization algorithm such as gradient descent to arrive at the appropriate weights. Two important parameters in the backpropagation process are the learning rate and momentum. The learning rate determines how quickly the optimization algorithm converges. If the parameter is set too large the optimization function may oscillate drastically while if it is too small the convergence time may tend towards infinity. This is an unfortunate and fundamental drawback of this method. The momentum parameter simply improves the performance of gradient descent by adding a

small constant value to each weight thereby making rapid changes in the optimization function less likely. The issue of discovering the network structure is unfortunately more complex and in this work was arrived at experimentally.

The structure of a Neural Network built with backpropagation with one hidden layer and containing three hidden neurons can be seen in Fig 2.13 for the iris data. The four feature inputs can be seen as feeding the hidden layer which in turn feeds the response neurons corresponding to the iris class labels. The synaptic weights can be seen between each node and constant neurons which arise during the optimization process are highlighted in blue. Also, the number of steps for convergence and the error rate of the network are indicated. This model performs respectively with 98% recognition and the code to produce this network can be found in Appendix B.

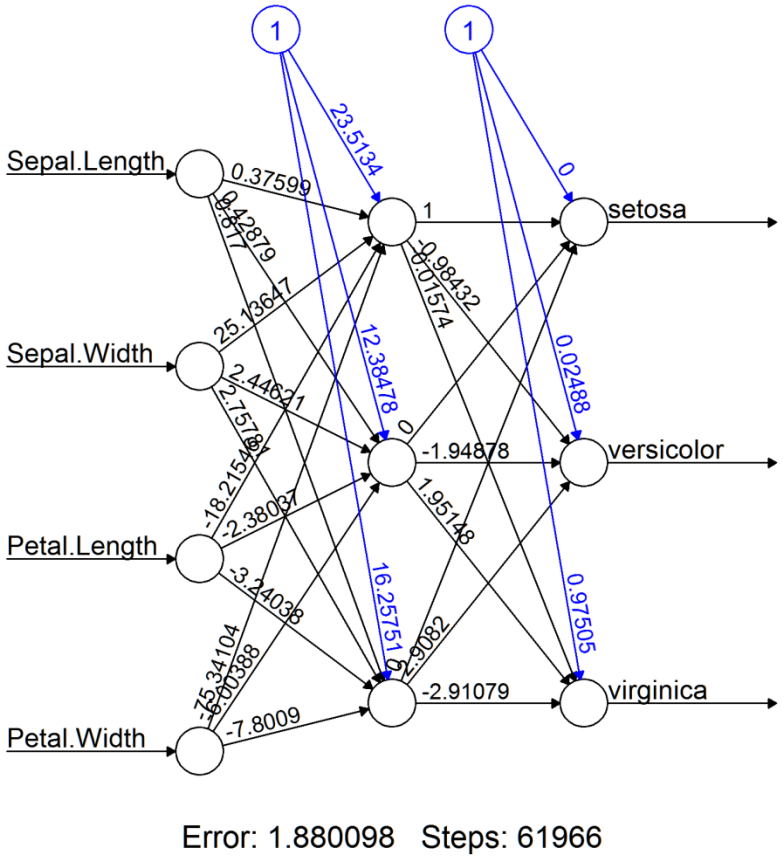


Fig. 2.13: Neural Network with 1 hidden layer and 3 hidden neurons for the Iris dataset

#### *2.2.4.7 Bagging*

A natural progression in classification is to assume that the combination of several simple base level classifiers will lead to improved accuracy; conceptually, wisdom of the crowd. The effect of combining multiple hypotheses can be viewed as a bias-variance decomposition [11]. The error rate for a particular learning algorithm is known as its bias and measures the extent to which the learning method has adapted to the problem. The issue of variance arises from the practical limitation of finite training data which can never be fully representative of the entire population to be learned. The total error of a classifier is simply a sum of its bias and variance and this concept will be discussed in more depth in the proceeding section. Meta-level classifiers attempt to reduce the variance component of this relationship.

The bagging, or bootstrap aggregating [102], algorithm attempts to generate new training data sets by randomly sampling with replacement from the original training dataset. The algorithm applies the chosen base-level classifier to each synthetic training set and allows the final class label to be chosen through majority voting. The technique is generally most effective when the underlying base level classifier is unstable; a small change in the training set results in a significant change in the decision function.

#### *2.2.4.8 Boosting: AdaBoostM1, MultiBoostAB*

The boosting technique relies on the same theoretical underpinnings as bagging; essentially addressing the bias-variance error of a classifier. The primary difference lies in the adopted weighting schemes; bagging assigns equal weighting to each classifier whereas boosting assigns higher weighing to the more successful classifier [11]. Whilst bagging trains each classifier separately the boosting methodology is iterative whereby each new classifier is influenced by the performance of those built previously.

The boosting algorithm begins by assigning equal weights to all classes in the training set. It then trains the chosen base-level classifier on this dataset. Based on these initial results a reweighting of the classes is performed whereby the weight of correctly classified classes is reduced and that of incorrectly classified classes increased. In the next iteration the base level classifier is trained on this reweighted data and in turn a

new-weighting scheme is derived. The scheme ceases once a predefined threshold is reached.

Boosting can produce significantly higher accuracy rates when compared with bagging [11]. However, the algorithm also has a higher tendency to overfit and thus must be treated with caution. In this work the classical boosting algorithm AdaBoostM1 [103] was employed with C4.5 classifier chosen as the base-level algorithm. We were also interested in investigating a hybrid algorithm which combines boosting with a variant of bagging to prevent over-fitting known as MultiBoostAB [103].

#### *2.2.4.9 Vote*

The final meta-level classifier investigated was the classical voting algorithm. The concept is very similar to that of bagging and boosting with the primary difference being the number of base-level classifiers chosen. Vote takes two or more base-level classifiers and based on a predefined combination rules merges the results into one prediction. The classical combination rule is the averaging of probability estimates of base-level classifiers but alternatives include taking the product, maximum or minimum of the probability estimates [11].

#### *2.2.4.10 Bias-Variance Decomposition, ROC & Cross Validation*

All classifiers are at risk of under- or over- fitting data. The core of this problem lies in the complexity of the classifier. Fig. 2.14 gives a graphical interpretation of the problem. This diagram demonstrates the typical behavior of the error of predictions on training and testing datasets as a function of the complexity of the classifier. The blue line represents the predication error on a training dataset and the red line the predication error on a testing dataset. Essentially, where our model is simple (few degrees of freedom) we tend to under-fit the data and when our model is complex (many degrees of freedom) we tend to over-fit the data [12].

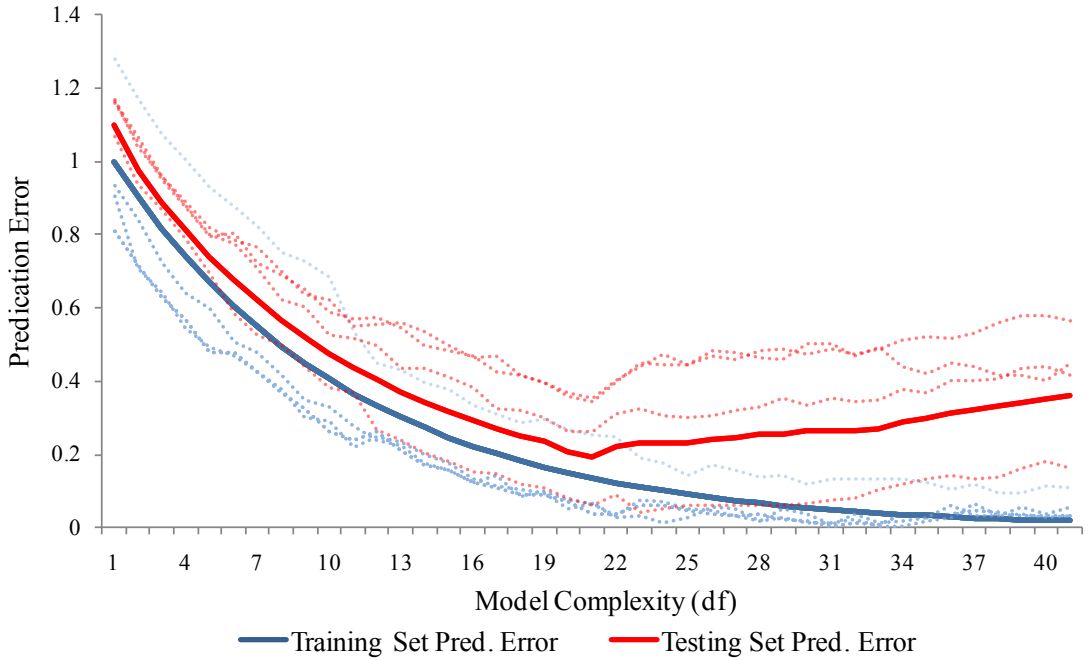


Fig. 2.14 The Bias-Variance trade-off of a classifier.

The terminology used in the machine learning community to describe these scenarios is bias and variance. The bias can be interpreted as the squared difference between the true mean and the expected value of our prediction. The variance is the variability of our estimate around this true mean [12]. Thus when our model has low complexity it is said to have high bias and low variance. Essentially, the model will be too generic and has under-fit itself to any specific structure in the training dataset and thus there may be a high error between the true mean and the estimated mean. Furthermore, as the model has not learnt anything of the structure of the problem it performs equally poorly on the test dataset. As we build ever increasingly complicated models we are making more of an effort to fit the training dataset and thus the prediction error goes down. It is said to have low bias as the estimated mean converges on the true mean but high variance as the model will not generalize well to test datasets as it has over-fit itself to noise and spurious trends in the training data. The key to note is in both circumstances we have high prediction error in our testing dataset. As previously noted meta-level classifiers attempt to reduce the variance component of this relationship.

Another important point to observe is the danger of reporting the accuracy of a classifier based on training data. A common technique to graphically report the accuracy of a classifier is through Receiver Operating Characteristic (ROC) plots. The ROC plots the True Positive Rate against the False Positive Rate or equivalently sensitivity against (1-specificity). The perfect classifier will appear in the top left hand corner of the plot when sensitivity and specificity of 1. As an example, Fig. 2.15 presents a ROC curve for a boosted and bagged decision tree. Here we are using a new dataset to demonstrate the power of meta-level classifiers – the *weather* dataset [104] consists of 35,000 daily observations from 45 Australian weather stations. The class label is binary yes / no on whether it will rain tomorrow. The features describe various weather parameters. Even with such a complicated dataset the boosted decision tree achieves 84% accuracy.

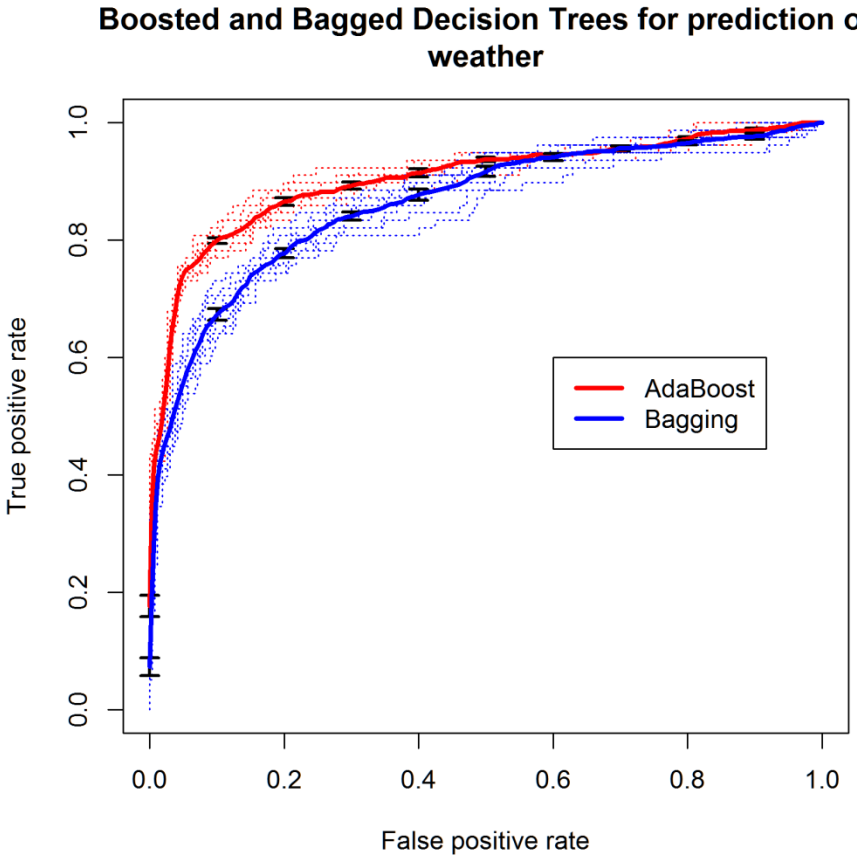


Fig. 2.15: ROC Curve for Boosted & Bagged Classifier

## *2.3 Physical Activity Recognition: SVM & MKL*

In the proceeding section we discuss the background of the second study conducted in this body of research, an analysis of physical activity recognition through support vector machines with multiple kernel learning. The journal paper arising from this work is presented in Chapter 4. To provide context and background the motivations and primary objectives behind this section of research are initially presented. This is followed by a review of relevant literature, a brief description of the hardware and software employed and an overview of the various algorithms investigated.

### *2.3.1 Motivation & Objective*

The core findings from our initial published work were from a dataset of 25 healthy subjects independent training data was found to outperform subject dependent data indicating that high recognition rates can be achieved without the need for prior user specific classifier training and secondly accelerometer based sensors attached to the wrist and ankle sensors were sufficient to maintain high levels of accuracy and therefore provided several options for embedding sensors in wearable electronics. However, this study was conducted in a controlled laboratory setting with a homogeneous healthy subject sample and therefore the logical next stage of research was to expand this into an older, more diverse population in a home environment. Therefore, a second study was conducted in a home environment with 5 elderly subjects using accelerometer based sensors to detect physical activities. However, in this study we concentrated on one specific type of classifier whose potential had been identified in the previous study – the Support Vector Machine and an expansion known as Multiple Kernel Learning.

### *2.3.2 Review of Relevant Literature*

As previously discussed in section 2.2.2, Support Vector Machines (SVMs) have proven popular in published work when large groups of classifiers have been compared for physical activity recognition [14], [35], [39], [63]. However, due to the power and flexibility of these classifiers numerous studies have been solely dedicated to them. Gyllensten et al [105] investigated the power of a SVM with a radial base function (RBF) kernel in classifying 6 activities using data from a single waist mounted

accelerometer. From a sample of 20 subjects the SVM marginally outperformed a Neural Network with an accuracy of 76%. Mannini et al [106] cascaded two RBF kernel SVMs together to identify dynamic and static activities and walking speed estimation in 6 subjects with a thigh mounted accelerometer achieving 99% accuracy in activity identification and 95% in speed estimation using 5-fold cross validation. Zhang et al [107] investigated a significant dataset of 60 subjects wearing accelerometers attached to each wrist and the waist employing a SVM with linear kernel to classify activities into one of sedentary, household, walking and running. The SVM achieved an overall accuracy of 97% outperforming decision trees and Bayesian classifiers. Fluery et al [108] achieved an accuracy of 86% classifying 7 physical activities with 13 subjects in a Health Smart Home using a range of sensors employing a SVM with a Gaussian kernel. This work was further extended in [109] by considering spatial and temporal knowledge with improved accuracy across several activities. Kilmartin et al [110] employed a polynomial kernel SVM trained on data from 40 subjects and tested on an independent dataset of 12 subjects to detect 5 distinct gait patterns achieving high levels of accuracy although the classifier was outperformed by a Multilayer Perceptron Neural Network. He et al [111] adopted a slight modification of the SVM known as a Relevance Vector Machine [112] applied to a dataset of 20 subjects wearing 5 sensors attached to the wrists, waist and ankles achieving an impressive 99% level of accuracy. Lau et al [113] used data from an accelerometer and gyroscope attached to the foot to train an RBF kernel SVM to distinguish between several walking conditions achieving 84% accuracy in a dataset of 3 subjects. Finally, Wu et al [114] investigated an RBF kernel SVM trained on data from a waist mounted accelerometer as subjects completed 6 unique activities. Interestingly, these authors used independent subjects for the training and testing and achieved an accuracy of 95%.

Several authors have employed the SVM technique in its natural form as a binary classifier, essentially separating subjects into one of two classes. Begg et al [115] employed a SVM classifier trained on a feature set derived from minimum foot clearance (MFC) data to differentiate between young and old gait patterns in a sample of 58 subjects. Using a linear kernel an accuracy of 83% was achieved. Wu et al [116] fed feature vectors consisting of the standard deviation of swing interval and signal turns

count into a polynomial kernel SVM and an accuracy of 90% in disguising between Parkinsonian and healthy subjects was achieved. Fukuchi et al [117] successfully distinguished between 17 young and 17 elderly subjects using a linear kernel SVM trained with 31 spatiotemporal parameters. Levinger et al [118] employed a Gaussian kernel SVM to classify gait patterns indicative of knee osteoarthritis with an accuracy of 89% in a dataset of 33 subjects. Kannoker et al [119] also investigated MFC data and further estimated the risk of falls using posterior probabilities from a SVM with strong results. Finally, Lai et al [120] employed ground reaction force data and a polynomial kernel SVM to differentiate between 27 subjects with and without patellofemoral pain syndrome achieving 89% accuracy.

As can be seen a significant range of approaches with SVMs have been adopted for activity recognition within the research community. Paramount to the successful application of this type of classifier is the kernel chosen and we discuss this in depth in section 2.3.4. Upon review of the literature we were unable to find an application of a particular type of kernel selection algorithm known as Multiple Kernel Learning applied to physical activity recognition. This finding coupled with the findings from the first study motivated our work for this second study.

### *2.3.3 Hardware / Software*

The same Witilt sensor [82], Fig. 2.6, was employed in the second study. As discussed in section 2.2.3.2, a software program deployed on a nearby laptop was used to synchronize, log and parse data for healthy younger adults during the first study. However, it was impractical to use the same hardware configuration in the second study in a home environment with older subjects. Therefore, a new program was developed on an iPAQ 6915 [121]. Incorporating open-source software, 32-Feet.Net [122], a Windows Mobile 5 [123] program to communicate with the accelerometer based sensors over a Serial Port Profile on a Widcomm / Broadcom Bluetooth stack [124] was developed. A simple GUI was developed for the device which allowed subjects to self-annotate the data. Once a data collection period was completed the data was downloaded from the device and analyzed in Matlab® and WEKA as previously described. Fig. 2.16 shows the custom GUI running on the IPAQ 6915 used for the second study.

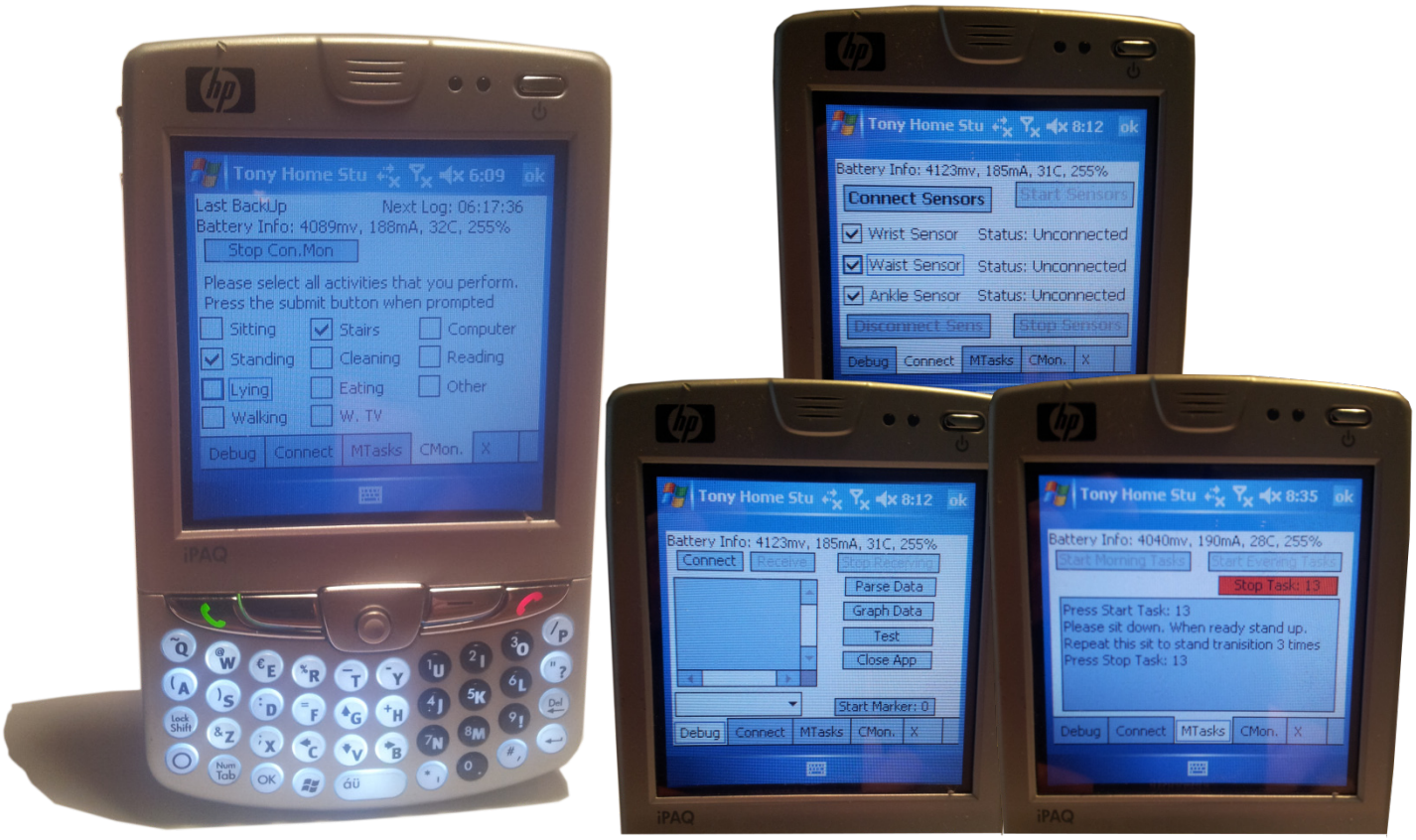


Fig. 2.16: GUI developed for the elderly home study running on an IPAQ 6915

### *2.3.4 The SVM & MKL Algorithms*

#### *2.3.4.1 The Support Vector Machine*

With Support Vector Machines (SVMs) we are essentially addressing a binary classification problem. The primary objective is, dependent on the dimensionality of the problem, to find a line, plane or hyperplane which *best* separates a given labeled dataset. The resulting SVM model can then be employed to classify samples from outside the training set. We present the theory of SVMs in several logical steps beginning with the definition of the simple dot product and hyperplane progressing through linear decision surfaces, perceptron learning and finally SVMs. This presentation follows closely to that provided in [90].

One of the cornerstones of SVMs is the concept of employing the dot product as a measure of similarity. Specifically, given two vectors $\bar{a} = (a_1, \cdots, a_n)$ and $\bar{b} = (b_1, \cdots, b_n)$ in $\mathbb{R}^n$ dimensional space the dot product of $\bar{a} \cdot \bar{b}$ can be interpreted from a geometric perspective as $\bar{a} \cdot \bar{b} = |\bar{a}||\bar{b}|cos(\gamma)$ where $\gamma$ is the angle between the two

vectors. Now, if we allow the two vectors to be unit vectors it is intuitive to see how the dot product acts as a measure of similarity; if the angle between the two vectors approaches $0^{\circ}$ then $\bar{a} \cdot \bar{b} \approx 1$ indicating similarity, if the angle approaches $180^{\circ}$ then $\bar{a} \cdot \bar{b} \approx -1$ which indicates similarity but in opposite direction and finally if the angle approaches $90^{\circ}$ then $\bar{a} \cdot \bar{b} \approx 0$ indicating dissimilarity.

A second keystone of SVMs is the concept of a separating hyperplane, Fig. 2.17. A hyperplane is nothing more than a line or plane in higher dimensions. Specifically, consider $\mathbb{R}^3$, a three dimensional dot product space where the normal vector $\overline{w} = (w_1, w_2, w_3)$ and a position vector $\bar{x} = (x, y, z)$ then $\overline{w} \cdot \bar{x} = b$ describes a plane. If we consider $\mathbb{R}^n$ then $\overline{w} \cdot \bar{x} = b$ describes a hyperplane in n-dimensional space.

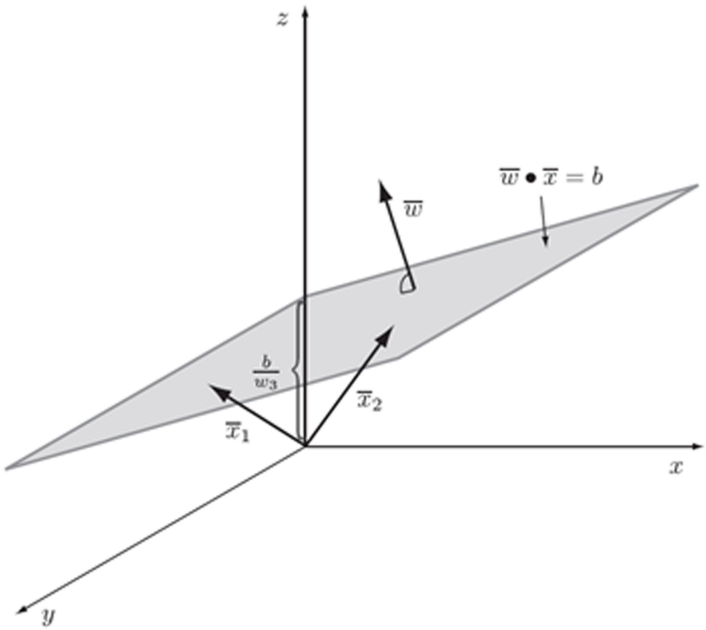


Fig. 2.17: A separating hyperplane defined by $\overline{w} \cdot \bar{x} = b$ where $\bar{x}_1$ and $\bar{x}_2$ are vectors in $\mathbb{R}^3$ three dimensional space.

If a hyperplane separates two classes it is known as a linear decision surface and from this we wish to define a linear decision function. As an example assume we have a linearly separable dataset consisting of points labeled -1 or 1 respectively. Given this we are guaranteed to find a line that perfectly separates the two training classes and thus our decision surface can be defined as: $g(\bar{x}) = \overline{w} \cdot \bar{x} = b$. Now imagine we wish to find the

label for some point $\bar{a} \in \mathbb{R}^2$ but which was not part of our original training set. To do this we need to create our decision function. We choose an arbitrary point, $\bar{c}$, on the decision surface: $g(\bar{c}) = \bar{w} \cdot \bar{c} = b$ and define a vector $\bar{z}$, such that $\bar{z} = \bar{a} - \bar{c}$. Now, we note that the dot product $\bar{w} \cdot \bar{z} = |\bar{w}||\bar{z}|cos(\gamma) = k$ will produce a positive value $k$ if $\bar{a}$ is above the decision surface and a negative value if it is below. Furthermore, it can be shown that $\bar{w} \cdot \bar{z} = g(\bar{a}) - b$ and thus our decision function is given by Equation 2.7

$$f(\bar{x}) = \begin{cases} +1 & if\ \mathrm{g}(\bar{\mathrm{x}}) - \mathrm{b} \geq 0 \\ -1 & if\ \mathrm{g}(\bar{\mathrm{x}}) - \mathrm{b} \leq 0 \end{cases} \forall\, \bar{x}\ \in\ \mathbb{R}^2 \tag{2.7}$$

We now generalize this to n-dimensional space and argue for some decision surface $\bar{w} \cdot \bar{x} = b$ in $\mathbb{R}^n$ the decision function is given by $f(\bar{x}) = sgn(\bar{w} \cdot \bar{x} - b)$ with $\bar{w}, \bar{x}\ \in\ \mathbb{R}^n, b\ \in\ \mathbb{R}$ and

$$sgn(k) = \begin{cases} +1 & if\ \mathrm{k} \geq 0 \\ -1 & if\ \mathrm{k} \leq 0 \end{cases} \forall\, k\ \in\ \mathbb{R} \tag{2.8}$$

The next key element is the concept of the perceptron which is considered the predecessor of Artificial Neural Networks. Within a perceptron an aggregation function sums $n$ weighted input signals, $\mathrm{x}_1, \cdots, \mathrm{x}_\mathrm{n}$ with weights $\mathrm{w}_1, \cdots, \mathrm{w}_\mathrm{n}$ with a bias of constant weight -1. The output of this aggregation function is in turn passed to a transfer function which assigns a $\pm 1$ label dependent on the sign of the input. Specifically, we can see a perceptron represents a decision function given by Equation 2.9

$$\bar{f}(x) = sgn\left(\left[\sum_{k=1}^{n} w_k x_k\right] - b\right) = sgn(\bar{\mathrm{w}} \cdot \bar{\mathrm{x}} - \mathrm{b}) \tag{2.9}$$

In the perceptron learning algorithm a greedy search heuristic is employed where the values of $\bar{\mathrm{w}}$ and b are adjusted through rotation and translation of the separating plane until a suitable decision surface is found. The majority of the adjustments to the plane will occur for points at the boundary between the two classes, the points most difficult to classify. A new counter variable, $\bar{a}$, is introduced to the perceptron training algorithm with points of significant difficulty near the boundary achieving a high counter value. We note that the normal vector $\bar{w}$ can be interpreted as a linear combination of the scaled versions of misclassified training set points: $\bar{w} = \sum_{i=1}^{l} a_i y_i x_i$ where $y_i$ represents class labels. The decision function can then be reformulated as Equation 2.10

$$\bar{f}(x) = sgn\left(\sum_{i=1}^{l} a_i y_i x_i \cdot \bar{\mathrm{x}} - b\right) \tag{2.10}$$

These two alternative presentations of the perceptron problem represent the primal and dual problem respectively. With this dual representation we see which training points exert the most pressure on our separating plane, a fundamental observation of SVMs.

A significant drawback of perceptron learning is that the decision surface are not guaranteed to be optimal. This problem is addressed by maximum-margin classifiers. Such a classifier attempts to simultaneously maximize the distance between the class boundaries and find a decision surface which is of equal distance between the class boundaries. This can be constructed as a convex optimization problem. We define a decision surface as optimal if it maximizes the margin from the supporting hyperplanes and is equidistant from each. Furthermore, we introduce the concept of a *support vector* which acts as a constraint on the supporting hyperplanes beyond which they cannot pass. Note, again we follow the derivation presented in [90]. Given a training set which is linearly separable, Equation 2.11

$$D = \{(\bar{x}_1, y_1, \bar{x}_2, y_2, \ldots, \bar{x}_l, y_l)\} \subseteq \mathbb{R}^{\mathrm{n}} \times \{+1, -1\} \tag{2.11}$$

The maximum margin decision surface $\bar{\mathrm{w}}^* \cdot \bar{\mathrm{x}} = \mathrm{b}^*$ is found through Equation 2.12

$$\begin{gathered} min\phi(\bar{w}, b) = \min_{\bar{w},b} \frac{1}{2} \bar{w} \cdot \bar{w} \\ \text{s.t. the constraints } \bar{w} \cdot (y_i \bar{x}_i) \geq 1 + y_i b \; \forall \; (\bar{x}_i, y_i) \in D \end{gathered} \tag{2.12}$$

The dot product as a measure of similarity, separating hyperplanes as decision functions, the primal and dual formation of perceptrons and maximum-margin classifiers leads naturally to the definition of SVMs. By employing Lagrangian optimization theory we find that the dual of the maximum-margin classifier is the Linear SVM. Again, given the training set in Equation 2.11 which is linearly separable then the Linear SVM is given by Equation 2.13

$$sgn\left(\sum_{i=1}^{l} \alpha_i^* y_i \bar{x}_i \cdot \bar{\mathrm{x}} - \sum_{i=1}^{l} \alpha_i^* y_i \bar{x}_i \cdot \bar{x} - \bar{x}_{SV^+} + 1\right) \tag{2.13}$$

where we define a support vector (sv) as a point $(\bar{x}_i, y_i) \in D$ whose Lagrangian multiplier is greater than zero. To find the dual offset tern we chose one support vector

$$(\bar{x}_{SV^+}, +1) \in \{(\bar{x}_i, +1) | (\bar{x}_i, +1) \in D, \alpha_i^* > 0\} \tag{2.14}$$

The Lagrangian dual of the maximum margin problem allows us to train our Linear SVM, Equation 2.15. Fig, 2.18 provides a graphical interpretation of the SVM.

$$\bar{\alpha}^* = arg\max_{\bar{\alpha}} \left( \sum_{i=1}^{l} \bar{\alpha} - \frac{1}{2} \sum_{i=1}^{l} \sum_{j=1}^{l} \alpha_i \alpha_j y_i y_j \bar{x}_i \cdot \bar{x}_j \right) s.t. \sum_{i=1}^{l} \alpha_i y_i = 0 \tag{2.15}$$

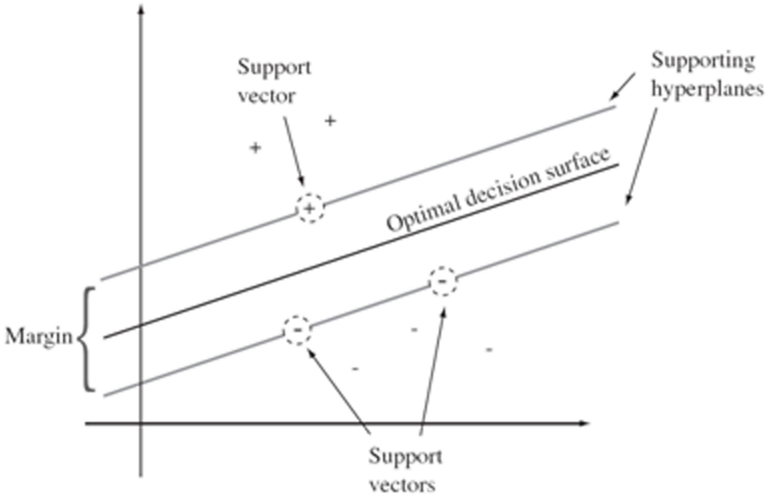


Fig. 2.18: Theoretical Support Vector Machine framework.

Through a technique known as the *kernel trick* we move from a space where data is not linearly separable, the input space, to a higher dimensional space, the feature space, where linear separability can be achieved. We assume we have a dataset for which there does not exist a linear decision surface in input space. Now we consider a function which maps our dataset into some higher dimensional feature space where a linearly separable decision function can be found. Specifically, $\hat{f}(\bar{x}) = sgn(\bar{w} \cdot \Phi(\bar{x}) - b)$ where $\Phi(\bar{x})$ performs the mapping from input to feature space producing the linear decision surface $\bar{w}^* \cdot \Phi(\bar{x}) = b$. A significant drawback of this decision function in this current format is the complexity of the decision function grows with the dimension of the feature space, as can be seen in Equation 2.16.

$$\begin{aligned}\hat{f}(\bar{x}) &= sgn(\overline{w} \cdot \Phi(\bar{\mathrm{x}}) - \mathrm{b}) = sgn(\overline{w}^* \cdot \Phi(\bar{\mathrm{x}}) - \mathrm{b}^*) \\ &= sgn\left(\sum_{i=1}^{d} w_i\, z_i - b\right)\end{aligned} \tag{2.16}$$

Once again the power of the dual representation is employed. We consider the dual of the normal vector $\overline{w}^* = \sum_{i=1}^{l} \alpha_i^* y_i\, \Phi(\bar{x}_i)$ where $l$ = the size of our training set. Our decision function is now given by Equation 2.17

$$\begin{aligned}sgn(\overline{w} \cdot \Phi(\bar{\mathrm{x}}) - \mathrm{b}) &= sgn\left(\sum_{i=1}^{l} \alpha_i^* y_i\, \Phi(\bar{x}_i) \cdot \Phi(\bar{\mathrm{x}}) - \mathrm{b}^*\right) \\ &= sgn\left(\sum_{i=1}^{l} \alpha_i^* y_i\, (\bar{x}_i \cdot \bar{\mathrm{x}}) - \mathrm{b}^*\right)\end{aligned} \tag{2.17}$$

The kernel trick can be seen in this last line. The actual value of the dot product in feature space is computed in input space and the complexity of our function is now proportional to the number of support vectors and not feature space dimensionality. Finally, the new decision function incorporating the kernel is shown in Equation 2.18

$$\hat{f}(\bar{x}) = sgn\left(\sum_{i=1}^{l} \alpha_i^* y_i\, \kappa(\bar{x}_i, \bar{x}) - b^*\right) \tag{2.18}$$

Kernel functions are the secret ingredient to SVMs and Fig. 2.19 presents a graphical interpretation of the kernel trick. In Fig. 2.19(a) we have data in $\mathbb{R}^2$ dimensional space. Clearly an optimally separating linear plane cannot be found in this input space. We would require a non-linear plane defined by $\bar{x} \cdot \bar{x} = 1$ (the circle). However, this can be avoided if we move the data into a $\mathbb{R}^3$ dimensional space, Fig. 2.19(b). Now, in this expanded feature space an optimally separating linear plane exists.

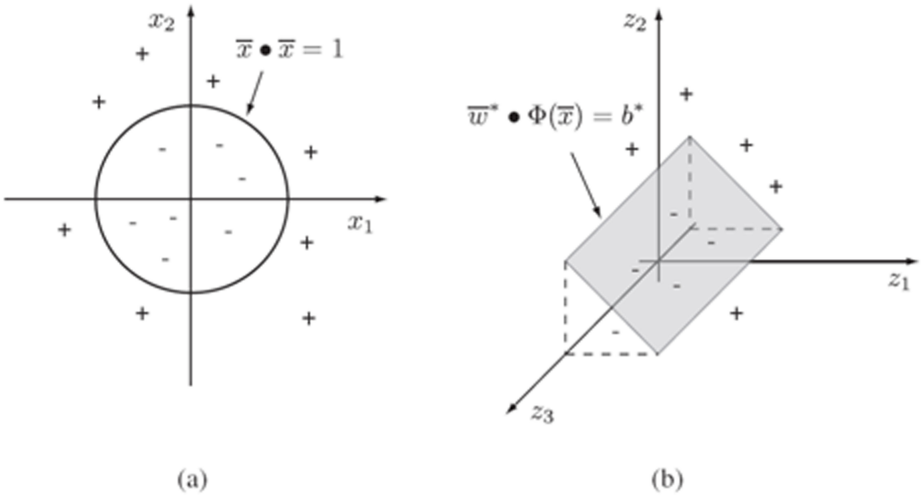


Fig. 2.19: The Kernel Trick. (a) $\mathbb{R}^2$ in input space (b) $\mathbb{R}^3$ in feature space

An important modification to the classical SVM is the concept of slack variables. Essentially, we introduce slack variables, $\xi_j$, into our supporting hyperplanes and allow some training samples to lie on the wrong side of the hyperplane, Equation 2.19

$$y_i(\overline{w} \cdot \bar{x}_i - b) + \xi_j - 1 \geq 0 \text{ AND } \xi_j \geq 0 \tag{2.19}$$

and introduce a cost variable $C$ into the optimization problem, Equation 2.20

$$\min_{\overline{w},\xi,b} \phi(\overline{w},\xi,b) = \min_{\overline{w},\xi,b}\left(\frac{1}{2}\overline{w} \cdot \overline{w} + C\sum_{i=1}^{l}\xi_i\right) \tag{2.20}$$

The optimization problem can now interpreted as a trade-off between the magnitude of the sum of the values of the slack variables and the width of the margin. A large $C$ forces a small margin with few slack variables whereas a small C forces a large margin with many slack variables.

#### *2.3.4.2 Multiple Kernel Learning*

As noted in the previous section one of the pivotal aspects of SVMs is the choice of kernel employed to map data from input space to feature space. As can be seen from Table 2.2 there exists a host of kernels to choose from with this list representing a small subset of well established kernels. The choice of kernel is highly dependent on the specific dataset with brute-force methods often employed to find the optimal kernel and

corresponding kernel parameters. The method of Multiple Kernel Learning (MKL) introduced by Bach et al [125] addresses the issue of kernel selection. MKL takes as input several kernels and evaluates various convex combinations, Equation 2.21

$$\kappa(\bar{x},\bar{y}) = \sum_{i=1}^{K} \lambda_i \kappa_i(\bar{x},\bar{y}) \;\; where \; \lambda_i \geq 0, \sum_i \lambda_i = 1 \tag{2.21}$$

We are searching for the weights $\lambda_i$ with higher weights attributed to more informative kernels. Practical implementation of the MKL technique was performed using SimpleMKL [126] and employing semi-infinite linear programming we have

$$\max_{\alpha} \left( \sum_{i=1}^{l} \alpha_i - \frac{1}{2} \sum_{i,j=1}^{l} \alpha_i \alpha_j y_i y_j \left[ \sum_{l=1}^{K} \lambda_l \kappa_l(\bar{x}_i, \bar{x}_l) \right] \right) \tag{2.22}$$
$$\text{s.t. } \textstyle\sum_{i=1}^{l} \alpha_i y_i = 0, \alpha_i = 0, \; \forall \; l \;\; \sum_l \lambda_l = 1 \; \lambda_l > 0 \; \forall \; l \;\; 0 \leq \alpha_i \leq C$$

This is equivalent to Equation 2.23

$$\min_{\bar{w},\xi,b,\lambda} \left( \frac{1}{2} \sum_{i=1}^{K} \frac{1}{\lambda_i} \overline{w}_i \cdot \overline{w}_i + C \sum_{i=1}^{l} \xi_{\mathrm{i}} \right) \tag{2.23}$$
$$s.t. \; \mathrm{y_i} \textstyle\sum_{i=1}^{K} w_i(\bar{x}_i) + \mathrm{b} \geq 1 - \xi_{\mathrm{j}}, \;\; \xi_{\mathrm{j}} \geq 0, \sum_i \lambda_i = 1 \; \forall \; i \; and \; C > 0$$

which we note is simply the SVM formulation. Essentially, a fixed weighting of kernels is used to final an initial $\alpha$, which in turn is used to solve for the corresponding $\lambda's$. This process is repeated until convergence criterion is satisfied. For a more detailed discussion of the topic the interested reader is referred to [126].

**Table 2.2 Functional form and parameters of several popular SVM Kernels**

| Kernel | Function $\kappa(\bar{x},\bar{y})$ | Parameters | Purpose |
|---|---|---|---|
| Linear | $\bar{x} \cdot \bar{y}$ | None | None |
| Gaussian (RBF) | $e^{-\gamma(\|\bar{x}-\bar{y}\|^2)}$ | $\gamma > 0$ | Kernel Width |
| Homogeneous Polynomial | $(\bar{x} \cdot \bar{y})^d$ | $d \geq 2$ | Poly. Degree |
| Sigmoid | $tanh(\gamma \cdot \bar{x} \cdot \bar{y} + \Theta)$ | $\gamma > 0, \Theta \in [-1,1]$ | Kernel Width |

#### *2.3.4.3 The Support Vector Machine: An Example*

A simple practical application of the SVM is now considered. The R code to reproduce this example can be found in Appendix B. To aid in the visualization of the hyperplane and support vectors a dataset consisting of numeric features in $\mathbb{R}^2$ with binary class labels is employed. The features are generated from a marginally skewed uniform random distribution with a class label of 1 assigned for a number between 0.25 and 0.75 in the first dimension. The split between class labels 0 and 1 is 52% / 48% respectively. Fig. 2.20 (a) displays the dataset and it can be seen that a non-linear plane is required to separate the classes. The predicative power of the SVM will be compared with logistic regression, a simple expansion on standard regression. When attempting to find a separating plane with logistic regression a prediction accuracy of 52% is achieved - essentially the same power as would have been achieved had we guessed all class labels were 0, as can be seen in Fig 2.20 (b). Now, using a SVM with a simple Gaussian kernel with a gamma parameter set equal to one a predicative accuracy of 72% is achieved as demonstrated in Fig. 2.20 (c). Essentially, the SVM technique drastically outperforms logistic kernel by performing the kernel trick, moving from non-separable input space to separable feature space, as previously described. However, it is very important to realize that the choice of kernel is imperative. To view this graphically the classification experiment is repeated with each of the kernels listed in Table 2.2. The linear kernel behaves essentially in the same manner as logistic regression and therefore the results are not shown. In Fig. 2.20 (d) shows the result of the SVM with polynomial kernel of degree 5. This kernel is ill-suited to the rectangular nature of the decision boundary required and thus only performs marginally better than logistic regression. The sigmoid kernel, Fig. 2.20 (e) with gamma parameter 1 produces a very unusual decision boundary and is clearly unsuited to the structure of this problem. Finally, Fig. 2.20 (f) presents the results of applying Multiple Kernel Learning. The R language does not contain an MKL implementation so this was conducted in Matlab®. Through application of the MKL technique it was found that each of features individually passed through a Gaussian kernel ($\gamma = 1$) produced an accuracy of 95%. This example clearly highlights the importance of kernel selection and the power of the MKL technique.

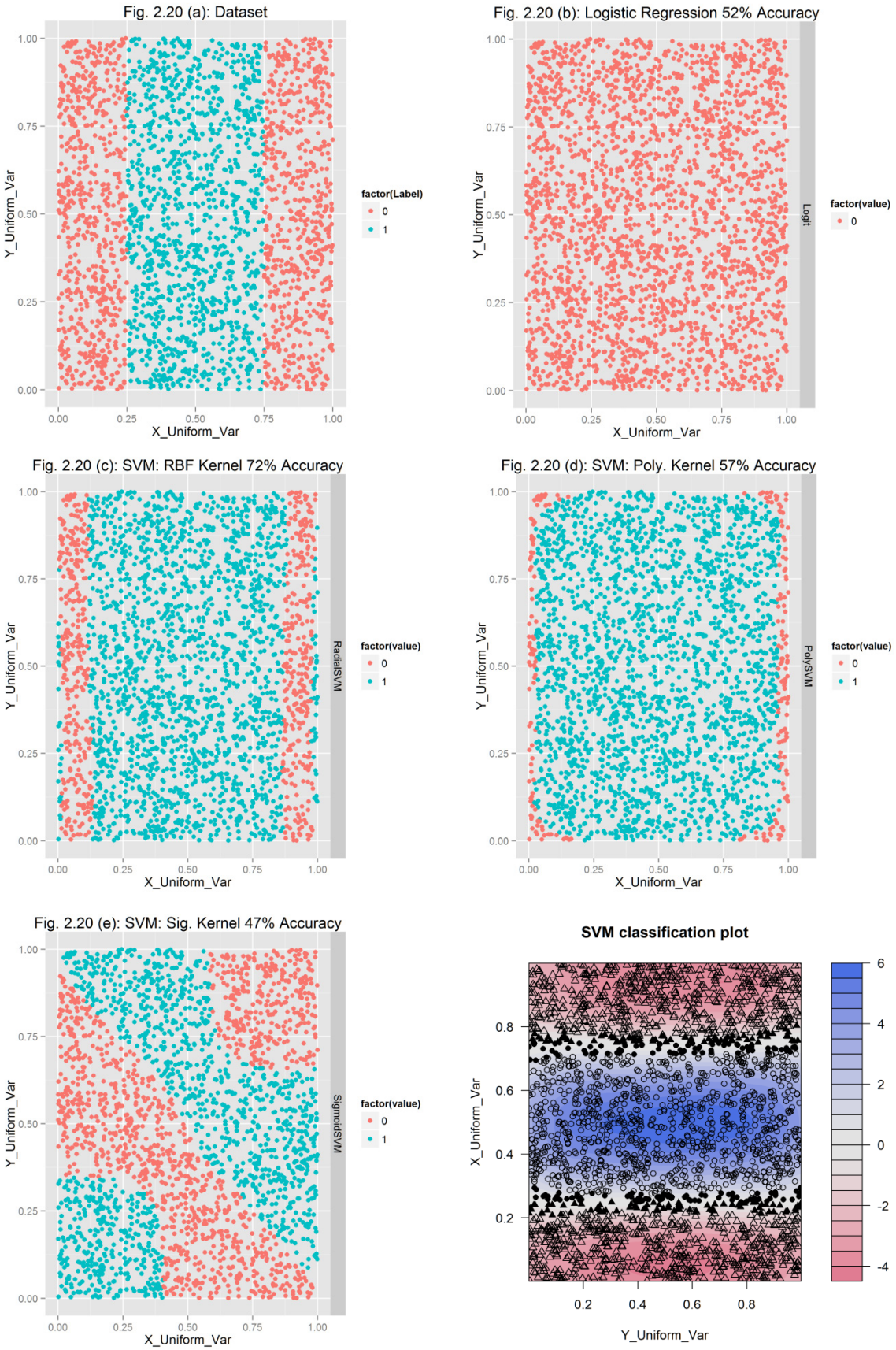


Fig. 2.20: Practical SVM Example

## *2.4 Epileptic Seizure Detection: Template Matching & DTW*

In the proceeding section we discuss the background of the third study conducted in this body of research, the development of a triaxial accelerometer based body sensor network to detect epileptic seizures. The journal paper arising from this work is presented in Chapter 5. To provide context and background the motivations and primary objectives behind this section of research are initially presented. This is followed by a review of relevant literature, a brief description of the hardware and software employed and an overview of the various algorithms investigated.

### *2.4.1 Motivation & Objective*

In this section of research we wished to investigate the applicability of accelerometer based sensors for remote monitoring of various neurodegenerative disorders. Specifically, the primary objective was to develop a practical body sensor network with accelerometer based sensors to detect epileptic seizure events. Our primary motivation was that seizure occurrence is a core criterion employed for treatment decisions in epilepsy and while the gold standard for seizure detection is EEG or video identification these techniques cannot be used to objectively quantify long-term seizure frequency. We successfully developed a system employing accelerometer based sensors combined with an internet based tablet to monitor seizure occurrence outside the laboratory setting without interfering with the subject's daily routine.

### *2.4.2 Review of Relevant Literature*

Epilepsy is a chronic neurological disorder which affects 0.5% - 1% of the world's population [127]. In Europe, in 2005 the estimated number of children and adolescents with active epilepsy was 0.9 million, 1.9 million in ages 20–64 years and 0.6 million in ages 65 years and older [127]. Approximately 20–30% of the epilepsy population has more than one seizure per month [127]. The estimated number of new cases per year amongst adolescents is 130,000, between adults 20–64 years it is 96,000 and 85,000 in the elderly 65 years and older [127]. Epileptic seizures are the manifestation of abnormal hypersynchronous discharges of populations of cortical neurons. The most common form of seizure is a tonic-clonic episode in which a phase of

tetanic muscle contraction (tonic) is followed by jerking of the affected body and limbs (clonic). The World Health Organization estimates that disability due to epilepsy accounts for approximately 1% of the global burden of disease and comparable to the worldwide burden of breast and lung cancer [128]. Approximately 67% of seizure events are controlled through anticonvulsant drug therapy with a further 7-8% treated with neurosurgical procedures. However, there remains 25% of patients whose seizures cannot be fully controlled by available therapy [128]. For these patients, medication titration through long term monitoring and analysis of EEG and video data can assist in the management of their seizure events [129]. This approach has significant advantages including high specificity and sensitivity of event detection. However, this methodology is only feasible for short periods of time and cannot be used to objectively quantify long-term seizure frequency. Furthermore, memory and consciousness may be affected due to complex seizure events and thus self-reporting of seizure incidence may be severely impaired [130]. However, seizure frequency is the primary criterion upon which neurologists make treatment decisions; the effectiveness of a given pharmacological treatment is based on evaluating its impact on the frequency of seizure events over an extended period of time [128], [131].

The use of accelerometry in detecting epileptic seizures is not a new concept. One of the most prominent authors on this topic is Nijsen et al [133-138]. From a sample of 18 subjects and 897 seizure events with triaxial accelerometers attached to the upper and lower limbs and chest this author demonstrated that accelerometry and EEG are complementary for seizure detection [133-134]. This work was continued in [135] where an investigation into nocturnal epileptic seizure events in seven mentally retarded patients was conducted. Nijsen et al [136-138] also investigated the use of short-term Fourier transforms and Wavelet transform with the short-term Fourier transform found to be more susceptible to false positives. Several other authors have also investigated the use of accelerometry for seizure detection. Schulc et al [139] attached a commercially available console controller containing a triaxial accelerometer to the forearm of 20 subjects. From a dataset of 4 seizure events a threshold based detection system achieved a sensitivity of 1 and specificity of 0.88. Becq et al [140] affixed a triaxial accelerometer and triaxial magnetometer to the affected limb and employed a Neural Network

classifier to a large dataset of seizure events with positive results. Lockmann et al [141] developed an accelerometer based device, SmartWatch, capable of detecting rhythmic, repetitive movement of an extremity. The device was attached to the dominant wrist of 40 subjects with 8 seizure events recorded. The author notes that a pattern recognition algorithm is used to detect seizure events but does not give more specific details. In similar work Kramer et al [142] embedded a triaxial accelerometer into a wrist bracelet and attached it to 13 subjects recording 22 seizure events. Again, specifics on the seizure detection algorithm are not provided but the authors note a high recognition rate. Jallon et al [143] proposed a seizure detection algorithm based on accelerometers attached to the wrist and chest using Hidden Markov Models achieved high recognition rates on a preliminary dataset of 2 subjects. One drawback with this approach was the high number of false positives. The authors continued this work in [144] describing how the system could be embedded in a home environment with alarms transmitted via an Ethernet gateway. Finally, Carlson et al [145] approached the problem from an alternative perspective. Rather than affixing accelerometers to a subject they were placed between the mattress and bed base in an effort to detect nocturnal seizure events. From a dataset of 64 subjects 8 seizure events were recorded and with a threshold detection system 5 events were identified but with a very high false positive rate (269 false positives).

Several other authors have employed alternative sensors for seizure detection. Minasyan et al [146] employed features derived from scalp EEG to train a Neural Network. From 14 subjects, 86 seizure events were recorded and an accuracy of 76% was achieved with few false positives. Shoeb et al [147] integrated seizure onset detection into an EEG recorder with an algorithm based on SVMs. Finally, Jones et al [148] proposed a body sensor network to detect the onset of seizure events based on monitoring ECG data for a change in heart rate prior to or at the onset of an event.

As can be seen, seizure detection through accelerometry is a popular research topic. However, upon completion of the literature review we felt that a practical and wearable body sensor network incorporating an advanced seizure detection algorithm which accounts for the temporal variability of seizures types across subjects had not been thoroughly investigated.

### *2.4.3 Hardware / Software*

The hardware foundation of our body sensor network was a Nokia N810 internet tablet [149]. This Linux-based device was chosen as it provides both USB client and host mode functionality, native support for C \ C++, a 400MHz processor and 2GB of internal memory. One severe drawback was that the device does not incorporate cell-phone capability however, this comes as standard in the N900. The SHIMMER (Sensing Health with Intelligence, Modularity, Mobility, and Experimental Reusability) [150] platform developed by Intel's Digital Health Group was employed as the core sensor for our third study. The sensor features dual radio functionality with a Roving Networks RN-41 Bluetooth Class 2 [151] module and a Chipcon CC2420 IEEE 802.15.4 module [152] which both communicate through a gigaAnt 2.4GHz Rufa antenna. SHIMMER also contains a Texas Instruments MSP430 microprocessor [153], a Freescale triaxial accelerometer [2], a rechargeable 250mAh lithium-ion battery and a micro-sd slot with a 2GB maximum flash storage which allows for approximately 40 days of continuous recording over 3 channels at a sampling rate of 100Hz. The device measures 1.75" x 0.8" x 0.5" and weighs approximately 10g. We further employed a Tmote base-station running TinyOS 2.0 [154] connected to the N810 to communicate over an 802.15.4 protocol to several SHIMMER sensors attached to the subject.

The software foundation of our body sensor network was Mercury, a platform for motion analysis of patients with neuromotor disorders [155]. Mercury is designed to overcome the challenges of long battery lifetime and high data fidelity and provides a high-level programming interface to develop policies for driving data collection and tuning sensor lifetime. Within Mercury the sensor node software is implemented in NesC using Pixie, an operating system for resource-aware programming of sensor networks [156]. On the N810 device we developed a program for storing and processing the received accelerometry data using the Maemo Software Development Kit [157]. Fig. 2.21 summarizes the software and hardware components of the body sensor network.

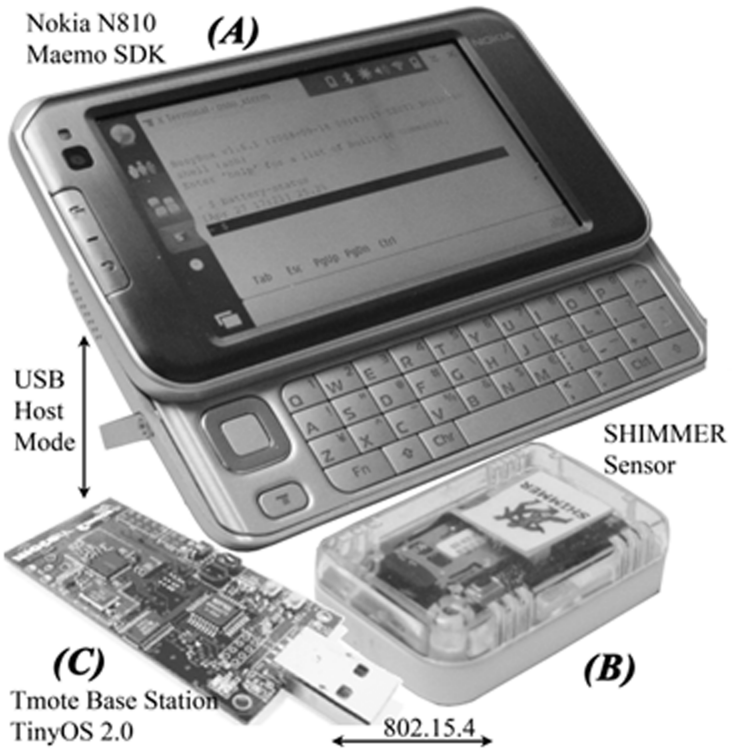


Fig. 2.21: Hardware components of the BSN. (A) Nokia N810, (B) SHIMMER sensor, (C), TMote Basestation, (D) Sensor attachment

### *2.4.4 Template Matching: The Dynamic Time Warping Algorithm*

From analysis of epileptic data we noted that seizure events exhibited a distinct spring like signature at the initiation and conclusion of each seizure event as can be seen in Fig. 2.22. Considering the unique signature of a seizure event we decided to investigate a template matching algorithm with a customized spring signal as our template. The equation of motion of a spring is defined by the second order linear differential equation

$$x'' = -\frac{k}{m}x - \frac{b}{m}x' \tag{2.24}$$

where $x$ is the position of the object, $m$ is the objects mass, $k$ is the spring stiffness and $b$ is a damping factor (friction).

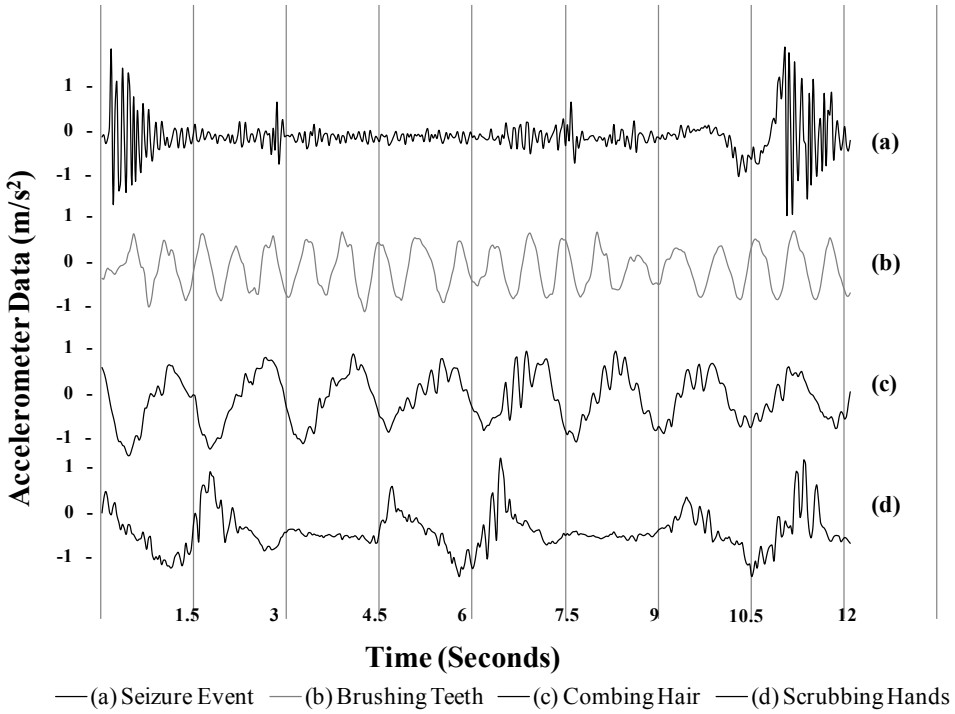


Fig. 2.22: Accelerometer data recorded from a wrist sensor

A non-trivial problem resides in the inherent temporal variability of seizure types. Accelerometry data from seizure events will be of different lengths, either compressed or stretched, dependant on the particular subject and severity of their symptoms. Therefore, we decided to incorporate the Dynamic Time Warping (DTW) [158] algorithm which takes such temporal nonlinearities into account.

The DTW algorithm recovers optimal alignments between two time sequences of different durations. This Warp-Path minimizes a cumulative distance measure consisting of *local* distances between aligned samples. The input signal is considered as a sequence of $n$ samples; $X = [x_1, x_2, x_3, \dots x_n]$ and the template is considered a sequence of $m$ samples; $Y = [y_1, y_2, y_3, \dots y_m]$. The DTW algorithm builds a matrix, $D[n \times m]$, in which each element represents the distance, $(x_i - y_j)^2$, between the *i-th* element of $X(i)$ and the *j-th* element of $Y(j)$. We then define the warping path W as a contiguous set of matrix elements that defines a mapping element between $X$ and $Y$. The k-element of $W$ is defined as $w_k = (i, j)_k$, Equation 2.25

$$W = w_1, w_2, w_3, \dots, w_k \tag{2.25}$$

The warping path is subject to several constraints; specifically, continuity restrictions which restrict the number of allowable steps in the warping path to adjacent cells in the matrix, boundary restrictions which require that the warping path must start and finish in diagonally opposite corner cells of the matrix and finally the warping path must be monotonic. There exist numerous warping paths that satisfy these requirements however, we want the path that minimizes the warping cost. Equation 2.26

$$\mathrm{DTW}(\mathrm{X},\mathrm{Y}) = \min\left\{\sqrt{\sum_{\mathrm{k}=1}^{\mathrm{k}} \mathrm{w}_{\mathrm{k}}}\right\} \tag{2.26}$$

This path can be found using dynamic programming to evaluate a recursive equation which defines the cumulative distance $\Phi(i,j)$ in the current cell and the minimum of the cumulative distances of the adjacent elements, Equation 2.27

$$\Phi(i,j) = d(x_i, y_i) + min\begin{Bmatrix} D(i,j-1) \\ D(i-1,j) \\ D(i-1,j-1) \end{Bmatrix} \tag{2.27}$$

#### *2.4.4.1 The Dynamic Time Warping Algorithm: An Example*

Similar to previous sections we will now discuss a practical example of the DTW algorithm. The implementation used in our published work was written in C++ and deployed on the N810 device however, the example which follows was generated with R code which is included in Appendix B and can easily be replicated.

For this example our template will be a simple single period cosine wave and we will investigate two input signals; the first will be a noisy single period shifted sine wave and the second a noisy two period shifted sine wave The template and input data can be seen in Fig. 2.23 (a) and Fig. 2.24 (a) respectively. We now apply the DTW algorithm to the data and the results can be seen in Fig. 2.23 (b) and Fig. 2.24 (b). These graphs are quite informative as we can explicitly see how the algorithm maps the template to the input signal and how it experiences considerable more difficulty in achieving this with the the second input dataset. Fig. 2.23 (c) and Fig. 2.24 (c) present the optimal warping path that was produced and it not surprising to note that the minimum warping cost found for input data 1 was approximately one half the minimum warping cost for input data 2. Finally, Fig. 2.23 (d-e) and Fig. 2.24 (d-e) present contour plots of the warping path and more interestingly the warped input data. For input data 1, Fig. 2.23 (e), we note the DTW algorithm was able to remove the phase shift and reduce the noise component. For input data 2, Fig. 2.24 (e), we note the DTW algorithm reshaped the data from a two phase to a noisy single phase signal with considerable difficulty.

As previously noted the epileptic seizure events observed demonstrated spring like signatures and thus a spring signal become our template and various physical activities; brushing teeth, combing hair, scrubbing hands became the input signals. Using the DTW algorithm epileptic seizure events were detected. For a deeper discussion please see Chapter 5.

**Fig. 2.23(a) DTW Example Dataset**

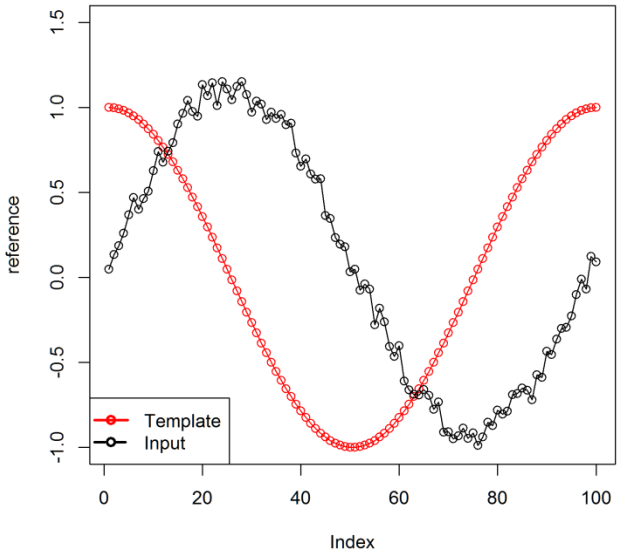


**Fig. 2.23(b) Template to Input Warping**

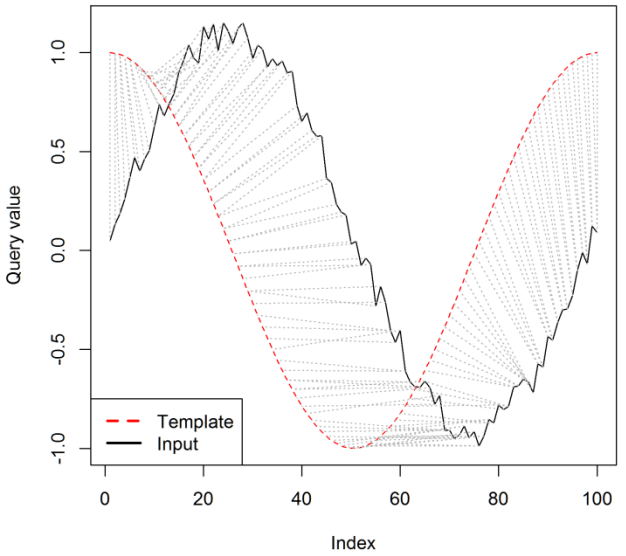


**Fig. 2.23(c) Warping Path**

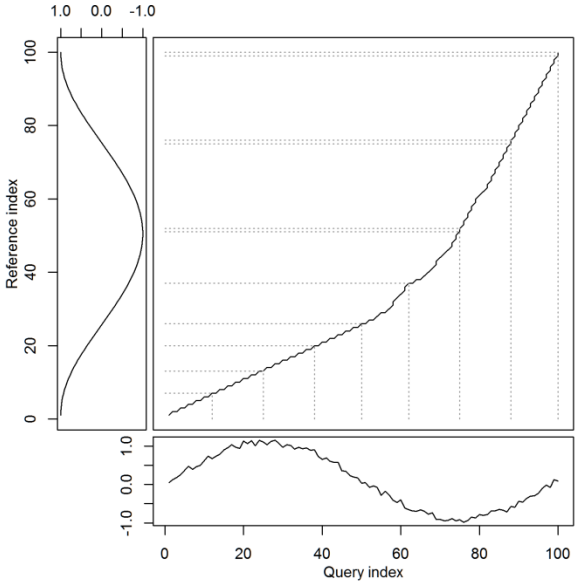


**Fig. 2.23(d) Warped Input**

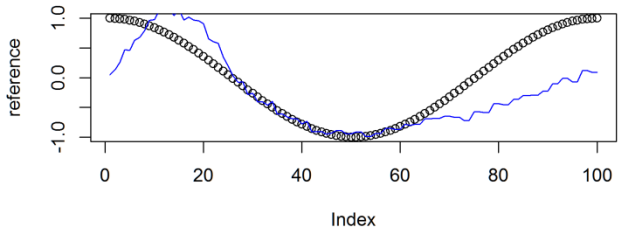


**Fig. 2.23(e) Warping Path Contour**

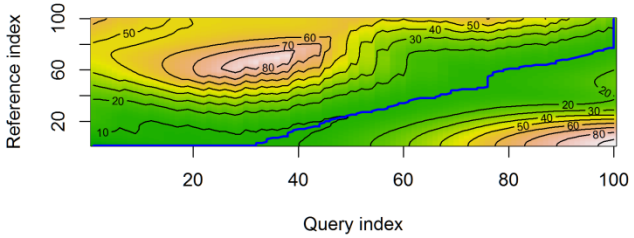

**Fig. 2.24(a) DTW Example Dataset**

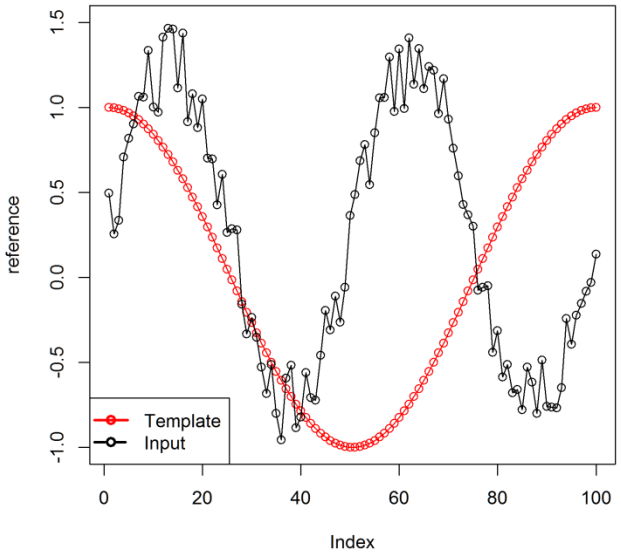


**Fig. 2.24(b) Template to Input Warping**

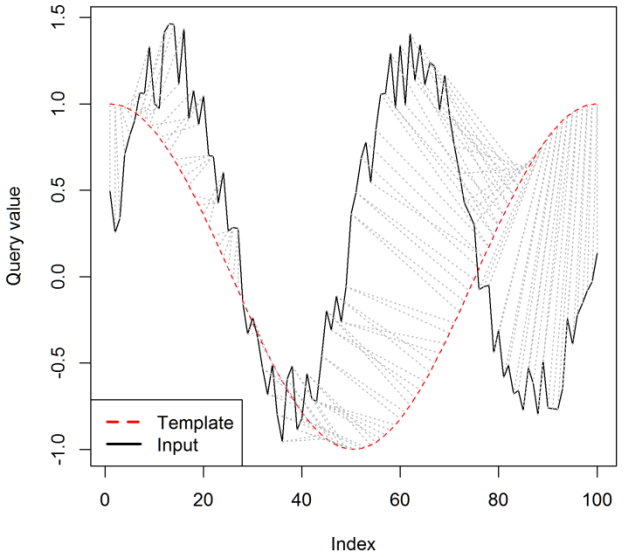


**Fig. 2.24(c) Warping Path**

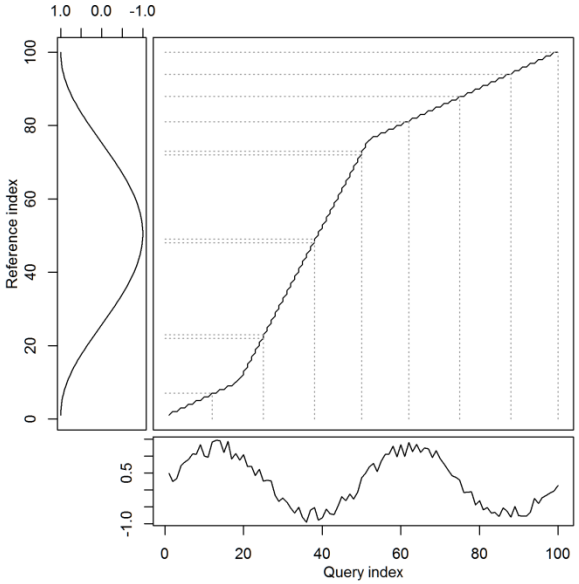


**Fig. 2.24(d) Warped Input**

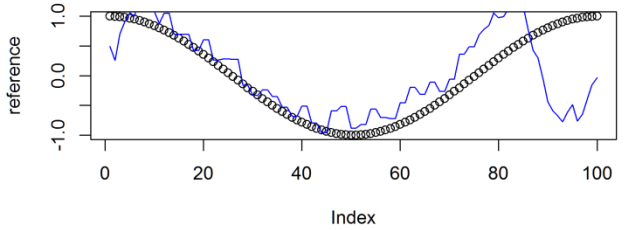


**Fig. 2.24(e) Warping Path Contour**

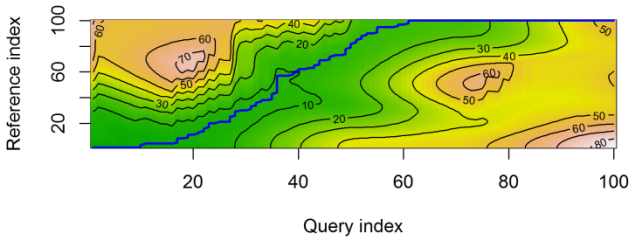

## *2.5 Huntington's Disease: Analyzing spatio-temporal gait parameters*

In the proceeding section we discuss the background of the fourth study conducted in this body of research, an analysis of gait and balance from a single body mounted triaxial accelerometer in presymptomatic and symptomatic Huntington's disease. The journal paper arising from this work is presented in Chapter 6. To provide context and background the motivations and primary objectives behind this section of research are initially presented. This is followed by a review of relevant literature, a brief description of the hardware and software employed and an overview of the various algorithms investigated. Furthermore, an analysis of the sit-to-stand transfer and Timed-Up and Go clinical test was conducted but not included in the journal paper and therefore is presented here for completeness.

### *2.5.1 Motivation & Objective*

In this section of research we considered a further application of accelerometer based sensors for analysis of various neurodegenerative disorders. Our primary objective was to investigate the capacity of a single triaxial accelerometer attached to the upper sternum in detecting gait and balance impairments in pre-manifest and manifest Huntington's disease subjects. Our primary motivations were the known limitations of commonly used ordinal based clinical tests and the considerable expense of laboratory-based walkways and other quantitative systems currently used to analyze Huntington's disease progression**.**

### *2.5.2 Review of Relevant Literature*

Huntington's disease is a neurodegenerative condition with primary symptoms of gait dysfunction, cognitive deficits and behavioural changes [159]. The disease is genetic with each child of an affected person having a 50% chance of developing the disease. To date there is no known treatment that prevents or slows progressive neuro-degeneration. The prevalence of the disease has been estimated at 4–10 affected individuals per 100,000 with higher incidence in women than in men [160]. Symptoms typically start to appear between the ages of 35 and 45 years with various recognized stages of disease progression. Specifically, a presymptomatic phase (PHD) is defined as

the period from HD gene identification through initial neuron degeneration with subtle changes in mood, cognition, balance and gait [161]. As the disease progressively worsens the symptomatic manifest stage (MHD) is defined by progressive motor deficits, cognitive disorders and behavioural changes. Specific to gait, significant decreases in stride length, gait velocity and cadence, higher variability in stride length and step-time and degradation in balance are seen [162-163]. The nature of these symptoms presents unique opportunities for analysis through accelerometry.

Several studies have investigated the various spatio-temporal gait parameters of HD subjects. Rao et al [164-166] employed a computerized walkway and found PHD subjects demonstrated decreased gait velocity, stride length and time in double support. They further identified a high correlation between these gait parameters and predicted years to onset. In a separate study they highlighted the limitations of ordinal based clinical tests by showing that the Functional Reach Test [164] and the traditional Timed up and Go (TUG) test [167] are not sensitive in detecting motor impairments in PHD subjects [168]. Devlal et al [169-171] also employed a computerized walkway to investigate the role of hypokinesia and bradykinesia in HD and found that PHD subjects demonstrated a shorter first step duration and lower-amplitude postural adjustments. Recent work by Panzera et al [172] again with a computerized walkway found MHD subjects generated significantly less rising force and significantly higher sway velocity at the centre of gravity while performing three functional postural tasks.

The analysis of spatio-temporal gait parameters through accelerometry in other subject populations has also attracted research interest. Moe-Nilssen et al [173] was one of the early researchers in this field investigating balance and walking using an accelerometer attached to the lumbar spine. The authors continued their work employing an unbiased autocorrelation procedure [174] to derive cadence, step length and measures of gait regularity and symmetry. In more recent papers the same author investigated the power of separation of step width and inter-stride trunk acceleration as measured using the unbiased autocorrelation algorithm in differentiating between fit and frail elderly achieving a sensitivity of 0.75 and specificity of 0.85 [175]. Again applying the unbiased autocorrelation procedure they found strong correlations between various gait

measurements from a triaxial accelerometer and concluded that different gait variability measures represent different constructs and should be included in gait analysis to enhance our understanding of variability in gait [176]. Tura et al [177] applied the autocorrelation procedure to measure gait regularity and symmetry in 10 amputees with strong performance. Zijlstra et al [178-180] attached accelerometers to the lower back and was able to model the trajectory of the body's centre of mass and from this derive various spatio-temporal gait parameters using an inverted pendulum model. In a more recent study the same author developed an algorithm based on accelerometer and gyroscopic data to quantify compensatory trunk movements during unconstrained walking and distinguished healthy subjects from subjects post hip surgery [180]. Brandes et al [181] applied the inverted pendulum model to accelerometry data from 20 young children and achieved a high degree of accuracy. Bautmans et al [182] conducted a large scale investigation with over 120 subjects into the potential of a triaxial accelerometer attached at the lumbar spine to differentiate between the healthy, elderly and elderly with increased fall risk. The inverted pendulum and autocorrelation techniques were employed in combination with several questionnaires. Acceleration patterns of the head and pelvis while walking on level and irregular surfaces were investigated with very strong results reported across all parameters. We employed both the unbiased autocorrelation algorithm and the inverted pendulum in this work and both are discussed in more detail in section 2.5.4.

Several other researchers have made significant contributions to this field. Kavanagh et al [10], [183-184] attached biaxial accelerometers to the head and lumbar spine and found that trunk accelerations in the anteroposterior (AP) axis associated with toe push-off were significantly lower for elderly subjects while negative head and trunk accelerations in the AP axis following heel contact were significantly higher for elderly subjects and the time delay between trunk and head accelerations experienced in the AP axis was significantly lower for elderly. Jasiewicz et al [185] demonstrated in a dataset of 26 healthy subjects that gait event detection through ankle mounted accelerometers was as accurate as footswitch detection. In similar work, Mansfield et al [186] investigated the use of accelerometers for heel strike detection with initial evidence indicating an 150ms delay between heel contact and the negative–positive change in

acceleration. Mizuike et al [187] affixed a triaxial accelerometer to the waist of 63 hemiplegic subjects and 21 healthy subjects and found that raw root mean square acceleration values were significantly higher in the healthy subjects. Sabatini et al [188] developed an ambulatory monitoring system consisting of accelerometers and gyroscopes to detect spatio-temporal gait parameters using a phase segmentation procedure. Menz et al [189] presented the concept of the harmonic ratio derived from acceleration profiles of the head and trunk while subjects walked on level and unlevel ground. The ratio is based on the premise that the unit of measurement from a continuous walking trial is a stride (two steps). A stable, rhythmic gait pattern should therefore repeat in multiples of two within any given stride. Accelerations patterns that do not repeat in multiples of two are problematic. This is similar in concept to the unbiased autocorrelation algorithm. Wark et al [190] developed an algorithm to establish a relationship with a biomechanical model for human gait. A linear predictive model was employed to identify key harmonic frequencies from a waist mounted accelerometer. Hartmann et al [191] determined intra-and inter-rater reliability of spatio-temporal gait parameters on different walking surfaces and under dual task conditions in an adult population using a trunk triaxial accelerometer. In an interesting adaption of machine learning algorithms discussed previously Sama et al [192] applied SVM regression in the analysis of spatio-temporal gait parameters with strong results in a Parkinsonian subject group.

Several researchers have also investigated the use of accelerometers to monitor balance. Moe-Nilssen el al [193] investigated balance in the young and elderly and found positive results once the constant gravity component and signal drift due to very low frequency body swap were removed. O'Sullivan et al [194] used an accelerometer attached to the lumbar spine to investigate whether accelerometry correlates with ordinal based clinical tests. The authors found a stepwise increase in root mean square accelerometer values with increasing task complexity in a group of healthy elderly and elderly with high fall risk. Helbostad et al [195] investigated the short-term repeatability of the measurement of body sway through accelerometers attached to the lumbar spine during quiet standing with very strong results.

The Timed-Up and Go (TUG) and Chair sit-to-stand (CSS) tests are well known clinical tests of mobility and fall risk [167]. The TUG test requires a subject to stand from a seated position, walk three meters, turn, walk back and return to a seated position. The CSS test requires a subject to transition from a seated to a standing position and back again as many times as possible in a 30 second window. Several researchers have sought to augment these tasks with accelerometers. Weiss [196] investigated whether the TUG could be analyzed with an accelerometer in a dataset of 17 Parkinsonian and 15 healthy subjects. A sensor was attached to the lumbar spine whilst subjects performed the TUG test and several parameters including sit-to-stand and stand-to-sit durations, range, slope, median and standard deviation were calculated. It was found that several of the parameters were significantly different between groups. Zampieri [197] attached 5 triaxial accelerometers to subjects as they completed the TUG test and found that peak arm swing velocity on the more affected side, average turning velocity, cadence and peak trunk rotation velocity were significantly different in Parkinsonian subjects when compared to healthy controls. Finally, Higashi et al [198] designed a threshold based algorithm using the pitch and yaw angular velocities of sensors attached to the waist and thigh. They found that total TUG time for a group of 10 hemiplegic subjects requiring supervision while walking was longer than a group of 10 hemiplegic independent walkers. They also found the RMS values of the independent group higher.

Although a considerable body of work has been devoted to the analysis of spatio-temporal gait parameters through accelerometers no work to date has considered the analysis of gait and balance through a single thorax mounted accelerometer in a Huntington's disease population and thus this study was conducted.

### *2.5.3 Hardware / Software*

A custom sensor was designed for this study, Fig. 2.25 (a). The AD_BRC sensor incorporates a $\pm 2.5g - 10g$ Freescale accelerometer [2], a Texas Instruments microprocessor [153], a 2000mAh lithium-ion battery and logs 250 readings to a micro-sd card every second. Battery voltage and a timestamp is stored every 12 seconds. We designed and fabricated an enclosure and label for the sensor, Fig. 2.25 (b)-(c) An interesting side effect of the development was an investigation into the various power drains on the sensor board. Not surprisingly, read and write cycles to the micro-sd card drew the most power however, surprisingly the brand of the micro–sd care chosen made a significant difference with the Verbatim card outperforming its competitors.

Similar to other studies which analyzed spatio-temporal gait parameters using accelerometers we employed the GAITRite® system [199] as our gold standard. The system consists of an instrumented walkway with sensors embedded within its surface. Sensors in the walkway record pressure applied at each footfall as a function of time. Data from the walkway is feed into some proprietary software where spatial and temporal gait parameters can be computed. The walkway used in this research was 481 cm long and 61 cm wide containing an active area of 16,149 sensors arranged in a grid pattern with a spatial resolution of 1.27cm and a sampling frequency of 60Hz. Menz et al [200] investigated the reliability of the GAITRite® system in a young and old population in quantifying spatio-temporal gait parameters and reported excellent ICC values (ICC=0.88-0.92). These results were mirrored in an independent study by Webster et al [201] (ICC=0.91-0.99). Finally, validity and reliability of the GAITRite® system has been established in a HD population by Rao et al [166] (ICC=0.86-0.95).

To monitor balance in this study subjects were asked to complete the clinically accepted Romberg test [202]. The test measures the length of time (max 30 secs) the subject can stand with ankle malleoli touching, arms crossed with palms touching the opposite shoulder. Subjects completed this test twice with the sensor attached to their upper sternum.

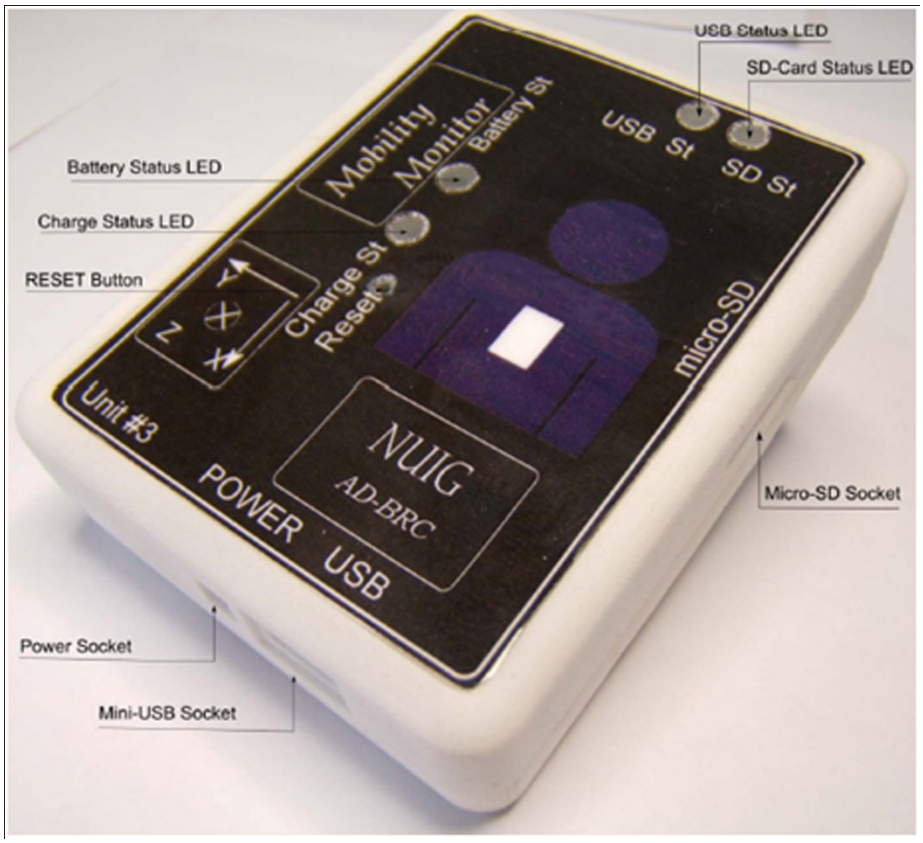


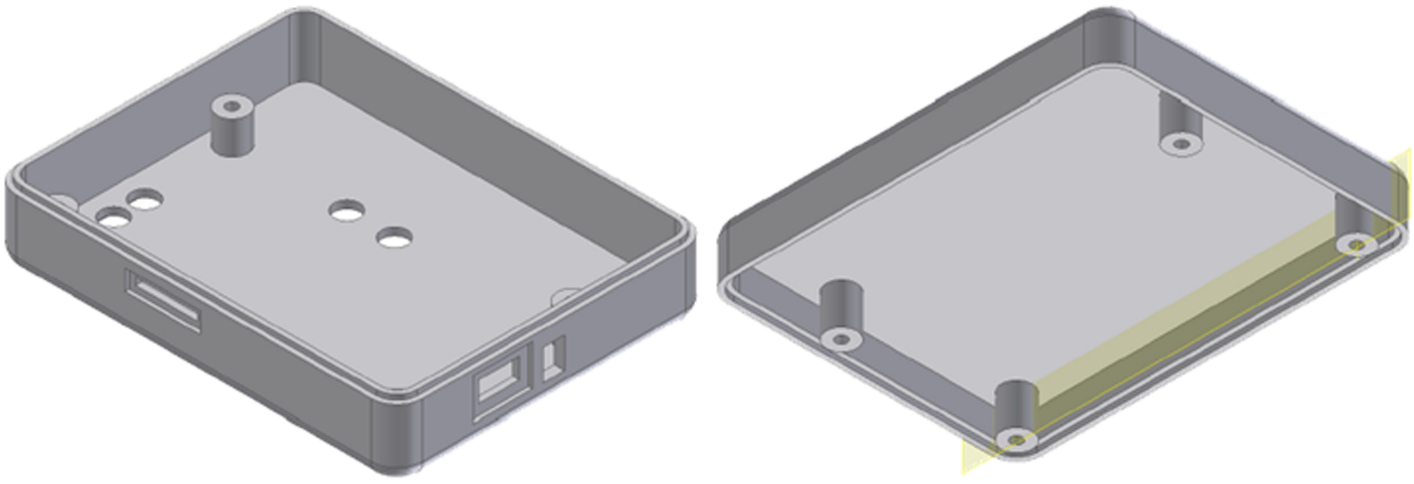

Fig. 2.25 (a) AD_BRC sensor (b)-(c) Enclosure base & lid

### *2.5.4 Analysis of the Gait Cycle through Accelerometry*

Inman et al [203] defines a gait cycle as the sequence occurring between consecutive heel-strikes of the same foot. The cycle can be divided into the stance and the swing phases which in turn can be subdivided into single and double support phases. With reference to Fig. 2.26, the stance phase constitutes approximately 60% of the gait cycle. Both feet are in contact with the ground during double support which represents 10% of the entire gait cycle at average walking speed. Double support percentage is directly proportional to walking velocity. Single-leg stance comprises approximately 40% of the normal gait cycle. The swing phase is subdivided into three phases: initial swing, mid-swing, and terminal swing. The initial swing phase commences as the foot is lifted from the floor and the swing leg is rapidly accelerated forward by hip and knee flexion along with ankle dorsiflexion. As the accelerating limb comes into alignment with the stance limb the body enters the mid-swing phase. As the limb begins to decelerate in preparation for contact with the floor the final terminal swing stage is reached. The body's center of mass (COM) is located midway between both hip joints, just anterior to the second sacral vertebra. The COM deviates in vertical and lateral sinusoidal displacements generating a *figure 8* in the frontal plane. In the vertical axis the COM goes through rhythmic upward and downward motion as it moves forward with the lowest and highest points reached during double support and mid-stance, respectively. In the lateral axis the pelvis shifts to the weight-bearing side dependent on which leg is in single support.

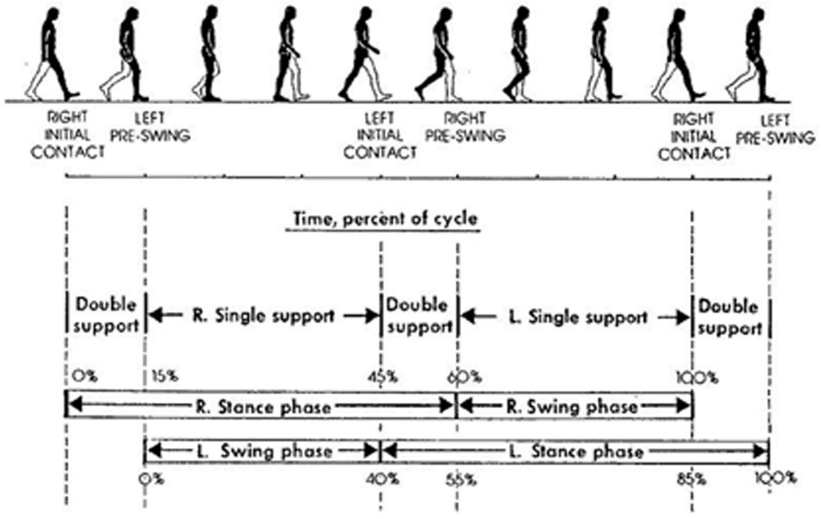


Fig. 2.26 Stages of the gait cycle [203]

#### *2.5.4.1 The Inverted Pendulum Model*

Zijlstra et al [178-180] introduced the inverted pendulum model. Longitudinal (LD) and anteroposterior (AP) axes accelerations follow a repeatable bi-phasic pattern during the gait cycle whereas mediolateral (ML) axis acceleration is characterized by a mono-phasic pattern. After mid-stance, during single support, an increase in AP acceleration can be expected as the body is falling forward and downward. Through the transition from single to double support, the forward fall of the body changes into an upward movement in which the forward movement decelerates. Therefore, foot contact should coincide with the peak of forward acceleration of the trunk [179].

Fig. 2.27 presents acceleration data from the LD, ML and AP axes for four gait cycles and Fig. 2.28 presents a breakdown of a complete gait cycle. Acceleration is shown as a solid line and displacement as a dashed line. Displacement is calculated from double integration of acceleration while taking into account drift and misalignment. (see the Appendix C for the specific calculation of displacement)

- Heel Strike (0 & 50% of the gait cycle): The AP axis reaches peak acceleration at heel strike followed by a period of deceleration.
- Double Support: Defined as the time between right leg heel strike & left leg toe off when both limbs are in contact with the ground simultaneously.
- Toe-Off: A slight indentation after heel strike can be seen in the LD axis which corresponds to toe-off. Displacement is sinusoidal between heel strikes.
- Left to Right Foot Placements: In the ML axis left-right accelerations of the trunk correspond to subsequent left and right foot placements. During the left support phase the COM accelerates to the right and vica-versa.

Step length can be estimated based on the change in pelvic displacement through double integration of the LD acceleration and then calculation of the difference between the maximum and minimum displacement during a stride cycle. Please see Appendix C for the integration algorithm employed. Subsequent step length can then be predicted using $2\sqrt{2lh - h^2}$ where l is the subject leg length and h the calculated pelvic amplitude [179]. Walking distance can be found through mean step length over a given duration multiplied by step number [179].

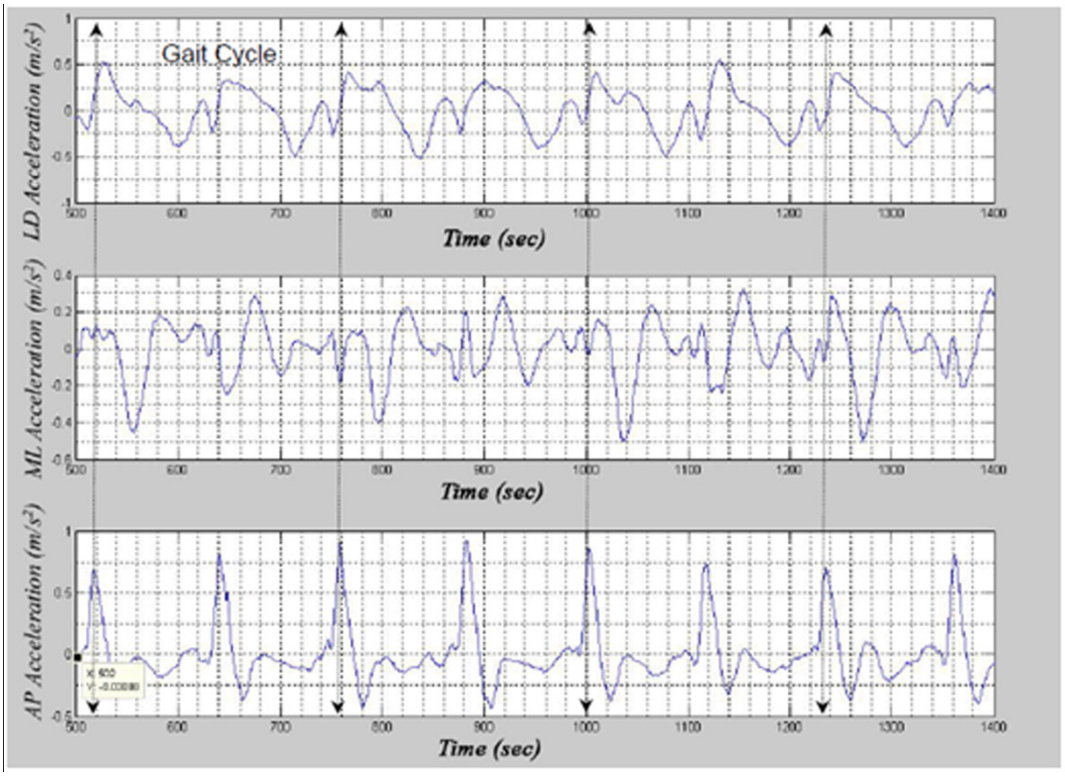


Fig. 2.27 Acceleration data from the LD, ML and AP axes for four gait cycles

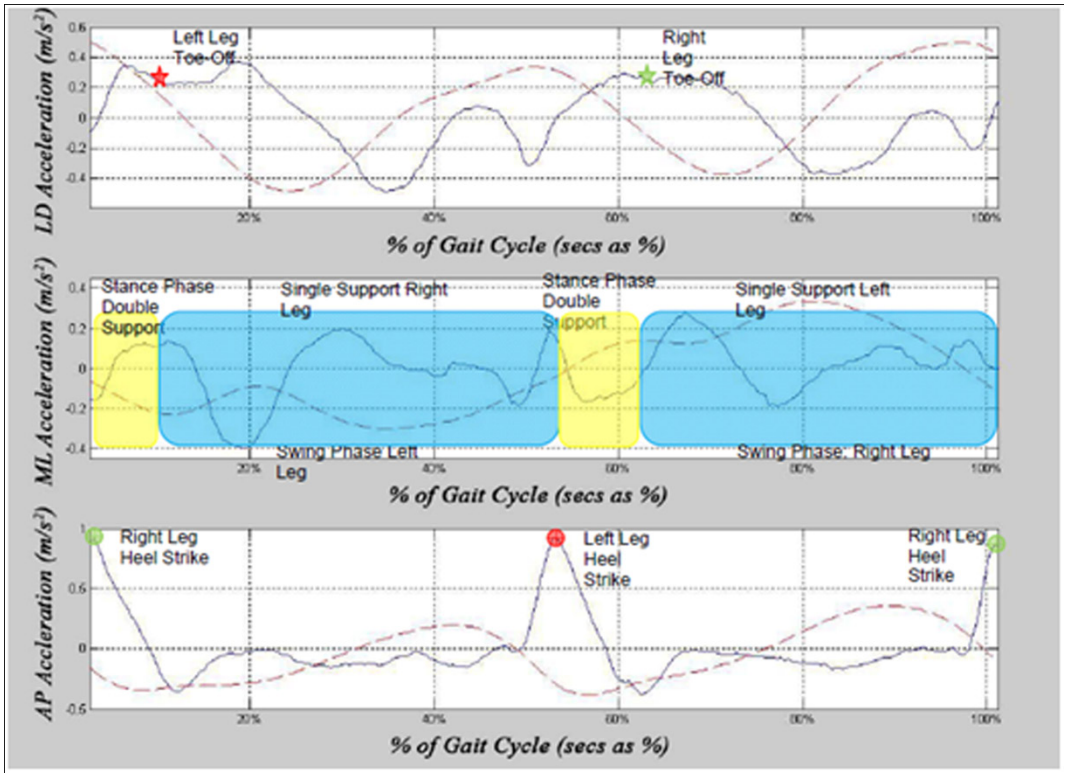


Fig. 2.28 Accelerometer decomposition of the gait cycle. Solid line: acceleration. Dashed line: displacement

### *2.5.4.2 The Unbiased Autocorrelation Procedure*

As noted in section 2.5.2 Moe-Nilsson et al [174] demonstrated that the unbiased autocorrelation procedure applied to trunk accelerations provides information concerning cadence, step length and symmetry of walking. Fig. 2.29 presents a plot of an autocorrelation sequence of several seconds of gait. From the AP or LD autocorrelation signal the first dominant period represents a phase shift equivalent to the number of samples per step. The first dominant period is identified as the first maximum value after the zeroth shift of the unbiased, normalized autocorrelation function. The autocorrelation method provides the opportunity to calculate a measure of gait regularity and symmetry. The term $d_1$ is defined as the phase lag equivalent to one step, $d_2$ is defined as the phase lag equivalent to one stride, $Ad_1$ is the autocorrelation coefficient for neighbouring steps and $Ad_2$ is the autocorrelation coefficient for neighbouring strides. The autocorrelation coefficient at the first dominant period is an expression of the regularity of the acceleration signal between neighbouring steps. Similarly, the second dominant period is an expression of the regularity of the acceleration signal between neighbouring strides. The closeness of $Ad_1$ and $Ad_2$ to one indicates step and stride regularity whereas the closeness of the ratio $\frac{Ad_1}{Ad_2}$ to one reflects symmetry.

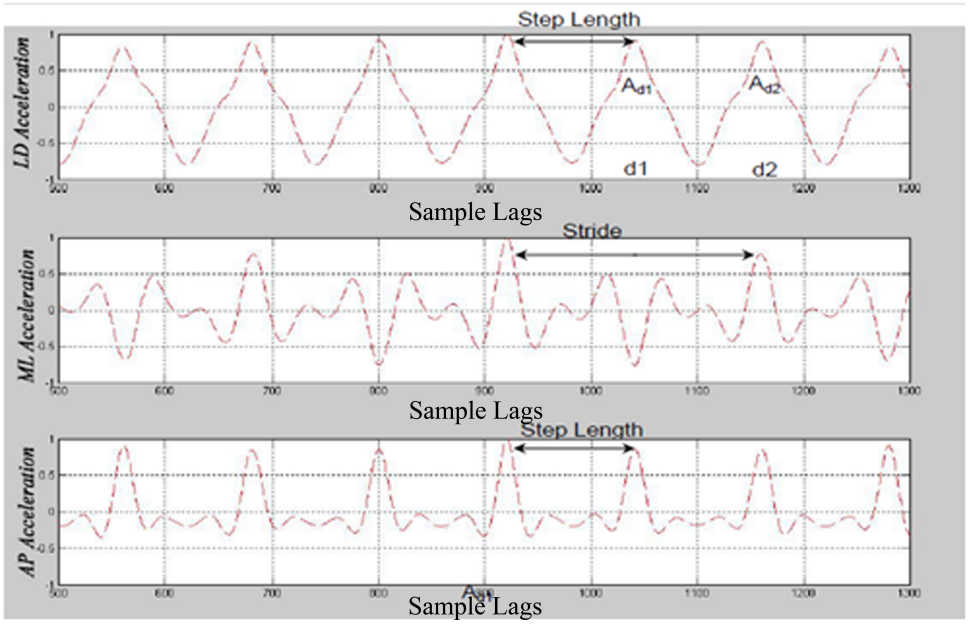


Fig. 2.29 Autocorrelation curves of the ML, LD and AP accelerations during walking.

#### *2.5.4.3 The Sit-to-Stand transition & the Timed Up and Go Test*

In this section of the thesis we also investigated the chair sit-to-stand transfer (CSS) and the Timed-Up and Go Test (TUG). This analysis has been presented in a conference format (Appendix A). Kerr et al [204] demonstrated that the sit-to-stand transition follows a structured sequence of events, Fig. 2.30. The CSS test is a physical performance evaluation used to assess lower-extremity function. Lower-extremity function has been shown to predict subsequent development of disability because it reflects the effects of chronic disease, coexisting conditions, and overall physiologic decline [204]. The test begins with the participant seated in the middle of the chair, arms crossed at the wrists and held against the chest, feet approximately shoulder-width apart and placed on the floor at an angle slightly back from the knees, with one foot slightly in front of the other to help maintain balance when standing. At the signal *go* the participant rises to a full stance and then returns back to the initial seated position. The participant is encouraged to complete as many full stands as possible within a 30 second time window. The TUG test requires a subject to stand from a seated position, walk three meters, turn, walk back and return to a seated position.

From the accelerometer data the component of the signal affected by gravity can be extracted with a high pass 3$^{rd}$ order elliptical filter as discussed in section 2.1.2. From this component the number of sit-stand transitions performed can be counted using a peak detection algorithm which finds the position, height, and approximate width of each peak by a least-squares curve-fitting technique with high accuracy. Furthermore, several subsections of the CSS and TUG movement were defined and quantified. These definitions can be seen in Table 2.3 and observed through cross reference with Fig. 2.31. Future research will investigate whether these parameters can be employed to find statistically significant differences between presymptomatic and symptomatic Huntington's disease subjects.

**Table 2.3. Quantitative parameters of the CSS / TUG tests**

| | | |
|---|---|---|
| 1. Test Duration | 4. Stit-to-Stand Range | 7. Stand-to-Sit Slope (Jerk) |
| 2. Sit-to-Stand Duration | 5. Stand-to-Sit Range | |
| 3. Stand-to-Sit Duration | 6. Sit-to-Stand Slope (Jerk) | |

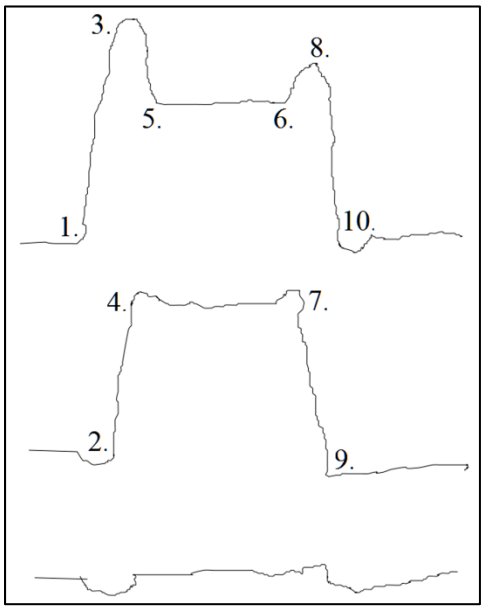


Fig.2.30 Analogue representation sit-to-stand transfer [203].

1. Initiation of forward lean
2. Initiation of vertical displacement
3. Final Forward Lean
4. Final vertical displacement
5. Final backward lean (recovery)
6. Initiation of forward lean
7. Initiation of vertical displacement

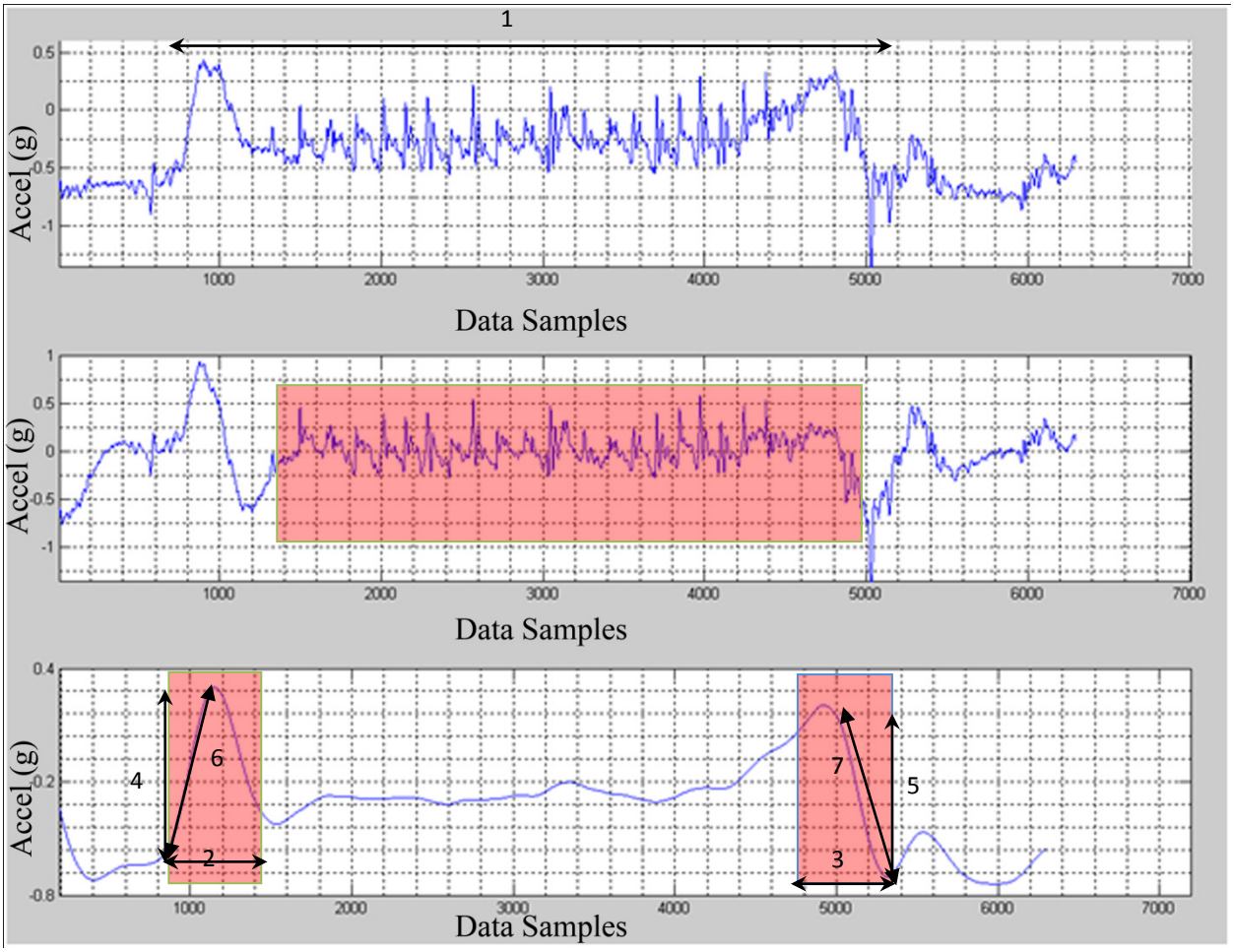


Fig. 2.31 (a) Raw data (b) Acceleration due to body movement (c) Acceleration due to gravity

## *2.6 Chapter Conclusion*

We have now concluded our background discussion of the four studies conducted in this body of research. The proceeding chapters present the journal papers arising from these studies.

## *2.7 References*

[1] Mathie, M. J., Coster, A. C., Lovell, N. H., & Celler, B. G. (2004). 'Accelerometry: providing an integrated, practical method for long-term, ambulatory monitoring of human movement', *Physiological Measurement*, vol. 25(2), pp. R1-20.

[2] Freescale MMA7260QT (2008), [Online]. Available: www.freescale.com (Accessed: July 2012)

[3] Cappozzo, A. (1982). 'Low frequency self-generated vibration during ambulation in normal men', *Journal of Biomechanics,* vol. 15(8), 599-609.

[4] Bhattacharya, A., McCutcheon, E. P., Shvartz, E., & Greenleaf, J. E. (1980). 'Body acceleration distribution and O2 uptake in humans during running and jumping', *Journal of Applied Physiology*, vol. 49(5), pp. 881-887.

[5] Aminian, K., Robert, P., Jequier, E., & Schutz, Y. (1995). 'Estimation of speed and incline of walking using neural network', *IEEE Transactions on Instrumentation and Measurement*, vol. 44(3), pp. 743-746.

[6] Aminian, K., & Najafi, B. (2004). 'Capturing human motion using body-fixed sensors: outdoor measurement and clinical applications', *Computer Animation and Virtual Worlds*, vol. 15(2), pp. 79-94.

[7] Bouten, C. V., Koekkoek, K. T., Verduin, M., Kodde, R., & Janssen, J. (1997). 'A triaxial accelerometer and portable data processing unit for the assessment of daily physical activity', *IEEE Transactions on Biomedical Engineering*, vol. 44(3), 136-147.

[8] Bourke, A. K., O'Donovan, K. J., & ÓLaighin, G. (2008). 'The identification of vertical velocity profiles using an inertial sensor to investigate pre-impact detection of falls', *Medical Engineering & Physics*, vol. 30(7), pp. 937.

[9] Moe-Nilssen, R., & Helbostad, J. L. (2004). 'Estimation of gait cycle characteristics by trunk accelerometry', *Journal of Biomechanics*, vol. 37(1), pp. 121-125.

[10] Kavanagh, J. J., Barrett, R. S., & Morrison, S. (2004). 'Upper body accelerations during walking in healthy young and elderly men', *Gait & Posture*, vol. 20(3), pp. 291-298.

[11] Witten, I. H. & Frank, E. (2005). '*Data Mining: Practical machine learning tools and techniques*', Morgan Kaufmann.

[12] Hastie, T., & Tibshirani, R. (2001). '*The Elements of Statistical Learning*', Springer Series in Statistics.

[13] Mannini, A., & Sabatini, A. M. (2010). 'Machine learning methods for classifying human physical activity from on-body accelerometers', *Sensors*, vol. 10(2), pp. 1154-1175.

[14] Bao, L., & Intille, S. (2004). 'Activity recognition from user-annotated acceleration data', *Pervasive Computing*, vol. 3001, pp. 1-17.

[15] Quinlan, J. R. (1993). '*C4. 5: programs for machine learning*', vol. 1, Morgan Kaufmann.

[16] Kwapisz, J. R., Weiss, G. M., & Moore, S. A. (2011). 'Activity recognition using cell phone accelerometers', *4th International Workshop on Knowledge Discovery from Sensor Data*, pp. 10-18.

[17] Bishop, C. M. (1995). 'Neural networks for pattern recognition', Oxford Press

[18] Paraschiv-Ionescu, A., Buchser, E. E., Najafi, B., & Aminian, K. (2004). 'Ambulatory system for the quantitative and qualitative analysis of gait and posture in chronic pain patients treated with spinal cord stimulation', *Gait & Posture*, vol. 20(2), pp. 113-125.

[19] Maekawa, T., Yanagisawa, Y., Kishino, Y., Ishiguro, K., Sakurai, Y., & Okadome, T. (2010). 'Object-based activity recognition with heterogeneous sensors on wrist', *Pervasive Computing*, vol. 6030, pp. 246-264.

[20] Parkka, J., Ermes, M., Korpipaa, P., Mantyjarvi, J., Peltola, J., & Korhonen, I. (2006). 'Activity classification using realistic data from wearable sensors', *IEEE Transactions of Information Technology in Biomedicine*, vol. 10(1), pp. 119-128.

[21] Pirttikangas, S., Fujinami, K., & Nakajima, T. (2006). 'Feature selection and activity recognition from wearable sensors', *Ubiquitous Computing*, vol. 4239, pp. 516-527.

[22] Moore, A., & Pelleg, D. (2000). 'X-means: Extending k-means with efficient estimation of clusters', *17th International Conference on Machine Learning*, vol. 1, pp. 727-734.

[23] Fahrenberg, J., Foerster, F., (1997). 'Assessment of posture and motion by multichannel piezoresistive accelerometer recordings', *Psychophysiology*, vol. 34(5), pp. 607-612.

[24] Forester, F., Smeja, M., & Fahrenberg, J. (1999). 'Detection of posture and motion by accelerometry: a validation study in ambulatory monitoring', *Computers in Human Behavior*, vol. 15(5), pp. 571-583.

[25] Mathie, M. J., Coster, A. C., Lovell, N. H., & Celler, B. G. (2003). 'Detection of daily physical activities using a triaxial accelerometer', *Medical and Biological Engineering and Computing*, vol. 41(3), pp. 296-301.

[26] Lee, S. H., Park, H. D., Hong, S. Y., & Kim, Y. H. (2003). 'A study on the activity classification using a triaxial accelerometer', *25th Annual International Conference of the IEEE Engineering in Medicine and Biology Society*, vol. 3, pp. 2941-2943.

[27] Sekine, M., Tamura, T., Akay, M., Fujimoto, T., Togawa, T., & Fukui, Y. (2002). 'Discrimination of walking patterns using wavelet-based fractal analysis', *IEEE Transactions on Neural Systems and Rehabilitation Engineering*, vol. 10(3), pp. 188-196.

[28] Sekine, M., Tamura, T., Togawa, T., & Fukui, Y. (2000). 'Classification of waist-acceleration signals in a continuous walking record', *Medical Engineering & Physics*, vol. 22(4), pp. 285-291.

[29] Najafi, B., Aminian, K., Loew, F., Blanc, Y., & Robert, P. (2000). 'An ambulatory system for physical activity monitoring in elderly', *1st Annual International Conference in Microtechnologies in Medicine and Biology*, pp. 562-566.

[30] Najafi, B., Aminian, K., Paraschiv-Ionescu, A., Loew, F., Bula, C. J., & Robert, P. (2003). 'Ambulatory system for human motion analysis using a kinematic sensor: monitoring of daily physical activity in the elderly', *Biomedical Engineering*, vol. 50(6), pp. 711-723.

[31] Herren, R., Sparti, A., Aminian, K., Schutz, Y., (1999). 'The prediction of speed and incline in outdoor running in humans using accelerometry', *Medicine and Science in Sports and Exercise*, vol. 31(7), pp. 1053-1059.

[32] Lakany, H. M. (2000). 'A generic kinematic pattern for human walking', *Neurocomputing*, vol. 35(1), pp. 27-54.

[33] Wang, N., Ambikairajah, E., Celler, B. G., & Lovell, N. H. (2008). 'Accelerometry based classification of gait patterns using empirical mode decomposition', *IEEE International Conference in Acoustics, Speech and Signal Processing*, pp. 617-620.

[34] Ibrahim, R. K., Ambikairajah, E., Celler, B., Lovell, N. H., & Kilmartin, L. (2008). 'Gait patterns classification using spectral features', *Irish Signals and Systems Conference*, pp. 98-102.

[35] Ravi, N., Dandekar, N., Mysore, P., & Littman, M. L. (2005). 'Activity recognition from accelerometer data', *Proceedings of National Conference Artificial Intelligence*, vol. 20, p. 1541

[36] Maurer, U., Smailagic, A., Siewiorek, D. P., & Deisher, M. (2006). 'Activity recognition and monitoring using multiple sensors on different body positions', *Wearable and Implantable Body Sensor Networks*, pp. 4-6.

[37] Olguin, D. O., & Pentland, A. S. (2006). 'Human activity recognition: Accuracy across common locations for wearable sensors', *MIT Media Lab.*

[38] Khan, A. M., Lee, Y. K., Lee, S. Y., & Kim, T. S. (2010). 'A triaxial accelerometer-based physical-activity recognition via augmented-signal features and a hierarchical recognizer', *IEEE Transactions in Information Technology in Biomedicine*, vol. 14(5), pp. 1166-1172.

[39] Mantyjarvi, J., Himberg, J., & Seppanen, T. (2001). 'Recognizing human motion with multiple acceleration sensors', *IEEE International Conference on Systems, Man, and Cybernetics*, vol. 2, pp. 747-752.

[40] Altun, K., Barshan, B., & Tunçel, O. (2010). 'Comparative study on classifying human activities with miniature inertial and magnetic sensors', *Pattern Recognition*, vol. 43(10), pp. 3605-3620.

[41] Hynes, M., Wang, H., McCarrick, E., & Kilmartin, L. (2011). 'Accurate monitoring of human physical activity levels for medical diagnosis and monitoring using off-the-shelf cellular handsets', *Personal and Ubiquitous Computing*, vol. 15(7), pp. 667-678.

[42] Veltink, P. H., Bussman, H. B., Koelma, H. M., Martens, W. L., & Lummel, R. C. (1993). 'The feasibility of posture and movement detection by accelerometry', *15th International Conference of the IEEE Engineering in Medicine and Biology Society*, pp. 1230-1231

[43] Bussmann, J. B., Culhane, K. M., Horemans, H. L., Lyons, G. M., & Stam, H. J. (2004). 'Validity of the prosthetic activity monitor to assess the duration and spatio-temporal characteristics of prosthetic walking', *IEEE Transactions on Neural Systems and Rehabilitation Engineering*, vol. 12(4), pp. 379-386.

[44] Bussmann, J. B. J., Van de Laar, Y. M., Neeleman, M. P., & Stam, H. J. (1998). 'Ambulatory accelerometry to quantify motor behaviour in patients after failed back surgery: a validation study', *Pain*, vol. 74(2), pp. 153-161.

[45] NiScanaill, C. N., Ahearne, B., & Lyons, G. M. (2006). 'Long-term telemonitoring of mobility trends of elderly people using SMS messaging', *IEEE Transactions of Information Technology in Biomedicine*, vol. 10(2), pp. 412-413.

[46] Lyons, G. M., Culhane, K. M., Hilton, D., Grace, P. A., & Lyons, D. (2005). 'A description of an accelerometer-based mobility monitoring technique', *Medical Engineering & Physics*, vol. 27(6), pp. 497-504.

[47] Karantonis, D. M., Narayanan, M. R., Mathie, M., Lovell, N. H., & Celler, B. G. (2006). 'Implementation of a real-time human movement classifier using a triaxial accelerometer for ambulatory monitoring', *IEEE Transactions in Information Technology in Biomedicine*, vol. 10(1), pp. 156-167.

[48] Allen, F. R., Ambikairajah, E., Lovell, N. H., & Celler, B. G. (2006). 'Classification of a known sequence of motions and postures from accelerometry data using adapted Gaussian mixture models', *Physiological Measurement*, vol. 27(10), pp. 935.

[49] Baek, J., Lee, G., Park, W., & Yun, B. J. (2004). 'Accelerometer signal processing for user activity detection', *Knowledge-Based Intelligent Information and Engineering Systems*, vol. 3215, pp. 610-617.

[50] Barralon, P., Noury, N., & Vuillerme, N. (2006). 'Classification of daily physical activities from a single kinematic sensor', *27th Annual International Conference of the IEEE Engineering in Medicine and Biology Society*, pp. 2447-2450.

[51] Barralon, P., Vuillerme, N., & Noury, N. (2006). 'Walk detection with a kinematic sensor: Frequency and wavelet comparison', *28th Annual International Conference of the IEEE Engineering in Medicine and Biology Society*, pp. 1711-1714.

[52] Betker, A. L., Moussavi, Z. M., & Szturm, T. (2006). 'Center of mass approximation and prediction as a function of body acceleration', *IEEE Transactions on Biomedical Engineering*, vol. 53(4), pp. 686-693.

[53] Bharatula, N. B., Stäger, M., Lukowicz, P., & Tröster, G. (2005). 'Empirical study of design choices in multi-sensor context recognition systems', *IFAWC-International Forum on Applied Wearable Computing*, pp.22.

[54] Bonnet, S., & Heliot, R. (2007). 'A magnetometer-based approach for studying human movements', *IEEE Transactions on Biomedical Engineering*, vol. 54(7), pp. 1353-1355.

[55] Boyle, J., Wark, T., Karunanithi, M., (2005). 'Wireless Personal Monitoring of Patient Movement and Vital Signs, e-Health Research Centre', *IEEE Computational Intelligence in Medicine and Healthcare*, pp. 34-41.

[56] Coley, B., Najafi, B., Paraschiv-Ionescu, A., & Aminian, K. (2005). 'Stair climbing detection during daily physical activity using a miniature gyroscope', *Gait & Posture*, vol. 22(4), 287-294.

[57] Culhane, K. M., Lyons, G. M., Hilton, D., Grace, P. A., & Lyons, D. (2004). 'Long-term mobility monitoring of older adults using accelerometers in a clinical environment', *Clinical Rehabilitation*, vol. 18(3), pp. 335-343.

[58] Ermes, M., Parkka, J., Mantyjarvi, J., & Korhonen, I. (2008). 'Detection of daily activities and sports with wearable sensors in controlled and uncontrolled conditions', *IEEE Transactions in Information Technology in Biomedicine*, vol. 12(1), pp. 20-26.

[59] Forester, F., Smeja, M., & Fahrenberg, J. (1999). 'Detection of posture and motion by accelerometry: a validation study in ambulatory monitoring', *Computers in Human Behavior*, vol. 15(5), pp. 571-583.

[60] Hendelman, D., Miller, K., Baggett, C., Debold, E., & Freedson, P. (2000). 'Validity of accelerometry for the assessment of moderate intensity physical activity in the field', *Medicine and Science in Sports and Exercise,* vol. 32(9), pp. S442.

[61] Herren, R., Sparti, A., Aminian, K., Schutz, Y., (1999). 'The prediction of speed and incline in outdoor running in humans using accelerometry', *Medicine and Science in Sports and Exercise*, vol. 31(7), pp. 1053-1059.

[62] Hester, T., Sherrill, D. M, Perreault, K., & Bonato, P. (2006). 'Identification of tasks performed by stroke patients using a mobility assistive device', *28th Annual International Conference of the IEEE in Engineering in Medicine and Biology Society,* pp. 1501-1504.

[63] Huynh, T., & Schiele, B. (2005). 'Analyzing features for activity recognition', *Proceedings of the 2005 Joint Conference on Smart Objects and Ambient Intelligence*, pp. 159-163.

[64] Huynh, T., & Schiele, B. (2006). 'Towards less supervision in activity recognition from wearable sensors', *10th IEEE International Symposium in Wearable Computers*, pp. 3-10

[65] Kern, N., Schiele, B., & Schmidt, A. (2003). 'Multi-sensor activity context detection for wearable computing'. *Ambient Intelligence*, vol. 2875, pp. 220-232.

[66] Krause, A., Siewiorek, D. P., Smailagic, A., & Farringdon, J. (2003). 'Unsupervised, dynamic identification of physiological and activity context in wearable computing', *7th IEEE International Symposium on Wearable Computers*, pp. 88.

[67] Lee, S. H., Park, H. D., Hong, S. Y., & Kim, Y. H. (2003). 'A study on the activity classification using a triaxial accelerometer', *25th Annual International Conference of the IEEE Engineering in Medicine and Biology Society*, vol. 3, pp. 2941-2943.

[68] Lester, J., Choudhury, T., Kern, N., Borriello, G., & Hannaford, B. (2005). 'A hybrid discriminative/generative approach for modeling human activities', *19th International Joint Conference on Artificial Intelligence*, pp. 766-772.

[69] Lester, J., Choudhury, T., & Borriello, G. (2006). 'A practical approach to recognizing physical activities', *Pervasive Computing*, vol. 3968, pp. 1-16.

[70] Liu J, Kanno T, Akashi M, Chen W, Wei W. (2006) 'Patterns of bipedal walking on tri-axial acceleration signals and their use in identifying falling risk of older people', *6th International Conference in Computer and Information Technology*, pp. 205-211.

[71] Lo, B., Atallah, L., Aziz, O., ElHew, & Yang, G. Z. (2007). 'Real-time pervasive monitoring for postoperative care', *4th International Workshop on Wearable and Implantable Body Sensor Networks*, pp. 122-127.

[72] Lukowicz, P., Junker, H., & Troester, G. (2002). 'WearNET: A distributed multi-sensor system for context aware wearables', *Ubiquitous Computing*, vol. 2498, pp. 361-370.

[73] Noury, N., Barralon, P., Couturier, P., Guillemaud, R., Mestais, C., & Provost, H. (2004). 'ACTIDOM-A MicroSystem based on MEMS for Activity Monitoring of the Frail Elderly in their Daily Life', *26th Annual International Conference in Engineering in Medicine and Biology Society*, vol. 2, pp. 3305-3308.

[74] Park, C., Chou, P. H., & Sun, Y. (2006). 'A wearable wireless sensor platform for interactive dance performances', 4th Annual IEEE International Conference in Pervasive Computing and Communications, pp. 6-10.

[75] Randell, C., & Muller, H. (2000). 'Context awareness by analysing accelerometer data', *4th International Symposium of Wearable Computers*, pp. 175-176.

[76] Salarian, A., Russmann, H., Vingerhoets, F. J., Burkhard, P. R., & Aminian, K. (2007). 'Ambulatory monitoring of physical activities in patients with Parkinson's disease', *IEEE Transaction in Biomedical Engineering*, vol. 54(12), pp. 2296-2299.

[77] Song, K. T., & Wang, Y. Q. (2005). 'Remote activity monitoring of the elderly using a two-axis accelerometer', *Proceedings of CACS Automatic Control Conference*, pp. 18-23.

[78] Tamura, T., Fujimoto., J., & Togawa, T. (1995). 'The design of an ambulatory physical activity monitor and it application to the daily activity of the elderly', *17th Annual Conference of IEEE Engineering in Medicine Biology Society*, vol. 2, pp. 1591-1592.

[79] Tapia, E., Intille, S., Lopez, L., & Larson, K. (2006). 'The design of a portable kit of wireless sensors for natural data collection', *Pervasive Computing*, vol. 10, pp. 117-134.

[80] Veltink, P. H., Bussmann, H., de Vries, W., Martens, W., & Van Lummel, R. C. (1996). 'Detection of static and dynamic activities using uniaxial accelerometers', *IEEE Transactions in Rehabilitation Engineering*, vol. 4(4), pp. 375-385.

[81] Yoshida, Y., Yonezawa, Y., Sata, K., & Caldwell, W. M. (2000). 'A wearable posture, behavior and activity recording system', *22nd Annual International Conference of the IEEE Engineering in Medicine and Biology Society*, vol. 2, pp. 1278-92.

[82] Witilt v2.5, Sparkfun (2012), [Online]. Available: www.sparkfun.com. (Accessed: Mar. 2012)

[83] Mitsumi Electric Bluetooth Module (2012), [Online] Available: www.mitsumi.co.jp/English (Accessed: Feb. 2012)

[84] FutureLec (2012), [Online]. Available: www.futurlec.com (Accessed: July 2012)

[85] Microsoft MFC, (1995) [Online]. Available: 'Microsoft Visual C++ Programming with MFC', (Accessed: Mar. 2012).

[86] Bluetooth Driver Stack, (2010), [Online]. Available: www.msdn.microsoft.com/en-us/library/ (Accessed: Mar. 2012)

[87] Widcomm Stack, (2010) [Online] Available: www.broadcom.com/ (Accessed: Feb. 2012)

[88] MATLAB r2010b, The MathWorks Inc., Nat, MA, USA (2012) [Online] Available www.mathworks.com (Accessed: Feb. 2012)

[89] Bishop, C. M. (2006). '*Pattern recognition and machine learning*', vol. 4, no. 4, Springer.

[90] Hamel, L. (2009). '*Knowledge discovery with support vector machines*', John Wiley

[91] Quinlan, J. R. (1993). '*C4. 5: programs for machine learning*', vol. 1, Morgan Kaufmann.

[92] Friedman, N., Geiger, D., & Goldszmidt, M. (1997). 'Bayesian network classifiers', *Machine Learning*, vol. 29(2), 131-163.

[93] Fix, E., & Hodges Jr, J. L. (1952). 'Discriminatory Analysis-Nonparametric Discrimination: Small Sample Performance', *University of California, Berkeley*.

[94] Cohen WW, (1995). 'Fast effective rule induction', *12th International Conference on Machine Learning*, pp. 115-123.

[95] Frank, A., & Asuncion, A. (2010). UCI Machine Learning Repository, Irvine, CA: University of California. *School of Information and Computer Science*, pp. 213-218.

[96] R Development Core Team (2011). '*R: A language and environment for statistical computing*', R Foundation for Statistical Computing.

[97] Cooper, G. F., & Herskovits, E. (1992). 'A Bayesian method for the induction of probabilistic networks from data', *Machine Learning*, vol. 9(4), 309-347.

[98] Aha, D. W. (1992). 'Tolerating noisy, irrelevant and novel attributes in instance-based learning algorithms', *International Journal Man-Machine* Study, vol. 36(2), pp. 267-287.

[99] Moore, A., & Pelleg, D. (2000). 'X-means: Extending k-means with efficient estimation of clusters', *17th International Conference on Machine Learning*, vol. 1, pp. 727-734.

[100] Cohen WW, (1995). 'Fast effective rule induction', *12th International Conference on Machine Learning*, pp. 115-123.

[101] Furnkranz, J., & Widmer, G. (1999). 'Incremental reduced error pruning', *International Conference on Machine Learning*, pp. 70-77.

[102] Breiman, L. (1996). 'Bagging predictors', *Machine Learning*, vol. 24(2), pp. 123-140

[103] Freund, Y., & Schapire, R. E. (1996). 'Experiments with a new boosting algorithm', *Machine Learning, 30th International Workshop*, pp. 148-156

[104] Commonwealth Bureau of Meteorolog (2011), [Online]. Available: www.bom.gov.au/ (Accessed: Mar. 2011)

[105] Gyllensten, I. C., & Bonomi, A. G. (2011). 'Identifying types of physical activity with a single accelerometer: Evaluating laboratory-trained algorithms in daily life', *IEEE Transactions in Biomedical Engineering*, vol. 58(9), pp. 2656-2663.

[106] Mannini, A., & Sabatini, A. M. (2011). 'On-line classification of human activity and estimation of walk-run speed from acceleration data using support vector machines', *33rd Annual International Conference of IEEE Engineering in Medicine and Biology Society,* pp. 3302-3305.

[107] Zhang, S., Rowlands, A. V., Murray, P., & Hurst, T. (2012). 'Physical Activity Classification Using the GENEA Wrist-Worn Accelerometer', *Medicine and Science in Sports and Exercise*, vol. 44(4), pp. 742-748.

[108] Fleury, A., Vacher, M., & Noury, N. (2010). 'SVM-based multimodal classification of activities of daily living in health smart homes: sensors, algorithms, and first experimental results', *IEEE Transactions in Information Technology in Biomedicine*, vol. 14(2), pp. 274-283.

[109] Fleury, A., Noury, N., & Vacher, M. (2010). 'Introducing knowledge in the process of supervised classification of activities of Daily Living in Health Smart Homes', *12th IEEE International Conference in e-Health Networking Applications and Services*, pp. 322-329.

[110] Kilmartin, L., Ibrahim, R. K., Ambikairajah, E., & Celler, B. (2009). 'Optimising recognition rates for subject independent gait pattern classification', *Irish Signals and Systems Conference*, pp. 1-6.

[111] He, W., Guo, Y., Gao, C., & Li, X. (2012). 'Recognition of human activities with wearable sensors', *Journal on Advances in Signal Processing*, vol. 1, pp. 108-121.

[112] Fletcher, T., (2010). 'Relevance Vector Machines Explained', [Online]. Available: www.cs.ucl.ac.uk/T.Fletcher/, (Accessed: April 2012)

[113] Lau, H. Y., Tong, K. Y., & Zhu, H. (2008). 'Support vector machine for classification of walking conditions using miniature kinematic sensors', *Medical and Biological Engineering and Computing*, vol. 46(6), pp. 563-573.

[114] Wu, Y., Chen, R., & She, M. (2011). 'Automated classification of human daily activities in ambulatory environment', *Software Engineering, Artificial Intelligence, Networking and Parallel / Distributed Computing,* vol. 368, pp.157-168.

[115] Begg, R., & Kamruzzaman, J. (2005). 'A machine learning approach for automated recognition of movement patterns using basic, kinetic and kinematic gait data', *Journal of Biomechanics*, vol. 38(3), pp. 401-408.

[116] Wu, Y., & Krishnan, S. (2010). 'Statistical analysis of gait rhythm in patients with Parkinson's disease', *IEEE Transactions on Neural Systems Rehabilitation Engineering*, vol. 18(2), pp. 150-158.

[117] Fukuchi, R. K., Eskofier, B. M., Duarte, M., & Ferber, R. (2011). 'Support vector machines for detecting age-related changes in running kinematics', *Journal of Biomechanics*, vol. 44(3), pp. 540-542..

[118] Levinger, P., Lai, D. T., Begg, R. K., Webster, K. E., & Feller, J. A. (2009). 'The application of support vector machines for detecting recovery from knee replacement surgery using spatio-temporal gait parameters', *Gait & Posture*, vol. 29(1), pp. 91-96.

[119] Khandoker, A. H., Lai, D. T., & Begg, R. K., (2007). 'Wavelet-based feature extraction for support vector machines for screening balance impairments in the elderly', *IEEE Transactions on Neural Systems and Rehabilitation Engineering*, vol. 15(4), pp. 587-597.

[120] Lai, D. T., Levinger, P., Begg, R. K., Gilleard, W., & Palaniswami, M. (2007). 'Identification of patellofemoral pain syndrome using a Support Vector Machine approach', *26th Annual International Conference of the IEEE Engineering in Medicine and Biology Society*, pp. 3144-3147.

[121] HP iPAQ 6915 (2006) [Online]. Available: www.o2.co.uk/deviceinfo/device-pdfs/hpipaq6915eng.pdf (Accessed: May 2012)

[122] 32Feet.net (2010) [Online]. Available: http://32feet.net/ (Accessed: Mar. 2012)

[123] Windows Mobile 5 SDK. (2010) [Online]. Available: www.microsoft.com/ (Accessed: Mar. 2012)

[124] Widcomm Stack, (2010) [Online] Available: www.broadcom.com/bt/ (Accessed: Feb. 2012)

[125] Bach, F.R., Lanckriet, G., & Jordan, M. I. (2004). 'Multiple kernel learning, conic duality, and the SMO algorithm', *21st International Conference on Machine Learning*, pp. 6-10.

[126] Rakotomamonjy, A., Bach, F., Canu, S., & Grandvalet, Y. (2008). 'SimpleMKL', *Journal of Machine Learning Research*, vol. 9, pp. 2491-2521.

[127] Hauser, W. A., & Hesdorffer, D.C. (1990). '*Epilepsy: frequency, causes, and consequences*', Epilepsy Foundation of America.

[128] Forsgren, L., Beghi, E., Oun, A., & Sillanpää, M. (2005). 'The epidemiology of epilepsy in Europe–a systematic review', *European Journal of Neurology*, vol. 12(4), pp. 245-253.

[129] Witte, H., & L.D, Iasemidis., (2003) 'Special issue on epileptic seizure prediction', *IEEE Transactions in Biological Engineering*, vol. 50, pp. 537-539.

[130] Deckers, C. L., Genton, P., & Schmidt, D. (2003). 'Current limitations of antiepileptic drug therapy: a conference review', *Epilepsy Research*, vol. 53(1-2), pp. 11-17.

[131] Tatum IV, W. O., Winters, L., Gieron, M., Ferreira, J., & Liporace, J. (2001). 'Outpatient seizure identification: results of 502 patients using computer-assisted ambulatory EEG', *Journal of Clinical Neurophysiology*, vol. 18(1), pp. 14-19.

[132] Murracy, C.J.L., Lopez, A.D. (1994) '*Global comparative assessment in the health sector; disease burden, expenditure*', World Health Organization.

[133] Nijsen, T. M., Cluitmans, P. J., (2005) 'The potential value of 3-D accelerometry for detection of motor seizures in severe epilepsy', *Epilepsy Behaviour,* vol. 7, pp. 74-84.

[134] Nijsen, T. M., Aarts, R. M., Arends, J. B., & Cluitmans, P. J. (2009). 'Automated detection of tonic seizures using 3-D accelerometry', *4th European Conference of International Federation for Medical and Biological Engineering*, pp. 188-191.

[135] Nijsen, T. M., Cluitmans, P. J., Arends, J. B., & Griep, P. A. (2007). 'Detection of subtle nocturnal motor activity from 3-D accelerometry recordings in epilepsy patients', *Biomedical Engineering*', vol. 54(11), pp. 2073-2081.

[136] Nijsen, T. M., Aarts, R. M., Cluitmans, P. J., & Griep, P. A. (2010). 'Time-frequency analysis of accelerometry data for detection of myoclonic seizures', *IEEE Transactions in Information Technology in Biomedicine*, vol. 14(5), pp. 1197-1203.

[137] Nijsen, T. M., Janssen, A. J., & Aarts, R. M. (2007). 'Analysis of a wavelet arising from a model for arm movements during epileptic seizures', *Program for Research on Integrated Systems and Circuits Conference*, pp. 19-24.

[138] Nijsen, T. M., Cluitmans, P. J., & Aarts, R. M. (2006). 'Short time Fourier and wavelet transform for accelerometric detection of myoclonic seizures', *IEEE Belgian Day on Biomedical Engineering*, pp. 7-8.

[139] Schulc, E., Unterberger, I., Saboor, S., Ertl, M. & Them, C. (2011). 'Measurement and quantification of generalized tonic–clonic seizures in epilepsy patients by means of accelerometry-An explorative study', *Epilepsy Research*, vol. 95(1), pp. 173-183.

[140] Becq, G., Bonnet, S., Minotti, L., Antonakios, M., Guillemaud, R., & Kahane, P. (2011). 'Classification of epileptic motor manifestations using inertial and magnetic sensors', *Computers in Biology and Medicine*, vol. 41(1), pp. 46-55.

[141] Lockmann, J., Fisher, R. S., & Olson, D. M. (2011). 'Detection of seizure-like movements using a wrist accelerometer', *Epilepsy & Behavior*, vol. 20(4), pp. 638-641.

[142] Kramer, U., & Kuzniecky, R. (2011). 'A novel portable seizure detection alarm system: preliminary results', *Journal of Clinical Neurophysiology*, vol. 28(1), pp. 36.

[143] Jallon, P., Bonnet, S., & Guillemaud, R. (2009). 'Detection system of motor epileptic seizures through motion analysis with 3D accelerometers', *27th Annual International Conference of the IEEE in Engineering in Medicine and Biology Society*, pp. 2466-2469

[144] Bonnet, S., Jallon, P., Bourgerette, A., Guillemaud, R. & Ejnes, D. (2011). 'An Ethernet motion-sensor based alarm system for epilepsy monitoring', *E-Health and Medical Communications*, vol. 32(2), pp. 155-157.

[145] Carlson, C., Arnedo, V., Cahill, M., & Devinsky, O. (2009). 'Detecting nocturnal convulsions: efficacy of the MP5 monitor', *Seizure*, vol. 18(3), pp. 225-227.

[146] Minasyan, G. R., Chatten, J. B., & Harner, R. N. (2010). 'Patient-specific early seizure detection from scalp EEG', *Journal of Clinical Neurophysiology*, vol. 27(3), pp. 163.

[147] Shoeb, A., Schachter, S., Schomer., S. T., & Guttag, J. (2006). 'Detecting seizure onset in the ambulatory setting: demonstrating feasibility', *7th Annual International Conference of the IEEE Engineering in Medicine and Biology Society*, pp. 3546-3550

[148] Jones, V. M., Tonis, T., Bults, R. B., van Beijnum, B., & Hermens, H. (2008). 'Biosignal and context monitoring: Distributed multimedia applications of body area networks in healthcare', *10th IEEE Workshop in Multimedia Signal Processing*, pp. 820-825.

[149] Nokia Corporation, (2012) [Online]. Available: www.nokia.com (Accessed: Feb. 2012)

[150] SHIMMER. (2012) [Online]. Available: www.shimmer.com (Accessed: Feb. 2012)

[151] Roving Networks, (2012) [Online] Available: www.rovingnetworks.com (Accessed: Mar. 2012)

[152] ChipCon CC2420, (2011) [Online]. Available: www.ti.com/lit/cc2420.pdf (Accessed: Feb. 2011)

[153] Texas Instruments MSP430, (2010) [Online] Available: www.ti.com (Accessed: Feb. 2012)

[154] TinyOS 2.0, (2011) [Online]. Available: www.docs.tinyos.net/ (Accessed: Feb. 2012)

[155] Lorincz, K., Chen, B. R., Challen, A. R., Patel, S., Bonato, P., & Welsh, M. (2009). 'Mercury: a wearable sensor network platform for high-fidelity motion analysis', *7th Annual Conference on Embedded Networked Sensor Systems*, pp. 183-196.

[156] Pixie Operating System, (2012) [Online] Available www.eecs.harvard.edu (Accessed: Mar. 2012)

[157] Maemo Online, (2010) [Online]. Available: www.maemo.org/. (Accessed: Feb. 2012)

[158] Keogh, E., & Ratanamahatana, C. A. (2005). 'Exact indexing of dynamic time warping', *Knowledge and Information Systems*, vol. 7(3), pp. 358-386.

[159] Quinn, L., & Rao, A. (2002). 'Physical therapy for people with Huntington disease: current perspectives', *Journal of Neurologic Physical Therapy*, vol. 26(3), pp. 145.

[160] Harper, P. S. (1992). 'The epidemiology of Huntington's disease', *Human Genetics*, vol. 89(4), pp. 365-376.

[161] Walker, F. O. (2007). 'Huntington's disease', *The Lancet*, vol. 36 (7), pp. 218-228.

[162] Ramos-Arroyo, M. A., Moreno, S., & Valiente, A. (2005). 'Incidence and mutation rates of Huntington's disease in Spain: experience of 9 years of direct genetic testing', *Journal of Neurology, Neurosurgery & Psychiatry*, vol. 76(3), pp. 337-342.

[163] Busse, M, Wiles, C, & Rosser, A. (2009). 'Mobility and falls in people with Huntington's disease', *Journal of Neurology, Neurosurgery & Psychiatry*, vol. 80(1), pp. 88-90.

[164] Rao, A. K., Quinn, L., & Marder, K.S. (2005). 'Reliability of spatiotemporal gait outcome measures in Huntington's disease', *Movement Disorders*, vol. 20(8), pp. 1033-1037.

[165] Rao, A. K., Muratori, L., Louis, E. D., Moskowitz, C. B., & Marder, K. S. (2009). 'Clinical measurement of mobility and balance impairments in Huntington's disease: Validity and responsiveness', *Gait & Posture*, vol. 29(3), pp. 433-436.

[166] Rao, A. K., Muratori, L., Louis, E. D., Moskowitz, C. B., & Marder, K. S. (2008). 'Spectrum of gait impairments in presymptomatic and symptomatic Huntington's disease', *Movement Disorders*, vol. 23(8), pp. 1100-1107.

[167] Geriatrics Society of America, British Geriatrics Society, and American Academy of Orthopaedic Surgeons Panel on Falls Prevention (2001) 'Guideline for the prevention of falls in older persons.' *Journal of the American Geriatrics Society*, vol. 49(5), pp. 664-672.

[168] Rao, A. K., Louis, E. D., & Marder, K. S. (2009). 'Clinical assessment of mobility and balance impairments in pre-symptomatic Huntington's disease', *Gait & Posture*, vol. 30(3), pp. 391-393.

[169] Delval, A., Krystkowiak, P., Blatt, E., & Defebvre, L. (2007). 'A biomechanical study of gait initiation in Huntington's disease', *Gait & Posture*, vol. 25(2), pp. 279-288.

[170] Delval, A., Bleuse, S., Simonin, C., Delliaux, M., Rolland, B., Destee, A., & Dujardin, K. (2011). 'Are gait initiation parameters early markers of Huntington's disease in pre-manifest mutation carriers?', *Gait & Posture*, vol. 34(2), pp. 202-207.

[171] Delval, A., Krystkowiak, P., Blatt, J. L., Labyt, E., Dujardin, K., & Defebvre, L. (2006). 'Role of hypokinesia and bradykinesia in gait disturbances in Huntington's disease', *Journal of Neurology*, vol. 253(1), pp. 73-80.

[172] Panzera, R., Salomonczyk, D., Pirogovosky, E., Simmons, R., Goldstein, J., Corey-Bloom, J., & Gilbert, P. E. (2011). 'Postural deficits in Huntington's disease when performing motor skills involved in daily living', *Gait & Posture*, vol. 33(3), pp. 457-461.

[173] Moe-Nilssen, R. et al. (1998). 'Test-retest reliability of trunk accelerometry during standing and walking', *Physical Medicine and Rehabilitation*, vol. 79(11), pp. 1377-1385.

[174] Moe-Nilssen, R., & Helbostad, J. L. (2004). 'Estimation of gait cycle characteristics by trunk accelerometry', *Journal of Biomechanics*, vol. 37(1), pp. 121-125.

[175] Moe-Nilssen, R., & Helbostad, J. L. (2005). 'Interstride trunk acceleration variability but not step width variability can differentiate between fit and frail older adults', *Gait & Posture*, vol. 21(2), pp. 164-170.

[176] Moe-Nilssen, R., Aaslund, M. K., C., & Helbostad, J. L. (2010). 'Gait variability measures may represent different constructs', *Gait & Posture*, vol. 32(1), pp. 98-101.

[177] Tura, A., Raggi, M., Rocchi, L., Cutti, A. G., & Chiari, L. (2010). 'Gait symmetry and regularity in transfemoral amputees assessed by trunk accelerations', *Journal Neuro-Engineering Rehabilitation*, vol. 7(4), pp. 13-17.

[178] Zijlstra, W., & Hof, A. L. (1997). 'Displacement of the pelvis during human walking: experimental data and model predictions', *Gait & Posture*, vol. 6(3), pp. 249-262.

[179] Zijlstra, W., & Hof, A. L. (2003). 'Assessment of spatio-temporal gait parameters from trunk accelerations during human walking', *Gait & Posture*, vol. 18(2), pp. 1-10.

[180] Zijlstra, A., Goosen, J. H., Verheyen, C. C., & Zijlstra, W. (2008). 'A body-fixed-sensor based analysis of compensatory trunk movements during unconstrained walking', *Gait & Posture*, vol. 27(1), pp. 164-167.

[181] Brandes, M., Zijlstra, W., van Lummel, R., & Rosenbaum, D. (2006). 'Accelerometry based assessment of gait parameters in children', *Gait & Posture*, vol. 24(4), pp. 482-486.

[182] Bautmans, I., Jansen, B., Van Keymolen, B., & Mets, T. (2011). 'Reliability and clinical correlates of 3D-accelerometry based gait analysis outcomes according to age and fall-risk', *Gait & Posture*, vol. 33(3), pp. 366-372.

[183] Kavanagh, J. J., Morrison, S., James, D. A., & Barrett, R. (2006). 'Reliability of segmental accelerations measured using a new wireless gait analysis system', *Journal of Biomechanics*, vol. 39(15), pp. 2863-2872.

[184] Kavanagh, J. J., & Menz, H. B. (2008). 'Accelerometry: a technique for quantifying movement patterns during walking', *Gait & Posture*, vol. 28(1), pp. 1-15.

[185] Jasiewicz, J. M., Allum, J. H., Middleton, A., Condie, P., Purcell, B., & Li, R. (2006). 'Gait event detection using linear accelerometers or angular velocity transducers in able-bodied and spinal-cord injured individuals', *Gait & Posture*, vol. 24(4), pp. 502-509.

[186] Mansfield, A., & Lyons, G. M. (2003). 'The use of accelerometry to detect heel contact events for use as a sensor in FES assisted walking', *Medical Engineering & Physics*, vol. 25(10), pp. 879-885.

[187] Mizuike, C., Ohgi, S., & Morita, S. (2009). 'Analysis of stroke patient walking dynamics using a tri-axial accelerometer', *Gait & Posture*, vol. 30(1), pp. 60-80.

[188] Sabatini, A. M., Martelloni, C., & Cavallo, F. (2005). 'Assessment of walking features from foot inertial sensing', *Biomedical Engineering*, vol. 52(3), pp. 486-494.

[189] Menz, H., Lord, S, & Fitzpatrick, R. (2003). 'Acceleration patterns of the head and pelvis when walking on level and irregular surfaces', *Gait & Posture*, vol. 18(1), pp. 35-46.

[190] Wark, T., Karunanithi, M., & Chan, W. (2006). 'A framework for linking gait characteristics of patients with accelerations of the waist', *27th Annual International Conference of the IEEE Engineering in Medicine and Biology Society*, pp. 7695-7698.

[191] Hartmann, A., Murer, K., de Bie, R. A., & de Bruin, E. D. (2009). 'Reproducibility of spatio-temporal gait parameters under different conditions in older adults using a trunk tri-axial accelerometer system', *Gait & Posture*, vol. 30(3), pp. 351.

[192] Sama, A, Català A, Rodríguez-Molinero A, Angulo, C., (2009). 'Extracting Gait Spatiotemporal Properties from Parkinson's Disease Patients'. *23rd Annual Conference on Neural Information Processing Systems*. pp. 12-15.

[193] Moe-Nilssen, R., & Helbostad, J. L. (2002). 'Trunk accelerometry as a measure of balance control during quiet standing', *Gait & Posture*, vol. 16(1), pp. 60-68.

[194] O'Sullivan, M., Blake, C., Cunningham, C., Boyle, G., & Finucane, C. (2009). 'Correlation of accelerometry with clinical balance tests in older fallers and non-fallers', *Age and Ageing*, vol. 38(3), pp. 308-313.

[195] Helbostad, J. L., Askim, T., & Moe-Nilssen, R. (2004). 'Short-term repeatability of body sway during quiet standing in people with hemiparesis and in frail older adults', *Archives of Physical Medicine and Rehabilitation*, vol. 85(6), pp. 993-999.

[196] Weiss, A., Herman, T., Plotnik, M., Giladi, N., & Hausdorff, J. M. (2010). 'Can an accelerometer enhance the utility of the Timed Up & Go Test when evaluating patients with Parkinson's disease?', *Medical Engineering & Physics*, vol. 32(2), pp. 119-125.

[197] Zampieri, C., Salarian, A., Carlson-Kuhta, P., Aminian, K., Nutt, J. G., & Horak, F. B. (2010). 'The instrumented timed up and go test: potential outcome measure for disease modifying therapies in Parkinson's disease', *Journal of Neurology, Neurosurgery & Psychiatry*, vol. 81(2), pp. 171-176.

[198] Higashi, Y., Yamakoshi, K., Fujimoto, T., Sekine, M., & Tamura, T. (2008). 'Quantitative evaluation of movement using the timed up-and-go test', *IEEE Engineering in Medicine and Biology Magazine*, vol. 27(4), pp. 38-46.

[199] The GAITRite Walkway (2010) [Online]. Available: www.gaitrite.com (Accessed: Feb. 2012)

[200] Menz, H. B., Latt, M. D., Tiedemann, A., Mun San Kwan, M., & Lord, S. R. (2004). 'Reliability of the GAITRite® walkway system for the quantification of temporo-spatial parameters of gait in young and older people', *Gait & Posture*, vol. 20(1), pp. 20-25.

[201] Webster, K. E., Wittwer, J. E., & Feller, J. A. (2005). 'Validity of the GAITRit® walkway system for the measurement of averaged and individual step parameters of gait', *Gait & Posture*, vol. 22(4), pp. 317-321.

[202] Khasnis, A., & Gokula, R. M. (2003). 'Romberg's test', *Journal of Postgraduate Medicine*, vol. 49(2), pp. 169-172.

[203] Inman, V.T (1967). 'Conservation of energy in ambulation', *Archives of Physical Medicine Rehabilitation*, vol. 48(9), pp. 484-8.

[204] Kerr, K. M., White, J. A., Barr, D. A., & Mollan, R. A. (1997). 'Analysis of the sit-stand-sit movement cycle in normal subjects', *Clinical Biomechanics*, vol. 12(4), pp. 236.

# CHAPTER III

# Comparing Supervised Learning Techniques on the Task of Physical Activity Recognition

**Accepted**

Dalton, A., & ÓLaighin, G. (2013). 'Comparing supervised learning techniques on the task of physical activity recognition', *IEEE Journal Biomedical & Health Informatics*, vol. 17, pp. 46-52

## *3.1 Abstract*

The objective of this study was to compare the performance of base-level and meta-level classifiers on the task of physical activity recognition. Five wireless kinematic sensors were attached to each subject (n=25) while they completed a range of basic physical activities in a controlled laboratory setting. Subjects were then asked to carry out similar self-annotated physical activities in a random order and in an unsupervised environment. A combination of time-domain and frequency-domain features were extracted from the sensor data including the first four central moments, zero-crossing rate, average magnitude, sensor cross-correlation, sensor auto-correlation, spectral entropy and dominant frequency components. A reduced feature set was generated using a wrapper subset evaluation technique with a linear forward search and this feature set was employed for classifier comparison. The meta-level classifier AdaBoostM1 with C4.5 Graft as its base-level classifier achieved an overall accuracy of 95%. Equal sized datasets of subject independent data and subject dependent data were used to train this classifier and high recognition rates could be achieved without the need for user specific training. Furthermore, it was found that an accuracy of 88% could be achieved using data from the ankle and wrist sensors only.

## *3.2 Introduction*

The World Health Organization (WHO) has reported that at least 60% of the world's population fails to achieve the minimum recommendation of 30 minutes of moderate intensity physical activity once a day [1]. The proportion of elderly people (aged 65 or over) in the European Union is predicted to rise from 16.4% in 2004 to 29.9% in 2050. The elderly dependency ratio, the population aged 65 or more as a percentage of population aged between 15 and 64, will rise from 24.5% in 2004 to 52.8% in 2050 [2]. A decline in physical activity can contribute to cardiovascular disease, depression [3] and hypertension [4].

Higher levels of physical activity are associated with lower mortality rates for both younger and older adults [5]. Increased mobility improves stamina and muscle strength and can improve psychological well-being and quality of life by increasing the ability to perform a greater range of activities of daily living (ADL). Ageing is associated with a

decline in physical activity levels [6-7]. The mobility status of older adults is, therefore, an important parameter and the ability to accurately monitor the extent to which an older person is active should provide useful clinically relevant data. The traditional method of monitoring a patient's physical activity patterns through interview and questionnaires has been found unreliable [8] . In rehabilitation medicine, as a reduction in mobility is a major problem for many older patients [9], continuous, unsupervised monitoring of the mobility status of these patients can enable effective evaluation of rehabilitation and other medical interventions. A parallel consideration is that the reported changes in demographics are expected to result in significant strain on future health care services, as older people are major users of these services. Home healthcare facilitated through telemedicine has been proposed as one way to reduce costs associated with healthcare provision.

A significant subsection of published work has concentrated on attaching accelerometer based sensors to several locations on the body and comparing various base-level and meta-level classifiers for activity recognition [10-21]. To date the most significant research conducted has been by Bao et al who gathered data from 20 subjects as they performed 20 self-annotated activities and used these data to compare several base-level classifiers with the C4.5 (J48) decision tree classifier achieving the highest accuracy [10-11]. Other studies have investigated using multiple sensor modalities attached at one location. Lester et al [12] attached a modal sensor board consisting of 8 unique sensors to the shoulder as subjects performed a range of activities. Ravi et al [14] reported on a pilot study with two subjects who performed eight standard activities with a sensor mounted at the waist. Several meta-level classifiers were compared and plurality voting was found to consistently outperform other classifiers. Base-level classifiers were also compared in [15] using a dataset of 6 subjects and C4.5 was found to outperform Naïve Bayes and k-Nearest-Neighbour classifiers. Khan et al employed a combination of Artificial Neural Networks and an autoregressive model achieving 97.9% accuracy across several activities. For a complete review we refer the reader to [16].

A significant number of these studies were preliminary in nature and used a small number of subjects. Contradictions on the accuracy of several classifiers have emerged; specifically for the Naïve Bayes classifier whose performance matched and outperformed several other techniques in [14] but in [10] the classifier was surpassed by k-Nearest

Neighbour (kNN) and C4.5 decision tree classifiers. Furthermore, a primary danger when using machine learning algorithms is over-fitting which can occur when training examples are rare with the classifier adjusting to very specific random features of the training data [17]. Following a review of the literature it was felt that a comprehensive comparison of base-level and meta-level classifiers was required.

This work is a continuation of that proposed in [21] where preliminary analysis was performed on 5 subjects. The long term objective of this work is the development of a robust, remote mobility monitoring system. We aim to contribute to the area of activity monitoring by gathering semi-naturalistic data from several kinematic sensors placed on different parts of the body and identifying the most reliable classifier and location for the sensor(s) in distinguishing Activities of Daily Living (ADLs). We explored a broad scope of concepts including a comparison of base-level and meta-level classifiers, the redundancy of time-domain and frequency domain features, the length of the segmentation window, subject dependant versus subject independent training data and the redundancy of sensor placement.

## *3.3 Method*

### *3.3.1 Study Protocol & Software Environment*

A study was conducted by recruiting 25 subjects, 10 male, 15 female (mean age: 23.6, SD: 2.41), who gave informed consent to a protocol approved by NUI Galway's Research Ethics Committee. Inclusion criteria specified that the subject be capable of significant levels of mobility in their everyday routine and not be dependent on a walking aid. For each subject, a three-phase protocol was adopted. In phase 1, subjects were asked to perform a directed sequence of activities (Table 3.1). In the second phase subjects were given a brief and purposefully ambiguous description of a set of activities similar to those in phase 1 and asked to perform these activities in a random order in an unsupervised environment. Subjects were asked to self-annotate each activity and were encouraged to perform the activities at their own pace and convenience. This method of semi-naturalistic data collection is similar to that presented in [10] where it is argued that data collected under these circumstances are more reflective of real-world conditions. During the third phase of the study, subjects were asked to return to the laboratory and instructed to repeat

**Table 3.1. List of Activities Performed**

| # | Basic Activities of Daily Living (ADLs) |
|---|---|
| 1 | Stand (30 seconds) |
| 2 | Lie Supine (60 seconds) |
| 3 | Lie Left Side (60 seconds) |
| 4 | Lie Right Side (60 seconds) |
| 5 | Walk on level Ground at normal speed (180 secs) |
| 6 | Jog (30 seconds) |
| 7 | Ascend stairs (16 steps) (30 seconds) |
| 8 | Descend stairs (16 steps) (30 seconds) |
| # | Transitions |
| 1 | Lie to Stand (30 seconds) (repeat x3) |
| 2 | Stand to Lie (30 seconds) (repeat x3) |
| 3 | Sit to Stand (30 seconds) (repeat x3) |
| 4 | Stand to Sit (30 seconds) (repeat x3) |
| # | Instrumental Activities of Daily Living (iADLs) |
| 1 | Make a sandwich, drink glass of water ~180 secs |
| 2 | Clean Windows (~120 seconds) |
| 3 | Dress (Shoes, shorts jumper) (~120 seconds) |
| 4 | Stretch (Arms, Legs, Torso) (~60 seconds each) |
| 5 | Vacuum floor (~120 seconds) |
| 6 | Computer Work (~180 seconds) |
| 7 | Read Newspaper (~180 seconds) |

the activities described in Table 3.1. This phase was conducted to ensure the repeatability of the measurements and to generate a larger training set for the classifiers.

A Microsoft Foundation Classes (MFC) based program was built to establish communication with the kinematic sensors over Bluetooth through virtual COM ports using a virtual serial port ActiveX control and to annotate the data as each activity was performed. This program also synchronized, logged and parsed the data. The piconet of sensors was synchronized using a Master-Slave algorithm [22] with a laptop acting as the master. The data gathered during phases one and three of the study were annotated by the researcher, while data collected during phase two were self-annotated by the subjects. The data gathered as the subject marked the start and end time of each activity were irrelevant and could affect the classification algorithms. Therefore, data within 15 seconds of each annotation were discarded, a similar technique to that adopted in previous activity monitoring studies [10]. Each phase took approximately 1 hour to complete for a total of 75 hours of recorded data. A MATLAB script was written to filter the raw data and to extract feature sets which were then converted into ARFF file format and fed into the Waikato Environment for Knowledge Analysis (WEKA) [17].

### *3.3.2 Sensor Specification, Placement & Attachment*

The sensor used in this study was a commercially available wireless accelerometer [23]. Data were sampled at a frequency of 135Hz and at a range of +/- 6g (9.81 $m/s^2$). These parameters compare favorably with those suggested by Bouten et al [24]. Five kinematic sensors were attached to a subject at the following sites: 1) just below the suprasternal notch, 2) left side of the chest over the lower ribs, 3) directly above the right hip, 4) wrist of the dominant hand and 5) ankle of the dominant leg. Two of the sensors ("1" and "2") were attached using a specifically designed vest [25]. The waist sensor was attached with a belt-clip. The wrist and ankle sensors were attached using standard medical strapping. The sensor attached on the left side of the chest was orientated with the X-Axis in the anteroposterior (AP) axis, the Y-Axis in the longitudinal (LD) axis and the Z-Axis in the mediolateral (ML) axis of the subject. All other sensors were orientated with the X-Axis in the ML axis, the Y-Axis in the LD axis and the Z-Axis in the AP of the subject. The sensor was calibrated prior to attachment by rotation of the accelerometer through six different known angles as outlined by Bourke et al [25]. To correct for any misalignment or tilt of the sensor caused by the site of attachment the accelerometer's capacity as an inclinometer was employed as outlined by Moe-Nilssen et al [26].

### *3.3.3 Classification & Feature Extraction*

#### *3.3.3.1 Feature Set*

In published work the standard approach is to select a fixed set of features [10] and a fixed sliding window length for the collection of activities being studied. Combinations of time-domain [15] and frequency-domain feature sets [27] have proven accurate and therefore we decided to extract a feature set consisting of the first four central moments, zero-crossing rate, average magnitude, sensor cross-correlation, sensor auto-correlation, spectral entropy and dominant frequency components (Table 3.2). A sliding window segmentation technique was used using a 128-sample sliding window with 50% overlap. This feature set was extracted for each sensor across each axis, generating 160 independent features. We performed initial exploratory examination of the feature space using Sammon's mapping [28] a nonlinear transformation technique that maps a high-dimensional space to a space of lower dimensionality by minimizing the Sammon's

**Table 3.2. The complete feature set**

| # | Time Domain Features |
|---|---|
| 1-4 | First Four Central Moments |
| 5,6 | Variance, Zero crossing rte |
| 7,8 | Short Term Average Magnitude, Auto-Correlation |
| 9 | Cross-Correlation between all sensors |
| # | Frequency Domain Features |
| 1,2 | Dominant Freq. Comp., Spectral Entropy |

stress error function. It is important to use a feature set with a high discriminative ability and to limit redundancy between features [29]. Redundant features not only increase the time required to train and test a classifier, they can also reduce their precision and recall. The wrapper evaluation was performed three times with a different base-classifier each time: C4.5 Graft, SVM and BayesNET respectively.

#### *3.3.3.2 Classifier Comparison*

A brute force comparison of base-level and meta-level classifiers was performed using the reduced feature set. Based on published work several different base-level classifiers were chosen including Decision Trees (C4.5), Bayesian Networks (Naïve Bayes, BayesNET), Nearest-Neighbour Lazy Classifiers (IB1, IBK, KStar), Rule Based Classifers (JRip), Support Vector Machines (LibSVM) and Neural Networks (Multilayer Perceptron). Several meta-level classifiers were also compared including AdaBoostM1, Bagging, MultiBoostAB and Vote. Meta-level classifiers merge the results of one or more base-level classifiers and, in general, generate a higher predictive accuracy then a single base-level classifier. For a full review of these classifiers see [17].

To compare the classifiers and to identify a principal classifier, we used the experimenter environment in the WEKA toolkit [17]. Ten-fold cross validation with 5 iterations per fold was used with each classifier independently selected as the baseline scheme. Within this environment WEKA uses the corrected resampled t-test for statistical comparison. The classifiers were trained and tested using two approaches;

*User Specific:* In the first approach the classifiers were trained on individual subject data gathered during phases 1 and 3 of the study and tested on that subjects' phase two data.

*Leave One-Subject Out*: In the second approach classifiers were trained on data from all three phases for all subjects except one. The classifiers were then tested on phase two data

of the subject left out. Both approaches were repeated for all subjects. We adopted these techniques to investigate the relationship between subject dependant and subject-independent data.

For the decision tree classifier C4.5 Graft we used a confidence factor of 0.30. The confidence factor addresses the issue of tree pruning. During the construction of a decision tree several branches may reflect anomalies due to noise or outliers in the training data. Tree pruning uses statistical measures to remove noise allowing for faster classification and improvement in the ability of the tree to correctly classify independent test data [30]. With the Naïve Bayes classifier we used kernel density estimators which improve performance if the assumption of a normal distribution is grossly incorrect [17]. For the BayesNET classifier we used the TAN search algorithm. For the kNN we determined the optimal number of neighbours using leave-one-out cross validation. For the JRip classifier we used three folds for pruning. For the SVM we used c-support vector classification from LibSVM [31] and a radial basis kernel (RBF) with automatic parameter selection through grid searching techniques. When the number of instances is considerably greater than the number of features, the use of a RBF kernel is recommended [32]. For the Multilayer Perceptron we used the approach of recursively evaluating values for the learning rate and momentum using cross validation [17].

#### *3.3.3.3 Window Size & Sensor Location Comparison*

In [33] it is argued that recognition rates can be increased by selecting features and window lengths for each activity separately. To compare the affect of varying window length, we extracted a reduced feature set using five window lengths; 32, 64, 128, 256 and 512 samples. At a sampling frequency of 135Hz this corresponds to 0.25, 0.5, 1, 2 and 4 seconds respectively. As an example, the activity jogging required on average 30 seconds to complete. Sampling at 135Hz produced 4050 samples for this activity and using a sliding window with 128 samples with 50% overlap produced approximately 63 unique windows and the reduced feature set was calculated across each window. The accuracy of several classifiers across these window lengths were compared within the WEKA Experimenter.

To establish the discriminatory power of each sensor location and to determine the minimum number of sensors required to maintain a high degree of accuracy, a comparison between the various combinations of sensor placement (31 in total) was adopted. An experiment was designed where the principal classifier was trained and tested on data from each combination of sensors independently. The reduced feature set and the optimal window size was used in conjunction with ten-fold cross validation.

## *3.4 Result*

### *3.3.4 Visualization of Feature Space*

The results of initial inspection of the feature space using Sammon's Mapping can be seen in Fig. 3.1. We present specific results for Activities of Daily Living (ADLs), transitions and instrumental ADLs respectively (iADLs). Table 3.3 presents the reduced feature set generated from a linear forward search.

### *3.3.5 Classifier Accuracy*

Table 3.4 summarizes the results for the comparison of base-level and meta-level classifiers. It is divided between *User Specific* and *Leave-One Subject Out* classifier training. To report the classifier accuracy we use the Kappa statistic which measures the agreement between predicted and observed categorizations of a dataset while correcting for agreement that occurs by chance. A Kappa of 1 indicates perfect agreement while a Kappa of 0 indicates agreement equivalent to chance [34]. Fig. 3.2 presents a Receiver Operating Characteristic (ROC) curve which is a graph of the true positive rate against the false positive rate for the activity *Dressing* which demonstrated high variability across subjects.

### *3.3.6 Window Size and Sensor Location Comparison*

Fig. 3.3 presents the results of comparing classifier accuracy across varying window size. Table 3.5 summarizes the results from our comparison of sensor placement.

**Table 3.4. Summary of classifier comparison**

| Classifier | (I) | (II) | (III) | Parameters |
|---|---|---|---|---|
| C4.5 Graft | 0.80 | 0.89 | 0.86 | Confidence: 0.30 |
| Naïve Bayes | 0.74 | 0.81 | 0.79 | Kernel Density Est. |
| BayesNET | 0.77 | 0.83 | 0.80 | Search: TAN |
| IB1 | 0.68 | 0.76 | 0.72 | Euclidean distance |
| IBK | 0.71 | 0.80 | 0.78 | # Neighbours: 5 |
| KStar | 0.72 | 0.80 | 0.78 | Global blending: 20 |
| JRip | 0.70 | 0.77 | 0.74 | # Folds: 3 |
| SVM | 0.78 | 0.86 | 0.82 | RBF Kernel |
| Multi Pcptrn. | 0.75 | 0.82 | 0.80 | LR: 0.3. M: 0.2 |
| AdaBoost | *0.83* | *0.95* | *0.92* | C4.5 Graft |
| AdaBoostM1 | 0.81 | 0.91 | 0.84 | SVM |
| Bagging | 0.81 | 0.90 | 0.83 | C4.5 Graft |
| MultiBoost | 0.81 | 0.92 | 0.82 | C4.5 Graft |
| Vote | 0.80 | 0.90 | 0.87 | C4.5Graft, SVM |

(I) User Specific Training: Kappa Stat.
(II) Leave One-Subject Out Training: Kappa Stat.
(III) Down Sampled Leave One-Subject Out Training: Kappa Stat.

**Table 3.3. The Reduced feature set**

| # | Time Domain Features |
|---|---|
| 1 | Wrist Y-Axis mean |
| 2 | Wrist Z-Axis Average Magnitude |
| 3 | Mid sternum Z-Axis mean |
| 4 | Ankle v Wrist Cross-Correlation |
| 5 | Ankle Z-Axis Average Magnitude |
| 6 | Ankle X Axis mean |
| 7 | Ankle Y-Axis mean |
| 8 | Mid sternum Y-Axis Average Mag. |
| 9 | Wrist Y-Axis mean |
| 10 | Ankle X-Axis Average Magnitude |
| 11 | Waist X-Axis Entropy |
| 12 | Ankle v Waist Cross-Correlation |
| 13 | Waist Y-Axis Entropy |
| 14 | Wrist X-Axis Zero Crossing Rate |

**Table 3.5. Sensor placement comparison with classifiers trained using Leave one-subject out protocol**

| Configuration | Kappa Statistic |
|---|---|
| All Sensors | 0.95 |
| Waist, Wrist & Ankle | 0.92 |
| Waist, Mid Sternum & Ankle | 0.90 |
| Wrist & Ankle | 0.88 |
| Mid Sternum & Ankle | 0.84 |
| Waist & Wrist | 0.83 |
| Waist & Ankle | 0.82 |
| Ankle Only | 0.80 |
| Wrist Only | 0.79 |
| Mid Sternum Only | 0.78 |
| Waist Only | 0.77 |
| Left Chest Only | 0.75 |

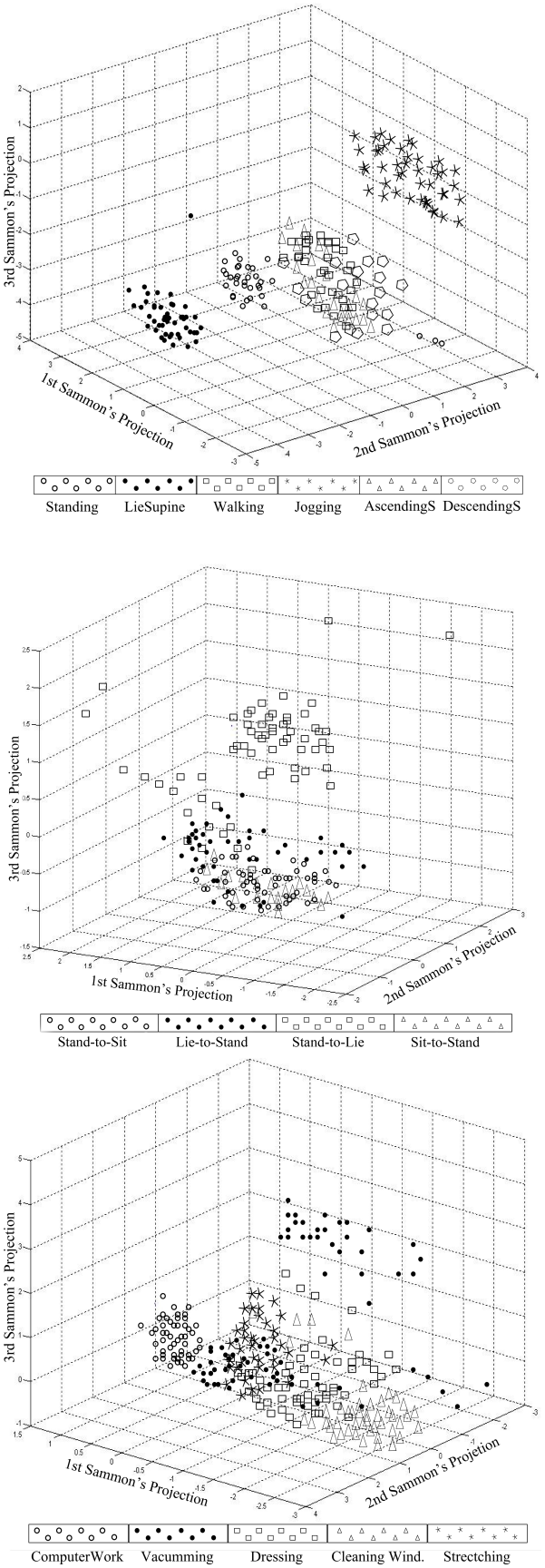


Fig 3.1. 3-D Sammon's-Map of the Feature Space (a) Basic ADL's, (b) Transitions and (c) iADLs

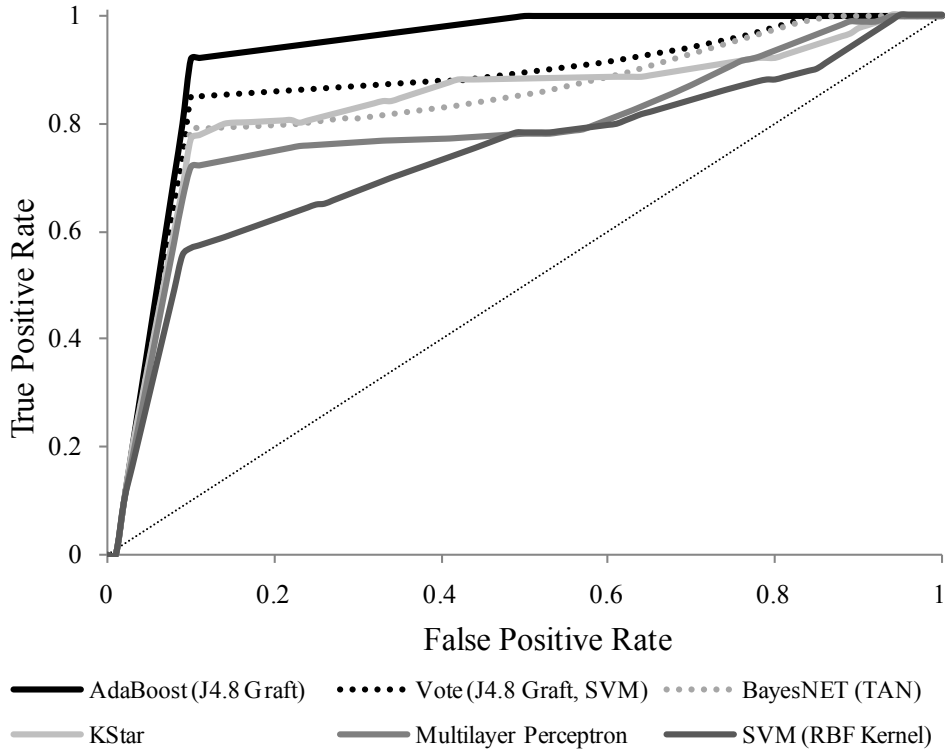


Fig. 3.2. ROC Curve for the activity: Dressing. True Positive Rate versus False Positive Rate

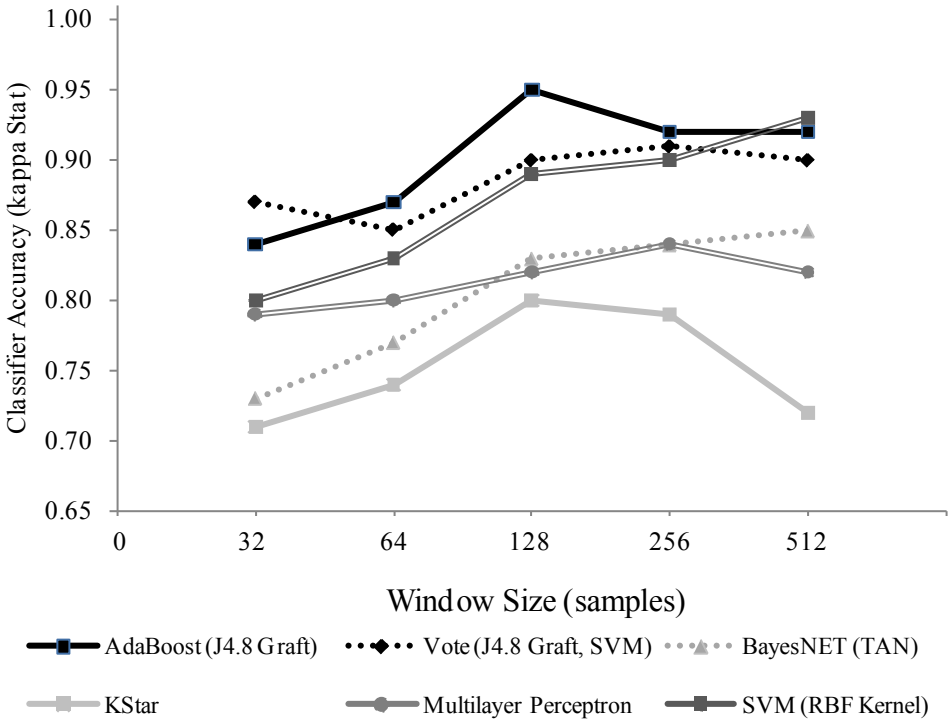


Fig. 3.3. Window Size Comparison, classifier Accuracy versus window size.

## *3.5 Discussion*

### *3.3.7 Analysis of Feature Space*

In Fig. 3.1(a) it can be seen that the activities *Standing*, *LieSupine* and *Jogging* all form unique compact clusters whereas *Walking* and *Ascending / Descending Stairs* are indistinguishable, as the features of these activities are quite similar. A similar problem can be seen in Fig 3.1(b) where four transitions are shown. Minor separation can only be seen between *StandtoLie* and the other transitions. Finally, in Fig. 3.1(c) we can see that *Computer Work* forms a unique cluster, as this activity predominantly generates movement in the wrist sensor. The other four activities appear to generate distinctive clusters but with considerable overlap highlighting the difficulty in differentiating "high-level" activities.

There are two fundamentally different approaches to feature set reduction. The filter method makes an independent assessment of the feature space based on general characteristics of the data whereas the wrapper method uses a classifier to recursively evaluate subsets of the feature space. In general, the wrapper method is considered superior however, this superiority comes at significant computational cost [17]. The wrapper subset evaluation technique we used to generate our reduced feature set also employed 10-fold cross validation within every subset evaluation to improve feature selection. The selection of the three base classifiers within the wrapper subset evaluation, C4.5 Graft, SVM and BayesNET, was based on the demonstrated accuracy of these classifiers in published work. It is also important to note that the linear forward search scheme employed is guaranteed to find locally but not globally optimal feature sets [17]. In published work there has been considerable dispersion among the choice of filter methods. Maurer et al employed a filter based technique which evaluates the worth of a feature set by considering the individual predicative ability of each feature along with the degree of correlation between them [15]. Lo et al also employed a filter based technique known as a Bayesian Framework for Feature Selection (BFFS) to rank the relevance of features [35]. Whereas Pirttikangas et al [36] and Palmerini et al [37] both employed wrapper selection techniques to evaluate the worth of features. Within our work we note that time-domain features from the wrist and ankle dominate and the cross-correlation between these sensors is rated as the fourth most important feature. Furthermore, the

mean of the accelerometer signal is rated as an important feature for all sensors which supports published work [15], [36]. The dominance of time-domain features is an encouraging result as these features require considerably less CPU cycles to compute and thus are more suitable for real-time portable systems.

### *3.3.8 Classifier Comparison*

It can be seen from Table 3.5 that C4.5 Graft produces the highest recognition accuracy among the base-level classifiers which corresponds with published work [10], [38]. The results of the Naïve Bayes and the BayesNET classifiers are significant. For these classifiers there has been conflicting findings in published work. In [14] the Naïve Bayes classifier matched and outperformed several other techniques however, in [10] the classifier was surpassed by kNN and C4.5. Naïve Bayes makes an inherent assumption that features are conditionally independent and modeled by a normal distribution. Bao et al argues that these assumptions are violated by features from accelerometer data and also that Bayesian algorithms require larger datasets. As previously noted we addressed these issues by using kernel density estimators with Naïve Bayes. These estimators can improve performance if the normality assumption is grossly incorrect. We also produced larger training sets by asking subjects to perform phase 3 of the protocol. A further problem of Naïve Bayes is its susceptibility to redundant features [17]. Feature reduction was performed in [15] where high accuracy with Naïve Bayes was achieved. From Table 3.5 we see Naïve Bayes outperforms all the Nearest Neighbour classifier's but is still below C4.5. Interestingly, the BayesNET classifier outperforms Naïve Bayes. BayesNET allows for the representation of more advanced probability distributions and is not hindered by the Naïve Bayes assumption of a normal distribution.

The fact that the Support Vector Machine achieves a higher Kappa statistic than BayesNET is noteworthy. There has been limited published work on comparing SVM to other classifiers for activity recognition. In [14] Naïve Bayes minimally outperformed SVM but in [27] SVM combined with multiple eigenspaces produced a significantly higher accuracy. Achieving satisfactory results with the SVM classifier with an RBF kernel requires appropriate kernel selection and fine-tuning of both the complexity parameter (C) and the scale parameter ($\gamma$) and as noted in section II (C) we employed

automatic parameter selection. However, we feel further investigation into SVM's for activity classification is warranted.

Among the meta-level classifiers, AdaBoostM1 with C4.5 Graft as its base-level classifier has the maximum Kappa statistic. It is interesting to note that boosting outperformed bagging and voting. Lester et al also reported success using the AdaBoost classifier with a Naïve Bayes base-level classifier and Hidden Markov Models (HMM). Similarly, with AdaBoost and a HMM base-level classifier, Maekawa et al achieved an 80% recognition rate across a range of ADLs with a host of sensors including accelerometers and microphones [40]. The activity *Dressing* distinguished a high variability across subjects and was therefore quite difficult to classify. It can be seen in Fig. 3.3 that AdaBoostM1 significantly outperforms the other classifiers for this activity.

### *3.3.9 User Specific vs. Independent Training*

A principle concern for the deployment of ubiquitous activity monitoring sensors is the level of user specific algorithm training required. Ideally, the classifiers should be robust and not require specific user adjustment. The two training techniques, discussed in section 3.3.3.2, were employed to address this question. From Table 3.4 we see that Leave One-Subject Out training continuously outperformed User Specific training. However, the accuracy of machine learning algorithms is inherently dependant on the amount of training data available and Leave One-Subject Out training has access to significantly more data than User Specific training. This issue was addressed by asking subjects to perform phase 3 of the protocol. Also, using re-sampling filters in the WEKA environment, a random sub-sample of the Leave One-Subject Out training set was generated for each subject. This subset was designed to be equal in size to the corresponding User Specific Training set, therefore allowing a balanced comparison. Interestingly, it can be seen from column III of Table 3.3 that Down Sampled Leave One-Subject Out training still outperforms User Specific training. This finding contradicts that of [10-11] where it is argued that given equal amounts of training data, user-specific training data can outperform generalized training sets. However, Bao et al notes that the accuracy of these preliminary results is limited by the low-number of subjects involved in this part of their study. Our results correlate with that presented by

Khan et al who used a combination of ANN's and an AR model to achieve an accuracy of 97.65% while using Leave One-Subject training out on a cohort of 6 subjects. We consider this a key result of our work; based on the dataset of 25 healthy subjects user specific input is not a prerequisite. While this is encouraging for user compliance in future deployment it must be noted that this is a relatively homogeneous dataset (10 m, 15 f , age: $23.62 \pm 2.41$, weight (kg): $71.84 \pm 5.38$, height (cm) $175.75 \pm 7.91$) and the lack of dispersion may have contributed to the power of Leave One-Subject Out training. As the primary goal is the development of a remote mentoring system the insights from this work need to be applied to a broader and more diverse study population.

### *3.3.10 Window Size and Sensor Location*

In Fig. 3.3 we see the majority of the classifiers reach their peak accuracy with a window size of 128 samples (1 second). This corresponds with the finding of [36], where a 1 second window size also produced optimal results. AdaBoostM1 with C4.5 Graft as its base-level classifier dominates for the higher window sizes but is outperformed by Vote at a window size of 32 samples. Interestingly, the accuracy of BayesNET improves with increasing window size. The calculation of feature sets from adaptive segmentation of the signal may lead to more robust classifiers and merits further investigation.

A key requirement for activity monitoring sensors is the achievement of a high compliance rate among end users and fundamental to achieving this is the placement of sensors in an unobtrusive and discreet manner. Previous work on this issue has shown that placement at the thigh and wrist [10] and wrist and left hip [39] achieve relatively high recognition rates. In Table 3.5 we see a Kappa statistic of 0.92 was achieved using sensors attached at the waist, wrist and ankle which resonates with published work. Of significant importance is the accuracy achieved by the combination of wrist and ankle sensors. This result reflects the importance placed on features calculated from these sensors during the feature selection process. The wrist and ankle should be highly favorable locations to the end-user and provide several options for embedding the sensors in wearable electronics.

We analyzed an aggregate confusion matrix for AdaBoostM1 with C4.5 Graft as its base-level classifier based on data from only the wrist and ankle sensors for all 25 subjects using Leave One-Subject Out training. Differentiating between opposing transitions is quite difficult with *Sit-to-Stand* transitions (0.857 AUC[3]) regularly confused with *Stand-to-Sit* transitions (0.842 AUC). During such transitions sensors attached to the wrist and ankle record a signal vector of considerably smaller magnitude to that recorded by sensors attached to the chest or waist although recognition rates for these transitions using five sensors show only marginal improvement, (0.884 AUC), highlighting the difficulty of classifying these transitions. Similarly, the classifier confuses the *Lie-to-Stand* transition (0.745 AUC) with a range of activities. This transition is naturally quite specific to each subject and therefore difficult to generalize. The power of the wrist-ankle combination can be seen in the accuracy achieved in distinguishing between *Ascending* (0.945 AUC) and *Descending* (0.951 AUC) stairs. In previous work it has proven difficult to discriminate between these two activities [10-14] with Lester et al using barometric pressure to make a distinction. Finally, the wrist-ankle combination achieves significant results in distinguishing between activities such as *Eating/Drinking* (0.957 AUC), *Cleaning Windows* (0.932 AUC) and *Dressing* (0.921 AUC).

## *3.6 Conclusion*

The two primary findings from this work we wish to emphasize are 1) from a dataset of 25 healthy subjects with AdaBoostM1 trained and tested with equal sized datasets, subject independent data was found to outperform subject dependent data indicating that high recognition rates can be achieved without the need for prior user specific training and 2) the dominance of the wrist and ankle sensors which provide several options for embedding sensors in wearable electronics. However, the homogeneity of our dataset warrants an extension of this research into an older, more diverse population in a home environment. Other notable areas of future research indentified are a deeper investigation of Support Vector Machine classification.

[3]Defined as the area under a ROC Curve, interpreted as the probability that the classifier ranks a randomly chosen positive instance above a randomly chosen negative instance

## *3.7 References*


[1] Puska P., H. Benaziza, D. Porter (2004). '*Physical Activity, WHO Sheet Physical Activity*', [Online]. Available: http://www.who.int/en/gs_pa.pdf. (Accessed: Mar. 2012)

[2] Eurostat (2005) '*Population Projections 2004-2050*', [Online] Available: www.europa.eu.int (Accessed: June 2012)

[3] Fox, K. R. (1999). 'The influence of physical activity on mental well-being', *Public Health Nutrition*, vol. 2(3a), pp. 411-418.

[4] Sobngwi, E., Mbanya, J. C., Unwin, A. P., & Alberti, K. G. (2002). 'Physical activity and its relationship with obesity, hypertension and diabetes in urban and rural Cameroon', *International Journal of Obesity and Related Metabolic Disorders*, vol. 26(7), pp. 1009-14.

[5] United States Public Health Service, Office of the Surgeon General, (1996). 'Physical activity and health: a report of the Surgeon General', *Jones & Bartlett Learning*.

[6] Westerterp, K. R., & Meijer, E. P. (2001). 'Physical Activity and Parameters of Aging A Physiological Perspective', *The Journals of Gerontology Series A: Biological Sciences and Medical Sciences*, vol. 56(A), pp. 7-12.

[7] Black, A. E., Coward, W. A., Cole, T. J., & Prentice, A. M. (1996). 'Human energy expenditure in affluent societies: an analysis of 574 doubly-labelled water measurements', *European Journal of Clinical Nutrition*, vol. 50(2), pp. 72.

[8] Lieberman, J. R., Dorey, F., Shekelle, P., Kilgus, D. J., & Finerman, G. A. (1996). 'Differences between Patients' and Physicians' Evaluations of Outcome after Total Hip Arthroplasty', *The Journal of Bone & Joint Surgery*, vol. 78(6), pp. 835-8.

[9] World Health Organization. (1980). 'International classification of impairment, disabilities, handicaps; a manual classification relating to the consequences of disease', *WHO*.

[10] Bao, L., & Intille, S. (2004). 'Activity recognition from user-annotated acceleration data', *Pervasive Computing*, vol. 3001, pp. 1-17.

[11] Mannini, A., & Sabatini, A. M. (2010). 'Machine learning methods for classifying human physical activity from on-body accelerometers', *Sensors*, vol. 10(2), pp. 1154-1175.

[12] Lester, J., Choudhury, T., & Borriello, G. (2006). 'A practical approach to recognizing physical activities', *Pervasive Computing*, vol. 3968, pp. 1-16.

[13] Karantonis, D. M., Narayanan, M. R., Mathie, M., Lovell, N. H., & Celler, B. G. (2006). 'Implementation of a real-time human movement classifier using a triaxial accelerometer for ambulatory monitoring', *IEEE Transactions in Information Technology in Biomedicine*, vol. 10(1), pp. 156-167.

[14] Ravi, N., Dandekar, N., Mysore, P., & Littman, M. L. (2005). 'Activity recognition from accelerometer data', *National Conference Artificial Intelligence*, vol. 20, p. 1541

[15] Maurer, U., Smailagic, A., Siewiorek, D. P., & Deisher, M. (2006). 'Activity recognition and monitoring using multiple sensors on different body positions', *Wearable and Implantable Body Sensor Networks*, pp. 4-6.

[16] Godfrey, A., Conway, R., Meagher, D., & ÓLaighin, G. (2008). 'Direct measurement of human movement by accelerometry', *Medical Engineering & Physics*, vol. 30(10), 1364-1386.

[17] Witten, I. H. & Frank, E. (2005). 'Data Mining: Practical machine learning tools and techniques', *Morgan Kaufmann*.

[18] NiScanaill, C. N., Ahearne, B., & Lyons, G. M. (2006). 'Long-term telemonitoring of mobility trends of elderly people using SMS messaging', *IEEE Transactions of Information Technology in Biomedicine*, vol. 10(2), pp. 412-413.

[19] Lyons, G. M., Culhane, K. M., Hilton, D., Grace, P. A., & Lyons, D. (2005). 'A description of an accelerometer-based mobility monitoring technique', *Medical Engineering & Physics*, vol. 27(6), pp. 497-504.

[20] Khan, A. M., Lee, Y. K., Lee, S. Y., & Kim, T. S. (2010). 'A triaxial accelerometer-based physical-activity recognition via augmented-signal features and a hierarchical recognizer', *IEEE Transactions in Information Technology in Biomedicine*, vol. 14(5), pp. 1166-1172.

[21] Dalton, A., Morgan, F., & Olaighin, G. (2008). 'A preliminary study of using wireless kinematic sensors to identify basic Activities of Daily Living', *30th Annual International Conference of the IEEE Engineering in Medicine and Biology Society*, pp. 2079-2082.

[22] Ringwald, M., & Romer, K. (2007). 'Practical time synchronization for bluetooth scatternets', *4th International Conference on Broadband Communications, Networks and Systems*, pp. 337-345.

[23] Sparkfun (2004). [Online]. Available: www.sparkfun.com (Accessed: Feb. 2012)

[24] Bouten, C. V., Koekkoek, K. T., Verduin, M., Kodde, R., & Janssen, J. (1997). 'A triaxial accelerometer and portable data processing unit for the assessment of daily physical activity', *IEEE Transactions on Biomedical Engineering*, vol. 44(3), 136-147.

[25] Bourke, A. K., O'Donovan, K. J., & ÓLaighin, G. M. (2007). 'Distinguishing falls from normal ADL using vertical velocity profiles', 29th Annual International Conference of the *IEEE Engineering in Medicine and Biology Society*, pp. 3176-3179.

[26] Moe-Nilssen, R., & Helbostad, J. L. (2004). 'Estimation of gait cycle characteristics by trunk accelerometry', *Journal of Biomechanics*, vol. 37(1), pp. 121-125.

[27] Huynh, T., & Schiele, B. (2006). 'Towards less supervision in activity recognition from wearable sensors', *10th IEEE International Symposium in Wearable Computers*, pp. 3-10.

[28] Sammon Jr, J. W. (1969). 'A nonlinear mapping for data structure analysis', *IEEE Transactions on Computers*, vol. 100(5), pp. 401-409.

[29] Kiani, K., Snijders, C., & Gelsema, E. S. (1997). 'Computerized analysis of daily life motor activity for ambulatory monitoring', *Technological Health Care*, vol. 5(4), pp. 307-318.

[30] Han, J., & Kamber, M. (2006). '*Data mining: concepts and techniques*', Morgan Kaufmann.

[31] Chang C, C. J. Lin (2004), 'LIBSVM: a library for support vector machines', [Online]. Available: http://www.csie.ntu.tw/~cjlin/libsvm. (Accessed: Feb. 2012)

[32] Hsu, C. W., Chang, C. C., & Lin, C. J. (2009). '*A practical guide to support vector classification*', [Online]. Available: www.csie.ntu.edu/guide.pdf.

[33] Huynh, T., & Schiele, B. (2005). 'Analyzing features for activity recognition', *2005 Joint Conference on Smart Objects and Ambient Intelligence*, pp. 159-163.

[34] Ben-David, A. (2008). 'Comparison of classification accuracy using Cohen's Weighted Kappa', *Expert Systems with Applications*, vol. 34(2), pp. 825-832.

[35] Lo, B., Atallah, L., Aziz, O., ElHew, & Yang, G. Z. (2007). 'Real-time pervasive monitoring for postoperative care', *4th International Workshop on Wearable and Implantable Body Sensor Networks*, pp. 122-127.

[36] Pirttikangas, S., Fujinami, K., & Nakajima, T. (2006). 'Feature selection and activity recognition from wearable sensor', *Ubiquitous Computing Systems,* vol. 4239, pp. 516-527.

[37] Palmerini, L., Rocchi, L., Mellone, S., Valzania, F., & Chiari, L. (2011). 'Feature selection for accelerometer-based posture analysis in Parkinson's disease', *IEEE Transactions of Information Technology in Biomedicine*, vol. 15(3), pp. 481-490.

[38] Kwapisz, J., & Moore, S. (2011). 'Activity recognition using cell phone accelerometers', *4th International Workshop on Knowledge Discovery from Sensor Data*, pp. 10-18.

[39] Olguin, D. O., & Pentland, A. S. (2006). 'Human activity recognition: Accuracy across common locations for wearable sensors', *MIT Media Lab*.

[40] Maekawa, T., Yanagisawa, Y., Kishino, Y., Ishiguro, K., Sakurai, Y., & Okadome, T. (2010). 'Object-based activity recognition with heterogeneous sensors on wrist', *Pervasive Computing*, vol. 6030,pp. 246-264.

# CHAPTER IV

# Physical Activity Recognition through Support Vector Machines with Multiple Kernel Learning

**Under Review:**
Dalton, A., ÓLaighin., G, (2012) " Physical Activity Recognition through Support Vector Machines with Multiple Kernel Learning," *Medical Engineering & Physics*

## *4.1 Abstract*

Our long term objective is the development of a robust remote mobility monitoring system employing supervised learning techniques and accelerometry data. In previous work the boosting classifier AdaBoostM1 with C4.5 Graft was found to perform well in classifying physical activities from a homogenous dataset of 25 young adults (age: $\mathbf{23.62 \pm 2.41}$) wearing 5 triaxial accelerometers in a laboratory setting. The objective of our current work was to classify various physical activities from a more diverse dataset and in a natural environment using Support Vector Machines (SVMs) with Multiple Kernel Learning (MKL). Therefore, we gathered data from 5 older adults (age: $\mathbf{60.4 \pm 6.95}$) in a home environment. In this work the boosting algorithm acted as a benchmark to several SVMs built with various kernel functions and to SVMs built with MKL. Kappa statistics of 0.97 and 0.86 for young adults and older adults respectively were achieved using the MKL technique. Furthermore, this classifier did not require subject specific training and a high level of accuracy was maintained using sensors attached at the mid-sternum, wrist and ankle..

## *4.2 Introduction*

It has been estimated that within the next several years people aged 65 or older will outnumber children under the age of 5. Furthermore, it is projected that the world's population aged 80 or more will increase by 233% by 2040 [1]. These and other statistics highlight the growing need for practical and reliable telemonitoring systems for home healthcare. As a result, research into the combination of kinematic sensors with advanced supervised learning algorithms towards the task of physical activity recognition has grown significantly over the previous several years.

Due to their size and ease-of-use accelerometer based sensors have been employed extensively for activity recognition within the research community. The characteristic approach has been to derive quantitative features from accelerometers attached to several locations on the body and attempt to recognize a subset of physical activities based on these features [2]-[19]. Considerable variety has emerged in the nature of algorithms adopted and range of features investigated. Several authors have employed heuristic style classifiers [2]-[4]. Notably, Karantonis et al [4] achieved an

accuracy of 90.8% when indentifying 12 activities across 6 subjects using a heuristic tree. Artificial Neural Networks (ANNs) have also attracted considerable attention [5]-[8] with Staudenmayer et al. [5] employing ANNs to explore physical activity metabolic equivalents (METs) and a significant range of physical activities with considerable accuracy. Long et al [9] utilised a Bayesian model on data from 24 subjects wearing a waist mounted triaxial accelerometer to achieve 80% accuracy. Investigation into Hidden Markov Models (HMMs) has also been conducted [10]-[11] with Lester et al [11] employing HMMs combined with boosting techniques to differentiate between 10 activities with an accuracy of 95%.

Researchers have also compared the predicative power of several classifiers on individual datasets. One of the most significant contributions to date has been by Bao et al [12] who gathered data from 20 subjects as they performed 20 self-annotated activities and used these data to compare several base-level classifiers with the C4.5 decision tree classifier achieving the highest accuracy. Ravi et al [13] investigated several meta-level classifiers on a dataset of 2 subjects and found plurality voting to consistently outperform other classifiers. Maurer et al [14] found C4.5 decision tree classifier outperformed Naïve Bayes and k-Nearest-Neighbour (kNNs) classifier on a dataset of 6 subjects. We recently explored a range of supervised learning algorithms on data from 25 subjects across a host of physical activities and found that AdaBoostM1 with C4.5 Graft as its base-level classifier achieved an accuracy of 95% [16].

Several publications have noted the power of a specific type of maximum margin classifier known as Support Vector Machines (SVMs) and the algorithm has proven capable of achieving accuracies comparable with other learning algorithms for physical activity recognition [12]-[13], [16]-[21]. The versatility of the SVM algorithm can be also seen in its varying use for fall detection [22], automatic seizure detection in the newborn [23] and analysis of walking with dropped foot [24]. However, we feel the full potential of SVMs for physical activity recognition has not yet been explored. The key ingredient for these maximum margin based classifiers is the choice of kernel which maps data from input space to feature space. The choice of kernel is highly dependent on the specific dataset with brute-force methods often employed to find the optimal kernel and corresponding kernel parameters. Multiple Kernel Learning (MKL) is a

technique which evaluates various convex combinations of kernels. This technique has shown very promising results in the identification of cognitive decline in healthy older adults [25] and the prediction of movements on a FX limit order book [26]. Although several researchers have compared standard kernels we are unaware of work which combines multiple kernels for physical activity recognition.

## *4.3 Method*

### *4.3.1. Study Protocol & Software Environment*

This study utilizes two independent datasets. The first dataset has been previously employed to compare several surprised learning algorithms [16]. This dataset, dataset I, consists of 25 healthy subjects, 10 male, 15 female. Data were gathered in a semi-naturalistic manner using a three-phase protocol. In phases 1 and 3, subjects performed a directed sequence of activities (Table 4.1). In the second phase subjects were given a brief and purposefully ambiguous description of a set of activities similar to those in phase 1 and asked to perform these activities in a random order in an unsupervised environment. Subjects were asked to self-annotate each activity and were encouraged to perform the activities at their own pace and convenience. A more detailed description of the protocol can be found in [16]. The second dataset, dataset II, consists of 5 healthy older adults, 2 male, 3 female. Data were gathered in the home environment of each subject with a similar three-phase protocol adopted. However, for this dataset the protocol was repeated over several days. Inclusion criteria for both datasets specified that the subject be capable of significant levels of mobility in their everyday routine and not be dependent on a walking aid. Table 4.2 summarises the two datasets.

### *4.3.2. Sensor Specification, Attachment & Software*

The same Bluetooth enabled triaxial accelerometer [27] was employed in gathering both datasets. Data were sampled at a frequency of 135Hz and at a range of +/- 6g (9.81 $m/s^2$). For all participants five kinematic sensors were attached at the following sites: (i) mid-sternum (ii) left side of the chest, (iii) above the right hip, (iv) wrist of the dominant hand and (v) ankle of the dominant leg.

**Table 4.1. List of Activities Performed**

| # | *Basic Activities of Daily Living (ADLs)* |
|---|---|
| 1 | Stand (30 seconds) |
| 2 | Lie Supine (60 seconds) |
| 3 | Lie Left Side (60 seconds) |
| 4 | Lie Right Side (60 seconds) |
| 5 | Walk on level Ground at normal speed (180 secs) |
| 6 | Jog (30 seconds) |
| 7 | Ascend stairs (16 steps) (30 seconds) |
| 8 | Descend stairs (16 steps) (30 seconds) |
| # | *Transitions* |
| 1 | Lie to Stand (30 seconds) (repeat x3) |
| 2 | Stand to Lie (30 seconds) (repeat x3) |
| 3 | Sit to Stand (30 seconds) (repeat x3) |
| 4 | Stand to Sit (30 seconds) (repeat x3) |
| # | *Instrumental Activities of Daily Living (iADLs)* |
| 1 | Make a sandwich, drink glass of water ~180 secs |
| 2 | Clean Windows (~120 seconds) |
| 3 | Dress (Shoes, shorts, jumper) (~120 seconds) |
| 4 | Stretch (Arms, Legs, Mid sternum) (~60 seconds each) |
| 5 | Vacuum floor (~120 seconds) |
| 6 | Computer Work (~180 seconds) |
| 7 | Read Newspaper (~180 seconds) |

**Table 4.2. Study Datasets**

| | *Dataset I: Healthy Younger Adults* | *Dataset II: Healthy Older Adults* |
|---|---|---|
| Age ($\mu \pm \sigma$) | $23.62 \pm 2.41$ | $60.40 \pm 6.95$ |
| Avg. Data Rec. (hours) ($\mu \pm \sigma$) | $3.01 \pm 0.31$ | $15.23 \pm 5.90$ |
| Sex | $10\ Male, 15\ Female$ | $2\ Male, 3\ Female$ |

Two of the sensors ((i) and (ii)) were attached using a specifically designed vest [28]. The waist sensor was attached with a belt-clip. The wrist and ankle sensors were attached using standard medical strapping. The sensor attached on the left side of the chest was orientated with the X-Axis in the anteroposterior (AP) axis, the Y-Axis in the longitudinal (LD) axis and the Z-Axis in the mediolateral (ML) axis of the subject. All other sensors were orientated with the X-Axis in the ML axis, the Y-Axis in the LD axis and the Z-Axis in the AP of the subject.

As discussed in [16] a software program deployed on a nearby laptop was used to synchronize, log and parse data for healthy younger adults from the first dataset. However, it was impractical to use the same hardware configuration in the home

**Table 4.3. Feature Set**

| # | *Time Domain Features* |
|---|---|
| 1-4 | First Four Moments |
| 5 | Zero Crossing Rate |
| 6 | Short Term Average Magnitude |
| 7 | Auto-Correlation |
| 8 | Cross-Correlation between all sensors |
| # | *Frequency Domain Features* |
| 1 | Dominant Freq. Comp. |
| 2 | Spectral Entropy |

environment with older subjects. Therefore, a new program was developed on an iPAQ 6915 [29]. Incorporating open-source software, 32-Feet.Net [30], a Windows Mobile 5 program to communicate with the accelerometer based sensors over a Serial Port Profile on a Widcomm / Broadcom Bluetooth stack was developed. Similar to dataset I, data gathered during phases one and three were annotated by the researcher who was present in the subject's home. However, data collected during phase two of the study were self-annotated by the subject by selecting from a dropdown list of activities in a simple GUI deployed on the iPAQ. A small tolerance level was incorporated as the subject marked the start and stop time of each activity; data within 15 seconds of each annotation were discarded, similar to published work [12].

### *4.3.3. Calibration & Feature Set*

The accelerometer based sensors were calibrated prior to attachment by rotation of the device through six different known angles as outlined by Bourke et al [31]. The site of attachment may cause unwanted misalignment or tilt of the sensor and to address this issue the accelerometer's capacity as an inclinometer was employed as outlined by Moe-Nilssen et al [32]. Table 4.3 summarizes the feature set calculated using a 128-sample sliding window with 50% overlap. This feature set was extracted for each sensor across each axis and is the same feature set calculated in previous work [16].

## *4.4 Classifier Specification*

In our previous work [16] we found that the boosting algorithm AdaBoostM1 with C4.5 Graft as its base-level classifier achieved an accuracy of 95% on dataset I. In this paper we build on these findings and explore SVMs with MKL. Therefore, the

boosting algorithm acts as a benchmark to which several combinations of SVMs with standard kernels and SVMs with MKL are compared. In the proceeding sections an overview of the various classifiers employed is given. As our core focus is SVMs with MKL these techniques are described in depth.

### *4.4.1. AdaBoostM1 & C4.5 Graft decision tree*

The construction of a decision tree can be defined recursively [33]. A specific feature is placed at the root node with a branch generated for each possible feature value which essentially generates data subsets. The process is recursively repeated for each subset and each feature until a class label is reached. The choice of which attribute to split on is based on a gain ratio; essentially the amount of information gained by making the decision at this node.

The boosting technique addresses the bias-variance error of a classifier [33]. The algorithm begins by assigning equal weights to all classes in the training set. It then trains the chosen base-level classifier on this dataset. Based on these initial results a reweighting of the classes is performed whereby the weight of correctly classified classes is reduced and that of incorrectly classified classes increased. In the next iteration the base level classifier is trained on this reweighted data and in turn a new-weighting scheme is derived. The scheme ceases once a predefined threshold is reached.

### *4.4.2. Support Vector Machine*

Support Vector Machines (SVMs) essentially address a binary classification problem. The primary objective is, dependent on the dimensionality of the problem, to find a line, plane or hyperplane which *best* separates a given labeled dataset [34]. The two cornerstones of SVMs are the concept of employing the dot product as a similarity score and the use of the perceptron as a learning mechanism. For a detailed discussion of SVM theory the reader is referred to Appendix 4A. Given a training set of instance-label pairs $(x_i, y_i), i = 1 \dots l$ where $x \epsilon \mathbb{R}^n$ represents a feature vector and $y \epsilon \{1, -1\}^l$ represents class labels then a SVM requires the solution to a quadratic optimization problem defined by Equation 4.1

$$\min_{\overline{w},\xi,b}\phi(\overline{w},\xi,b) = \min_{\overline{w},\xi,b}\left(\frac{1}{2}\overline{w}\cdot w + C\sum_{i=1}^{l}\xi_i\right) \quad (4.1)$$
$$\text{s.t. } y_i(\overline{w}\cdot\bar{x}_i - b) + \xi_j - 1 \geq 0\,,\ \xi_j \geq 0\ \forall\ i\ and\ C > 0$$

The power of SVMs lies in the ease from which we can move from the linear to the nonlinear form. Through a technique known as the *kernel trick* we move from a space where data is not linearly separable, the input space, to a linearly separable higher dimensional space, the feature space. The choice of kernel is not arbitrary and must adhere to several constraints [34]. Table 4.4 summarizes several popular kernel functions and their respective parameters.

**Table 4.4. SVM Kernels**

| *Kernel* | $\kappa(\bar{x},\bar{y})$ | *Parameters* |
|---|---|---|
| Linear | $\bar{x}\cdot\bar{y}$ | *None* |
| Gaussian (RBF) | $e^{-(\gamma\|\bar{x}-\bar{y}\|^2)}$ | $\gamma > 0$ |
| Homo. Polynomial | $(\bar{x}\cdot\bar{y})^d$ | $d \geq 2$ |
| Sigmoid | $tanh(\gamma\bar{x}^T\bar{y} + \Theta)$ | $\gamma > 0, \Theta \in [-1,1]$ |

### *4.4.3. Multiple Kernel Learning*

As previously discussed feature-space mapping through the choice of kernel is highly dependent on the specific dataset with empirical grid searching techniques often employed. The method of MKL introduced by Bach et al. [35] addresses the issue of kernel selection. MKL takes as input $K$ kernels and evaluates various convex combinations as shown in Equation. 4.2

$$\kappa(\bar{x},\bar{y}) = \sum_{i=1}^{K}\lambda_i\kappa_i(\bar{x},\bar{y})\ \ where\ \lambda_i \geq 0, \sum_i \lambda_i = 1 \quad (4.2)$$

Essentially, we are searching for the weights $\lambda_i$ with higher weights attributed to more informative kernels. In this work practical implementation of the MKL technique was performed using SimpleMKL [36]. By employing semi-infinite linear programming the multiple kernel dual problem is defined by Equation 4.3

$$\max_{\alpha}\left(\sum_{i=1}^{l}\alpha_i - \frac{1}{2}\sum_{i,j=1}^{l}\alpha_i\alpha_j y_i y_j\left[\sum_{l=1}^{K}\lambda_l\kappa_l(\bar{x}_i,\bar{x}_l)\right]\right) \quad (4.3)$$
$$\text{s.t. } \textstyle\sum_{i=1}^{l}\alpha_i y_i = 0, \alpha_i = 0,\ \forall\ l\ \ \sum_l \lambda_l = 1\ \lambda_l > 0\ \forall\ l\ \ 0 \leq \alpha_i \leq C$$

This is equivalent to Equation 4.4

$$\min_{\bar{w},\xi,b,\lambda}\left(\frac{1}{2}\sum_{i=1}^{K}\frac{1}{\lambda_i}\bar{w}_i\cdot\bar{w}_i + C\sum_{i=1}^{l}\xi_{\mathrm{i}}\right) \qquad (4.4)$$
$$s.t.\ \mathrm{y_i}\sum_{i=1}^{K} w_i(\bar{x}_i) + \mathrm{b} \geq 1-\xi_{\mathrm{j}},\ \xi_{\mathrm{j}} \geq 0, \sum_i \lambda_i = 1\ \forall\ i\ and\ C > 0$$

A fixed weighting of kernels is used to final an initial $\alpha$ which in turn is used to solve for the equivalent kernel weights $\lambda_i$. This process is repeated until the convergence criterion is satisfied. For a detailed discussion the interested reader is referred to [36].

### *4.4.4. Classifier Software, Training & Testing*

The Waikato Environment for Knowledge Analysis (WEKA v3.6 [33] ) provides Java based implementations of AdaBoostM1, C4.5 Graft and SVMs with various kernels. Unfortunately, it does not yet include MKL for SVMs and therefore we utilized the open source Matlab (v. 7.11) library SimpleMKL [36]. Ten-fold cross validation and the one-against-one for multi-class SVMs was employed.

For all analysis datasets I and II were treated independently. Feature set reduction was performed using wrapper subset evaluation with a linear forward search in WEKA. Similar to our previous work the wrapper evaluation was performed three times with a different base-classifier each time: C4.5 Graft, SVM (RBF kernel) and BayesNET respectively [16]. An interesting advantage of the MKL technique is that it provides implicit feature ranking through the weights and therefore we also used SVM with MKL using an RBF kernel to generate a comparable reduced feature set.

Two approaches were used for classifier training and testing

- *User Specific*: Classifiers were trained on individual subject data gathered during phases one and three of the study and tested on that subjects' phase two data.
- *Leave One-Subject Out*: Classifiers were trained on data from all three phases for all subjects except one. The classifiers were then tested on phase two data of the subject left out

Both approaches were repeated for all subjects using the reduced feature set. We adopted these techniques to investigate the relationship between subject dependant and subject-independent data. For both approaches a total of six classifiers were compared; AdaBoostM1 with C4.5, four SVMs with the various kernels from Table 4.4 and finally

an SVM with MKL. The free parameters of the various kernels were optimized using a grid searching technique. Specifically, the $\gamma$ parameter controls the width of the Gaussian kernel, the $d$ parameter controls the power of the polynomial kernel and finally the $\gamma$ and $\Theta$ parameters control the scaling and shifting of the sigmoid kernel respectively. In a similar manner the optimal cost parameter $C$ for all kernels was found. For the SVM with MKL analysis we allowed each feature in the reduced feature set be expressed by each kernel in Table 4.4. We further explored various combinations of kernels, e.g. 50% linear 50% gaussian etc. In this manner we essentially had ten SVM with MKL classifiers however, for brevity only the optimal results will be presented.

We also investigated the discriminatory power of each sensor location and the minimum number of sensors required to maintain a high degree of accuracy. Using the most accurate classifier found from the previous analysis the discriminatory powers of various combinations of sensors were compared for datasets I and II.

## *4.5 Results*

### *4.5.1. Reduced Feature Set*

Table 4.5 presents the result of the feature reduction process. The results of similar analysis on dataset I are reprinted in the left hand column for comparison [16].

**Table 4.5. Reduced Feature Set**

| # | *Dataset I* | *Dataset II* |
|---|---|---|
| 1 | Wrist Y-Axis mean | Mid sternum Z-Axis mean |
| 2 | Wrist Z-Axis avg. mag. | Wrist Z-Axis avg. mag. |
| 3 | Mid sternum Z-Axis mean | Ankle Z-Axis avg. mag. |
| 4 | Ankle v Wrist cross-corr | Wrist Y-Axis mean |
| 5 | Ankle Z-Axis avg. mag. | Mid strnm X-Axis avg. mag. |
| 6 | Ankle X Axis mean | Ankle v Wrist cross-corr |
| 7 | Ankle Y-Axis mean | Mid strnm v Waist cross-corr |
| 8 | Mid strnm Y-Axis Avg. mag. | Wrist X-Axis zero cross rate |
| 9 | Wrist Y-Axis mean | Wrist Y-Axis avg. mag. |
| 10 | Ankle X-Axis avg. mag. | Mid sternum X-Axis mean |
| 11 | Waist X-Axis entropy | Ankle X-Axis zero cross rate |
| 12 | Ankle v Waist cross-corr | Mid sternum Y-Axis mean |
| 13 | Waist Y-Axis entropy | Ankle v Waist cross-corr |
| 14 | Wrist X-Axis zero cross rate | Waist X-Axis zero cross rate |

### *4.5.2. Classifier Comparison*

Table 4.6 presents the results of the classifier comparison on datasets I and II respectively. Classifier accuracy is presented using the Kappa statistic [39]. As discussed in section 4.4.4 both datasets were compared using *User Specific* and *Leave One-Subject Out* Training. The accuracy of machine learning algorithms is inherently dependant on the amount of training data available and *Leave One-Subject Out* training has access to significantly more data than *User Specific* training. This issue was addressed by asking subjects to perform phase 3 of the protocol. Also, using re-sampling filters in the WEKA environment, a random sub-sample of the *Leave One-Subject Out* training set was generated for each subject. This subset is represented by column (3) in Table 4.6 and was designed to be equal in size to the corresponding *User Specific Training* set, therefore allowing a balanced comparison. Fig. 4.1 presents a ROC curve for the *Dressing*. The ROC curve is plotted with the True Positive Rate, the ratio of *Dressing* activities detected by the classifier to the total number of *Dressing* activities on the Y-Axis and the False Positive Rate, the ratio of *Dressing* activities erroneously detected by the algorithm to the total number of *non-dressing* activities, on the X-Axis. From the ROC curves we can determine if a classifier is conservative (low false positive rate) or liberal (high false positive rate). Furthermore, the Area under the ROC curve (AUC) is a useful and commonly used metric for comparing classifiers [37]. This is interpreted as the probability that the classifier ranks a randomly chosen positive instance above a randomly chosen negative instance [37]. Table 4.7 presents AUC values across several activities for both datasets calculated from the most informative sensors.

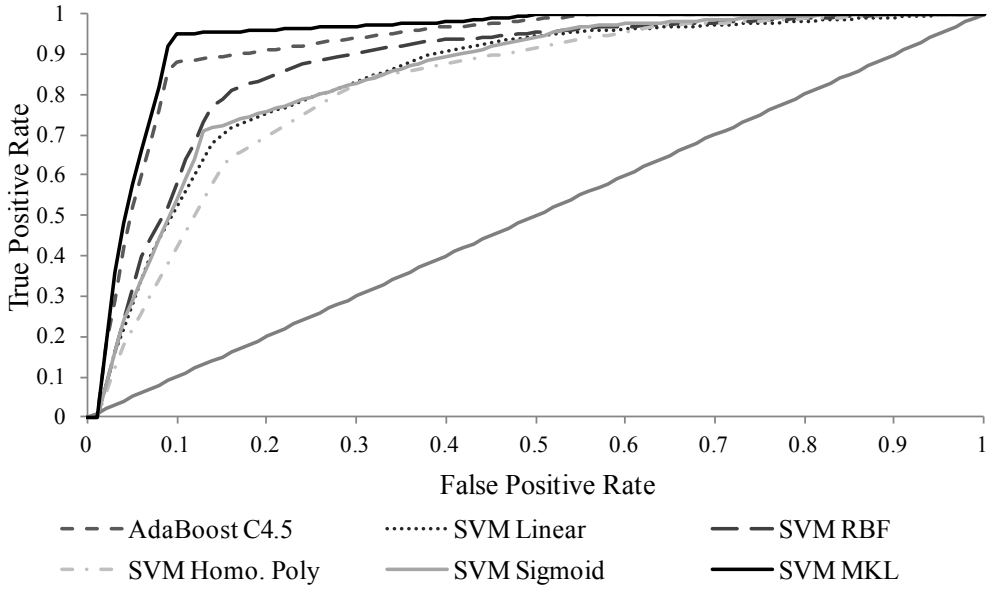


**Fig. 4.1.** ROC Curve for the activity *dressing*

**Table 4.6. Classifier Comparison Datasets I and II**

| *Classifier* | *Dataset I* | | | *Dataset II* | | |
|---|---|---|---|---|---|---|
| | (1) | (2) | (3) | (1) | (2) | (3) |
| AdaBoostM1 C4.5 | 0.83 | 0.95 | 0.92 | 0.71 | 0.75 | 0.73 |
| SVM Linear | 0.68 | 0.75 | 0.72 | 0.60 | 0.65 | 0.63 |
| SVM RBF | 0.78 | 0.86 | 0.83 | 0.63 | 0.67 | 0.65 |
| SVM Homo. Poly | 0.71 | 0.74 | 0.72 | 0.55 | 0.61 | 0.59 |
| SVM Sigmoid | 0.68 | 0.71 | 0.70 | 0.61 | 0.64 | 0.63 |
| SVM MKL | *0.89* | *0.97* | *0.95* | *0.78* | *0.86* | *0.83* |

(1) User Specific Training: Kappa Stat.
(2) Leave One-Subject Out Training: Kappa Stat.
(3) Down Sampled Leave One-Subject Out Training

**Table 4.7 AUC from Datasets I & II**

| *Task* | *Dataset I* | *Dataset II* | |
|---|---|---|---|
| | *AdaBoost* | *AdaBoost* | *SVM MKL* |
| Lie-to-Stand transition | 0.745 | 0.655 | 0.790 |
| Stand-to-Sit transition | 0.842 | 0.688 | 0.812 |
| Sit-to-Stand transition | 0.857 | 0.720 | 0.795 |
| Dressing | 0.921 | 0.755 | 0.810 |
| Cleaning Windows | 0.932 | 0.747 | 0.840 |
| Ascending / Descending Stairs | 0.948 | 0.705 | 0.863 |

### *4.5.3. Sensor Location Comparison*

Table 4.8 presents the results for sensor location comparison. Results for only *Leave One-Subject Out* training are reported.

**Table 4.8 Sensor placement comparison Datasets I & II**

| *Configuration* | *Dataset I* | *Dataset II* |
|---|---|---|
| All Sensors | 0.97 | 0.86 |
| Mid-Sternum, Wrist, Ankle | 0.89 | 0.81 |
| Wrist & Ankle | 0.88 | 0.75 |
| Ankle Only | 0.80 | 0.68 |
| Wrist Only | 0.78 | 0.66 |
| Mid Sternum Only | 0.76 | 0.67 |

## *4.6 Discussion*

### *4.6.1. Reduced Feature Set*

By analyzing the right hand column of Table 4.5 we can see that time domain features from the wrist, ankle and mid-sternum sensors were among the most informative features. Although, there is some overlap between the reduced feature sets for both datasets we note the mid-sternum sensor was not seen as important for features from dataset I. Furthermore, feature set reduction is not an exact science with plausible alternatives including correlation-feature selection [14], forward-backward searching [38] and the filter method [33]. Reassuringly, the reduced feature set generated by the SVM MKL weightings follows closely to that shown in Table 4.5.

### *4.6.2. Classifier & Sensor Location Comparison*

Results in Table 4.6 are presented using the Kappa statistic. There exists a considerable range of performance measures for binary classification problems including classification rate, precision, sensitivity, specificity, G-mean, F-score, Youden's index $\gamma$ and the Kappa statistic [39]. Each measure comes with its own advantages and disadvantages however, in multi-class problems, like the one we considered in this work, the most commonly used and applicable metrics are classification rate and the Kappa statistic [40]-[41]. Classification rate is the number of true positives relative to the total number of classifications [39]. The Kappa statistic evaluates the portion of true positives which can be attributed to the classifier itself

relative to all the classifications that be cannot be attributed to chance alone [40]. It is calculated as $\frac{P_0-P_c}{1-P_c}$ where $P_0$ is the total agreement probability and $P_c$ is the agreement probability which is due to chance. The statistic ranges from -1 implying total disagreement to 1 implying perfect agreement. Ben-David et al [40] conducted an extensive investigation of this statistic by comparing it with classification rate across 15 different datasets and 5 well-known classifiers. They found that the probability of a true positive being the result of mere chance was 33%. Therefore, the standard classification rate may under or over estimate the power of a classification scheme and the author recommends the application of the chance adjusted Kappa statistic. Of significant importance is that the Kappa statistic is affected by skewed distributions commonly known as the prevalence and bias problem [42] however, the dataset employed in this work did not suffer from such problems.

An SVM MKL mixture of 50% linear kernels and 50% Gaussian kernels achieved an accuracy of 0.97 and 0.86 for datasets I and II respectively. The reduction in performance for AdaBoostM1 C4.5 from dataset I to dataset II could be attributed to a smaller sample size however, it is more likely to be attributed to the increase in variance of activity performance across the older subject group. The results of dataset II reflect the real power of the MKL technique in allowing each feature select an optimal kernel. Furthermore, the SVM with RBF kernel classifier outperformed all other SVMs trained with individual kernels.

These results agree with published work. Gyllensten et al [17] achieved, in a laboratory environment, an accuracy of 95.1% using a single waist mounted triaxial accelerometer for 7 physical activities across 20 young subjects using an SVM with RBF kernel. Although, a comparable accuracy was achieved their activity set was smaller. Interestingly, classifier accuracy fell to 75.6% when tested outside the laboratory. We feel this further reflects the power of the MKL technique on dataset II however, we note our reduced sample size of 5 subjects. Fluery et al [20] achieved an accuracy of 86.21% classifying seven physical activities in a Smart Home using a range of sensors employing an SVM with Gaussian kernel. Interestingly, this work was further extended in [21] by considering spatial and temporal knowledge with slightly improved accuracy. Interestingly, the activity *Dressing* also proved difficult to classify in their

work; 80% recognition when combining spatial and temporal information. By analyzing Table 4.4 we can see that the MKL technique significantly outperforms this level. Zhang et al [22] conducted a large scale study monitoring 60 subjects wearing triaxial accelerometers attached to each wrist and the waist while they performed 16 semi-structured activities in a laboratory setting. Accuracy levels greater than 99% were achieved for C4.5 decision trees and an SVM with linear kernel. However, the 16 activities were subcategorized into four distinct labels; sedentary, household, walking and running and the authors' note this may have attributed to the accuracy levels.

For practical application of this work the classifiers should be robust and not require specific user training. From Table 4.6 we see that *Leave One-Subject Out* Training consistently outperforms *User Specific* Training. This result is consistent even when accommodation for sample size is made with *Down Sampled Leave One-Subject Out* Training, In Table 4.8 for dataset I the combination of wrist and ankle sensors maintained a comparably high accuracy as reflected by the dominant features in Table 4.5. For dataset II the combination of features attached at the mid-sternum, wrist and ankle maintained respectable accuracy levels. Previous work on this issue has shown that placement at the thigh and wrist [12], wrist and left hip [43] and waist and right-wrist [22] achieve relatively high recognition rates. While embedding sensors in wearable electronics for the wrist and ankle should be feasible attachment at the mid-sternum might pose additional difficulties.

In our previous work [16] we noted that dataset I is relatively homogeneous (10 males, 15 females, age: $23.62 \pm 2.41$, weight (kg): $71.84 \pm 5.38$, height (cm) $175.75 \pm 7.91$) and the lack of dispersion may have contributed to the power of *Leave One-Subject Out* training in that study. In our present work the characteristics of dataset II are (2 male, 3 female, age: $60.4 \pm 6.95$, weight (kg): $60.84 \pm 12.11$, height (cm) $148.55 \pm 9.14$). From observing subjects in both datasets we note that subjects in dataset II had considerably more difficulty completing tasks such as *Postural transitions*, *Ascending / Descending stairs*, *Dressing* and *Cleaning Windows* with some subjects halting for brief periods mid-task. Furthermore, the competency with which subjects completed tasks varied more dramatically in dataset II when compared with dataset I. By analyzing Table 4.7 we find that the SVM MKL mixture achieved higher

AUC metrics for dataset II across these difficult to classify activities when compared to AdaBoostM1 with C4.5. We note that the AUC values for dataset I come from wrist and ankle sensor data and the AUC values for dataset II comes from mid-sternum, wrist and ankle sensor data. That *Leave One-Subject Out* training outperformed *User Specific* Training across both datasets provides more confidence that user specific data are not required for classifier training.

## *4.7 Conclusion*

In this work the boosting classifier AdaBoostM1 with C4.5 Graft was compared to several SVMs built with various kernel functions and with SVMs built with Multiple Kernel Learning on the task of physical activity recognition. Two datasets of 25 young adults and 5 older adults were used with each subject wearing an array of triaxial accelerometers and completing a range of physical activities. An SVM MKL mixture of 50% linear kernels and 50% Gaussian kernels achieved Kappa statistics of 0.97 and 0.86 for young adults and older adults respectively. Furthermore, it was found that this classifier did not require subject specific training and a high level of accuracy could be maintained using sensors attached at the mid-sternum, wrist and ankle. Future work will explore expanding the older adult training set and incorporating more physical activities.

**Appendix 4A**

The first two cornerstones of SVM theory are the dot product and the separating hyperplane. Firstly, the dot product can be employed as a measure of similarity. Specifically, given two unit vectors $\bar{c} = (c_1, \cdots, c_n)$ and $\bar{d} = (d_1, \cdots, d_n)$ in $\mathbb{R}^n$, the dot product of $\bar{c} \cdot \bar{d}$ can be interpreted from a geometric perspective as $\bar{c} \cdot \bar{d} = |\bar{c}|\left|\bar{d}\right|cos(\gamma)$ where $\gamma$ is the angle between the two vectors. If the angle approaches $0^{\circ}$ then $\bar{c} \cdot \bar{d} \approx 1$ indicating similarity, if the angle approaches $180^{\circ}$ then $\bar{c} \cdot \bar{d} \approx -1$ indicating similarity but in opposite direction and finally if the angle approaches $90^{\circ}$ then $\bar{c} \cdot \bar{d} \approx 0$ indicating dissimilarity. Secondly, given a normal vector $\overline{w} = (w_1, \cdots, w_n)$, a position vector $\bar{x} = (x_1, \cdots, x_n)$ both in $\mathbb{R}^n$ and an offset term $b \, \epsilon \, \mathbb{R}$ then $\overline{w} \cdot \bar{x} = b$ describes a hyperplane in n-dimensional space. If this hyperplane separates our labeled data it can

be used in conjunction with the similarity interpretation of the dot product to define a decision function as

$$f(\bar{x}) = sgn(\overline{w} \cdot \bar{x} - b) \text{ s.t. } sgn(k) = \begin{cases} +1 & if \text{ k} \geq 0 \\ -1 & if \text{ k} < 0 \end{cases} \forall\, k \in \mathbb{R} \quad with\, \overline{w}, \bar{x} \in \mathbb{R}^n, b \in \mathbb{R} \tag{A4.1}$$

The next two cornerstones of SVM theory are the perceptron algorithm and maximum margin classifiers. A perceptron represents a decision function defined in Equation A4.2

$$\hat{f}(\bar{x}) = sgn\left(\sum_{k=1}^{n} w_k x_k - b\right) = sgn(\overline{\text{w}} \cdot \bar{\text{x}} - \text{b}) \tag{A4.2}$$

In the perceptron learning algorithm a greedy search heuristic is used where the values of $\overline{\text{w}}$ and b are adjusted through rotation and translation of the separating plane until a suitable decision surface is found. Importantly, the vast majority of the adjustments to the plane will occur for points at the boundary between the two classes, the points most difficult to classify. We now define a variable $a$ to count the number of adjustments with $a \approx 0$ for points easy to classify and $a \gg 1$ for points difficult to classify, e.g. points at the boundary. Significantly, we now no longer need to compute the normal vector but rather we can define it in terms of $a$

$$\overline{w} = \left(\sum_{i=1}^{l} a_i y_i \bar{\text{x}}_i\right) \tag{A4.3}$$

If we now substitute Equation A4.3 into Equation A4.1 we have

$$\hat{f}(\bar{x}) = sgn\left(\sum_{k=1}^{l} a_k y_k x_k \cdot \bar{\text{x}} - b\right) \tag{A4.4}$$

Equation A4.2 can be understood as the primal and Equation A4.4 as the dual of the perceptron problem.

Unfortunately, a significant drawback is that this decision surface is not guaranteed to be optimal, a problem addressed by maximum-margin classifiers. A decision surface is defined as optimal if it maximizes the margin from the supporting hyperplanes and is equidistant from each hyperplane. Furthermore, we can interpret the counter variables $a$ as support vectors which act as constraints on the supporting hyperplanes beyond which they cannot pass. Fortunately, such a problem is convex and

can be solved via quadratic programming techniques. Specifically, we define the maximum margin decision surface as:

$$\min_{\bar{w},b}\phi(\bar{w},b)=\min_{\bar{w},b}\frac{1}{2}\bar{w}\cdot\bar{w}\ \ st.\ y_i(\bar{w}\cdot\bar{x}_i-b)-1\geq 0\ \forall i \tag{A4.5}$$

Finally, by employing Lagrangian optimization theory we find that the dual of the maximum-margin classifier is the Linear SVM. For a full derivation the interested reader is referred to [34]. Given a linearly seperable training set where $x$ represents our feature vector and $y$ represents class labels, Equation A4.6 results

$$D=\{(\bar{x}_1,y_1,\bar{x}_2,y_2,\dots,\bar{x}_l,y_l)\}\subseteq\mathbb{R}^{\mathbf{n}}\times\{+1,-1\} \tag{A4.6}$$

then the Linear SVM is given by:

$$sgn\left(\sum_{i=1}^{l}\alpha_i^*y_i\bar{x}_i\cdot\bar{\mathrm{x}}-\sum_{i=1}^{l}\alpha_i^*y_i\bar{x}_i\cdot\bar{x}-\bar{x}_{SV^+}+1\right) \tag{A4.7}$$

where sv is a point $(\bar{x}_i,y_i)\in D$ whose Lagrangian multiplier > 0

We define a kernel function $\Phi(\bar{\mathrm{x}})$ to map from input space to feature space.

$$\hat{f}(\bar{x})=sgn(\bar{w}\cdot\Phi(\bar{\mathrm{x}})-\mathrm{b})=sgn\left(\sum_{i=1}^{d}w_i\,z_i-b\right) \tag{A4.8}$$

However, in the format of Equation 4.8 the complexity of the decision function grows with the dimension of the feature space. Once again the power of the dual representation is employed. If we consider the dual of the normal vector given in Equation A4.9

$$\bar{w}=\left(\sum_{i=1}^{l}a_iy_i\Phi(\bar{x}_i)\right) \tag{A4.9}$$

our decision function is now

$$\begin{aligned}sgn(\bar{w}\cdot\Phi(\bar{\mathrm{x}})-\mathrm{b})&=sgn\left(\sum_{i=1}^{l}a_iy_i\Phi(\bar{x}_i)\cdot\Phi(\bar{x})-b\right)\\&=sgn\left(\sum_{i=1}^{l}a_iy_i(\bar{x}_i\cdot\bar{x})-b\right)\end{aligned} \tag{A4.10}$$

Essentially, the actual value of the dot product in feature space is computed in input space and the complexity of our function is now proportional to the number of support

vectors and not feature space dimensionality. By incorporating a kernel function $\kappa$ the new decision function is shown in Equation A4.11

$$\hat{f}(\bar{x}) = sgn\left(\sum_{i=1}^{l} \alpha_i \, y_i \kappa(\bar{x}_i \bar{x}) - b\right) \tag{A4.11}$$

One final but important modification to the classical SVM framework is the concept of slack variables. This adjustment is required as a real life dataset will be a combination of both signal and noise. Therefore slackness is introduced into the supporting hyperplanes and some training samples are allowed to lie on the wrong side of their respective hyperplane. Slack variables, $\xi_j$, are introduced into the primal optimization problem and their influence is controlled by a cost parameter C

$$\begin{gathered} \min_{\overline{w},\xi,b} \phi(\overline{w},\xi,b) = \min_{\overline{w},\xi,b}\left(\frac{1}{2}\overline{w}\cdot w + C\sum_{i=1}^{l}\xi_i\right) \\ \text{s.t. } y_i(\overline{w}\cdot \bar{x}_i - b) + \xi_j - 1 \geq 0\,,\ \xi_j \geq 0\ \forall\ i\ and\ C > 0 \end{gathered} \tag{A4.12}$$

Essentially a penalty term is introduced into the optimization and a trade-off between the size of the margin and the size of the error allowed is made. Selecting larger $C$ values will be seen as costly to the optimization and a small margin will be found. Conversely, a smaller $C$ value will induce a larger margin.

## *4.8 References*


[1]. Kinsella, K., & He, W. (2009). 'Census Bureau, International Population Reports. *An Aging World: 2008'*, [Online]. Available: www.census.gov/p95-09-1.pdf (Accessed: May 2012)

[2]. Forester, F., Smeja, M., & Fahrenberg, J. (1999). 'Detection of posture and motion by accelerometry: a validation study in ambulatory monitoring', *Computers in Human Behavior*, vol. 15(5), pp. 571-583.

[3]. Mathie, M. J., Coster, A. C., Lovell, N. H., Celler, B. G., Lord, S. R., & Tiedemann, A. (2004). 'A pilot study of long-term monitoring of human movements in the home using accelerometry', *Journal of Telemedicine and Telecare*, vol. 10(3), pp. 144-151.

[4]. Karantonis, D. M., Narayanan, M. R., Mathie, M., Lovell, N. H., & Celler, B. G. (2006). 'Implementation of a real-time human movement classifier using a triaxial accelerometer

for ambulatory monitoring', *IEEE Transactions in Information Technology in Biomedicine*, vol. 10(1), pp. 156-167.

[5]. Staudenmayer, J., Pober, D., Crouter, S., & Freedson, P. (2009). 'An artificial neural network to estimate physical activity energy expenditure and identify physical activity type from an accelerometer', *Journal of Applied Physiology*, vol. 107(4), pp. 1300-1307.

[6]. Mantyjarvi, J., Himberg, J., & Seppanen, T. (2001). 'Recognizing human motion with multiple acceleration sensors', *IEEE International Conference on Systems, Man, and Cybernetics*, vol. 2, pp. 747-752.

[7]. Parkka, J., Ermes, M., Korpipaa, P., Mantyjarvi, J., Peltola, J., & Korhonen, I. (2006). 'Activity classification using realistic data from wearable sensors', *IEEE Transactions of Information Technology in Biomedicine*, vol. 10(1), pp. 119-128.

[8]. Khan, A. M., Lee, Y. K., Lee, S. Y., & Kim, T. S. (2010). 'A triaxial accelerometer-based physical-activity recognition via augmented-signal features and a hierarchical recognizer', *IEEE Transactions in Information Technology in Biomedicine*, vol. 14(5), pp. 1166-1172.

[9]. Long, X., Yin, B., & Aarts, R. M. (2009). 'Single-accelerometer-based daily physical activity classification', *28th Annual International Conference of the IEEE in Engineering in Medicine and Biology Society*, pp. 6107-6110.

[10]. Minnen, D., Starner, T., Ward, J. A., Lukowicz, P., & Troster, G. (2005). 'Recognizing and discovering human actions from on-body sensor data', *IEEE International Conference in Multimedia*, pp. 1545-1548.

[11]. Lester, J., Choudhury, T., Kern, N., Borriello, G., & Hannaford, B. (2005). 'A hybrid discriminative/generative approach for modeling human activities', *19th International Joint Conference on Artificial Intelligence*, pp. 766-772.

[12]. Bao, L., & Intille, S. (2004). 'Activity recognition from user-annotated acceleration data', *Pervasive Computing*, vol. 3001, pp. 1-17.

[13]. Ravi, N., Dandekar, N., Mysore, P., & Littman, M. L. (2005). 'Activity recognition from accelerometer data', *Proceedings of National Conference Artificial Intelligence*, vol. 20, pp. 1541-1550

[14]. Maurer, U., Smailagic, A., Siewiorek, D. P., & Deisher, M. (2006). 'Activity recognition and monitoring using multiple sensors on different body positions', *Wearable and Implantable Body Sensor Networks*, pp. 4-6.

[15]. Ermes, M., Parkka, J., Mantyjarvi, J., & Korhonen, I. (2008). 'Detection of daily activities and sports with wearable sensors in controlled and uncontrolled conditions', *IEEE Transactions in Information Technology in Biomedicine*, vol. 12(1), pp. 20-26.

[16]. Dalton, A., & ÓLaighin, G. (2012). 'Comparing supervised learning techniques on the task of physical activity recognition', *IEEE Transactions on Information Technology in Biomedicine*, article in press.

[17]. Gyllensten, I. C., & Bonomi, A. G. (2011). 'Identifying types of physical activity with a single accelerometer: Evaluating laboratory-trained algorithms in daily life', *IEEE Transactions in Biomedical Engineering*, vol. 58(9), pp. 2656-2663.

[18]. Mannini, A., & Sabatini, A. M. (2011). 'On-line classification of human activity and estimation of walk-run speed from acceleration data using support vector machines', *33rd Annual International Conference of the IEEE Engineering in Medicine and Biology Society*, pp. 3302-3305.

[19]. Zhang, S., Rowlands, A. V., Murray, P., & Hurst, T. (2012). 'Physical Activity Classification Using the GENEA Wrist-Worn Accelerometer', *Medicine and Science in Sports and Exercise*, vol. 44(4), pp. 742-748.

[20]. Fleury, A., Vacher, M., & Noury, N. (2010). 'SVM-based multimodal classification of activities of daily living in health smart homes: sensors, algorithms, and first experimental results', *IEEE Transactions in Information Technology in Biomedicine*, vol. 14(2), pp. 274-283.

[21]. Fleury, A., Noury, N., & Vacher, M. (2010). 'Introducing knowledge in the process of supervised classification of activities of Daily Living in Health Smart Homes', *12th IEEE International Conference in e-Health Networking Applications and Services*, pp. 322-329.

[22]. Zhang, T., & Liu, P. (2006). 'Fall detection by wearable sensor and one-class SVM algorithm', *Intelligent Computing in Control and Information Sciences*, pp. 858-863.

[23]. Doyle, O. M., Temko, A., Marnane, W., Lightbody, G., & Boylan, G. B. (2010). 'Heart rate based automatic seizure detection in the newborn', *Medical Engineering & Physics*, vol. 32(8), pp. 829-839.

[24]. Lau, H. Y., Tong, K. Y., & Zhu, H. (2008). 'Support vector machine for classification of walking conditions using miniature kinematic sensors', *Medical and Biological Engineering and Computing*, vol. 46(6), pp. 563-573.

[25]. Filipovych, R., Resnuck, S., Davatzikos, (2011). 'MultiKernel Classification for Integration of Clinical and Imaging Data: Application to Prediction Cognitive Decline in Older Adults', *Machine Learning Medical Imaging*, pp. 26-29

[26]. Fletcher, T., Hussain, Z., Shawe-Taylor, J. (2010) 'Multiple kernel learning on the limit order book', *Proceedings Journal of Machine Learning Research*, vol. 11, pp. 167–174\

[27]. Witilt 3, Sparkfun (2011) [Online]. Available: www.sparkfun.com. (Accessed: June 2012)

[28]. Bourke, A. K., O'Donovan, K. J., & ÓLaighin, G. M. (2007). 'Distinguishing falls from normal ADL using vertical velocity profiles', *29th Annual International Conference of the IEEE Engineering in Medicine and Biology Society*, pp. 3176-3179.

[29]. HP iPAQ 6915 (2006) [Online]. Available: www.o2.co.uk/deviceinfo/device-pdfs/hpipaq6915eng.pdf (Accessed: May 2012)

[30]. 32Feet.net (2010) [Online]. Available: http://32feet.net/ (Accessed: Mar. 2012)

[31]. Bourke, A. K., O'Donovan, K. J., & ÓLaighin, G. (2008). 'The identification of vertical velocity profiles using an inertial sensor to investigate pre-impact detection of falls', *Medical Engineering & Physics*, vol. 30(7), pp. 937.

[32]. Moe-Nilssen, R., & Helbostad, J. L. (2002). 'Trunk accelerometry as a measure of balance control during quiet standing', *Gait & Posture*, vol. 16(1), pp. 60-68.

[33]. Witten, I. H. & Frank, E. (2005). '*Data Mining: Practical machine learning tools and techniques*', Morgan Kaufmann.

[34]. Hamel, L. (2009). '*Knowledge discovery with support vector machines'*, John Wiley

[35]. Bach, F. R., Lanckriet, G, & Jordan, M. I. (2004). 'Multiple kernel learning, conic duality, and the SMO algorithm', *21st International Conference on Machine Learning*, p. 6-10.

[36]. Rakotomamonjy, A., Bach, F., Canu, S., & Grandvalet, Y. (2008). 'SimpleMKL', *Journal of Machine Learning Research*, vol. 9, pp. 2491-2521.

[37]. Bradley, A. P. (1997). 'The use of the area under the ROC curve in the evaluation of machine learning algorithms', *Pattern Recognition*, vol. 30(7), pp. 1145-1159

[38]. Pirttikangas, S., & Nakajima, T. (2006). 'Feature selection and activity recognition from wearable sensors', *Ubiquitous Computing Systems*, vol. 4239, pp. 516-527.

[39]. Galar, M., Fernández, A., Barrenechea, E., Bustince, H., & Herrera, F. (2011). 'An overview of ensemble methods for binary classifiers in multi-class problems: Experimental study on one-vs-one and one-vs-all schemes', *Pattern Recognition*, vol. 44(8), pp. 1761-1776.

[40]. Ben-David, A. (2007). 'A lot of randomness is hiding in accuracy', *Engineering Applications of Artificial Intelligence,* vol. 20(7), pp. 875-885.

[41]. Ben-David, A. (2008). 'About the relationship between ROC curves and Cohen's kappa', *Engineering Applications of Artificial Intelligence*, vol. 21(6), pp. 874-882.

[42]. Gwet, K. (2002). 'Kappa statistic is not satisfactory for assessing the extent of agreement between raters', *Statistical Methods for Interrater Reliability Assessment*, vol. 1(6), p. 1-6

[43]. Olguın, D. O., & Pentland, A. S. (2006). 'Human activity recognition: Accuracy across common locations for wearable sensors'*, MIT Media Lab*

# CHAPTER V

# Development of a body sensor network to detect motor patterns of epileptic seizures

**Accepted**

Dalton, A., Patel, S., Chowdhury, A., Welsh, M., Pang, T., Schachter, S., ÓLaighin, G., & Bonato, P. (2012). 'Development of a body sensor network to detect motor patterns of epileptic seizures', *IEEE Transactions on Biomedical Engineering*, vol. 59 (11), pp. 3204-3211.

## *5.1 Abstract*

The objective of this work was the development of a remote monitoring system to monitor and detect simple motor seizures. Using accelerometer-based kinematic sensors, data were gathered from subjects undergoing medication titration at the Beth Israel Deaconess Medical Center. Over the course of the study subjects repeatedly performed a predefined set of Instrumental Activities of Daily Living (iADLs). During the monitoring sessions, EEG and video data were also recorded and provided the gold standard for seizure detection. To distinguish seizure events from iADLs we developed a template matching algorithm. Considering the unique signature of seizure events and the inherent temporal variability of seizure types across subjects, we incorporated a customized mass-spring template into the dynamic time warping algorithm. We then ported this algorithm onto a commercially available internet tablet and developed our body sensor network on the Mercury platform. We designed several policies on this platform to compare the tradeoffs between feature calculation, raw data transmission and battery lifetime. From a dataset of 21 seizures, the sensitivity for our template matching algorithm was found to be 0.91 and specificity of 0.84. We achieved a battery lifetime of 10.5 hours on the Mercury platform.

## *5.2 Introduction*

Epilepsy is one of the most common neurological disorders affecting almost 60 million people worldwide [1]. Epileptic seizures are the manifestation of abnormal hypersynchronous discharges of populations of cortical neurons. The most common form of seizure is a tonic-clonic episode in which a phase of tetanic muscle contraction (tonic) is followed by jerking of the affected body and limbs (clonic). Approximately 67% of seizure events are controlled through anticonvulsant drug therapy with a further 7-8% treated with neurosurgical procedures. However, there remains 25% of patients whose seizures cannot be fully controlled by available therapy [1]. For these patients, medication titration through long term monitoring and analysis of EEG and video data can assist in the management of their seizure events [2]. This approach has significant advantages including high specificity and sensitivity of event detection. Unfortunately, this methodology is practically only feasible for short periods of time and therefore

cannot be used to objectively quantify long-term seizure frequency. Furthermore, memory and consciousness may be affected due to complex seizure events, and thus, self-reporting of seizure incidence may be severely impaired [3]. However, seizure frequency is the primary criterion upon which physicians make treatment decisions; the effectiveness of a given pharmacological treatment is based on evaluating its impact on the frequency of seizure events over an extended period of time [1], [4].

In the context of epileptic seizure detection using accelerometers, the most significant work to date has been by Nijsen et al [5-8]. A total of 897 seizures were seen in 288 hours of data obtained from 18 patients with drug resistant seizures who experienced high seizure frequencies [5]. This study showed that accelerometry and EEG are complementary for seizure detection in a number of patients. A continuation of this work was seen in [7] where a system to support offline analysis of seizure events was designed by defining six features which represent the main characteristics of movement associated with tonic seizures. These features were incorporated into a Fisher's linear discriminant analysis and a successful detection rate of 0.80 and a positive predictive value of 0.35 was achieved. This work was extended further in [8] where several time frequency and time-scale methods were investigated. Other studies have concentrated on classifying seizures with EEG data. Classification methods include Neural Networks [9], zero crossing rate analysis [10], decision trees [11] and support vector machines [12]. By using accelerometer-based sensors, only seizures that express themselves in stereotyped motor behavior can be detected. Collectively, these are known as motor seizures and our work concentrates on simple motor seizures; specifically myoclonic (a sudden jerk) and clonic (rhythmic jerking) events.

Several key factors have contributed to a growing interest in the development of remote monitoring systems. Primary among these are the demands of an aging population. The proportion of elderly people (aged 65 or over) in the European Union is predicted to rise from 16.4% in 2004 to 29.9% in 2050. The elderly dependency ratio, the population aged 65 or more as a percentage of population aged between 15 and 64, will rise from 24.5% in 2004 to 52.8% in 2050 [13]. This trend is mirrored in the United States where in 2000, people aged 65 and older made up 12.3% of the population, while by 2030, they will constitute 19.2%, with growth projected to level off such that this

cohort represents 20% of the population in 2050 [14]. Secondary motivations are the ever increasing availability of high bandwidth public wireless networks and the advances in Micro-Electro-Mechanical Systems (MEMS) technology.

In the context of our current work the most pertinent publications have been by Jones et al [15-16] and Shoeb et al [17]. In [16], a Body Sensor Network (BSN) to warn of the onset of an epileptic seizure event was developed during the Dutch Freeband Awareness project. The algorithm is based on monitoring ECG data for a change in heart rate prior to or at the onset of a seizure event and the system performance measures that are key to the success of this network are also presented. In [17], a method of integrating seizure onset detection into a commercially available ambulatory EEG recorder was proposed with an algorithm based on support vector decomposition [12]. Lockmann et al [18] developed an accelerometer based device, SmartWatch, capable of detecting rhythmic, repetitive movement of an extremity. A similar "Motion Sensor" device was proposed in [19].

Considering that seizure frequency is the primary criterion for treatment decisions, the aging population, and recent technological advances we believe there exists both a need and the available hardware and software architectures to develop a real-time, seizure detection telemonitoring system. Within this work we have endeavored to develop such a system based on wearable kinematic sensors and internet tablet technology.

## *5.3 Materials & Methods*

### *5.3.1. Data Collection*

Five subjects were recruited; 2 male, 3 female (mean age: 37.6 SD: 14.63) and studied at Beth Israel Deaconess Medical Center. Each subject gave informed consent to a protocol approved by Spaulding Hospital Institutional Review Board. Subjects with non-motor partial seizures and unusually violent seizures were excluded.

**Table 5.1. Study Details & Seizure Events**

| # | Length of recording | Sensor Location | ADLs/iADLs Sessions | Seizures Avg. Len |
|---|---|---|---|---|
| 1 | 8H across 1 day | RH, RA, RL, LRL | 1 | 1 (15sec) |
| 2 | 20H across 3 days | All | 4 | 4 (22sec) |
| 3 | 42H across 5 days | All except RA | 8 | 2 (16sec) |
| 4 | 7H across 1 day | RH, LH, RA, LA | 1 | 6 (12sec) |
| 5 | 53H across 4 days / 3 nights | All except LRL LLL | 5 | 8 (21sec) |

RH: Right-Hand, LH: Left-Hand, RA: Right Arm, LA: Left Arm
RL: Right-Leg, LL: Left-Leg, LRL: Lower right leg, LLL: Lower left leg

In this paragraph, a brief overview of the methodology will be given with specific details provided in proceeding sections. For each subject data were gathered over several days with the subjects wearing the sensors for several hours each day (Table 5.1). When battery power was drained, sensors were replaced. The sensors were attached at several locations dependent on the severity of the subject's symptoms using latex-free COBAN. On each morning and evening of a recording session, a researcher would initiate and directly guide the subject through a predefined set of Activities of Daily Living (ADLs) and Instrumental ADLs (iADLs) (Table 5.2). Not all sessions could be completed for every subject. We wished to investigate iADLs which are similar in movement and duration to simple seizure events.

During the entire recording process EEG and video data were also recorded and the offline analysis of these data by EEG technicians provided the timestamps and gold standard detection of seizure event activity to annotate our data and define the specificity and sensitivity of our detection algorithm. Post the recording session data were filtered and passed through a template matching algorithm to identify seizure events. Independently, this algorithm was deployed and tested on a body sensor network based on commercially available sensor and cellular technology.

**Table 5.2. List of Activities Performed**

| # | ADLs | # | Transitions |
|---|---|---|---|
| 1 | Sit (30 seconds) | 4 | Sit to Stand (repeat x3) |
| 2 | Stand (30 seconds) | 5 | Stand to Sit (repeat x3) |
| 3 | Walk (60 seconds) | | |
| # | Instrumental Activities of Daily Living (iADLs) | | |
| 6 | Reach for a cup (repeat x3) | 8 | Comb hair (~30 seconds) |
| 7 | Brush teeth (~30 seconds) | 9 | Scrub hands (~30 seconds) |
| 10 | Ride Indoor Bicycle (Subject 5 only) | | |

### *5.3.2. Sensor Specification & Initial Data Processing*

In this study, we used the SHIMMER (Sensing Health with Intelligence, Modularity, Mobility, and Experimental Reusability) platform developed by Intel's Digital Health Group [20]. The sensor features dual radio functionality with a Roving Networks RN-41 Bluetooth Class 2 module and a Chipcon CC2420 IEEE 802.15.4 module which both communicate through a gigaAnt 2.4GHz Rufa antenna. SHIMMER also contains a Texas Instruments MSP430 microprocessor, a Freescale triaxial accelerometer, a rechargeable 250mAh lithium-ion battery and a MircoSD slot with a 2GB maximum flash storage which allows for approximately 40 days of continuous recording over 3 channels at a sampling rate of 100Hz. The device measures 1.75" x 0.8" x 0.5" and weighs approximately 10g.

Data from the SHIMMER sensors were calibrated and converted into G values ($m/s^2$) by rotating each axis of the sensor through its maximum and minimum orientation and then implementing standard calibration formulae [21]. The data were then high pass filtered with a $3^{rd}$ order elliptical filter. This filter serves to separate the two primary components of the accelerometer signal: the component from acceleration due to gravity and the component from acceleration of the body [21]. With a sampling frequency of 100Hz we used a sliding window of 100 samples in width to generate a feature set which included mean, standard deviation, variance, zero-crossing rate, RMS, approximate entropy and autocorrelation. We performed initial exploratory analysis of this feature space using Sammon's Mapping; a nonlinear transformation technique that maps a high-dimensional space to a space of lower dimensionality by minimizing the Sammon's Stress error function [22]. To investigate the discriminatory power of each individual feature, we calculated the separation between seizure events and ADLs / iADLs for each member of our feature set independently. If seizure events and ADLs / iADLs could be separated by individual features, then the power and resource demands on a mobile platform would be significantly reduced.

### *5.3.3. Template Matching Algorithm*

#### *5.3.3.1. Spring Template*

Considering the unique signature of a seizure event we also decided to investigate a template matching algorithm. We noted that our recorded seizure events exhibited a distinct spring like signature at the initiation and conclusion of each seizure event as can be seen in Fig. 5.1. We therefore adopted a customized spring signal as our template.

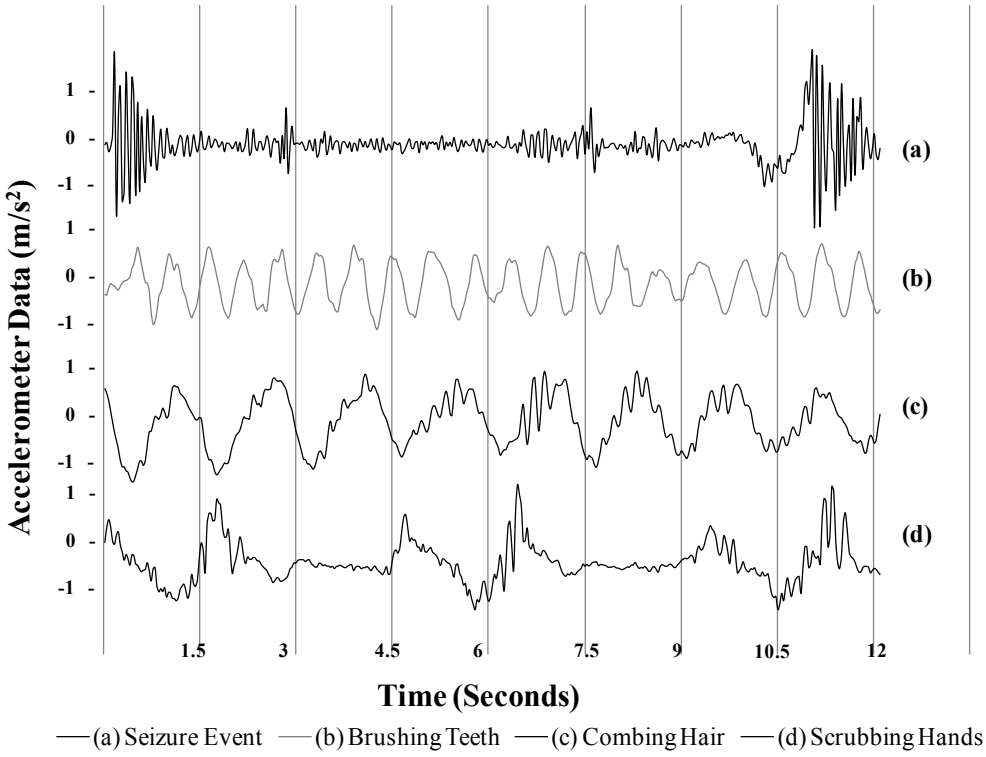


Fig. 5.1 Data recorded from a seizure event and three iADLs

The equation of motion of a spring is defined by the second order linear differential equation

$$x'' = -\frac{k}{m}x - \frac{b}{m}x' \tag{5.1}$$

where $x$ is the position of the object, $m$ is the objects mass, $k$ is the spring stiffness and $b$ is a damping factor (friction).

#### *5.3.3.2. Dynamic Time Warping*

A non-trivial problem resides in the inherent temporal variability of seizure types across subjects. Accelerometry data from seizure events will be of different lengths, either compressed or stretched, dependant on the particular patient and severity of their symptoms. Therefore, we decided to incorporate the Dynamic Time Warping (DTW) algorithm [24] which takes such temporal nonlinearities into account.

The DTW algorithm recovers optimal alignments between two time sequences of different durations. This *Warp-Path* minimizes a cumulative distance measure consisting of 'local' distances between aligned samples. The input signal, in this case our accelerometer data, is considered as a sequence of $n$ samples; $X = [x_1, x_2, x_3, \dots x_n]$ and the template, in this case our spring template, is considered a sequence of $m$ samples; $Y = [y_1, y_2, y_3, \dots y_m]$. The DTW algorithm builds a matrix, $D[n \times m]$, in which each element represents the distance, $(x_i - y_j)^2$, between the *i-th* element of $X(i)$ and the *j-th* element of $Y(j)$. We then define the *warping path* $W$ as a contiguous set of matrix elements that defines a mapping element between $X$ and $Y$. The *k-element* of $W$ is defined as $w_k = (i, j)_k$:

$$W = w_1, w_2, w_3, \dots, w_k \tag{5.2}$$

The warping path is subject to several constraints; specifically, continuity restrictions which restrict the number of allowable steps in the warping path to adjacent cells in the matrix, boundary restrictions which require that the warping path must start and finish in diagonally opposite corner cells of the matrix and finally the warping path must be monotonic. There exist numerous warping paths that satisfy these requirements however, we are only interested in the path that minimizes the *warping cost*.

$$\mathrm{DTW(X,Y)} = \min\left\{\sqrt{\sum_{k=1}^{k} w_k}\right\} \tag{5.3}$$

This path can be found using dynamic programming to evaluate a recursive equation which defines the cumulative distance $\Phi(i, j)$ in the current cell and the minimum of the cumulative distances of the adjacent elements.

$$\Phi(i,j) = d(x_i, y_i) + min\begin{Bmatrix} D(i, j-1) \\ D(i-1, j) \\ D(i-1, j-1) \end{Bmatrix} \tag{5.4}$$

For our dataset, seizure duration ranged from 12-25 seconds and the average duration of the distinct spring like signature at the initiation and conclusion of a seizure event was 1 second (Fig. 5.1). The DTW algorithm, in its raw format, has a quadratic time and space complexity ($O(n^2)$) and is thus suitable for this problem as our seizure events are of short-duration. With a sampling frequency of 100Hz and a sliding window of 1 second this led to a DTW matrix of $[128 * 128]$ samples. In our Body Sensor Network discussed later we also employed fixed rather than dynamic memory allocation to improve memory and CPU usage [23]. For a full description of the DTW algorithm, the reader is referred to [24]. We defined a motor activity as a seizure event as follows: if the warping cost fell below a defined threshold, it was considered a potential seizure event and if the warping cost fell below the threshold again within the next 25 seconds, it was marked as an actual seizure event. This constraint of requiring a second occurrence of the template helps reduce false detections caused by short-term seizure-like motor activities and a similar approach was adopted in [16]. We split our dataset into training and test sets (60 / 40 split) and recursively tested a range of parameters for the differential equation of the spring to find the optimized template in the training set. For each iteration we ran the updated template across our test set and as noted in section 5.3.2 we used the offline analysis of the EEG and video data as the gold standard detection of seizures.

### *5.3.4. Body Sensor Network*

One of our primary objectives was the development of a practical, real-time, telemonitoring system. At this initial stage of research our BSN could not be deployed on subjects and thus we present a proof of concept although the capacities of the developed system were evaluated on real subject data. After careful consideration of several platforms we decided to base our development on the Nokia N810 internet tablet [25] (Fig. 5.2). This Linux-based device provides both USB client and host mode functionality, native support for C \ C++, a 400MHz processor and 2GB of internal memory. One severe drawback was that the device does not incorporate cell-phone capability however, this comes as standard in the N900.

The hardware components of our BSN consist of a Tmote base-station (Fig. 5.2 (C)) running TinyOS 2.0 connected to an N810 (Fig. 5.2 (A)) in USB host mode. This base-station communicates over an 802.15.4 protocol to several SHIMMER sensors (Fig. 5.2 (B)) attached to the subject which transmit recorded accelerometry data to the base-station. On occurrence of a seizure event an alert message is sent to a specified emergency number via Wi-Fi or GSM (N900). The N810 has a built-in GPS receiver and thus the longitude and latitude of the subject is encoded within the alert message.

The software component of our BSN is based on Mercury, a platform for motion analysis of patients with neuromotor disorders [26]. Mercury is designed to overcome the challenges of long battery lifetime and high data fidelity and provides a high-level programming interface to develop policies for driving data collection and tuning sensor lifetime. Within Mercury the sensor node software is implemented in NesC using the Pixie operating system. We based our N810 software development on the Maemo SDK [27]. Using these and other tools we deployed Mercury and our seizure detection algorithm on the N810.

### *5.3.5. Mercury Driver Policies*

To test the robustness and performance of our BSN, we designed several driver policies on the Mercury platform. For the driver policies (1) and (2) we simulated a real-life data collection scenario by transmitting data from several SHIMMER sensors attached to a healthy subject while simultaneously executing the seizure detection algorithm on real data gathered during the initial study stored locally on the device. We also wanted to explore some of the more powerful components of the Mercury platform such as on-node feature calculation and energy schedulers. The drawback of these components is that they are not compatible with our current template matching algorithm and thus, we developed further driver policies, (3) and (4), from the perspective of a generic evaluation of our BSN.

The N810 incorporates a CPU scaling governor which allows for various power configurations. For each driver policy, the governor was set to OnDemand which opportunistically throttles down the CPU to 165MHz [25]. The battery of the N810's 1500mAh lithium-ion battery and the CPU load were logged using a python script.

#### *5.3.5.1. Standard Driver*

After establishing reliable communication between the N810 and SHIMMER sensors, the standard driver performed round-robin downloads from each sensor to the N810 which simultaneously executed the seizure detection algorithm.

#### *5.3.5.2. Activity Filter Driver*

The activity-filter driver policy saves energy during periods of sensor inactivity. The sensor calculates the signal magnitude of accelerometer data and only transmits data when an activity threshold is exceeded. We defined this threshold by calculating the signal magnitude of the data gathered from our study population while at rest.

#### *5.3.5.3. On-Node Feature Calculation Driver*

Mercury provides the option of calculating and transmitting feature blocks in real-time on the SHIMMER sensor. To date it implements a feature set including: peak velocity, maximum peak-to-peak amplitude, mean, RMS, and RMS of the jerk. The use of feature blocks over raw sample blocks provides a significant advantage in both on-node storage and power usage [26]. We used a driver policy that continuously transmits the complete feature set to the N810.

#### *5.3.5.4. Lifetime-Target Driver*

One of the most powerful tools on the Mercury platform is the ability to define a lifetime target. Based on initial battery capacity, radio bandwidth, energy measurements and a battery lifetime target the base-station can schedule data transmissions from SHIMMER nodes in an opportunistic fashion. Data will only be downloaded if the sensor has "excess energy" according to the energy scheduler. The driver qseudocode is presented in Lorincz et al [26]. Essentially, the driver will not download data unless it has surplus energy.

## *5.4 Results*

### *5.4.1. Visualization of Feature Space*

The results of initial inspection of the feature space using Sammon's Mapping can be seen in Fig. 5.3 in which we have grouped ADLs and iADLs together.

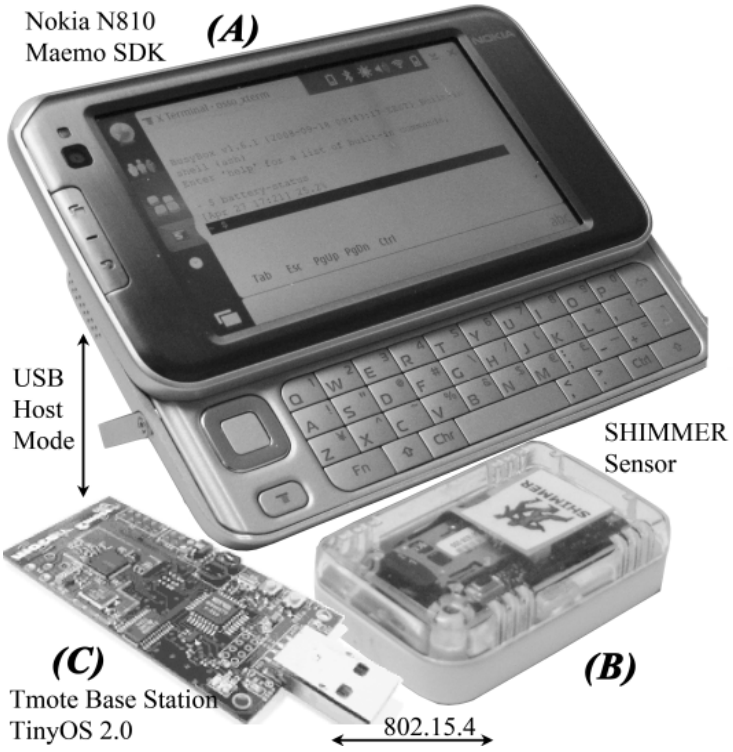


Fig. 5.2: Hardware components of the BSN.

(A) Nokia N810, (B) SHIMMER sensor, (C) TMote Basestation

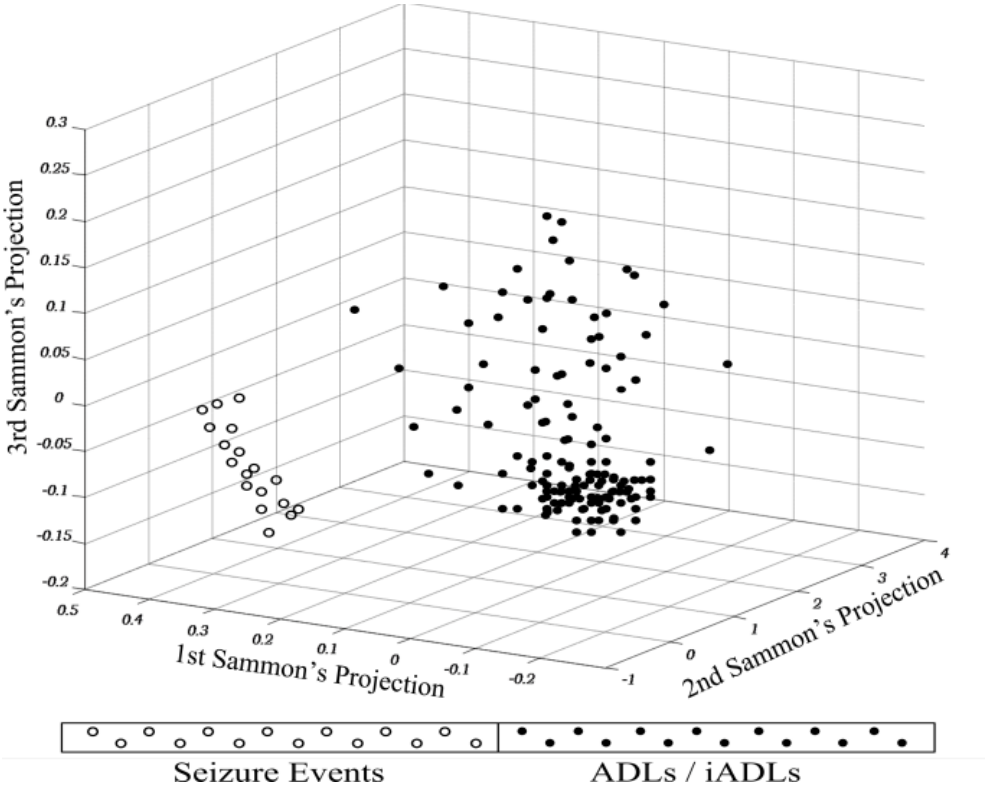


Fig. 5.3. Sammons Map of Feature Space

### *5.4.2. Individual Feature Analysis*

From our investigation of the discretionary power of individual features, we found the strongest separation for RMS. Fig. 5.4 presents the respective box plots for iADLs and seizure events for one subject.

### *5.4.3. Template matching Algorithm*

We note that we did not test the discriminatory power of the spring template individually; rather, all analysis was performed incorporating the DTW algorithm. The box plot in Fig. 5.5 and the receiver operator characteristic (ROC) curves shown in Fig. 5.6 represent the results of our template matching algorithm using a spring template and incorporating the DTW algorithm. The ROC curve is plotted with the True Positive Rate, the ratio of seizure events detected by the algorithm to the total number of seizure events, on the *Y*-Axis and the False Positive Rate, the ratio of seizure events erroneously detected by the algorithm to the total number of non-seizure events, on the *X*-Axis. The three ROC curves represent various combinations of parameters for the differential equation of a spring.

### *5.4.4. Sensor Network Driver Policies*

As described in section 5.3.4 we ported our seizure detection algorithm onto the N810 and tested the robustness of our BSN by developing several driver policies on the Mercury platform. Fig. 5.7 presents the battery lifetime of the various policies. We also calculated the average CPU usage of the N810 for each driver policy over the length of the BSN evaluation. To place these results in context, we also present battery and CPU usage for two extreme states of the N810:

*Idle:* In this state, GPS, Wi-fi and Bluetooth were off (flight mode), the backlight was set to minimum brightness and the CPU scaling governor was set to *Powersave.* This policy uses a more assertive algorithm then the *OnDemand* policy

*Aggressive:* In this state, GPS, Wi-fi and Bluetooth were on, the backlight was set to full brightness and the CPU scaling governor was set to *Performance*. With this policy the N810 does not throttle down and is kept at a constant 400MHz.

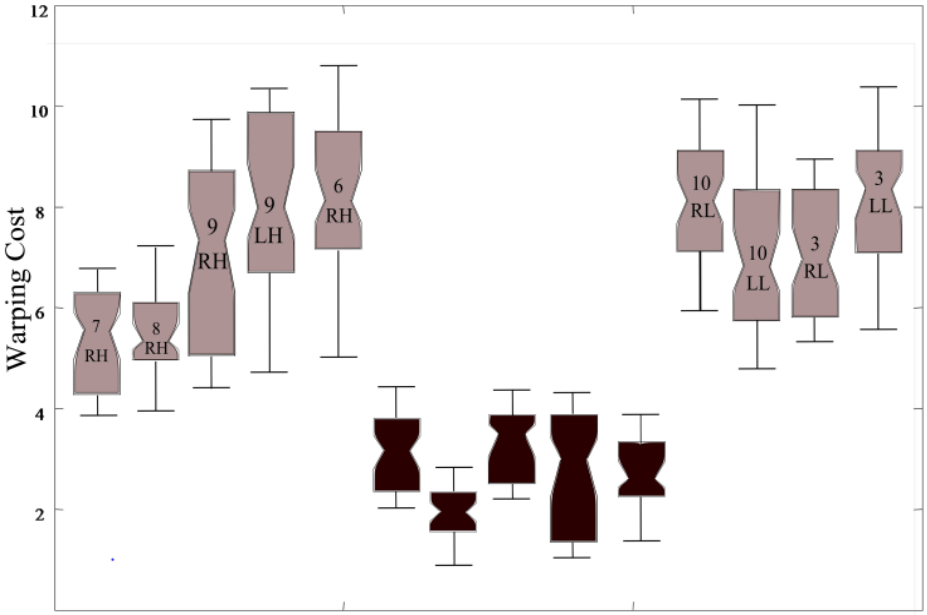


The values within the grey boxplots correspond to the activities in Table 5.2.
The black boxplots represent seizure events.
The boxplots were generated on data from subject 5
RH: Right Hand. LH: Left Hand. RL: Right Leg. LL: Left Leg

Fig. 5.4. RMS Boxplots

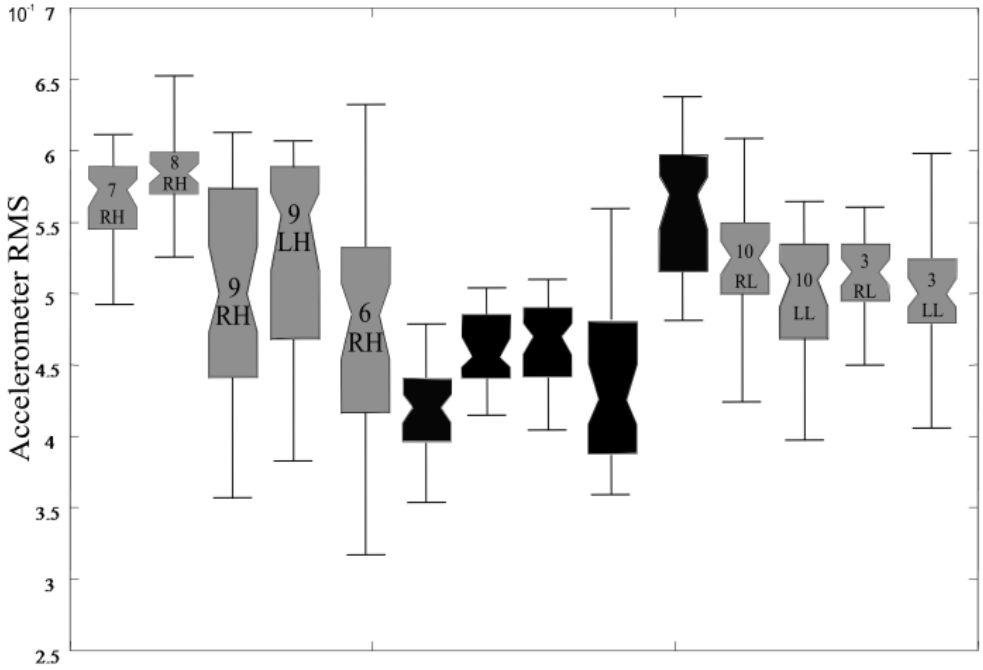


The values within the grey boxplots correspond to the activities in Table 5.2
The black boxplots represent seizure events.
The boxplots were generated on data from subject 5
RH: Right Hand. LH: Left Hand. RL: Right Leg. LL: Left Leg

Fig. 5.5. Boxplots for spring template and DTW

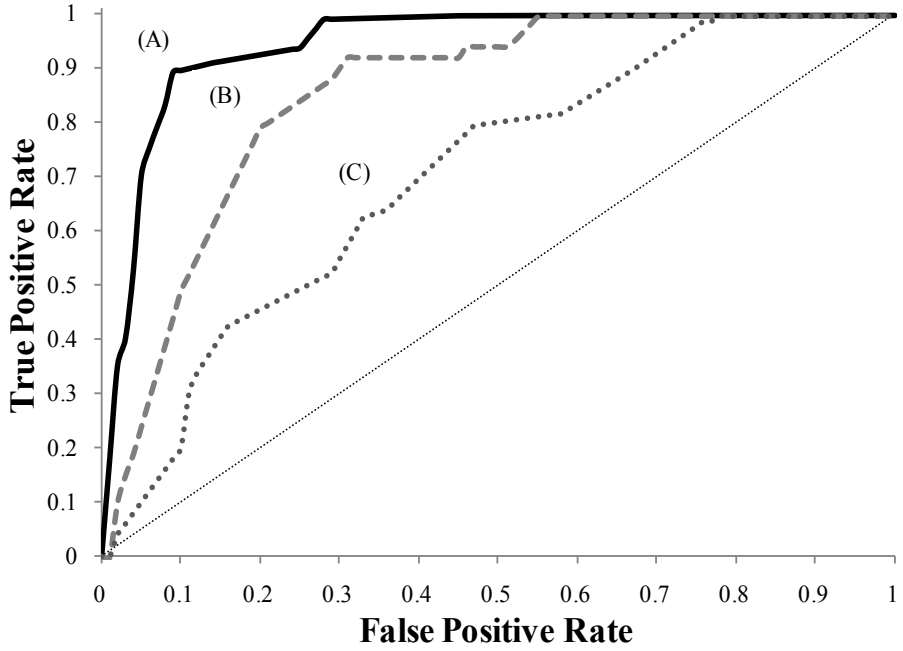


a) Mass (m) = 50. Spring Stiffness (k) = 40. Damping Factor (b) = 4
(b) Mass (m) = 30. Spring Stiffness (k) = 10. Damping Factor (b) = 2
(c) Mass (m) = 20. Spring Stiffness (k) = 3. Damping Factor (b) = 2
Fig. 5.6. ROC Curve for various spring templates and DTW

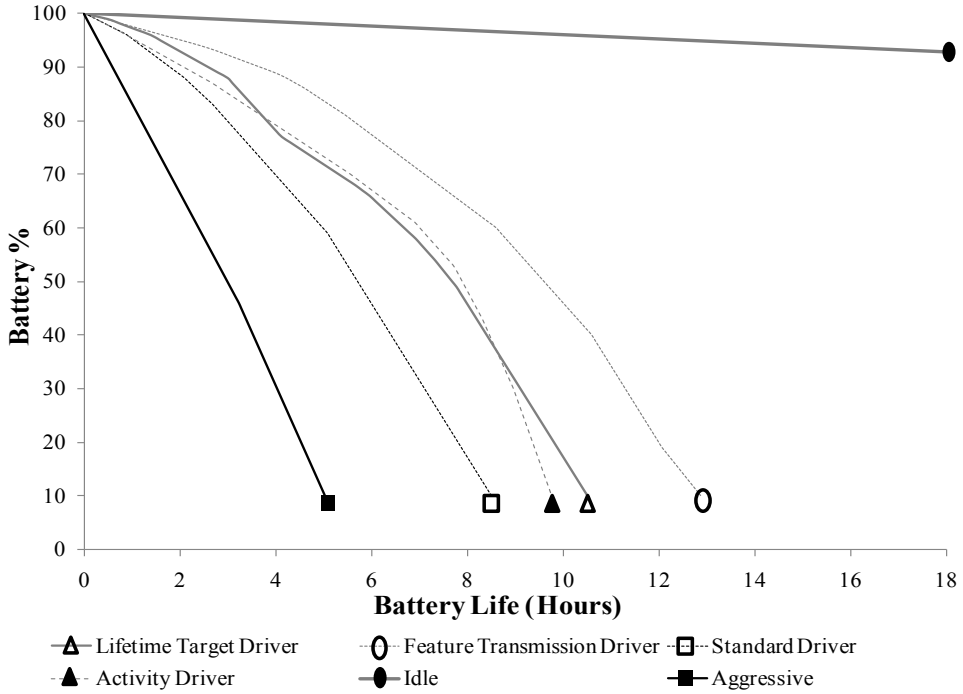


Fig. 5.7. Mercury driver policies battery lifetime

## *5.5 Discussion*

### *5.5.1. Analysis of Feature Space*

Within the Sammon's Map in Fig. 5.3, the seizure events and ADLs / iADLs form unique clusters and demonstrate strong separation. This analysis suggested that individual features may serve to distinguish seizure events. However, by analyzing Fig. 5.4 we can see that even the most robust feature failed to demonstrate any separation. We further investigated the discriminatory power of combinations of features but found no improvement in separation, and thus, we proceeded to investigate the potential of the template matching approach. These findings are in contrast to those reported by Schul et al [28] where a threshold based detection system achieved a sensitivity of 1 and specificity of 0.88 on a dataset of 4 seizures. The sensitivity and specificity in our dataset for RMS was very poor, 0.13 and 0.25 respectively. It is difficult to make statistically sound comparisons as both datasets are preliminary in nature. Deeper research into various non-linear combinations of these features such as decision tress or support vector machines would be of considerable interest.

### *5.5.2. Template Matching Algorithm Evaluation*

In Fig. 5.5, we can see the significant improvement in separation between seizure events and ADLs / iADLs although some overlap still exists. Some minor confusion still exists between the activities *Combing Hair / Brushing Teeth* and seizure events. This is to be expected as the motor activities for these movements are quite analogous. Analyzing Fig. 5.6 the sensitivity for our template matching algorithm was found to be 0.91 and specificity of 0.84. In our dataset we had 19 ADL / iADL sessions and from this we gathered 305 distinct ADLs / iADLs. A specificity of 0.84 yielded 50 false positives. Nijsen et al [8] investigated various time frequency and time-scale methods for seizure detection. A sensitivity of 0.80 and specificity of 0.87 across their entire dataset was achieved. While we achieved higher performance measures, our dataset was smaller and less diverse. Interestingly, Nijsen et al [8] is capable of distinguishing between tonic and clonic seizure events. Shoeb et al [17] developed a real-time patient-specific seizure onset detector based on support-vector decomposition of EEG data. Although the real-time implementation was not thoroughly tested on actual subject data

an offline analysis of the algorithm achieved a sensitivity of 97% with the support vector trained on three previous seizure events. From 139 seizures it declared 15 false positives. The *SmartWatch* proposed in [18] correctly indentified 7 out of 8 seizure events. However, a drawback of this system is the high-rate of false positives (204). Specifically, the authors note problems with iADLs; an issue our template matching algorithm addresses in our small dataset. A further improvement to our work would be incorporation of a cost matrix into the algorithm, such that false positives are attributed a higher cost. However, such an implementation is more suited towards supervised learning algorithms such as decision trees and Support Vector Machines.

Although we observed the distinct spring like signature across the dataset we cannot draw statistically significant conclusions until a larger sample size is analyzed. However, we believe that this is a step closer to a reliable seizure detection algorithm.

### *5.5.3. Body Sensor Network Evaluation*

In [29] several key parameters of a practical remote monitoring system are discussed with battery lifetime and wearability identified as primary factors. By analyzing Fig. 5.6 we can see the upper and lower bounds for the N810's 1500mAh battery are approximately 5.75 hours (aggressive usage) and 250 hours (idle usage), respectively. Of our developed driver policies which simultaneously transmit data and run our seizure detection algorithm, ((1) and (2)), the activity-filter driver lasts for approximately 10.5 hours with the standard driver lasting approximately 9 hours. This improvement in lifetime is explained by its reduced CPU usage of 7.1% versus 9.3% for the standard driver.

For the driver policies lifetime target driver and on-node feature calculation, we see a battery lifetime of approximately 11 and 14 hours with CPU usage of 6.9% and 4.8% respectively. For both drivers, we did not run the seizure detection algorithm. In an ideal environment, the on-node feature block represents 30 seconds worth of data, consumes 600 bytes of flash memory and draws 249μJ during transmission whereas a sample block represents 1 second of data, consumes 1200 bytes and draws 19958μJ to transmit an equivalent amount of data [26]. Thus, using the on-node feature calculation driver saves energy both on the SHIMMER nodes and the N810.

The performance of the lifetime-target driver is quite interesting. We set the lifetime target to 15 hours and, as noted in section 5.3.5.4, using an energy scheduler, the Mercury platform strictly adheres to this objective. However, the energy consumption of the various individual sensors on the SHIMMER node explains the poor performance of battery consumption on the N810 using this driver. Sampling the accelerometer consumes 2805μJ of energy whereas sampling the gyroscope consumes 53163μJ which is by far the most energy hungry operation on the node [26]. Disabling the gyroscope and continuously logging and transmitting accelerometry data will allow a SHIMMER node using a 250mAh battery to live for 22 hours. As further noted in Lorincz et al [26] the SHIIMER battery life plateaus for target lifetimes equal to or greater than 12 hours with all sensors enabled. We note that during our evaluation, both the gyroscope and the accelerometer sensors were enabled as future development of this BSN will incorporate the combined data. Setting a target lifetime of 15 hours ensures the SHIMMER nodes will have enough power to continuously transmit data and thus the performance of the lifetime target driver closely mimics the activity-filter driver, a result that is mirrored in CPU usage. Therefore, we conclude that while running our seizure detection algorithm with the activity-filter driver, the battery lifetime of our BSN is approximately 10.5 hours. In [16] a battery lifetime of 7.83 hours was achieved with a 3000mAh battery. Lockmann et al [18] achieved a battery lifetime of 30 hours. Finally, we note that our implementation of the DTW is not optimal. Improvements approaching linear space and time complexity could be achieved by implementing the FastDTW algorithm [30] which would also influence battery and CPU consumption.

In the context of wearability and high end-user compliance we believe our BSN has significant potential. The SHIMMER sensor is designed for research purposes and, thus, is not optimized for size and weight. Accelerometer based sensors can be easily incorporated into wearable devices with little inconvenience to the subject [17-18], Furthermore, the N810 is analogous in size and weight to the standard smart phone. We believe the battery life of the BSN should mimic that of modern smart phones which require, on average, charging once a day on moderate usage. As previously discussed the number of false positive may be addressed by a cost sensitive matrix with the design of such a matrix a compromise between accuracy and practicality.

## *5.6 Conclusion*

In this work we described the development of a BSN to detect motor patterns of epileptic seizures based on wearable kinematic sensors and the N810 internet tablet. The detection algorithm incorporates a mass-spring template into the dynamic time warping algorithm. From a sample set of 19 ADLs / iADLs sessions providing 305 unique ADLs / iADLs events and 21 seizure events from 5 subjects the algorithm achieves a sensitivity of 0.91 and specificity of 0.84 with a battery lifetime of approximately 10.5 hours for the BSN.

The proposed system has several limitations which provide significant opportunities for future exploration. Our sample size is not sufficiently large to draw statistically significant conclusions and, thus, as more data is collected rigorous analysis can be performed and other algorithms investigated. Additionally, battery consumption on the N810 warrants further investigation. If an algorithm to detect motor seizures based on features calculated on-node could be developed then battery lifetime could be significantly extended. Finally, the BSN is still in a proof of concept phase and thus must be evaluated in a real life scenario. We believe this work presents the first steps towards the development of a practical real-time, seizure detection telemonitoring system.

## *5.7 References*

[1] Witte, H., & L.D, Iasemidis., (2003) 'Special issue on epileptic seizure prediction', *IEEE Transactions in Biological Engineering*, vol. 50, pp. 537-539.

[2] Deckers, C., Genton, P., Sills, G., & Schmidt, D. (2003). 'Current limitations of antiepileptic drug therapy: a conference review', *Epilepsy Research*, vol. 53(1), pp. 11-17.

[3] Tatum IV, W. O., Winters, L., Gieron, M., Ferreira, J., & Liporace, J. (2001). 'Outpatient seizure identification: results of 502 patients using computer-assisted ambulatory EEG', *Journal of Clinical Neurophysiology*, vol. 18(1), pp. 14-19.

[4] Schmidt, D., Elger, C., & Holmes, G. L. (2002). 'Pharmacological overtreatment in epilepsy-Mechanisms and management', *Epilepsy Research*, vol. 52(1), pp. 3-14.

[5] Nijsen, T. M., Cluitmans, P. J., (2005) 'The potential value of 3-D accelerometry for detection of motor seizures in severe epilepsy', *Epilepsy Behaviour*, vol. 7, pp. 74-84.

[6] Nijsen, T. M., Cluitmans, P. J., Arends, J. B., & Griep, P. A. (2007). 'Detection of subtle nocturnal motor activity from 3-D accelerometry recordings in epilepsy patients', *IEEE Transactions in Biomedical Engineering*, vol. 54(11), pp. 2073-2081.

[7] Nijsen, T. M., Aarts, R. M., Arends, J. B., & Cluitmans, P. J. (2009). 'Automated detection of tonic seizures using 3-D accelerometry', *4th European Conference of International Federation for Medical and Biological Engineering*, pp. 188-191.

[8] Nijsen, T. M., Aarts, R. M., Cluitmans, P. J., & Griep, P. A. (2010). 'Time-frequency analysis of accelerometry data for detection of myoclonic seizures', *IEEE Transactions in Information Technology in Biomedicine*, vol. 14(5), pp. 1197-1203.

[9] Gabor, A. J., Leach, R. R., & Dowla, F. U. (1996). 'Automated seizure detection using a self-organizing neural network', *Electroencephalography and Clinical Neurophysiology*, vol. 99(3), pp. 257-266.

[10] Conradsen, I., Beniczky, S., Wolf, P., & Sorensen, H. B. (2012). 'Automated Algorithm for Generalized Tonic–Clonic Epileptic Seizure Onset Detection Based on sEMG Zero-Crossing Rate', *IEEE Transactions on Biomedical Engineering*, vol. 59(2), pp. 579-585.

[11] Qu, H., & Gotman, J. (1993). 'Improvement in seizure detection performance by automatic adaptation to the EEG of each patient', *Electroencephalography and Clinical Neurophysiology*, vol. 86(2), pp. 79-87.

[12] Shoeb, A., Edwards, H., Connolly, J., Bourgeois, B., Ted Treves, S., & Guttag, J. (2004). 'Patient-specific seizure onset detection', *Epilepsy & Behavior*, vol. 5(4), pp. 483-498.

[13] Eurostat (2005) '*Population Projections 2004-2050*', [Online] Available: www.europa.eu.int (Accessed: June 2012)

[14] United States Department of Commerce. Bureau of the Census. Population, (1996) [Online]. Available www.census.gov/idbpyr.html. (Accessed: Apr. 2012)

[15] Jones, V. M., Tonis, T., Bults, R. B., van Beijnum, B., & Hermens, H. (2008). 'Biosignal and context monitoring: Distributed multimedia applications of body area networks in healthcare', *10th IEEE Workshop in Multimedia Signal Processing*, pp. 820-825.

[16] AWARENESS (2010), '*Freeband AWARENESS project*', [Online] Available: http://www.freeband.nl/project.cfm?id=494&language=en (Accessed: Apr. 2012)

[17] Shoeb, A., Schachter, D., Treves, S. T., & Guttag, J. (2006). 'Detecting seizure onset in the ambulatory setting: demonstrating feasibility', *7th Annual International Conference IEEE Engineering in Medicine and Biology Society*, pp. 3546-3550

[18] Lockmann, J., Fisher, R. S., & Olson, D. M. (2011). 'Detection of seizure-like movements using a wrist accelerometer', *Epilepsy & Behavior*, vol. 20(4), pp. 638-641.

[19] Kramer, U., Kipervasser, S., & Kuzniecky, R. (2011). 'A novel portable seizure detection alarm system: preliminary results', *Journal of Clinical Neurophysiology*, vol. 28, pp. 36.

[20] SHIMMER. (2012) [Online]. Available: www.shimmer-research.com (Accessed: Feb. 2012)

[21] Mathie, M. (2003). 'Monitoring and interpreting human movement patterns using a triaxial accelerometer', Doctoral dissertation, The University of New South Wales.

[22] Sammon Jr, J. W. (1969). 'A nonlinear mapping for data structure analysis', *IEEE Transactions on Computers*, vol. 100(5), pp. 401-409.

[23] Niezen, G., & Hancke, G. P. (2009). 'Evaluating and optimising accelerometer-based gesture recognition techniques for mobile devices', *9th IEEE Region 8 Conference AFRICON*, 2009, pp. 1-6.

[24] Keogh, E., & Ratanamahatana, C. A. (2005). 'Exact indexing of dynamic time warping', *Knowledge and Information Systems*, vol. 7(3), pp. 358-386.

[25] Nokia Corporation, (2012) [Online]. Available: www.nokia.com//phones/ (Accessed: Feb. 2012)

[26] Lorincz, K., Chen, B. R., Challen, A. R., Patel, S., Bonato, P., & Welsh, M. (2009). 'Mercury: a wearable sensor network platform for high-fidelity motion analysis', *7th Annual Conference on Embedded Networked Sensor Systems*, pp. 183-196.

[27] Maemo Online, (2010) [Online]. Available: www.maemo.org/. (Accessed: Feb. 2012)

[28] Schulc, E., Unterberger, I., Hilbe, J., Ertl, M. & Them, C. (2011). 'Measurement and quantification of generalized tonic–clonic seizures in epilepsy patients by means of accelerometry—An explorative study', *Epilepsy Research*, vol. 95(1), pp. 173-183.

[29] Milenković, A., Otto, C., & Jovanov, E. (2006). 'Wireless sensor networks for personal health monitoring: Issues and an implementation', *Computer Communications*, vol. 29(13), pp. 2521-2533.

[30] Salvador, S., & Chan, P. (2007). 'Toward accurate dynamic time warping in linear time and space', *Intelligent Data Analysis*, vol. 11(5), pp. 561-580.

# CHAPTER VI

# Analysis of gait and balance through a single triaxial accelerometer in presymptomatic and symptomatic Huntington's disease

**Accepted**

Dalton, A., Khalil, H., Busse, M., Rosser, A., van Deursen, R., & ÓLaighin, G. (2012). 'Analysis of gait and balance through a single triaxial accelerometer in presymptomatic and symptomatic Huntington's disease', *Gait & Posture*, vol. 37(1), pp. 49-54.

## *6.1 Abstract*

*Purpose:* To investigate the capacity of a single triaxial accelerometer sensor in detecting gait and balance impairments in pre-manifest and symptomatic Huntington's disease (HD) subjects.

*Methods*: Fourteen manifest HD (MHD) (age: $51.83 \pm 14.8$), ten pre-manifest HD (PHD) (age: $44.8 \pm 11.7$) and ten healthy subjects (HLY) (age: $56.4 \pm 10.9$) were recruited. The sensor was attached to the upper sternum as subjects completed gait and Romberg balance tests. An inverted pendulum model of the body's centre of mass and an unbiased autocorrelation procedure were employed to derive gait parameters from the triaxial accelerometer signal. The accuracy of the gait measurements were compared to those recorded by a computerized walkway.

*Results*: Strong agreement was seen between the sensor and the walkway; cadence ($\text{ICC} = 0.95$ $\text{CI} = [0.75\ 0.97]$), velocity ($\text{ICC} = 0.94$ $\text{CI} = [0.75\ 0.97]$) and step length ($\text{ICC} = 0.89$ $\text{CI} = [0.77\ 0.95]$). Sensor derived velocity was significantly higher in HLY ($p < 0.001$) and PHD ($p < 0.005$) when compared to MHD. Step and stride length was significantly longer in HLY ($p < 0.05$) and PHD ($p < 0.001$) when compared to MHD. Significant differences between subject groups across all four balance tasks ($p < 0.0001$) were found.

*Conclusion:* An accelerometer based sensor may be an effective means of differentiating between pre-manifest and manifest Huntington's disease subjects.

## *6.2 Introduction*

Huntington's disease (HD) is an autosomal dominant neurodegenerative condition with a principal symptom of progressive movement disorder [1]. The prevalence of the disease has been estimated at 4–10 affected individuals per 100,000 with higher incidence in women than in men. Considerable research has been conducted into the progression of gait disorder through the various stages of HD. Specifically, manifest HD (MHD) subjects experience decreased stride length, gait velocity and cadence [2-4], higher variability in stride length and step-time [5] and significant degradation in balance [4]. Further investigation into gait impairments in pre-manifest HD (PHD) subjects (gene carriers not yet demonstrating motor symptoms and functional

decline) has also generated attention. Rao et al [3] employed a computerized walkway and found PHD subjects demonstrated decreased gait velocity, stride length and time in double support. They further identified a high correlation between these gait parameters and predicted years to onset. Devlal et al [5], [7] investigated the role of akinesia in HD and found that PHD subjects demonstrated a shorter first step duration and lower-amplitude postural adjustments. Panzera et al [8] found MHD subjects generated significantly less rising force and significantly higher sway velocity at the centre of gravity while performing three functional postural tasks.

These studies highlight the advantages of quantitative gait analysis in HD populations however; laboratory-based systems are typically expensive and are not available in all clinical settings. Furthermore, Rao et al [9] has highlighted the limitations of ordinal based clinical tests by showing that the Functional Reach Test and the traditional Timed up and Go (TUG) test are not sensitive in detecting motor impairments in PHD subjects. Therefore, a significant interest has grown in the development of alternative gait analysis tools.

Accelerometry has shown significant potential in the measurement of spatio-temporal gait parameters [10-13] however, caution must be exercised as reduced accuracy at decreased gait speed has been shown for commercially available activity monitors [13]. By modeling the trajectory of the body's centre of mass using an inverted pendulum model Zijlstra et al [10] was able to accurately derive several gait parameters. Moe-Nilssen et al [11] demonstrated how an unbiased autocorrelation procedure may be employed to derive cadence and step length. Significantly, the autocorrelation method also provides the opportunity to calculate a measure of gait regularity and symmetry. These techniques demonstrated high reliability when applied to a population of 121 elderly by Bautsman et al [12].

Accelerometry has also been used to investigate balance [14-17]. O'Sullivan et al [14] demonstrated a high correlation between accelerometry and the Berg Balance Scale (BBS) in a population of 21 elderly subjects. Accelerometery measured during quiet standing has also been adapted to differentiate between young and old healthy subjects [15]. In a HD population fourteen MHD subjects demonstrated lower balance

confidence and impairments on clinical measures of balance when compared to nine healthy controls [17].

The objective of this study was to investigate the capacity of a single accelerometer based sensor to derive spatio-temporal parameters of gait and balance in a HD population and investigate its potential to differentiate between subject groups. This is a continuation of previously presented work where an investigation of an instrumented TUG test was performed [18].

## *6.3 Methods*

### *6.3.1. Participants*

Fourteen manifest HD (age: $51.83 \pm 14.8$), ten pre-manifest HD (age: $44.8 \pm 11.7$) and ten healthy subjects (age: $56.4 \pm 10.9$) were recruited from the South Wales HD service. All subjects gave their written informed consent before participation in accordance with local research ethics requirements (09/WSE02/24). The healthy (HLY) control group consisted of 2 students, 2 staff, 2 family members and 4 friends recruited from outside the University. The inclusion criterion for the PHD subjects was a positive genetic test for HD, a diagnostic confidence score of three or less as rated by a neurologist indicating the absence of definitive motor signs of HD. The inclusion criterion for MHD subjects was a positive genetic test for HD and a score of four on the motor diagnostic confidence scale of the Unified Huntington's Disease Rating Scale (UHDRS) [19]. This scale accesses motor function, cognition, behaviour and functional abilities therefore providing a uniform assessment of the clinical features and course of HD. Subject exclusion criteria included a history of coexisting neurological conditions such as stroke and severe visual problems. For HD subjects scores on the motor section of the UHDRS and the Total Functional Capacity (TFC) scale were recorded. The total motor score has 31 items with a maximum possible score of 124 (indicating maximum disability), and includes tests of chorea, dystonia, rigidity, bradykinasia, coordination, balance and gait.

### *6.3.2. Apparatus and procedure*

#### *6.3.2.1. Accelerometer*

An accelerometer based sensor [18] was attached to the thorax of each subject as they completed the clinical tests. The AD_BRC sensor contains a $\pm 2.5\text{g} - 10\text{g}$ triaxial accelerometer, a Texas Instruments microprocessor, a 2000mAh lithium-ion battery and samples data at a frequency of 250Hz. The sensor was calibrated prior to attachment by rotation of the accelerometer through six different known angles as outlined by Bourke et al [20]. To correct for any misalignment or tilt of the sensor caused by the site of attachment the accelerometer's capacity as an inclinometer was employed as outlined by Moe-Nilssen et al [15]. Data from the sensor were high-pass filtered with a 3rd order normalized elliptical filter with a passband frequency of 0.25Hz, 0.01 dB of ripple in the passband and 100 dB of attenuation in the stopband [10].

#### *6.3.2.2. Gait Analysis*

The inverted pendulum model proposed by Zijlstra et al [10] was used to extract spatio-temporal gait parameters. Furthermore, by employing an unbiased autocorrelation procedure [11] and subsequently analyzing the ratio of the correlation coefficients at the first and second dominant periods observations on gait regularity and symmetry were made. Step and stride regularity were calculated across the anteriorposterior (AP), mediolateral (ML) and longitudinal (LD) axes respectively. Coefficient of variation ($CV = 100 * \mu/\sigma$) for step time, step length, stride length and step time asymmetry [12] were also calculated. Step time asymmetry calculates the ratio of the difference between mean step time of individual legs to the combined mean step time of both legs. The accuracy of the accelerometer was gauged against the parameters provided by a GAITRite® system (CIR Systems, Inc.: Havertown, PA). This 4.8 meter long instrumented walkway uses embedded sensors to record pressure applied at each footfall as a function of time. Menz et al [21] investigated the reliability of the GAITRite® system in a young and old population in quantifying spatio-temporal gait parameters and reported excellent ICC values ($ICC = 0.88 - 0.92$). These results were mirrored in an independent study by Webster et al [22] ($ICC = 0.91 - 0.99$). Finally, validity and reliability of the GAITRite® system has also been established in a HD population [3]

($ICC = 0.86 - 0.95$). Each participant was asked to perform five trials of walking at their comfortable pace with all statistical analysis performed on respective mean values. As noted by Hof et al [23] several gait parameters are speed dependant and thus the spatio-temporal variables were normalized using subject specific height prior to statistical analysis. Subjects were instructed to begin walking two meters before the edge of the walkway and stop two meters beyond the end of the walkway. Finally, subjects were given a practice trial at the beginning of the testing session.

#### *6.3.2.3. Balance*

Balance and postural control were assessed using the Romberg (RB) test [24]. The test measures the length of time (max 30 secs) the subject can stand with ankle malleoli touching, arms crossed with palms touching the opposite shoulder. Each test was conducted twice with all statistical analysis performed on the mean of both attempts. As previously discussed the sensor was calibrated and compensation for possible tilt was considered. A further issue specific to these type of balance tests is that a subject may slowly shift their position during the testing period (a shift unrelated to balance control) and this can result in a low frequency drift over time [15]. Thus the triaxial signal was detrended using a second-order polynomial fit curve [14]. Finally, for the center 80% of data of each task the root mean square of the ML and AP axes along with the combined instantaneous vector sum $\left(\sqrt{a_{ML}^2 + a_{AP}^2 + a_{LD}^2}\right)$ were calculated.

### *6.3.3. Statistical Analysis*

Signal processing and parameter extraction was performed using MATLAB (Matlab 7.10.0, The MathWorks USA) and statistical analysis was performed using PASW-Statistics 17.0.1 (SPSS Inc., Illinois, USA). The levels of agreement between the sensor and GAITRite® were assessed by intraclass correlation coefficients (ICCs) of the type $(2, k)$. For each parameter the assumption of a normal distribution was assessed by a Kolmogorov–Smirnov Goodness of Fit test ($p < 0.05$). Dependent on this analysis group differences were assessed using either a one-way ANOVA ($p < 0.05$) or a Kruskal-Wallis ($p < 0.05$) test, respectively. Post-hoc analysis was performed with Tukey HSD tests or a Mann-Whitney U-test with appropriate Bonferroni correction

(adjusted alpha: $p < 0.0125$) for multiple comparisons. Using Receiver Operating Characteristics (ROC) curve analysis the sensitivity and specificity of statistically significant variables was investigated. Specifically, the discriminatory power of a parameter can be evaluated by area under the ROC Curve (AUC) – a larger area is indicative of higher sensitivity and specificity [25].

### *6.4 Results*

Table 6.1 summarizes subject characteristics. HLY subjects were generally older and taller than both PHD and MHD subjects but these differences were not significant ($p < 0.05$). PHD subject's weight was generally greater than that of HLY and MHD subjects but again this was not significant ($p < 0.05$). All PHD subjects scored either 0 ($n = 6$) or 1 ($n = 4$) on diagnostic confidence. PHD had UHDRS total motor scores ($4.8 \pm 5.3$) and TFC ($13 \pm 0$) indicating that clinical examination detected no specific motor impairments and no functional limitations in these individuals. MHD subjects had UHDRS total motor scores ($54.15 \pm 13.02$) and TFC ($6.33 \pm 2.18$).

**Table 6.1**
**Subject Characteristics ($HLY_n = 10$, $PHD_n = 10$, $MHD_n = 14$)**
**$\bar{x} \pm s$ = Mean ± Standard Deviation**

| *Characteristic* | *Healthy* ($\bar{x} \pm s$) | *Pre-manifest HD* ($\bar{x} \pm s$) | *Manifest HD* ($\bar{x} \pm s$) |
|---|---|---|---|
| *Age (year)* | $56.45 \pm 10.93$ | $44.81 \pm 11.79$ | $51.83 \pm 14.82$ |
| *Sex* | $5M$ / $5F$ | $4M$ / $6F$ | $8M$ / $6F$ |
| *Weight (kg)* | $75.91 \pm 7.62$ | $81.86 \pm 27.94$ | $68.38 \pm 9.35$ |
| *Height (cm)* | $171.15 \pm 6.66$ | $171.05 \pm 9.94$ | $167.58 \pm 8.72$ |
| *Right Leg (cm)* | $93.00 \pm 5.52$ | $92.55 \pm 5.63$ | $89.88 \pm 3.62$ |
| *Left Leg (cm)* | $92.60 \pm 5.24$ | $92.15 \pm 5.87$ | $89.67 \pm 3.68$ |
| *UHDRS MS* | *NA* | $4.80 \pm 5.30$ | $54.15 \pm 13.02$ |
| *UHDRS TFC* | *NA* | $13 \pm 0$ | $6.33 \pm 2.18$ |

#### *6.3.4. Gait Analysis*

Table 6.2 compares the gait parameters derived from the accelerometer to those recorded by the GAITRite® software across all subject groups. The accelerometer sensor displayed excellent agreement to the GAITRite® system for cadence (ICC = 0.95 [0.75 0.97]) and velocity (ICC = 0.94 [0.75 0.97]). Agreement was very good for

step length (ICC = 0.89 [0.77 0.95]), step time (ICC = 0.88 [0.72 0.94]) and stride length (ICC = 0.88 [0.71 0.95]) respectively. Table 6.3 presents means and standard deviations across each subject group and the respective statistical group differences. Fig. 6.1 (A-F) presents box plots representing the parameters which were statistically significant between subject groups. Sensor derived velocity was significantly higher in HLY ($p < 0.001$) and PHD ($p < 0.005$) when compared to MHD. Step and stride length was significantly longer in HLY ($p < 0.001$) and PHD ($p < 0.005$) when compared to MHD. No significant group differences were found for cadence and step time. Interestingly, significant group differences were found between each subject category for each coefficient of variation parameter. HLY step time CV, step length CV and stride length CV were significantly different from PHD ($p < 0.005$) and from MHD ($p < 0.001$). PHD step time CV, step length CV and stride length CV were significantly different from MHD ($p < 0.01$). No significant difference was found for step time asymmetry. Finally, step and stride regularity were significantly different between all three groups in the ML axis (ML Step ( $p < 0.001$ ), ML Stride: ($p < 0.005$) ) and LD axis (LD Step: ($p < 0.002$), LD Stride: ($p < 0.002$) . Similarly, for the AP axis step and stride regularity demonstrated significant group differences (AP Step: ($p < 0.002$ ) AP Stride: ($p < 0.002$) ) with the exception of stride regularity between PHD and MHD.

**Table 6.2**
**Gait Analysis (All subject groups combined. n=34)**
**$\bar{x} \pm s$ = Mean $\pm$ Standard Deviation**

| Parameter | GAITRite® ($\bar{x} \pm s$) | AD_BRC ($\bar{x} \pm s$) | ICC [$CI$] |
|---|---|---|---|
| Velocity (m/s) | $1.17 \pm 0.29$ | $1.21 \pm 0.31$ | 0.94 [0.75 0.97] |
| Cadence (s/m) | $109.76 \pm 13.84$ | $108.86 \pm 14.95$ | 0.95 [0.75 0.97] |
| Step Length(m) | $0.58 \pm 0.11$ | $0.57 \pm 0.13$ | 0.89 [0.77 0.95] |
| Step Time (s) | $0.56 \pm 0.08$ | $0.54 \pm 0.09$ | 0.88 [0.72 0.94] |
| Stride Length. (m) | $1.18 \pm 0.23$ | $1.23 \pm 0.22$ | 0.88 [0.71 0.95] |

### *6.3.5. Balance Analysis*

The lower section of Table 6.3 presents the calculated root mean square values after appropriate adjustment for tilt and low frequency drift. Although separate values were calculated for the ML and AP axes, very similar results were found from analysis

of the vector sum and thus only these values are used. Kruskal-Wallis analysis revealed significant differences between subject groups across all four balance tasks ($p < 0.0001$)

**Table 6.3**
**Sensor Gait Analysis ($HLY_n = 10$, $PHD_n = 10$, $MHD_n = 14$)**
**ML = Mediolateral, AP = Anteriorposterior, LD = Longitudinal**

| Parameter | Healthy ($\bar{x} \pm s$) | Pre-manifest HD ($\bar{x} \pm s$) | Manifest HD ($\bar{x} \pm s$) |
|---|---|---|---|
| Velocity (m/s) | $1.44 \pm 0.15^{\dagger d}$ | $1.30 \pm 0.21^{\dagger b}$ | $0.96 \pm 0.29$ |
| Cadence (s/m) | $110.74 \pm 7.95$ | $111.80 \pm 15.82$ | $105.20 \pm 18.33$ |
| Step Length (m) | $0.65 \pm 0.06^{\dagger d}$ | $0.64 \pm 0.10^{\dagger b}$ | $0.48 \pm 0.13$ |
| Step Time (s) | $0.51 \pm 0.03$ | $0.52 \pm 0.06$ | $0.60 \pm 0.11$ |
| Stride Length (m) | $1.38 \pm 0.10^{\dagger d}$ | $1.33 \pm 0.15^{\dagger b}$ | $1.02 \pm 0.19$ |
| Step Time Coeff. of Var. | $2.61 \pm 0.51^{\star b,d}$ | $5.45 \pm 2.40^{\dagger a}$ | $11.78 \pm 6.21$ |
| Step Length Coeff. of Var. | $2.13 \pm 0.39^{\star b,d}$ | $5.34 \pm 2.82^{\dagger a}$ | $16.31 \pm 10.70$ |
| Stride Length Coeff of Var | $2.01 \pm 0.25^{\star b,d}$ | $4.70 \pm 2.29^{\dagger a}$ | $13.81 \pm 8.64$ |
| Step Time Asymmetry | $2.17 \pm 1.39$ | $3.54 \pm 2.11$ | $5.43 \pm 3.08$ |
| ML Step Regularity | $-0.75 \pm 0.10^{\star d}$ | $-0.54 \pm 0.12^{\dagger d}$ | $-0.35 \pm 0.10$ |
| ML Stride Regularity | $0.69 \pm 0.10^{\star b}$ | $0.53 \pm 0.10^{\dagger b}$ | $0.34 \pm 0.13$ |
| AP Step Regularity | $0.81 \pm 0.09^{\star c}$ | $0.67 \pm 0.05^{\dagger c}$ | $0.50 \pm 0.14$ |
| AP Stride Regularity | $0.79 \pm 0.08^{\star c}$ | $0.57 \pm 0.12$ | $0.50 \pm 0.11$ |
| LD Step Regularity | $0.78 \pm 0.09^{\star c}$ | $0.58 \pm 0.09^{\dagger c}$ | $0.37 \pm 0.13$ |
| LD Stride Regularity | $0.72 \pm 0.09^{\star c}$ | $0.52 \pm 0.12^{\dagger c}$ | $0.29 \pm 0.16$ |
| Romberg Balance Tests | | | |
| Eyes Open Feet Together | $0.025 \pm 0.003^{\dagger e}$ | $0.026 \pm .004^{\dagger e}$ | $0.035 \pm 0.003$ |
| Eyes Closed Feet Together | $0.026 \pm 0.004^{\star d,e}$ | $0.031 \pm .002^{\dagger e}$ | $0.038 \pm 0.005$ |
| Eyes Open Feet Apart | $0.020 \pm 0.005^{\dagger e}$ | $0.022 \pm .005^{\dagger e}$ | $0.029 \pm 0.005$ |
| Eyes Closed Feet Apart | $0.023 \pm 0.003^{\star b,e}$ | $0.025 \pm .003^{\dagger e}$ | $0.034 \pm 0.004$ |

$\bar{x} \pm s$ = Mean $\pm$ Standard Deviation
† Significantly different from Manifest HD
⋆ Significantly different from Pre-manifest HD and Manifest HD
[a] ($p < 0.01$) [b] ($p < 0.005$) [c] ($p < 0.002$) [d] ($p < 0.001$) [e] ($p < 0.0001$)

Post-hoc analysis found significant differences between HLY & MHD and PHD & MHD across all balance tasks ($p < 0.0001$) however, significant differences between HLY & PHD were only found for tasks requiring eyes closed; Eyes-Closed Feet-Together ($p < 0.001$) and Eyes-Closed Feet-Apart ($p < 0.005$). Table 6.4 presents the ROC curve analysis. Several parameters displayed very high sensitivity and specificity for HLY vs. PHD & MHD. However, these values are slightly reduced for HLY vs. PHD. Notably, mediolateral step regularity demonstrated perfect distinction across subjects with and without the HD mutation.

**Table 6.4**
**ROC Analysis ($HLY_n$ = 10, $PHD_n$ = 10, $MHD_n$ = 14)**
**HLY = Healthy, PHD = Pre-manifest HD, MHD = Manifest HD.**
**ML= Mediolateral, AP= Anteriorposterior, LD = Longitudinal**

| Parameter (Optimal Threshold) | HLY vs. PHD & MHD | | HLY vs. PHD | |
|---|---|---|---|---|
| | Sens. | Spec. | Sens. | Spec. |
| Velocity (1.31m/s) | 83 | 80 | 60 | 80 |
| Step Length (0.58m) | 76 | 90 | 50 | 90 |
| Stride Length (1.35m) | 78 | 90 | 50 | 90 |
| Stride Length Coeff of Var. (2.65) | 91 | 90 | 80 | 90 |
| Step Time Coeff of Var. (3.06) | 83 | 100 | 80 | 100 |
| ML Step Regularity (−0.64) | 100 | 100 | 100 | 100 |
| AP Stride Regularity (0.69) | 91 | 90 | 50 | 80 |
| LD Step Regularity (0.69) | 91 | 90 | 80 | 90 |
| Eyes Closed Feet Together (0.029) | 93 | 100 | 50 | 90 |

Step Regularity: First dominant peak from autocorrelation procedure ($A_{d1}$) Regularity of the acceleration between consecutive steps.
Stride Regularity: Second dominant peak from unbiased ($A_{d2}$) autocorrelation procedure: Regularity of the acceleration between consecutive strides
Sens. = Sensitivity ($\sum TP/\ (\sum TP + \sum FN) * 100$); probability of a positive test among subjects with HD
Spec. = Specificity ($\sum TN/\ (\sum TN + \sum FP) * 100$); probability of a negative test for subjects without HD

## *6.5 Discussion*

Our results demonstrate the capacity of a single triaxial accelerometer attached at the sternum in differentiating between pre-manifest and manifest Huntington's disease subjects. Specifically, MHD subjects exhibited lower velocity, shorter step and stride length, inferior gait symmetry / regularity and greater postural sway when compared to HLY and PHD subjects.

The strong agreement between the AD_BRC sensor and the GAITRite® software across all five spatio-temporal parameters (velocity, cadence, step length, step time and stride length) demonstrates the accuracy of the sensor and reiterates the reliability of the inverted pendulum [10] model. As noted in section 6.3.2.2 normalization of spatio-temporal variables by subject specific height was performed however, we found this procedure had little impact on the raw data. We believe this can be attributed to the lack of dispersion among our sample height data and as noted by Hof et al [23] in homogenous datasets the normalization procedure may have minimal effect.

Significant group differences were found for several gait parameters. Specifically, step time CV and stride length CV were significantly different across all subject groups. They results are consistent with studies of a larger sample size conducted by Rao et al [6], Devlal et al [7] and Tabrizi et al [26]. Our results did not reveal significant group differences between HLY and PHD for velocity ($p<0.06$) and stride length ($p<0.06$). Furthermore, cadence did not demonstrate any significant group differences. In contrast, both Devlal et al [7] and Rao et al [6] found velocity and stride length to be significantly different across all subject groups. For cadence Devlal et al [7] found significant differences between HLY and PHD ($p<0.01$) and Rao et al [6] found significant differences between healthy subjects and subjects in stages two ($p<0.01$) and three ($p<0.003$) of the disease; we did not create subgroups by manifest HD stage.

Step and stride length decreased with each subject group. Furthermore, significant group differences were found across all gait regularity components and mediolateral step regularity demonstrated strong discriminative power. Although we were unable to find published work investigating step and stride regularity using the unbiased autocorrelation procedure and step time asymmetry in a HD population, these results correspond to published work employing alternative measurement techniques and varying populations. Rao et al [6] noted that PHD subjects tended to spend a larger percentage of time in stance and have increased step time variability with the severity of these symptoms increasing with disease progression. Tura et al [27] found that AP step regularity and LD stride regularity could distinguish between ten amputees and ten healthy subjects. Stride-to-stride variability has also proven useful in distinguishing between Parkinsonian subjects with freezing of gait and those without [28]. For step time asymmetry Bautmans et al [12] also found no significant difference in a cohort of 121 elderly subjects.

For balance analysis the root mean square values increased with task complexity from Eyes-Open Feet-Apart to Eyes-Closed Feet-Together across all subject groups. Although, we were unable to find published work investigating accelerometry data for balance analysis in a HD population several studies have employed similar techniques in varying populations. In an investigation of postural instability, stance with feet close together was found to be a highly sensitive test in a sample of 20 HD subjects [29].

Using accelerometry O'Sullivan et al [14] was able to distinguish between various test conditions except between that of Eyes-Open and Eyes-Closed. They speculate since both balance tasks only represent a marginally different challenge to balance control and as their subjects stood with feet apart, increased mediolateral stability was demonstrated. Our dataset tends to agree with this observation as a significant difference was found for Eyes-Open Feet-Apart vs. Eyes-Closed Feet-Together ($p<0.0007$). Several studies investigated balance while standing on a mat or foam surface [14-17] and it is plausible that the sensitivity and specificity of our results might change with the addition of such a surface in the protocol.

The optimal thresholds from the ROC curve analysis, velocity (1.3142m/s) and stride length (1.349m), align with recent studies [6-7]. The parameters derived from both gait and balance demonstrated high sensitivity and specificity thus reinforcing the argument for inclusion of quantitative evaluation in clinical assessment of HD. However, we note the caution raised by Devlal et al [7]. With a large study population of 57 healthy subjects they found standard gait parameters were not sensitive enough to detect PHD status however, an increase in stride-to-stride variability was found sufficient to differentiate between PHD & HLY (sensitivity and specificity < 0.9). In comparison Tabrizi et al [26] found GAITRite® stride length CV to be a sufficient biomarker in a very large study population. Although measures of step and stride regularity and balance were not investigated in these studies we recognize the necessity of large scale longitudinal studies employing accelerometry in a HD population.

Our site of attachment for the triaxial accelerometer was the thorax just below the suprasternal notch and this placement might be considered a limitation of the study. We chose this location as we wish to incorporate fall detection in future development. The majority of referenced work affixed a sensor over the L3 region of the spine which is close to where COM is believed to be during quiet standing [10]. From analysis of the data we note the accelerometry patterns at the level of the thorax are an attenuated version of those closer to the COM. This conclusion is also supported in the literature where accelerations measured at the level of the head correlate with and are dampened versions of those at inferior levels [30].

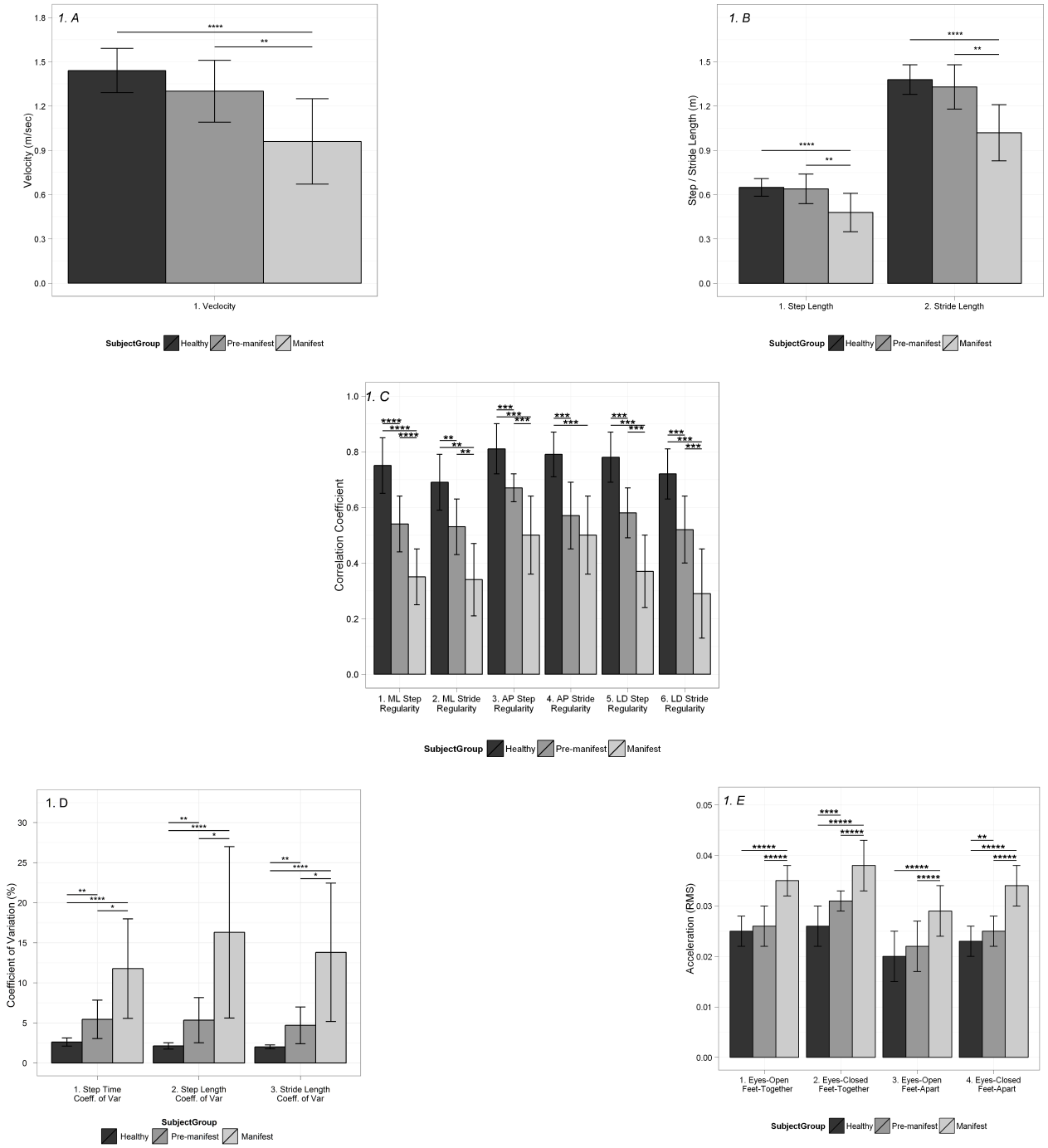


**Fig. 6.1.**

Box plots $(\text{mean} \pm \text{standard deviation})$ presenting the statistically significant parameters from the gait analysis

Fig 1 (A): velocity, Fig 1 (B) step length, stride length, Fig. 1 (C) step and stride regularity across the ML, AP and LD axes respectively, Fig. 1 (D) Step time coefficient of variation, step length coefficient of variation and stride length coefficient of variation, Fig. 1 (E) Romberg balance tasks

(Note the absolute values of ML Step Regularity are presented)

Step Regularity: First dominant peak from autocorrelation procedure $(A_{d1})$ Regularity of the acceleration between consecutive steps.

Stride Regularity: Second dominant peak from unbiased $(A_{d2})$ autocorrelation procedure: Regularity of the acceleration between consecutive strides

$^{*}(p < 0.01)$ $^{**}(p < 0.005)$ $^{***}(p < 0.002)$ $^{****}(p < 0.001)$ $^{*****}(p < 0.0001)$

A significant advantage of our work is the incorporation of a high sampling frequency (Fs=250Hz). A low sampling rate increases the probability of temporal aliasing especially in heel strike detection [29] and a higher sampling rate (>100 Hz) could improve the accuracy of step / stride regularity and step-time asymmetry.

### *6.6 Conclusion*

The objective of this study was to investigate the capacity of a single accelerometer based sensor to derive spatio-temporal parameters of gait and balance in a HD population and investigate its potential to differentiate between subject groups. The sensor showed excellent agreement to a computerized walkway across a range of spatio-temporal parameters and demonstrated significant discriminatory power between healthy, pre-manifest HD and manifest HD subjects across a host of gait and balance parameters. Specifically, we note the excellent discriminatory power of velocity, stride length coefficient of variation, ML step regularity and LD step regularity. These results highlight the sensors capacity to detect and quantify the variability in task performance across subject groups and its significant potential for employment in monitoring for disease onset in HD.

### *6.7 References*

[1] Quinn, L., & Rao, A. (2002). 'Physical therapy for people with Huntington disease: current perspectives and case report', *Journal of Neurologic Physical Therapy*, vol. 26(3), pp. 145.

[2] Ramos-Arroyo, M. A., Moreno, S., & Valiente, A. (2005). 'Incidence and mutation rates of Huntington's disease in Spain: experience of 9 years of direct genetic testing', *Journal of Neurology, Neurosurgery & Psychiatry*, vol. 76(3), pp. 337-342.

[3] Rao, A. K., Quinn, L., & Marder, K. S. (2005). 'Reliability of spatiotemporal gait outcome measures in Huntington's disease', *Movement Disorders*, vol. 20, pp. 1033-1037.

[4] Busse, M, Wiles, C, & Rosser, A. (2009). 'Mobility and falls in people with Huntington's disease', *Journal of Neurology, Neurosurgery & Psychiatry*, vol. 80(1), pp. 88-90.

[5] Delval, A., Krystkowiak, P., Blatt, E., & Defebvre, L. (2007). 'A biomechanical study of gait initiation in Huntington's disease', *Gait & Posture*, vol. 25(2), pp. 279-288.

[6] Rao, A. K., Muratori, L., Louis, E. D., Moskowitz, C. B., & Marder, K. S. (2008). 'Spectrum of gait impairments in presymptomatic and symptomatic Huntington's disease', *Movement Disorders*, vol. 23(8), pp. 1100-1107.

[7] Delval, A., Bleuse, S., Simonin, C., Delliaux, M., Rolland, B., Destee, A., & Dujardin, K. (2011). 'Are gait initiation parameters early markers of Huntington's disease in pre-manifest mutation carriers?', *Gait & Posture*, vol. 34(2), pp. 202-207.

[8] Panzera, R., Salomonczyk, D., Pirogovosky, E., Simmons, R., Goldstein, J., Corey-Bloom, J., & Gilbert, P. E. (2011). 'Postural deficits in Huntington's disease when performing motor skills involved in daily living', *Gait & Posture*, vol. 33(3), pp. 457-461.

[9] Rao, A. K., Louis, E. D., & Marder, K. S. (2009). 'Clinical assessment of mobility and balance impairments in pre-symptomatic Huntington's disease', *Gait & Posture*, vol. 30(3), pp. 391-393.

[10] Zijlstra, W., & Hof, A. L. (2003). 'Assessment of spatio-temporal gait parameters from trunk accelerations during human walking', *Gait & Posture*, vol. 18(2), pp. 1-10.

[11] Moe-Nilssen, R., & Helbostad, J. L. (2004). 'Estimation of gait cycle characteristics by trunk accelerometry', *Journal of Biomechanics*, vol. 37(1), pp. 121-125.

[12] Bautmans, I., Jansen, B., Van Keymolen, B., & Mets, T. (2011). 'Reliability and clinical correlates of 3D-accelerometry based gait analysis outcomes according to age and fall-risk', *Gait & Posture*, vol. 33(3), pp. 366-372.

[13] Storti, K. L., Pettee, K. K., Brach, J. S., Talkowski, J. B., Richardson, C. R., & Kriska, A. M. (2008). 'Gait speed and step-count monitor accuracy in community-dwelling older adults', *Medicine and Science in Sports and Exercise*, vol. 40(1), pp. 59.

[14] O'Sullivan, M., Blake, C., Cunningham, C., Boyle, G., & Finucane, C. (2009). 'Correlation of accelerometry with clinical balance tests in older fallers and non-fallers', *Age and Ageing*, vol. 38(3), pp. 308-313.

[15] Moe-Nilssen, R., & Helbostad, J. L. (2002). 'Trunk accelerometry as a measure of balance control during quiet standing', *Gait & Posture*, vol. 16(1), pp. 60-68.

[16] Helbostad, J. L., Askim, T., & Moe-Nilssen, R. (2004). 'Short-term repeatability of body sway during quiet standing in people with hemiparesis and in frail older adults', *Archives of Physical Medicine and Rehabilitation,* vol. 85(6), pp. 993-999.

[17] Goldberg, A., Schepens, S. L., Feely, S. M., Garbern, L. J., & Conti, G. E. (2010). 'Deficits in stepping response time are associated with impairments in balance and mobility in people with Huntington disease', *Journal of the Neurological Sciences*, vol. 298(1), pp. 91-95.

[18] Khalil, H., Dalton, A., van Deursen, R., Rosser, A., ÓLaighin, G., & Busse, M. (2010). 'F17 The use of an accelerometer to evaluate the performance of timed up and go test in pre-symptomatic and symptomatic huntington's disease', *Journal of Neurology, Neurosurgery & Psychiatry*, A28-A28.

[19] Kremer, H. P. H. (1996). 'Unified Huntington's disease rating scale: reliability and consistency', *Movement Disorders*, vol 11(2), pp. 136-140.

[20] Bourke, A. K., O'Donovan, K. J., & ÓLaighin, G. (2008). 'The identification of vertical velocity profiles using an inertial sensor to investigate pre-impact detection of falls', *Medical Engineering & Physics*, vol. 30(7), pp. 937.

[21] Menz, H. B., Latt, M. D., Tiedemann, A., Mun San Kwan, M., & Lord, S. R. (2004). 'Reliability of the GAITRite® walkway system for the quantification of temporo-spatial parameters of gait in young and older people', *Gait & Posture*, vol. 20(1), pp. 20-25.

[22] Webster, K. E., Wittwer, J. E., & Feller, J. A. (2005). 'Validity of the GAITRit® walkway system for the measurement of averaged and individual step parameters of gait', *Gait & Posture*, vol. 22(4), pp. 317-321.

[23] Hof, At L. 'Scaling gait data to body size', Gait & Posture, vol. 4(3), pp. 222-223.

[24] Khasnis, A., & Gokula, R. M. (2003). 'Romberg's test', *Journal of Postgraduate Medicine*, vol. 49(2), pp. 169-172.

[25] Hosmer David, W., & Stanley, L. (2000). '*Applied logistic regression*', John Wiley.

[26] Tabrizi, S. J., Langbehn, D. R., Leavitt, B. R., Roos, R. A., & Stout, J. C. (2009). 'Biological and clinical manifestations of Huntington's disease in the longitudinal TRACK-HD study: cross-sectional analysis of baseline data', *The Lancet Neurology*, vol. 8(9), pp. 791-801.

[27] Tura, A., Raggi, M., Rocchi, L., Cutti, A. G., & Chiari, L. (2010). 'Gait symmetry and regularity in transfemoral amputees assessed by trunk accelerations', *Journal Neuro-Engineering Rehabilitation*, vol. 7(4), pp. 13-17.

[28] Hausdorff, J. M., Schaafsma, J. D., Balash, Y. L., Gurevich, T., & Giladi, N. (2003). 'Impaired regulation of stride variability in Parkinson's disease subjects with freezing of gait', *Experimental Brain Research*, vol. 149(2), pp. 187-194.

[29] Senden, R., Grimm, B., Heyligers, I. C., Savelberg, H. H. C. M., & Meijer, K. (2009). 'Acceleration-based gait test for healthy subjects: reliability and reference data', *Gait & Posture*, vol. 30(2), pp. 192-196

[30] Kavanagh, J. J., Barrett, R. S., & Morrison, S. (2004). 'Upper body accelerations during walking in healthy young and elderly men', Gait & Posture, vol. 20(3), pp. 291-298.

# CHAPTER VII

# Summary

# & Conclusion

## *7.1 Chapter Overview*

In this thesis we investigated the practical application of accelerometer based sensors as tools to remotely monitor various physical activities and neuro-degenerative disorders. This chapter summarizes the core findings of each of the four studies conducted and provides suggestions for future avenues of research.

## *7.2 Activity Recognition in Healthy & Elderly Subjects*

The first two studies in this body of work focused on physical activity recognition using base-level and meta-level learning classifiers trained on accelerometry data. Upon completion of a significant literature review it was concluded that the published work was fragmented and disjointed and a large scale study combining many of the insights from previous work was warranted. Our key objectives were to 1. Perform a brute force comparison of the most popular machine learning classifiers, 2. Analyze the redundancy of time-domain and frequency domain features, 3. Compare user-specific and user-independent training sets and 4. Investigate whether the window size by which data are segmented or the location of sensor attachment affects classifier accuracy. During the study, 25 healthy subjects wore 5 accelerometer based sensors as they completed a range of physical activities. A set of time domain and frequency domain feature sets were derived from the raw data and used to train and test the supervised classifiers. Our final results from this initial study were that the meta-level classifier AdaBoostM1 with C4.5 Graft as its base-level classifier achieved an overall accuracy of 95%. Furthermore, high recognition rates could be achieved without the need for user specific training. Finally, an accuracy of 88% could be achieved using data from the ankle and wrist sensors only with a window size of 128 samples (1 second).

Our initial study was conducted in a controlled laboratory setting with a homogeneous healthy subject sample and therefore we progressed to the next stage of research by expanding into an older, more diverse population in a home environment. By employing the same accelerometer based sensors and list of activities from the initial study, data were gathered from 5 elderly subjects in their home environment. Furthermore, we focused specifically on Support Vector Machine (SVM) classifiers employing Multiple Kernel Learning (MKL). Our final results from the second study were that an SVM MKL mixture of 50% linear kernels

and 50% gaussian kernels achieved an accuracy of 86% for older adults. Furthermore, this classifier did not require subject specific training and a high level of accuracy was maintained using sensors attached at the mid-sternum, wrist and ankle.

### *7.3 Epileptic Seizure Detection*

In the third study conducted in this thesis we developed a Body Sensor Network (BSN) to detect motor patterns of epileptic seizures. Our primary motivation for this work was that miniature accelerometer based sensors combined with an internet based tablet could be attached to a subject and seizure occurrence outside the laboratory setting could be monitored without interfering with the subject's daily routine. Several accelerometer based sensors were attached to 5 epileptic subjects as they performed a predefined set of physical activities across multiple days in a hospital environment. During the monitoring sessions EEG and video data were also recorded and provided the gold standard for seizure detection. A template matching algorithm which accommodated for the unique signature of seizure events and the inherent temporal variability of seizure types across subjects by incorporating a customized mass-spring template into the dynamic time warping algorithm was designed. Furthermore, we built a proof-of-concept BSN incorporating wireless accelerometer sensors and a commercially available internet tablet. We investigated several driver policies on a specifically designed software research platform. Our primary results from this third study were a sensitivity of 0.91 and specificity of 0.84 from 21 tonic-clonic seizure events for the template matching algorithm and a 10.5 hours battery lifetime for the BSN.

### *7.4 Spatio-temporal gait analysis in Huntington's Disease*

In the fourth and final study conducted in this body of research we investigated the capacity of a single triaxial accelerometer sensor to detect gait and balance impairments in pre-symptomatic and symptomatic Huntington's disease (HD) subjects. Our primary motivations were the known limitations of commonly used ordinal based clinical tests and the considerable expense of laboratory-based walkways and other quantitative systems currently used to monitor Huntington's disease. Thirty-four subjects were recruited (10 healthy (HLY), 10 pre-manifest HD (PHD), 14 manifest HD (MHD)) and a custom built triaxial accelerometer based

sensor was attached to the upper sternum as subjects completed gait and balance tests. By employing an inverted pendulum model of the body's centre of mass and an unbiased autocorrelation procedure several gait parameters were derived from the accelerometer signal. The accuracy of these gait measurements was compared to those recorded by a computerized walkway and furthermore, we investigated whether the parameters could be used to distinguish between subjects in various stages of disease progression. Our primary results from this study were strong agreement between the accelerometer based sensor and the computerized walkway across a range of gait parameters including cadence, velocity and step length. Furthermore, it was found that sensor derived velocity was significantly higher in HLY and PHD when compared to MHD and step and stride length was significantly longer in HLY and PHD when compared to MHD. Finally, significant differences between subject groups across all four balance tasks were found.

### *7.5 Future Work*

There are significant opportunities for future research arising from this thesis. Specifically, the elderly study population for the analysis of physical activities in the home environment should be expanded. Although we are confident that our comparisons of subject dependant versus subject independent training data were rigorous a larger sample would confirm this hypothesis. A further clear area of extension would be embedding the accelerometer based sensors in everyday wearable electronics and gathering data in a truly natural environment without researcher intervention. The iPAQ software developed in the second study should be sufficient for deployment however, the sensors employed are too bulky for long term use. The wrist, ankle and mid-sternum were identified as sufficient locations to maintain a high degree of accuracy and Bluetooth enabled accelerometer based sensors could easily be incorporated into ankle and wrist bracelets. The mid-sternum is slightly more restrictive and perhaps a sensor could be incorporated into clothing. The final key piece to the puzzle is how these data are fed back into and incorporated within the medical decision process. We strongly feel that the techniques indentified in these two studies address several of the engineering problems associated with remote mobility monitoring and these results could be incorporated into a larger geriatrics study, driven more from a medical perspective rather than from an engineering perspective.

With regards the Epileptic seizure detection study the next stage of research should be deployment of the Body Sensor Network on a subject in their home environment. Although, extensive testing was conducted in the research environment, unforeseen issues will naturally arise in a real life environment. Furthermore, a larger sample of accelerometer based subject data would need to be collected to verify whether the spring based template matching algorithm is truly applicable across the subject population. Our personal opinion is that while the spring-like seizure signature may not be as pronounced in subjects from outside the study population, it is possible that certain parameterizations of the spring function specific to the physiology of certain subject subgroups may be applicable. For example, it is plausible that various parameterizations of the template may be required based on subject sex, height, weight and seizure magnitude. This question can only be addressed with a large sample size.

Finally, as noted in section 2.5.4.3, analysis of the sit-to-stand transfer and Timed-Up and Go clinical tests were conducted as part of the study of Huntington's disease subjects. We are currently investigating whether parameters derived from these tests can be employed to find statistically significant differences between presymptomatic and symptomatic Huntington's disease subjects. As this study demonstrated that an accelerometer based sensor affixed to the upper chest is capable of distinguishing between Huntington's subject subgroups the next stage of research should investigate whether these tests can be conducted in the subject's home. Specifically, rather than requiring a subject to attend a laboratory session involving expensive research equipment, a strict protocol could be conducted in the subjects home with the sensor downloading data to a nearby base station. It would also be quite feasible for a researcher to monitor these sessions remotely. We strongly feel this is an area of research worth exploring.

In conclusion, we feel the body of research consisting of the four studies conducted demonstrates the practical application of accelerometer based sensors as tools to monitor various physical activities and neuro-degenerative disorders. Furthermore, we believe this work lays the foundation for future meaningful and exciting work in this field.

# BIBLIOGRAPHY

32Feet.net (2010) [Online]. Available: http://32feet.net/ (Accessed: Mar. 2012)

AWARENESS (2010), '*Freeband AWARENESS project*', [Online] Available: http://www.freeband.nl/project.cfm?id=494&language=en (Accessed: Apr. 2012)

Age Concern England, (2012), 'The age agenda 2008: public policy and older people', *London, Age Concern England*.

Aha, D. W. (1992). 'Tolerating noisy, irrelevant and novel attributes in instance-based learning algorithms', *International Journal Man-Machine Study*, vol. 36(2), pp. 267-287.

Allen, F. R., Ambikairajah, E., Lovell, N. H., & Celler, B. G. (2006). 'Classification of a known sequence of motions and postures from accelerometry data using adapted Gaussian mixture models', *Physiological Measurement*, vol. 27(10), pp. 935-941.

Altun, K., Barshan, B., & Tunçel, O. (2010). 'Comparative study on classifying human activities with miniature inertial and magnetic sensors', *Pattern Recognition*, vol. 43(10), pp. 3605-3620.

Aminian, K., & Najafi, B. (2004). 'Capturing human motion using body-fixed sensors: outdoor measurement and clinical applications', *Computer Animation and Virtual Worlds*, vol. 15(2), pp. 79-94.

Aminian, K., Robert, P., Jequier, E., & Schutz, Y. (1995). 'Estimation of speed and incline of walking using neural network', *IEEE Transactions on Instrumentation and Measurement*, vol. 44(3), pp. 743-746.

Bach, F. R., Lanckriet, G.R, & Jordan, M. I. (2004). 'Multiple kernel learning, conic duality, and the SMO algorithm', *21st International Conference on Machine Learning,* pp. 6-10.

Baek, J., Lee, G., Park, W., & Yun, B. J. (2004). 'Accelerometer signal processing for user activity detection', *Knowledge-Based Intelligent Information and Engineering Systems,* vol. 3215, pp. 610-617.

Bao, L., & Intille, S. (2004). 'Activity recognition from user-annotated acceleration data', *Pervasive Computing*, vol. 3001, pp. 1-17.

Barralon, P., Noury, N., & Vuillerme, N. (2006). 'Classification of daily physical activities from a single kinematic sensor', *27th Annual International Conference of the IEEE Engineering in Medicine and Biology Society,* pp. 2447-2450.

Barralon, P., Vuillerme, N., & Noury, N. (2006). 'Walk detection with a kinematic sensor: Frequency and wavelet comparison', *28th Annual International Conference of the IEEE Engineering in Medicine and Biology Society,* pp. 1711-1714.

Bautmans, I., Jansen, B., Van Keymolen, B., & Mets, T. (2011). 'Reliability and clinical correlates of 3D-accelerometry based gait analysis outcomes according to age and fall-risk', *Gait & Posture*, vol. 33(3), pp. 366-372.

Becq, G., Bonnet, S., Minotti, L., Antonakios, M., Guillemaud, R., & Kahane, P. (2011). 'Classification of epileptic motor manifestations using inertial and magnetic sensors', *Computers in Biology and Medicine*, vol. 41(1), pp. 46-55.

Begg, R., & Kamruzzaman, J. (2005). 'A machine learning approach for automated recognition of movement patterns using basic, kinetic and kinematic gait data', *Journal of Biomechanics*, vol. 38(3), pp. 401-408.

Ben-David, A. (2008). 'About the relationship between ROC curves and Cohen's kappa', *Engineering Applications of Artificial Intelligence*, vol. 21(6), pp. 874-882.

Ben-David, A. (2008). 'Comparison of classification accuracy using Cohen's Weighted Kappa', *Expert Systems with Applications*, vol. 34(2), pp. 825-832.

Ben-David, A. (2007). 'A lot of randomness is hiding in accuracy', *Engineering Applications of Artificial Intelligence*, vol. 20(7), pp. 875-885.

Betker, A. L., Moussavi, Z. M., & Szturm, T. (2006). 'Center of mass approximation and prediction as a function of body acceleration', *IEEE Transactions on Biomedical Engineering*, vol. 53(4), pp. 686-693.

Bharatula, N. B., Stäger, M., Lukowicz, P., & Tröster, G. (2005). 'Empirical study of design choices in multi-sensor context recognition systems', *IFAWC-International Forum on Applied Wearable Computing*, pp.22.

Bhattacharya, A., McCutcheon, E. P., Shvartz, E., & Greenleaf, J. E. (1980). 'Body acceleration distribution and O2 uptake in humans during running and jumping', *Journal of Applied Physiology*, vol. 49(5), pp. 881-887.

Bishop, C. M. (2006). '*Pattern recognition and machine learning',* vol. 4, no. 4, Springer.

Bishop, C. M. (1995). '*Neural networks for pattern recognition*', Oxford Press

Black, A. E., Coward, W. A., Cole, T. J., & Prentice, A. M. (1996). 'Human energy expenditure in affluent societies: an analysis of 574 doubly-labelled water measurements', *European Journal of Clinical Nutrition*, vol. 50(2), pp. 72.

Bluetooth Driver Stack, (2012) [Online]. Available: www.msdn.microsoft.com/en-us/library/, (Accessed: Mar. 2012)

Bonnet, S., & Heliot, R. (2007). 'A magnetometer-based approach for studying human movements', *IEEE Transactions on Biomedical Engineering*, vol. 54(7), pp. 1353-1355.

Bonnet, S., Jallon, P., Bourgerette, A., Guillemaud, R. & Ejnes, D. (2011). 'An Ethernet motion-sensor based alarm system for epilepsy monitoring', *E-Health and Medical Communications* , vol. 32(2), pp. 155-157.

Bourke, A. K., O'Donovan, K. J., & ÓLaighin, G. M. (2007). 'Distinguishing falls from normal ADL using vertical velocity profiles', *29th Annual International Conference of the IEEE Engineering in Medicine and Biology Society,* pp. 3176-3179.

Bourke, A. K., O'Donovan, K. J., & ÓLaighin, G. (2008). 'The identification of vertical velocity profiles using an inertial sensor to investigate pre-impact detection of falls', *Medical Engineering & Physics*, vol. 30(7), pp. 937.

Bouten, C. V., Koekkoek, K. T., Verduin, M., Kodde, R., & Janssen, J. (1997). 'A triaxial accelerometer and portable data processing unit for the assessment of daily physical activity', *IEEE Transactions on Biomedical Engineering*, vol. 44(3), 136-147.

Boyle, J., Wark, T., Karunanithi, M., (2005). 'Wireless Personal Monitoring of Patient Movement and Vital Signs, e-Health Research Centre', *IEEE Computational Intelligence in Medicine and Healthcare*. pp. 34-41.

Bradley, A. P. (1997). 'The use of the area under the ROC curve in the evaluation of machine learning algorithms', *Pattern Recognition*, vol. 30(7), pp. 1145-1159.

Brandes, M., Zijlstra, W., van Lummel, R., & Rosenbaum, D. (2006). 'Accelerometry based assessment of gait parameters in children', *Gait & Posture*, vol. 24(4), pp. 482-486.

Breiman, L. (1996). 'Bagging predictors', *Machine Learning*, vol. 24(2), pp. 123-140.

Busse, M, Wiles, C, & Rosser, A. (2009). 'Mobility and falls in people with Huntington's disease', *Journal of Neurology, Neurosurgery & Psychiatry*, vol. 80(1), pp. 88-90.

Bussmann, J. B., Culhane, K. M., Horemans, H. L., Lyons, G. M., & Stam, H. J. (2004). 'Validity of the prosthetic activity monitor to assess the duration and spatio-temporal characteristics of prosthetic walking', *IEEE Transactions on Neural Systems and Rehabilitation Engineering,* vol. 12(4), pp. 379-386.

Bussmann, J. B. J., Van de Laar, Y. M., Neeleman, M. P., & Stam, H. J. (1998). 'Ambulatory accelerometry to quantify motor behaviour in patients after failed back surgery: a validation study', *Pain*, vol. 74(2), pp. 153-161.

Cappozzo, A. (1982). 'Low frequency self-generated vibration during ambulation in normal men', *Journal of Biomechanics*, vol. 15(8), 599-609.

Carers UK, (2009). 'Policy Briefing: Facts about carers', *Carers UK*, London.

Carlson, C., Arnedo, V., Cahill, M., & Devinsky, O. (2009). 'Detecting nocturnal convulsions: efficacy of the MP5 monitor', *Seizure*, vol. 18(3), pp. 225-227.

Chang C, C. J. Lin (2004), '*LIBSVM: a library for support vector machines*', [Online]. Available: http://www.csie.ntu.tw/~cjlin/libsvm. (Accessed: Feb. 2012)

ChipCon CC2420 (2011) [Online]. Available: www.ti.com/cc242.pdf (Accessed: Feb. 2011)

Cohen WW, (1995). 'Fast effective rule induction', *12th International Conference on Machine Learning,* pp. 115-123.

Coley, B., Najafi, B., Paraschiv-Ionescu, A., (2005). 'Stair climbing detection during daily physical activity using a miniature gyroscope', *Gait & Posture*, vol. 22(4), 287-294.

Commonwealth Bureau of Meteorolog (2011), [Online]. Available: www.bom.gov.au/ (Accessed: Mar. 2011)

Conradsen, I., Beniczky, S., Wolf, P., & Sorensen, H. B. (2012). 'Automated Algorithm for Generalized Tonic–Clonic Epileptic Seizure Onset Detection Based on sEMG Zero-Crossing Rate', *IEEE Transactions on Biomedical Engineering*, vol. 59(2), pp. 579-585.

Cooper, G. F., & Herskovits, E. (1992). 'A Bayesian method for the induction of probabilistic networks from data', *Machine Learning*, vol. 9(4), 309-347.

Culhane, K. M., Lyons, G. M., Hilton, D., Grace, P. A., & Lyons, D. (2004). 'Long-term mobility monitoring of older adults using accelerometers in a clinical environment', *Clinical Rehabilitation*, vol. 18(3), pp. 335-343.

Dalton, A., Patel, S., Chowdhury, A., Welsh, M., Pang, T., Schachter, S., ÓLaighin, G., & Bonato, P. (2012). 'Development of a body sensor network to detect motor patterns of epileptic seizures', *IEEE Transactions on Biomedical Engineering*, vol. 59 (11), pp. 3204-3211.

Dalton, A., & ÓLaighin, G. (2013). 'Comparing supervised learning techniques on the task of physical activity recognition', *IEEE Journal of Health & Biomedical Informatics,* vol. 17, pp. 46-52.

Dalton, A., Morgan, F., & Olaighin, G. (2008). 'A preliminary study of using wireless kinematic sensors to identify basic Activities of Daily Living', *30th Annual International Conference of the IEEE Engineering in Medicine and Biology Society,* pp. 2079.

Dalton, A., Khalil, H., Busse, M., Rosser, A., van Deursen, R., & ÓLaighin, G. (2012). 'Analysis of gait and balance through a single triaxial accelerometer in presymptomatic and symptomatic Huntington's disease', *Gait & Posture*, vol. 37(1), pp. 49-54.

Deckers, C. L., Genton, P., Sills, G. J., & Schmidt, D. (2003). 'Current limitations of antiepileptic drug therapy: a conference review', *Epilepsy Research*, vol. 53(1-2), pp. 11-17.

Delval, A., Bleuse, S., Simonin, C., Delliaux, M., Rolland, B., Destee, A., & Dujardin, K. (2011). 'Are gait initiation parameters early markers of Huntington's disease in pre-manifest mutation carriers?', *Gait & Posture*, vol. 34(2), pp. 202-207.

Delval, A., Krystkowiak, P., Blatt, E., & Defebvre, L. (2007). 'A biomechanical study of gait initiation in Huntington's disease', *Gait & Posture*, vol. 25(2), pp. 279-288.

Delval, A., Krystkowiak, P., Blatt, J. L., Labyt, E., Dujardin, K., & Defebvre, L. (2006). 'Role of hypokinesia and bradykinesia in gait disturbances in Huntington's disease', *Journal of Neurology*, vol. 253(1), pp. 73-80.

Dorsey, E. R., Constantinescu, R., Thompson, J. P., Biglan, K. M., Holloway, R. G., Kieburtz, K., & Tanner, C. M. (2007). 'Projected number of people with Parkinson disease in the most populous nations, 2005 through 2030', *Neurology*, vol. 68(5), pp. 384-386.

Doyle, O. M., Temko, A., Marnane, W., Lightbody, G., & Boylan, G. B. (2010). 'Heart rate based automatic seizure detection in the newborn', *Medical Engineering & Physics*, vol. 32(8), pp. 829-839.

Ermes, M., Parkka, J., Mantyjarvi, J., & Korhonen, I. (2008). 'Detection of daily activities and sports with wearable sensors in controlled and uncontrolled conditions', *IEEE Transactions in Information Technology in Biomedicine*, vol. 12(1), pp. 20-26.

Eurostat (2005) '*Population Projections 2004-2050*', [Online] Available: www.europa.eu.int (Accessed: June 2012)

Fahrenberg, J., Foerster, F., (1997). 'Assessment of posture and motion by multichannel piezoresistive accelerometer recordings', *Psychophysiology*, vol. 34(5), pp. 607-612.

Filipovych, R., Resnuck, S., Davatzikos, (2011). 'MultiKernel Classification for Integration of Clinical and Imaging Data: Application to Prediction Cognitive Decline in Older Adults', *Machine Learning Medical Imaging*, pp. 26-29

Fix, E., & Hodges Jr, J. L. (1952). 'Discriminatory Analysis-Nonparametric Discrimination: Small Sample Performance', *University of California, Berkeley*.

Fletcher, T., Hussain, Z., Shawe-Taylor, J. (2010) 'Multiple kernel learning on the limit order book', *Proceedings Journal of Machine Learning Research*, vol. 11, pp. 167–174

Fletcher, T., (2010). 'Relevance Vector Machines Explained', [Online]. Available: www.cs.ucl.ac.uk/T.Fletcher/, (Accessed: April 2012)

Fleury, A., Noury, N., & Vacher, M. (2010). 'Introducing knowledge in the process of supervised classification of activities of Daily Living in Health Smart Homes', *12th IEEE International Conference in e-Health Networking Applications and Services,* pp. 322-329.

Fleury, A., Vacher, M., & Noury, N. (2010). 'SVM-based multimodal classification of activities of daily living in health smart homes: sensors, algorithms, and first experimental results', *IEEE Transactions in Information Technology in Biomedicine,* vol. 14(2), pp. 274-283.

Forester, F., Smeja, M., & Fahrenberg, J. (1999). 'Detection of posture and motion by accelerometry: a validation study in ambulatory monitoring', *Computers in Human Behavior*, vol. 15(5), pp. 571-583.

Forsgren, L., Beghi, E., Oun, A., & Sillanpää, M. (2005). 'The epidemiology of epilepsy in Europe–a systematic review', *European Journal of Neurology*, vol. 12(4), pp. 245-253.

Fox, K. R. (1999). 'The influence of physical activity on mental well-being', *Public Health Nutrition*, vol. 2(3a), pp. 411-418.

Frank, A., & Asuncion, A. (2010). UCI Machine Learning Repository, Irvine, CA: University of California. *School of Information and Computer Science*, pp. 213-218.

Freescale MMA7260QT (2008), [Online]. Available: www.freescale.com (Accessed: July 2012)

Freund, Y., & Schapire, R. E. (1996). 'Experiments with a new boosting algorithm', *Machine Learning, 30th International Workshop,* pp. 148-156

Friedman, N., Geiger, D., & Goldszmidt, M. (1997). 'Bayesian network classifiers', *Machine Learning*, vol. 29(2), 131-163.

Fukuchi, R. K., Eskofier, B. M., Duarte, M., & Ferber, R. (2011). 'Support vector machines for detecting age-related changes in running kinematics', *Journal of Biomechanics*, vol. 44(3), pp. 540-542.

FutureLec, (2012) [Online]. Available: www.futurlec.com/Microchip/ (Accessed: July 2012)

Furnkranz, J., & Widmer, G. (1999). 'Incremental reduced error pruning', *International Conference on Machine Learning*, pp. 70-77.

Gabor, A. J., Leach, R. R., & Dowla, F. U. (1996). 'Automated seizure detection using a self-organizing neural network', *Electroencephalography and Clinical Neurophysiology*, vol. 99(3), pp. 257-266.

Galar, M., Fernández, A., Barrenechea, E., Bustince, H., & Herrera, F. (2011). 'An overview of ensemble methods for binary classifiers in multi-class problems: Experimental study on one-vs-one and one-vs-all schemes', *Pattern Recognition*, vol. 44(8), pp. 1761-1776.

Godfrey, A., Conway, R., Meagher, D., & ÓLaighin, G. (2008). 'Direct measurement of human movement by accelerometry', *Medical Engineering & Physics*, vol. 30(10), 1364-1386.

Goldberg, A., Schepens, S. L., Feely, S. M., Garbern, L. J., & Conti, G. E. (2010). 'Deficits in stepping response time are associated with impairments in balance and mobility in people with Huntington disease', *Journal of the Neurological Sciences*, vol. 298(1), pp. 91-95.

Geriatrics Society of America, British Geriatrics Society, and American Academy of Orthopaedic Surgeons Panel on Falls Prevention (2001) 'Guideline for the prevention of falls in older persons.' *Journal of the American Geriatrics Society*, vol. 49(5), pp. 664-672.

Gwet, K. (2002). 'Kappa statistic is not satisfactory for assessing the extent of agreement between raters', *Statistical Methods for Inter-rater Reliability Assessment*, vol. 1(6), pp. 1-6.

Gyllensten, I. C., & Bonomi, A. G. (2011). 'Identifying types of physical activity with a single accelerometer: Evaluating laboratory-trained algorithms in daily life', *IEEE Transactions in Biomedical Engineering*, vol. 58(9), pp. 2656-2663.

Hamel, L. (2009). '*Knowledge discovery with support vector machines*', John Wiley

Han, J., & Kamber, M. (2006). '*Data mining: concepts and techniques*', Morgan Kaufmann.

Harper, P. S. (1992). 'The epidemiology of Huntington's disease', *Human Genetics*, vol. 89(4), pp. 365-376.

Hartmann, A., Murer, K., de Bie, R. A., & de Bruin, E. D. (2009). 'Reproducibility of spatio-temporal gait parameters under different conditions in older adults using a trunk tri-axial accelerometer system', *Gait & Posture*, vol. 30(3), pp. 351.

Hastie, T., & Tibshirani, R. (2001). '*The Elements of Statistical Learning',* Springer Series in Statistics.

Hausdorff, J. M., Schaafsma, J. D., Balash, Y. L., Gurevich, T., & Giladi, N. (2003). 'Impaired regulation of stride variability in Parkinson's disease subjects with freezing of gait', *Experimental Brain Research*, vol. 149(2), pp. 187-194.

Hauser, W. A., & Hesdorffer, D.C. (1990). '*Epilepsy: frequency, causes, and consequences*', Epilepsy Foundation of America.

He, W., Guo, Y., Gao, C., & Li, X. (2012). 'Recognition of human activities with wearable sensors', *Journal on Advances in Signal Processing*, vol. 1, pp. 108-121.

Helbostad, J. L., Askim, T., & Moe-Nilssen, R. (2004). 'Short-term repeatability of body sway during quiet standing in people with hemiparesis and in frail older adults', *Archives of Physical Medicine and Rehabilitation*, vol. 85(6), pp. 993-999.

Hendelman, D., Miller, K., Baggett, C., Debold, E., & Freedson, P. (2000). 'Validity of accelerometry for the assessment of moderate intensity physical activity in the field', *Medicine and Science in Sports and Exercise*, vol. 32(9), pp. S442-449.

Herren, R., Sparti, A., Aminian, K., Schutz, Y., (1999). 'The prediction of speed and incline in outdoor running in humans using accelerometry', *Medicine and Science in Sports and Exercise*, vol. 31(7), pp. 1053-1059.

Hester, T., Sherrill, D. M, Perreault, K., & Bonato, P. (2006). 'Identification of tasks performed by stroke patients using a mobility assistive device', *28th Annual International Conference of the IEEE in Engineering in Medicine and Biology Society,* pp. 1501-1504.

Higashi, Y., Yamakoshi, K., Fujimoto, T., Sekine, M., & Tamura, T. (2008). 'Quantitative evaluation of movement using the timed up-and-go test', *IEEE Engineering in Medicine and Biology Magazine*, vol. 27(4), pp. 38-46.

Hof, At L. 'Scaling gait data to body size', *Gait & Posture,* vol. 4(3), pp. 222-223.

Hosmer David, W., & Stanley, L. (2000). '*Applied logistic regression*', John Wiley.

HP iPAQ 6915 (2006) [Online]. Available: www.o2.co.uk/deviceinfo/device-pdfs/hpipaq6915eng.pdf (Accessed: May 2012)

Hsu, C. W., Chang, C. C., & Lin, C. J. (2009). '*A practical guide to support vector classification'*, [Online]. Available: www.csie.ntu.edu/guide.pdf.

Huynh, T., & Schiele, B. (2005). 'Analyzing features for activity recognition', *Joint Conference on Smart Objects and Ambient Intelligence,* pp. 159-163.

Huynh, T., & Schiele, B. (2006). 'Towards less supervision in activity recognition from wearable sensors', *10th IEEE International Symposium in Wearable Computers,* pp. 3-10.

Hynes, M., Wang, H., McCarrick, E., & Kilmartin, L. (2011). 'Accurate monitoring of human physical activity levels for medical diagnosis and monitoring using off-the-shelf cellular handsets', *Personal and Ubiquitous Computing*, vol. 15(7), pp. 667-678.

Ibrahim, R. K., Ambikairajah, E., Celler, B., Lovell, N. H., & Kilmartin, L. (2008). 'Gait patterns classification using spectral features', *Irish Signals and Systems Conference,* pp. 98-102.

Inman, V.T (1967). 'Conservation of energy in ambulation', *Archives of Physical Medicine Rehabilation*, vol. 48(9), pp. 484-492.

Jallon, P., Bonnet, S., Antonakios, M., & Guillemaud, R. (2009). 'Detection system of motor epileptic seizures through motion analysis with 3D accelerometers', *27th Annual International Conference of the IEEE in Engineering in Medicine and Biology Society*, pp. 2466-2469

Jasiewicz, J. M., Allum, J. H., Middleton, A., Condie, P., Purcell, B., & Li, R. C. T. (2006). 'Gait event detection using linear accelerometers or angular velocity transducers in able-bodied and spinal-cord injured individuals', *Gait & Posture*, vol. 24(4), pp. 502-509.

Jones, V. M., Tonis, T., Bults, R. B., van Beijnum, B., & Hermens, H. (2008). 'Biosignal and context monitoring: Distributed multimedia applications of body area networks in healthcare', *10th IEEE Workshop in Multimedia Signal Processing,* pp. 820-825.

Karantonis, D. M., Narayanan, M. R., Mathie, M., Lovell, N. H., & Celler, B. G. (2006). 'Implementation of a real-time human movement classifier using a triaxial accelerometer for ambulatory monitoring', *IEEE Transactions in Information Technology in Biomedicine*, vol. 10(1), pp. 156-167.

Kavanagh, J. J., & Menz, H. B. (2008). 'Accelerometry: a technique for quantifying movement patterns during walking', *Gait & Posture*, vol. 28(1), pp. 1-15.

Kavanagh, J. J., Barrett, R. S., & Morrison, S. (2004). 'Upper body accelerations during walking in healthy young and elderly men', *Gait & Posture*, vol. 20(3), pp. 291-298.

Kavanagh, J. J., Morrison, S., James, D. A., & Barrett, R. (2006). 'Reliability of segmental accelerations measured using a new wireless gait analysis system', *Journal of Biomechanics*, vol. 39(15), pp. 2863-2872.

Keogh, E., & Ratanamahatana, C. A. (2005). 'Exact indexing of dynamic time warping', *Knowledge and Information Systems*, vol. 7(3), pp. 358-386.

Kern, N., Schiele, B., & Schmidt, A. (2003). 'Multi-sensor activity context detection for wearable computing'. *Ambient Intelligence*, vol. 2875, pp. 220-232.

Kerr, K. M., White, J. A., Barr, D. A., & Mollan, R. A. (1997). 'Analysis of the sit-stand-sit movement cycle in normal subjects', *Clinical Biomechanics*, vol. 12(4), pp. 236.

Khalil, H., Dalton, A., van Deursen, R., Rosser, A., ÓLaighin, G., & Busse, M. (2010). 'F17 The use of an accelerometer to evaluate the performance of timed up and go test in pre-symptomatic and symptomatic huntington's disease', *Journal of Neurology, Neurosurgery & Psychiatry*, A28-A28.

Khan, A. M., Lee, Y. K., Lee, S. Y., & Kim, T. S. (2010). 'A triaxial accelerometer-based physical-activity recognition via augmented-signal features and a hierarchical recognizer', *IEEE Transactions in Information Technology in Biomedicine*, vol. 14(5), pp. 1166-1172.

Khandoker, A. H., Lai, D. T., & Begg, R. K., (2007). 'Wavelet-based feature extraction for support vector machines for screening balance impairments in the elderly', *IEEE Transactions on Neural Systems and Rehabilitation Engineering*, vol. 15(4), pp. 587-597.

Khasnis, A., & Gokula, R. M. (2003). 'Romberg's test', *Journal of Postgraduate Medicine*, vol. 49(2), pp. 169-172.

Kiani, K., Snijders, C., & Gelsema, E. S. (1997). 'Computerized analysis of daily life motor activity for ambulatory monitoring', *Technological Health Care,* vol. 5(4), pp. 307-318.

Kilmartin, L., Ibrahim, R. K., Ambikairajah, E., & Celler, B. (2009). 'Optimising recognition rates for subject independent gait pattern classification', *Irish Signals and Systems Conference,* pp. 1-6.

Kinsella, K., & He, W. (2009). '*Census Bureau, International Population Reports. An Aging World: 2008',* [Online]. Available: www.census.gov/p95-09-1.pdf (Accessed: May 2012)

Kramer, U., Kipervasser, S., & Kuzniecky, R. (2011). 'A novel portable seizure detection alarm system: preliminary results', *Journal of Clinical Neurophysiology*, vol. 28(1), pp. 36.

Krause, A., Siewiorek, D. P., Smailagic, A., & Farringdon, J. (2003). 'Unsupervised, dynamic identification of physiological and activity context in wearable computing', *7th IEEE International Symposium on Wearable Computers,* pp. 88.

Kremer, H. P. H. (1996). 'Unified Huntington's disease rating scale: reliability and consistency', *Movement Disorders*, vol. 11(2), pp. 136-140.

Kwapisz, J. R., Weiss, G. M., & Moore, S. A. (2011). 'Activity recognition using cell phone accelerometers', *4th International Workshop on Knowledge Discovery from Sensor Data*, pp. 10-18.

Lai, D. T., Levinger, P., Begg, R. K., Gilleard, W., & Palaniswami, M. (2007). 'Identification of patellofemoral pain syndrome using a Support Vector Machine approach', *26th Annual International Conference of the IEEE Engineering in Medicine and Biology Society*, pp. 3144-3147.

Lakany, H. M. (2000). 'A generic kinematic pattern for human walking', *Neurocomputing*, vol. 35(1), pp. 27-54.

Lau, H. Y., Tong, K. Y., & Zhu, H. (2008). 'Support vector machine for classification of walking conditions using miniature kinematic sensors', *Medical and Biological Engineering and Computing*, vol. 46(6), pp. 563-573.

Lee, S. H., Park, H. D., Hong, S. Y., Lee, K. J., & Kim, Y. H. (2003). 'A study on the activity classification using a triaxial accelerometer', *25th Annual International Conference of the IEEE Engineering in Medicine and Biology Society*, vol. 3, pp. 2941-2943.

Lester, J., Choudhury, T., Kern, N., Borriello, G., & Hannaford, B. (2005). 'A hybrid discriminative/generative approach for modeling human activities', *19th International Joint Conference on Artificial Intelligence*, pp. 766-772.

Lester, J., Choudhury, T., & Borriello, G. (2006). 'A practical approach to recognizing physical activities', *Pervasive Computing*, vol. 3968, pp. 1-16.

Levinger, P., Lai, D. T., Begg, R. K., Webster, K. E., & Feller, J. A. (2009). 'The application of support vector machines for detecting recovery from knee replacement surgery using spatio-temporal gait parameters', *Gait & Posture*, vol. 29(1), pp. 91-96.

Lieberman, J. R., Dorey, F., Shekelle, P., Kilgus, D. J., & Finerman, G. A. (1996). 'Differences between Patients' and Physicians' Evaluations of Outcome after Total Hip Arthroplasty', *The Journal of Bone & Joint Surgery*, vol. 78(6), pp. 835-8.

Liu J, Kanno T, Akashi M, Chen W, Wei W. (2006) 'Patterns of bipedal walking on tri-axial acceleration signals and their use in identifying falling risk of older people', *6th International Conference in Computer and Information Technology*, pp. 205-211.

Lo, B., Atallah, L., Aziz, O., ElHew, & Yang, G. Z. (2007). 'Real-time pervasive monitoring for postoperative care', *4th International Workshop on Wearable and Implantable Body Sensor Networks*, pp. 122-127.

Lockmann, J., Fisher, R. S., & Olson, D. M. (2011). 'Detection of seizure-like movements using a wrist accelerometer', *Epilepsy & Behavior*, vol. 20(4), pp. 638-641.

Long, X., Yin, B., & Aarts, R. M. (2009). 'Single-accelerometer-based daily physical activity classification', *28th Annual International Conference of the IEEE in Engineering in Medicine and Biology Society*, pp. 6107-6110.

Lorincz, K., Chen, B. R., Challen, A. R., Patel, S., Bonato, P., & Welsh, M. (2009). 'Mercury: a wearable sensor network platform for high-fidelity motion analysis', *7th Annual Conference on Embedded Networked Sensor Systems,* pp. 183-196.

Lukowicz, P., Junker, H., Staeger, M., & Troester, G. (2002). 'WearNET: A distributed multi-sensor system for context aware wearables', *Ubiquitous Computing*, vol. 2498, pp. 361-370.

Lyons, G. M., Culhane, K. M., Hilton, D., Grace, P. A., & Lyons, D. (2005). 'A description of an accelerometer-based mobility monitoring technique', *Medical Engineering & Physics*, vol. 27(6), pp. 497-504.

MATLAB r2010b, The MathWorks Inc., Nat, MA, USA (2012) [Online] Available: www.mathworks.com (Accessed: Feb. 2012)

Maekawa, T., Yanagisawa, Y., Kishino, Y., Ishiguro, K., Sakurai, Y., & Okadome, T. (2010). 'Object-based activity recognition with heterogeneous sensors on wrist', *Pervasive Computing*, vol. 6030, pp. 246-264.

Maemo Online, (2010) [Online]. Available: www.maemo.org/. (Accessed: Feb. 2012)

Mannini, A., & Sabatini, A. M. (2011). 'On-line classification of human activity and estimation of walk-run speed from acceleration data using support vector machines', *33rd Annual International Conference of the IEEE Engineering in Medicine and Biology Society*, pp. 3302-3305.

Mannini, A., & Sabatini, A. M. (2010). 'Machine learning methods for classifying human physical activity from on-body accelerometers', *Sensors*, vol. 10(2), pp. 1154-1175.

Mansfield, A., & Lyons, G. M. (2003). 'The use of accelerometry to detect heel contact events for use as a sensor in FES assisted walking', *Medical Engineering & Physics*, vol. 25(10), pp. 879-885.

Mantyjarvi, J., Himberg, J., & Seppanen, T. (2001). 'Recognizing human motion with multiple acceleration sensors', *IEEE International Conference on Systems, Man, and Cybernetics*, vol. 2, pp. 747-752.

Mathie, M. (2003). '*Monitoring and interpreting human movement patterns using a triaxial accelerometer*', Doctoral dissertation, The University of New South Wales.

Mathie, M. J., Coster, A. C., Lovell, N. H., Celler, B. G., Lord, S. R., & Tiedemann, A. (2004). 'A pilot study of long-term monitoring of human movements in the home using accelerometry', *Journal of Telemedicine and Telecare*, vol. 10(3), pp. 144-151.

Mathie, M. J., Coster, A. C., Lovell, N. H., & Celler, B. G. (2003). 'Detection of daily physical activities using a triaxial accelerometer', *Medical and Biological Engineering and Computing*, vol. 41(3), pp. 296-301.

Mathie, M. J., Coster, A. C., Lovell, N. H., & Celler, B. G. (2004). 'Accelerometry: providing an integrated, practical method for long-term, ambulatory monitoring of human movement', *Physiological Measurement*, vol. 25(2), pp. R1-20.

Maurer, U., Smailagic, A., Siewiorek, D. P., & Deisher, M. (2006). 'Activity recognition and monitoring using multiple sensors on different body positions', *Wearable and Implantable Body Sensor Networks,* pp. 4-6.

Menz, H. B., Latt, M. D., Tiedemann, A., Mun San Kwan, M., & Lord, S. R. (2004). 'Reliability of the GAITRite® walkway system for the quantification of temporo-spatial parameters of gait in young and older people', *Gait & Posture*, vol. 20(1), pp. 20-25.

Menz, H. B., Lord, S. R., & Fitzpatrick, R. C. (2003). 'Acceleration patterns of the head and pelvis when walking on level and irregular surfaces', *Gait & Posture*, vol. 18(1), pp. 35-46.

Microsoft MFC, (1995) [Online]. Available: '*Microsoft Visual C++ Programming with MFC*', (Accessed: Mar. 2012).

Milenković, A., Otto, C., & Jovanov, E. (2006). 'Wireless sensor networks for personal health monitoring: Issues and an implementation', *Computer Communications*, vol. 29(13), pp. 2521-2533.

Minasyan, G. R., Chatten, J. B., & Harner, R. N. (2010). 'Patient-specific early seizure detection from scalp EEG', *Journal of Clinical Neurophysiology,* vol. 27(3), pp. 163.

Minnen, D., Starner, T., Ward, J. A., Lukowicz, P., & Troster, G. (2005). 'Recognizing and discovering human actions from on-body sensor data', *IEEE International Conference* in *Multimedia,* pp. 1545-1548.

Mitsumi Electric Bluetooth Module, (2012) [Online] Available: www.mitsumi.co.jp/English (Accessed: Feb. 2012)

Mizuike, C., Ohgi, S., & Morita, S. (2009). 'Analysis of stroke patient walking dynamics using a tri-axial accelerometer', *Gait & Posture*, vol. 30(1), pp. 60-80.

Moe-Nilssen, R., Aaslund, M. K., C., & Helbostad, J. L. (2010). 'Gait variability measures may represent different constructs', *Gait & Posture*, vol. 32(1), pp. 98-101.

Moe-Nilssen, R., & Helbostad, J. L. (2005). 'Interstride trunk acceleration variability but not step width variability can differentiate between fit and frail older adults', *Gait & Posture*, vol. 21(2), pp. 164-170.

Moe-Nilssen, R., & Helbostad, J. L. (2002). 'Trunk accelerometry as a measure of balance control during quiet standing', *Gait & Posture*, vol. 16(1), pp. 60-68.

Moe-Nilssen, R., & Helbostad, J. L. (2004). 'Estimation of gait cycle characteristics by trunk accelerometry', *Journal of Biomechanics*, vol. 37(1), pp. 121-125.

Moe-Nilssen, R. et al. (1998). 'Test-retest reliability of trunk accelerometry during standing and walking', *Archives of Physical Medicine and Rehabilitation*, vol. 79(11), pp. 1377-1385.

Moore, A., & Pelleg, D. (2000). 'X-means: Extending k-means with efficient estimation of clusters', *17th International Conference on Machine Learning*, vol. 1, pp. 727-734.

Murracy, C.J.L., Lopez, A.D. (1994) '*Global comparative assessment in the health sector; disease burden, expenditur*e', World Health Organization.

Myers, R. H. (2004). 'Huntington's disease genetics', *NeuroRx*, vol. 1(2), pp. 255-262.

Najafi, B., Aminian, K., Loew, F., Blanc, Y., & Robert, P. (2000). 'An ambulatory system for physical activity monitoring in elderly', *1st Annual International Conference in Microtechnologies in Medicine and Biology,* pp. 562-566.

Najafi, B., Aminian, K., Paraschiv-Ionescu, A., Loew, F., Bula, C. J., & Robert, P. (2003). 'Ambulatory system for human motion analysis using a kinematic sensor: monitoring of daily physical activity in the elderly', *Biomedical Engineering,* vol. 50(6), pp. 711-723.

Niezen, G., & Hancke, G. P. (2009). 'Evaluating and optimising accelerometer-based gesture recognition techniques for mobile devices', *9th IEEE Region 8 Conference AFRICON, 2009*, pp. 1-6.

Nijsen, T. M., Cluitmans, P. J., Arends, J. B., & Griep, P. A. (2007). 'Detection of subtle nocturnal motor activity from 3-D accelerometry recordings in epilepsy patients', *IEEE Transactions in Biomedical Engineering,* vol. 54(11), pp. 2073-2081.

Nijsen, T. M., Cluitmans, P. J. (2005) 'The potential value of 3-D accelerometry for detection of motor seizures in severe epilepsy', *Epilepsy Behaviour*, vol. 7(1), pp. 74-84.

Nijsen, T. M., Aarts, R. M., Arends, J. B., & Cluitmans, P. J. (2009). 'Automated detection of tonic seizures using 3-D accelerometry', *4th European Conference of International Federation for Medical and Biological Engineering*, pp. 188-191.

Nijsen, T. M., Aarts, R. M., Cluitmans, P. J., & Griep, P. A. (2010). 'Time-frequency analysis of accelerometry data for detection of myoclonic seizures', *IEEE Transactions in Information Technology in Biomedicine,* vol. 14(5), pp. 1197-1203.

Nijsen, T. M., Janssen, A. J., & Aarts, R. M. (2007). 'Analysis of a wavelet arising from a model for arm movements during epileptic seizures', *Program for Research on Integrated Systems and Circuits Conference,* pp. 19-24.

Nijsen, T. M., Cluitmans, P. J., & Aarts, R. M. (2006). 'Short time Fourier and wavelet transform for accelerometric detection of myoclonic seizures', *IEEE Belgian Day on Biomedical Engineering*, pp. 7-8.

Nokia Corporation, (2012) [Online]. Available: www.nokia.com//phones/ (Accessed: Feb. 2012)

Noury, N., Barralon, P., Couturier, P., Guillemaud, R., Mestais, C., & Provost, H. (2004). 'ACTIDOM-A MicroSystem based on MEMS for Activity Monitoring of the Frail Elderly in their Daily Life', *26th Annual International Conference in Engineering in Medicine and Biology Society,* vol. 2, pp. 3305-3308.

NiScanaill, C. N., Ahearne, B., & Lyons, G. M. (2006). 'Long-term telemonitoring of mobility trends of elderly people using SMS messaging', *IEEE Transactions of Information Technology in Biomedicine,* vol. 10(2), pp. 412-413.

O'Sullivan, M., Blake, C., Cunningham, C., Boyle, G., & Finucane, C. (2009). 'Correlation of accelerometry with clinical balance tests in older fallers and non-fallers', *Age and Ageing*, vol. 38(3), pp. 308-313.

United States Public Health Service, Office of the Surgeon General, (1996). 'Physical activity and health: a report of the Surgeon General', *Jones & Bartlett Learning*.

Olguın, D. O., & Pentland, A. S. (2006). 'Human activity recognition: Accuracy across common locations for wearable sensors', *MIT Media Lab*.

Palmerini, L., Rocchi, L., Mellone, S., Valzania, F., & Chiari, L. (2011). 'Feature selection for accelerometer-based posture analysis in Parkinson's disease', *IEEE Transactions of Information Technology in Biomedicine,* vol. 15(3), pp. 481-490.

Panzera, R., Salomonczyk, D., Pirogovosky, E., Simmons, R., Goldstein, J., Corey-Bloom, J., & Gilbert, P. E. (2011). 'Postural deficits in Huntington's disease when performing motor skills involved in daily living', *Gait & Posture*, vol. 33(3), pp. 457-461.

Paraschiv-Ionescu, A., Buchser, E. E., Najafi, B., & Aminian, K. (2004). 'Ambulatory system for the quantitative and qualitative analysis of gait and posture in chronic pain patients treated with spinal cord stimulation', *Gait & Posture*, vol. 20(2), pp. 113-125.

Park, C., Chou, P. H., & Sun, Y. (2006). 'A wearable wireless sensor platform for interactive dance performances', *4th Annual IEEE International Conference in Pervasive Computing and Communications,* pp. 6-10.

Parkka, J., Ermes, M., Korpipaa, P., Mantyjarvi, J., Peltola, J., & Korhonen, I. (2006). 'Activity classification using realistic data from wearable sensors', *IEEE Transactions of Information Technology in Biomedicine,* vol. 10(1), pp. 119-128.

Pirttikangas, S., Fujinami, K., & Nakajima, T. (2006). 'Feature selection and activity recognition from wearable sensors', *Ubiquitous Computing Systems*, vol. 4239, pp. 516-527.

Pixie Operating System (2012) [Online] Available www.eecs.harvard.edu (Accessed: Mar. 2012)

Puska P., H. Benaziza, D. Porter (2004). '*Physical Activity, WHO Sheet Physical Activity*', [Online]. Available: http://www.who.int/en/gs_pa.pdf. (Accessed: Mar. 2012)

Qu, H., & Gotman, J. (1993). 'Improvement in seizure detection performance by automatic adaptation to the EEG of each patient', *Electroencephalography and Clinical Neurophysiology*, vol. 86(2), pp. 79-87.

Quinlan, J. R. (1993). '*C4. 5: programs for machine learning*', vol. 1, Morgan Kaufmann.

Quinn, L., & Rao, A. (2002). 'Physical therapy for people with Huntington disease: current perspectives and case report', *Journal of Neurologic Physical Therapy*, vol. 26(3), pp. 145.

R Development Core Team (2011). '*R: A language and environment for statistical computing*', R Foundation for Statistical Computing.

Rakotomamonjy, A., Bach, F., Canu, S., & Grandvalet, Y. (2008). 'SimpleMKL', *Journal of Machine Learning Research*, vol. 9, pp. 2491-2521.

Ramos-Arroyo, M. A., Moreno, S., & Valiente, A. (2005). 'Incidence and mutation rates of Huntington's disease in Spain: experience of 9 years of direct genetic testing', *Journal of Neurology, Neurosurgery & Psychiatry*, vol. 76(3), pp. 337-342.

Randell, C., & Muller, H. (2000). 'Context awareness by analysing accelerometer data', *4th International Symposium of Wearable Computers,* pp. 175-176.

Rao, A. K., Louis, E. D., & Marder, K. S. (2009). 'Clinical assessment of mobility and balance impairments in pre-symptomatic Huntington's disease', *Gait & Posture*, vol. 30(3), pp. 391-393.

Rao, A. K., Muratori, L., Louis, E. D., Moskowitz, C. B., & Marder, K. S. (2009). 'Clinical measurement of mobility and balance impairments in Huntington's disease: Validity and responsiveness', *Gait & Posture*, vol. 29(3), pp. 433-436.

Rao, A. K., Muratori, L., Louis, E. D., Moskowitz, C. B., & Marder, K. S. (2008). 'Spectrum of gait impairments in presymptomatic and symptomatic Huntington's disease', *Movement Disorders*, vol. 23(8), pp. 1100-1107.

Rao, A. K., Quinn, L., & Marder, K. S. (2005). 'Reliability of spatiotemporal gait outcome measures in Huntington's disease', *Movement Disorders*, vol. 20(8), pp. 1033-1037.

Ravi, N., Dandekar, N., Mysore, P., & Littman, M. L. (2005). 'Activity recognition from accelerometer data', *Proceedings of National Conference Artificial Intelligence,* vol. 20, pp. 1541-1550

Ringwald, M., & Romer, K. (2007). 'Practical time synchronization for bluetooth scatternets', *4th International Conference on Broadband Communications, Networks and Systems,* pp. 337-345.

Roving Networks, (2012) [Online] Available: www.rovingnetworks.com/ (Accessed: Mar. 2012)

Sabatini, A. M., Martelloni, C., Scapellato, S., & Cavallo, F. (2005). 'Assessment of walking features from foot inertial sensing', *Biomedical Engineering,* vol. 52(3), pp. 486-494.

Salarian, A., Russmann, H., Vingerhoets, F. J., Burkhard, P. R., & Aminian, K. (2007). 'Ambulatory monitoring of physical activities in patients with Parkinson's disease', *IEEE Transaction in Biomedical Engineering,* vol. 54(12), pp. 2296-2299.

Salvador, S., & Chan, P. (2007). 'Toward accurate dynamic time warping in linear time and space', *Intelligent Data Analysis*, vol. 11(5), pp. 561-580.

Sama, A, Català A, Rodríguez-Molinero A, Angulo, C., (2009). 'Extracting Gait Spatiotemporal Properties from Parkinson's Disease Patients'. *23rd Annual Conference on Neural Information Processing Systems*, pp. 12-15.

Sammon Jr, J. W. (1969). 'A nonlinear mapping for data structure analysis', *IEEE Transactions on Computers*, vol. 100(5), pp. 401-409.

Schmidt, D., Elger, C., & Holmes, G. L. (2002). 'Pharmacological overtreatment in epilepsy-Mechanisms and management', *Epilepsy Research*, vol. 52(1), pp. 3-14.

Schulc, E., Unterberger, I., Saboor, S., Hilbe, J., Ertl, M. & Them, C. (2011). 'Measurement and quantification of generalized tonic–clonic seizures in epilepsy patients by means of accelerometry—An explorative study', *Epilepsy Research*, vol. 95(1), pp. 173-183.

Sekine, M., Tamura, T., Akay, M., Fujimoto, T., Togawa, T., & Fukui, Y. (2002). 'Discrimination of walking patterns using wavelet-based fractal analysis', *IEEE Transactions on Neural Systems and Rehabilitation Engineering*, vol. 10(3), pp. 188-196.

Sekine, M., Tamura, T., Togawa, T., & Fukui, Y. (2000). 'Classification of waist-acceleration signals in a continuous walking record', *Medical Engineering & Physics*, vol. 22(4), pp. 285-291.

Senden, R., Grimm, B., Heyligers, I. C., Savelberg, H. H. C. M., & Meijer, K. (2009). 'Acceleration-based gait test for healthy subjects: reliability and reference data', *Gait & Posture*, vol. 30(2), pp. 192-196.

SHIMMER (2012) [Online]. Available: www.shimmer-research.com (Accessed: Feb. 2012)

Shoeb, A., Edwards, H., Connolly, J., Bourgeois, B., Ted Treves, S., & Guttag, J. (2004). 'Patient-specific seizure onset detection', *Epilepsy & Behavior*, vol. 5(4), pp. 483-498.

Shoeb, A., Schachter, S., Schomer, D., Treves, S. T., & Guttag, J. (2006). 'Detecting seizure onset in the ambulatory setting: demonstrating feasibility', *7th Annual International Conference of the IEEE Engineering in Medicine and Biology Society,* pp. 3546-3550

Skovronsky, D. M., Lee, V. M. Y., & Trojanowski, J. Q. (2006). 'Neurodegenerative diseases: new concepts of pathogenesis and their therapeutic implications', *Annual Review of Pathology-mechanisms of Disease*, vol. 1, pp. 151-170.

Sobngwi, E., Mbanya, J. C., Unwin, A. P., & Alberti, K. G. (2002). 'Physical activity and its relationship with obesity, hypertension and diabetes in urban and rural Cameroon', *International Journal of Obesity and Related Metabolic Disorders,* vol. 26(7), pp. 1009-14.

Song, K. T., & Wang, Y. Q. (2005). 'Remote activity monitoring of the elderly using a two-axis accelerometer', *Proceedings of CACS Automatic Control Conference*, pp. 18-23.

Sparkfun (2004). [Online]. Available: www.sparkfun.com (Accessed: Feb. 2012)

Stanton, M. W., & Rutherford, M. K. (2006). 'The high concentration of US health care expenditures', *US Department of Health & Human Services: Agency for Healthcare Research and Quality*, pp. 6-16.

Staudenmayer, J., Pober, D., Crouter, S., & Freedson, P. (2009). 'An artificial neural network to estimate physical activity energy expenditure and identify physical activity type from an accelerometer', *Journal of Applied Physiology*, vol. 107(4), pp. 1300-1307.

Storti, K. L., Pettee, K. K., Brach, J. S., Talkowski, J. B., Richardson, C. R., & Kriska, A. M. (2008). 'Gait speed and step-count monitor accuracy in community-dwelling older adults', *Medicine and Science in Sports and Exercise*, vol. 40(1), pp. 59.

Tabrizi, S. J., Langbehn, D. R., Leavitt, B. R., Roos, R. A., & Stout, J. C. (2009). 'Biological and clinical manifestations of Huntington's disease in the longitudinal TRACK-HD study: cross-sectional analysis of baseline data', *The Lancet Neurology*, vol. 8(9), pp. 791-801.

Tamura, T., Fujimoto, T., Huang, J., & Togawa, T. (1995). 'The design of an ambulatory physical activity monitor and it application to the daily activity of the elderly', *17th Annual Conference of the IEEE Engineering in Medicine Biology Society,* vol. 2, pp. 1591-1592.

Tapia, E., Intille, S., Lopez, L., & Larson, K. (2006). 'The design of a portable kit of wireless sensors for naturalistic data collection', *Pervasive Computing*, vol. 10, pp. 117-134.

Tatum IV, W. O., Winters, L., Gieron, M., Ferreira, J., & Liporace, J. (2001). 'Outpatient seizure identification: results of 502 patients using computer-assisted ambulatory EEG', *Journal of Clinical Neurophysiology*, vol. 18(1), pp. 14-19.

Texas Instruments MSP430, (2010) [Online] Available: www.ti.com (Accessed: Feb. 2012)

The GAITRite Walkway, (2010) [Online]. Available: www.gaitrite.com/ (Accessed: Feb. 2012)

TinyOS 2.0, (2011) [Online]. Available: www.docs.tinyos.net/ (Accessed: Feb. 2012)

Tura, A., Raggi, M., Rocchi, L., Cutti, A. G., & Chiari, L. (2010). 'Gait symmetry and regularity in transfemoral amputees assessed by trunk accelerations', *Journal Neuro-Engineering Rehabilitation*, vol. 7(4), pp. 13-17.

United States Department of Commerce. Bureau of the Census. Population, (1996) [Online]. Available www.census.gov/idbpyr.html. (Accessed: Apr. 2012)

Veltink, P. H., Bussman, H. B., Koelma, H. M., Martens, W. L., & Lummel, R. C. (1993). 'The feasibility of posture and movement detection by accelerometry', *15th International Conference of the IEEE Engineering in Medicine and Biology Society*, pp. 1230-1231

Veltink, P. H., Bussmann, H., de Vries, W., Martens, W., & Van Lummel, R. C. (1996). 'Detection of static and dynamic activities using uniaxial accelerometers', *IEEE Transactions in Rehabilitation Engineering*, vol. 4(4), pp. 375-385.

Walker, F. O. (2007). 'Huntington's disease', *The Lancet*, vol. 36 (7), pp. 218-228.

Wang, N., Ambikairajah, E., Celler, B. G., & Lovell, N. H. (2008). 'Accelerometry based classification of gait patterns using empirical mode decomposition', *IEEE International Conference in Acoustics, Speech and Signal Processing,* pp. 617-620.

Wark, T., Karunanithi, M., & Chan, W. (2006). 'A framework for linking gait characteristics of patients with accelerations of the waist', *27th Annual International Conference of the IEEE Engineering in Medicine and Biology Society,* pp. 7695-7698.

Webster, K. E., Wittwer, J. E., & Feller, J. A. (2005). 'Validity of the GAITRit® walkway system for the measurement of averaged and individual step parameters of gait', *Gait & Posture*, vol. 22(4), pp. 317-321.

Weiss, A., Herman, T., Plotnik, M., Maidan, I., Giladi, N., & Hausdorff, J. M. (2010). 'Can an accelerometer enhance the utility of the Timed Up & Go Test when evaluating patients with Parkinson's disease?', *Medical Engineering & Physics*, vol. 32(2), pp. 119-125.

Westerterp, K. R., & Meijer, E. P. (2001). 'Physical Activity and Parameters of Aging A Physiological Perspective', *The Journals of Gerontology Series A: Biological Sciences and Medical Sciences*, vol. 56(A), pp. 7-12.

White, C. (2007). 'Health care spending growth: How different is the United States from the rest of the OECD?', *Health Affairs*, vol. 26(1), pp. 154-161.

Widcomm Stack, (2010) [Online] Available: www.broadcom.com/bt/ (Accessed: Feb. 2012)

Windows SDK. (2010) [Online]. Available: www.microsoft.com (Accessed: Mar. 2012)

Witilt v2, Sparkfun, (2009) [Online]. Available: www.sparkfun.com. (Accessed: Mar. 2012)

Witilt v3, Sparkfun, (2011) [Online]. Available: www.sparkfun.com. (Accessed: June 2012)

Witte, H., & L.D, Iasemidis., (2003) 'Special issue on epileptic seizure prediction', *IEEE Transactions in Biological Engineering*, vol. 50, pp. 537-539.

Witten, I. H. & Frank, E. (2005). '*Data Mining: Practical machine learning tools and techniques*', Morgan Kaufmann.

World Health Organization. (1980). '*International classification of impairment, disabilities, handicaps; a manual classification relating to the consequences of disease*', WHO.

Wu, Y., Chen, R., & She, M. (2011). 'Automated classification of human daily activities in ambulatory environment', *Software Engineering, Artificial Intelligence, Networking and Parallel / Distributed Computing,* vol. 368, pp.157-168.

Wu, Y., & Krishnan, S. (2010). 'Statistical analysis of gait rhythm in patients with Parkinson's disease', *IEEE Transactions on Neural Systems Rehabilitation Engineering*, vol. 18(2), pp. 150-158.

Wyke, A. (2009). 'Fixing Healthcare Professionals Perspective' *Economist Intelligence Unit*

Yoshida, Y., Yonezawa, Y., Sata, K., Ninomiya, I., & Caldwell, W. M. (2000). 'A wearable posture, behavior and activity recording system', *22nd Annual International Conference of the IEEE Engineering in Medicine and Biology Society,* vol. 2, pp. 1278-92.

Zampieri, C., Salarian, A., Carlson-Kuhta, P., Aminian, K., Nutt, J. G., & Horak, F. B. (2010). 'The instrumented timed up and go test: potential outcome measure for disease modifying therapies in Parkinson's disease', *Journal of Neurology, Neurosurgery & Psychiatry*, vol. 81(2), pp. 171-176.

Zhang, S., Rowlands, A. V., Murray, P., & Hurst, T. (2012). 'Physical Activity Classification Using the GENEA Wrist-Worn Accelerometer', *Medicine and Science in Sports and Exercise*, vol. 44(4), pp. 742-748.

Zhang, T., Wang, J., & Liu, P. (2006). 'Fall detection by wearable sensor and one-class SVM algorithm', *Intelligent Computing in Control and Information Sciences*, vol. 345, pp. 858-863.

Zijlstra, A., Goosen, J. H., Verheyen, C. C., & Zijlstra, W. (2008). 'A body-fixed-sensor based analysis of compensatory trunk movements during unconstrained walking', *Gait & Posture*, vol. 27(1), pp. 164-167.

Zijlstra, W., & Hof, A. L. (1997). 'Displacement of the pelvis during human walking: experimental data and model predictions', *Gait & Posture*, vol. 6(3), pp. 249-262.

Zijlstra, W., & Hof, A. L. (2003). 'Assessment of spatio-temporal gait parameters from trunk accelerations during human walking', *Gait & Posture*, vol. 18(2), pp. 1-10.

# APPENDIX

# APPENDIX A

## Journal Publications

Dalton, A., & ÓLaighin, G. (2012). 'Comparing supervised learning techniques on the task of physical activity recognition', *IEEE Journal of Health & Biomedical Informatics,* vol. 17, pp. 46-52 http://ieeexplore.ieee.org

Dalton, A., & ÓLaighin, G. (2012). 'Physical activity recognition through support vector machines with multiple kernel learning', *Medical Engineering & Physics*, *under review.*

Dalton, A., Patel, S, Chodury, A., Welsh, M, Pang, T, Schachter, S., ÓLaighin, G., & Bonato, P. (2012). 'Development of a body sensor network to detect motor patterns of epileptic Seizures', *IEEE Transactions on Biomedical Engineering*, vol. 59 (11), pp. 3204-3211 http://ieeexplore.ieee.org

Dalton, A., Khalil, H., Busse, M., Rosser, A., van Deursen, R., & ÓLaighin, G. (2012). 'Analysis of gait and balance through a single triaxial accelerometer in presymptomatic and symptomatic Huntington's disease', *Gait & Posture*, vol. 37(1), pp. 49-54. www.gaitposture.com

## Conference Publications

Dalton, A, Scanaill, C.N., Carew, S., Lyons, D., & ÓLaighin, G. (2007). 'A clinical evaluation of a remote mobility monitoring system based on SMS messaging', *29th Annual International Conference of IEEE Engineering in Medicine and Biology Society*, pp. 237-233.

Dalton, A., Morgan, F., & ÓLaighin, G. (2008). 'A preliminary study of using wireless kinematic sensors to identify basic Activities of Daily Living', *30th Annual International Conference of IEEE Engineering in Medicine and Biology Society,* pp. 2079-2082.

Dalton, A, & ÓLaighin, G. (2009). 'Identifying activities of daily living using wireless kinematic sensors and data mining algorithms', *IEEE Wearable & Implantable Body Sensor Networks*, pp. 87-91.

Dalton, A., Patel, S., Mancinelli, C., Hughes, R., Shih, L., ÓLaighin, G., & Bonato, P. (2009). 'Analyzing the decision space of deep brain stimulation settings' *35th Annual IEEE Northeast Bioengineering Conferenc*e, pp.12-15

Dalton, A., Patel, S., Chowdhury, A., Welsh, M., Pang, T., Schachter, S., ÓLaighin, G., & Bonato, P. (2010) 'Detecting epileptic seizures with wearable sensor technologies', *1st Annual AMA-IEEE Medical Technology Conference,* pp. 73-74.

Khalil, H., Dalton, A., van Deursen, R., Rosser, A., ÓLaighin, G., & Busse, M. (2010). 'The use of an accelerometer to evaluate the performance of timed up and go test in pre-symptomatic and symptomatic Huntington's disease', *Journal of Neurology, Neurosurgery & Psychiatry*, pp. 28-29.

# APPENDIX B

## R-Code

```
#Anthony Dalton - Sept. 2012
#Requires Packages: Party, klaR, e1071, neuralnet, caret, RWeka, ROCR, kernlab and ggplot2.
#Built using RStudio v. 0.96
#Reference: R and Data Mining: Examples and Case Studies, Machine Learning for Hackers

#Clean Workspace
rm(list = ls())

#Install Required Packages
install.packages('party');install.packages('klaR');install.packages('e1071');install.packages('neuralnet');install.pac
kages('caret');
install.packages('RWeka');install.packages('ROCR');install.packages('kernlab');install.packages('ggplot2');

#Load Required Packages
library(party);library(klaR);library(e1071);library(neuralnet);library(caret);
library(RWeka);library(ROCR);library(kernlab);library(ggplot2);

#Set up Train & Test Data
str(iris)
set.seed(1234)
ind <- sample(2, nrow(iris), replace=TRUE, prob=c(0.7, 0.3))
trainData <- iris[ind==1,]
testData <- iris[ind==2,]

#Fig 2.10: C4.5 Decision Tree
myFormula <- Species ~ Sepal.Length + Sepal.Width + Petal.Length + Petal.Width
iris_ctree <- ctree(myFormula, data=trainData)
table(predict(iris_ctree), trainData$Species)

plot(iris_ctree)

testPred <- predict(iris_ctree, newdata = testData)
table(testPred, testData$Species)

#Fig 2.11: Naive Bayes Marginal Distributions
rm(list = ls())
install.packages('klaR')
library(klaR)
data(iris)
mN <- NaiveBayes(Species ~ ., data = iris)
plot(mN,lwd=5);
mK <- NaiveBayes(Species ~ ., data = iris, usekernel = TRUE)
plot(mK)
plot(mN,lwd=3,n=10000);

#Naive Bayes Marginal Prediction
set.seed(1234)
ind <- sample(2, nrow(iris), replace=TRUE, prob=c(0.7, 0.3))
trainData <- iris[ind==1,]
testData <- iris[ind==2,]
model <- naiveBayes(Species~., data=trainData)
prediction <- predict(model, testData[,-5])
```

```
table(prediction, testData[,5])

#Fig 2.12: K-Means Clustering
rm(list = ls())
set.seed(3)

iris.km <- kmeans(iris[, -5], 3, iter.max = 1000)
tbl <- table(iris[, 5], iris.km$cluster)
iris.dist <- dist(iris[, -5])
iris.mds <- cmdscale(iris.dist)
c.chars <- c("*", "o", "+")[as.integer(iris$Species)]
a.cols <- rainbow(3)[iris.km$cluster]

plot(iris.mds, col = a.cols,cex=2, pch = c.chars, main="IBK Clustering",xlab = "Dimension 1", ylab = "Dimension 2")
leg.txt <- c("Setoso","Versicolor","Virginica")
legend("bottomright", leg.txt,col=c("red","green","blue"), pch=c("*", "o", "+") )

idx <- sample(1:dim(iris)[1], 40)
irisSample <- iris[idx,]
irisSample$Species <- NULL
hc <- hclust(dist(irisSample), method="ave")
plot(hc, hang = -1, labels=iris$Species[idx])

#JRip
rm(list = ls())
library(caret)
library(RWeka)
data(iris)
TrainData <- iris[,1:4]
TrainClasses <- iris[,5]
jripFit <- train(TrainData, TrainClasses,method = "JRip")
jripFit$finalModel

#Fig 2.13: Nueral Networks
library(neuralnet)
set.seed(1234)
ind <- sample(2, nrow(iris), replace=TRUE, prob=c(0.7, 0.3))
trainData <- iris[ind==1,]
testData <- iris[ind==2,]
nnet_iristrain <-trainData
#Binarize the categorical output
nnet_iristrain <- cbind(nnet_iristrain, trainData$Species == 'setosa')
nnet_iristrain <- cbind(nnet_iristrain, trainData$Species == 'versicolor')
nnet_iristrain <- cbind(nnet_iristrain, trainData$Species == 'virginica')
names(nnet_iristrain)[6] <- 'setosa'
names(nnet_iristrain)[7] <- 'versicolor'
names(nnet_iristrain)[8] <- 'virginica'
nn <- neuralnet(setosa+versicolor+virginica ~ Sepal.Length + Sepal.Width +Petal.Length + Petal.Width, data=nnet_iristrain, hidden=c(3))

plot(nn)
mypredict <- compute(nn, testData[-5])$net.result
# Consolidate multiple binary output back to categorical output
maxidx <- function(arr) {
 return(which(arr == max(arr)))
}
idx <- apply(mypredict, c(1), maxidx)
prediction <- c('setosa', 'versicolor', 'virginica')[idx]
table(prediction, testData$Species)
```

```
#Fig 3.11 SVM.
#df data is from R and Data Mining: Examples and Case Studies, Machine Learning for Hackers
library(ggplot2)
library(e1071)
df<-read.csv('C:/Users/Owmer/Documents/My Dropbox/Dalton PhD/WriteUp/Images/df.csv')
ggplot(df, aes(x = X_Uniform1_Var, y = Y_Uniform_Var, color = factor(Label)))+geom_point() + ggtitle("Fig. 2.20 (a): Dataset")

logit.fit <- glm(Label ~ X_Uniform_Var + Y_Uniform_Var,family = binomial(link = 'logit'),data = df)
logit.predictions <- ifelse(predict(logit.fit) > 0, 1, 0)
library("reshape")
df <- cbind(df,data.frame(Logit = ifelse(predict(logit.fit) > 0, 1, 0)))

df$Label<-NULL
predictions <- melt(df, id.vars = c('X_Uniform_Var', 'Y_Uniform_Var'))
ggplot(predictions, aes(x = X_Uniform_Var, y = Y_Uniform_Var, color = factor(value))) +    geom_point() + facet_grid(variable ~ .)+ ggtitle("Fig. 2.20 (b): Logistic Regression 52% Accuracy")

df<-read.csv('C:/Users/Owmer/Documents/My Dropbox/Dalton PhD/WriteUp/Images/df.csv')
rbf.svm.fit <- svm(Label ~ X_Uniform_Var + Y_Uniform_Var, data = df, kernel = 'radial')
df <- cbind(df,data.frame(RadialSVM = ifelse(predict(rbf.svm.fit ) > 0, 1, 0)))
with(df, mean(Label == ifelse(predict(rbf.svm.fit) > 0, 1, 0)))
df$Label<-NULL
predictions <- melt(df, id.vars = c('X_Uniform_Var', 'Y_Uniform_Var'))
ggplot(predictions, aes(x = X_Uniform_Var, y = Y_Uniform_Var, color = factor(value))) +    geom_point() + facet_grid(variable ~ .)+ ggtitle("Fig. 2.20 (c): SVM: RBF Kernel 72% Accuracy")

df<-read.csv('C:/Users/Owmer/Documents/My Dropbox/Dalton PhD/WriteUp/Images/df.csv')
poly.svm.fit <- svm(Label ~ X_Uniform_Var + Y_Uniform_Var, data = df, kernel = 'polynomial',degree=8)
df <- cbind(df,data.frame(PolySVM = ifelse(predict(poly.svm.fit ) > 0, 1, 0)))
with(df, mean(Label == ifelse(predict(poly.svm.fit) > 0, 1, 0)))
df$Label<-NULL
predictions <- melt(df, id.vars = c('X_Uniform_Var', 'Y_Uniform_Var'))
ggplot(predictions, aes(x = X_Uniform_Var, y = Y_Uniform_Var, color = factor(value))) +    geom_point() + facet_grid(variable ~ .)+ ggtitle("Fig. 2.20 (d): SVM: Poly. Kernel 57% Accuracy")

df<-read.csv('C:/Users/Owmer/Documents/My Dropbox/Dalton PhD/WriteUp/Images/df.csv')
sig.svm.fit <- svm(Label ~ X_Uniform_Var + Y_Uniform_Var, data = df, kernel = 'sigmoid')
df <- cbind(df,data.frame(SigmoidSVM = ifelse(predict(sig.svm.fit ) > 0, 1, 0)))
with(df, mean(Label == ifelse(predict(sig.svm.fit) > 0, 1, 0)))
df$Label<-NULL
predictions <- melt(df, id.vars = c('X_Uniform_Var', 'Y_Uniform_Var'))
ggplot(predictions, aes(x = X_Uniform_Var, y = Y_Uniform_Var, color = factor(value))) +    geom_point() + facet_grid(variable ~ .)+ ggtitle("Fig. 2.20 (e): SVM: Sig. Kernel 47% Accuracy")


## DTW Algorithm

rm(list = ls())
install.packages('dtw')
library(dtw)
## A noisy sine wave as query
idx<-seq(0,4*pi,len=100);
query<-sin(idx)+runif(100)/2;
## A cosine is for reference; sin and cos are offset by 25 samples
idx<-seq(0,2*pi,len=100);
```

```
reference<-cos(idx)
plot(reference,type="o",col="red",ylim=c(-1,1.5)); lines(query,col="black",type="o");
title("Fig. 2.24(a) DTW Example Dataset")
legend('bottomleft',c("Template","Input"),lty=c(1,2), pch=21:21,lwd=c(2.5,2.5),col=c("red","black"))

dtw(query,reference,step=asymmetricP1,keep=TRUE)->alignment;
alignment$distance
dtwPlotTwoWay(alignment);
title("Fig. 2.24(b) Template to Input Warping")
legend('bottomleft',c("Template","Input"),lty=c(2,1),lwd=c(2.5,2.5),col=c("red","black"))

hq <- (0:8)/8
hq <- round(hq*100) # indices in query for pi/4 .. 7/4 pi
hw <- (alignment$index1 %in% hq) # where are they on the w. curve?
hi <- (1:length(alignment$index1))[hw]; # get the indices of TRUE elems
dtwPlotThreeWay(alignment,match.indices=hi,main="");
title("Fig. 2.24(c) Warping Path")

wq<-warp(alignment,index.reference=FALSE);
wt<-warp(alignment,index.reference=TRUE)
alignment<-dtw(query,reference,keep=TRUE);
par(mfrow=c(2,1));
plot(reference,main="");
title("Fig. 2.24(d) Warped Input")
lines(query[wq],col="blue");

## A profile of the cumulative distance matrix
## Contour plot of the global cost
dtwPlotDensity(alignment,main="")
title("Fig. 2.24(e) Warping Path Contour")
```

# APPENDIX C

## Acceleration, Velocity & Displament

#Anthony Dalton - Sept. 2012
#Reference: Slifka L, (2003), 'An accelerometer based approach to measuring displacement of a vehicle body*', Master's Thesis, University of Michigan*.

With reference to Equation AC.1, acceleration is the first derivative of velocity and the second derivative of displacement. A double integration, Equations AC.2 and AC.3, technique can be employed to derive these parameters from raw accelerometer data. Both the initial velocity and initial position are required. A further complication is the d.c. bias imposed by the gravitational vector embedded within the raw acceleration data which cannot be completely removed.

$$a(t) = \frac{dv}{dt} = \frac{d^2x}{dt^2} \tag{AC.1}$$

$$v(t) = v(t_0) + \int_{t_0}^{t} a(\tau)d\tau \tag{AC.2}$$

$$x(t) = x(t_0) + \int_{t_0}^{t} v(\tau)d\tau \tag{AC.3}$$

To address some of these issues a five stage algorithm was adopted in this thesis. For more information please see Slifka et al.

- Employ a high pass 3rd order elliptical filter to minimize the accelerometer drift caused by the gravitational vector
- Perform cumulative trapezoidal numerical integration on the raw acceleration data to find velocity
- Employ a high pass 3rd order elliptical filter to eliminate the requirement for an initial velocity value.
- Perform cumulative trapezoidal numerical integration on the calculated velocity to compute displacement
- Employ a high pass 3rd order elliptical filter to eliminate to eliminate the requirement for an initial displacement measurement.

# APPENDIX D

# AD-BRC Users Manual

# AD-BRC

# MOBILITY MONITOR

# USER MANUAL

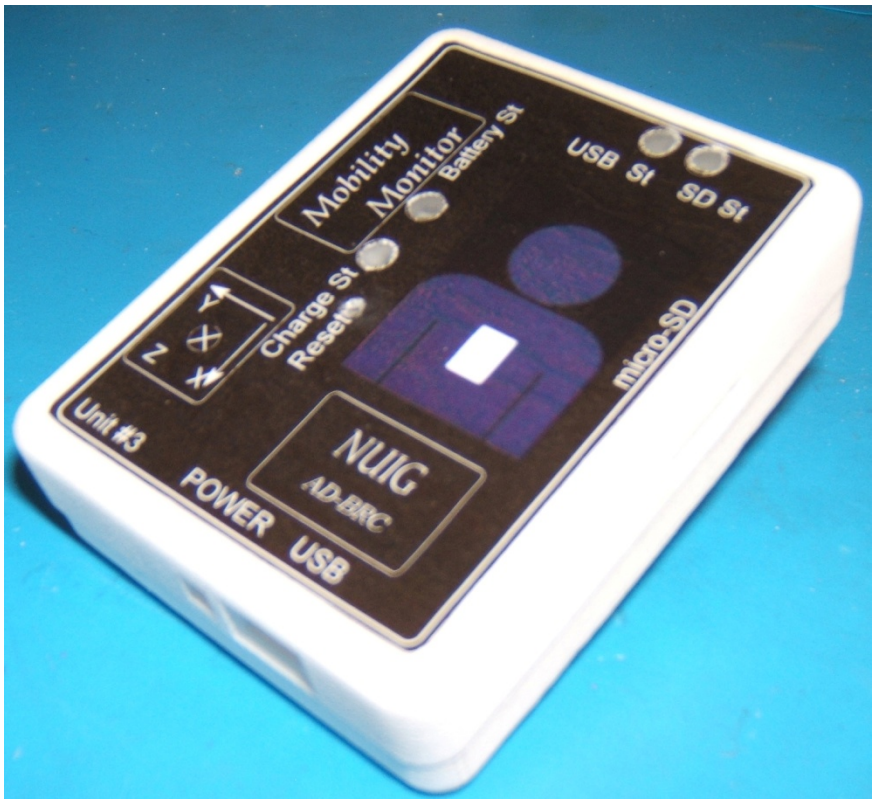

# Table of Contents

# Functional Overview

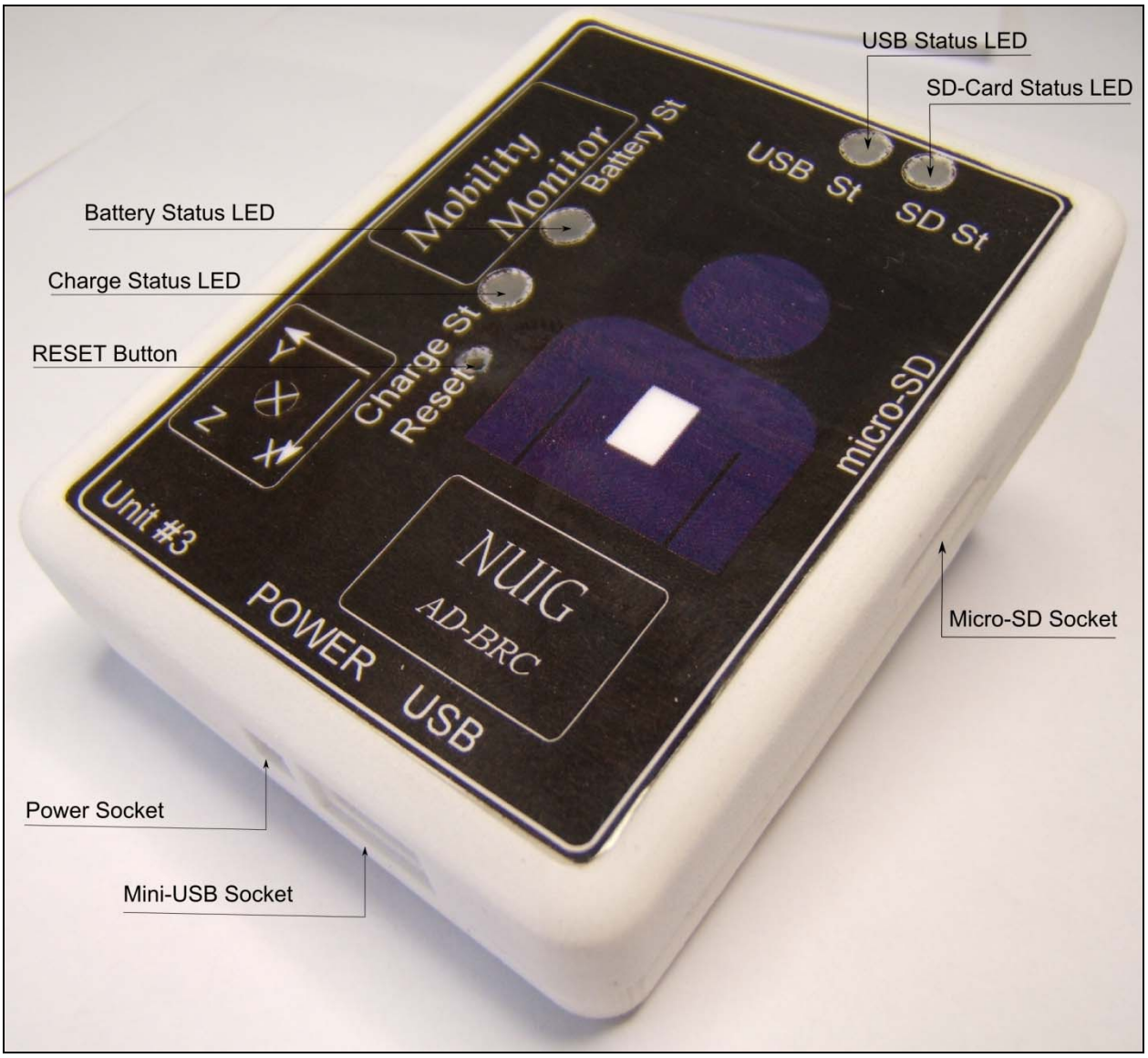


*Fig.1. Mobility Monitor Functional Overview*

# Summary of Operation

This mobility monitor will record movement data from a subject. During operation data is stored on a micro-SD card. After 8.5 days the monitor will automatically go into a sleep mode. Data can be downloaded from the monitor over USB or directly from the micro-SD card. Once downloaded the data can be analyzed to indentify fall and mobility events. The monitor can be reset to its original settings using the embedded reset button.

# Device Setup

Prior to each 8 day recording session the following steps should be followed.

1. Reformat the micro-SD card.
2. Recharge the monitor to its full capacity.
3. Insert the micro-sd card and reset the monitor
4. Calibrate the monitor
5. Attach the monitor to the subject

Post each 8 day recording session the following steps should be followed.

1. Download the data from the monitor
2. Upload the data for post processing
3. Follow steps 1-5 above prior to the next recording session.

# Reformat the micro-SD card.

***Important Notes***:

The micro-SD card must be formatted to FAT 32 file system and with a default allocation size.

Formatting the mirco-SD card means deleting all information from it. This process must only be done when data from the previous session has been successfully downloaded and saved to a PC.

Extreme care must be used when handling the micro-SD cards.

***Instructions***

- Remove the card from the micro-SD socket, as in Fig 2.
- This is a Push-Pop micro-sd card. Push in the card with a needle and it will pop out
- **Do not use excessive force**


*Fig.2. Removing the micro-SD card.*

- Insert the micro-SD card into the standard SD holder and insert this into the SD slot on your PC.

- Double click *My Computer* and you will be see a new drive, *Logger x.*
- Right Click on *Logger x* and select *Format* from the drop down menu, as in Fig 3.

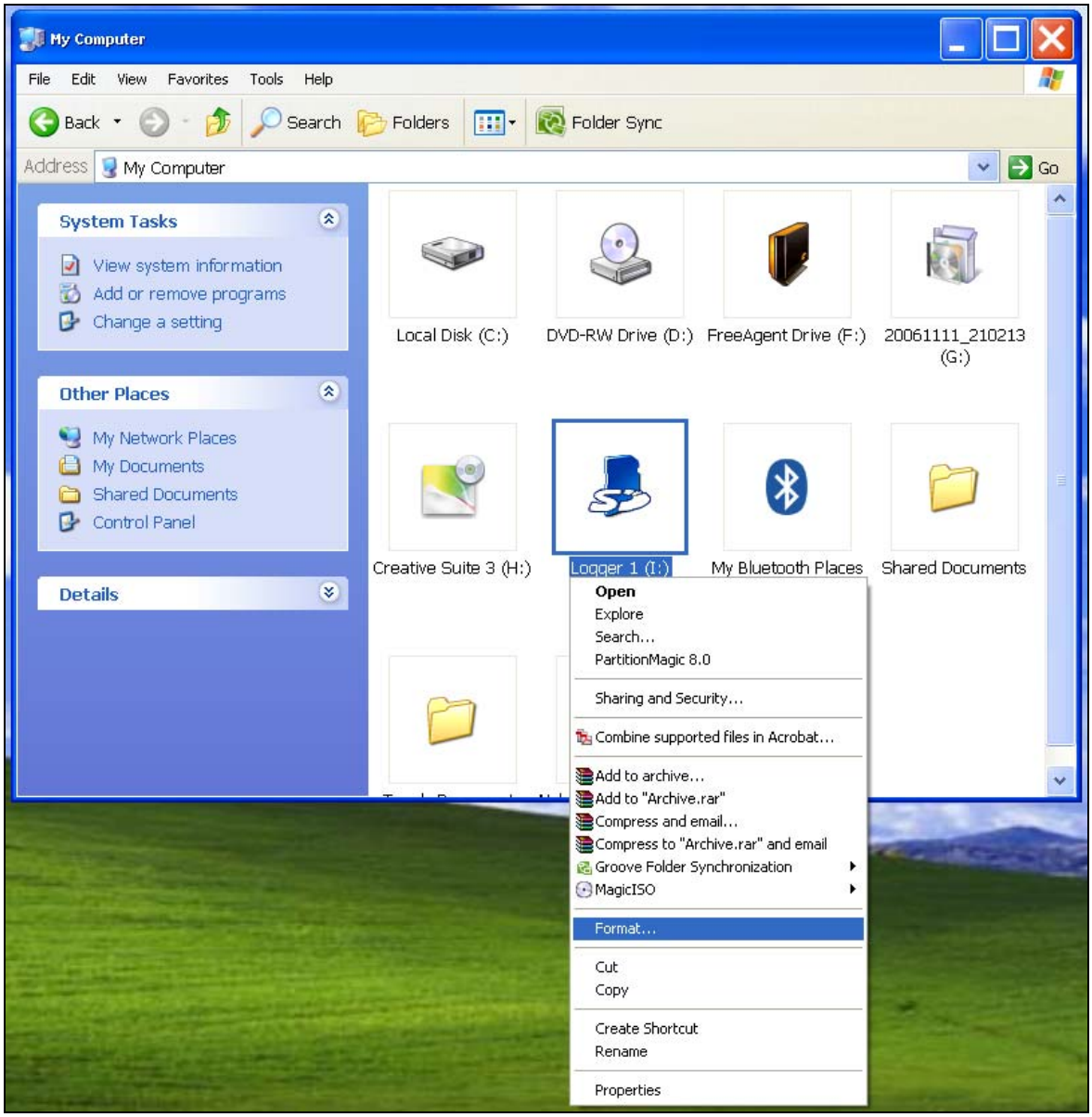


*Fig.3. Selecting Format for Logger x.*

- In the *Format* pop up box ensure the following are set, as in Fig 4:

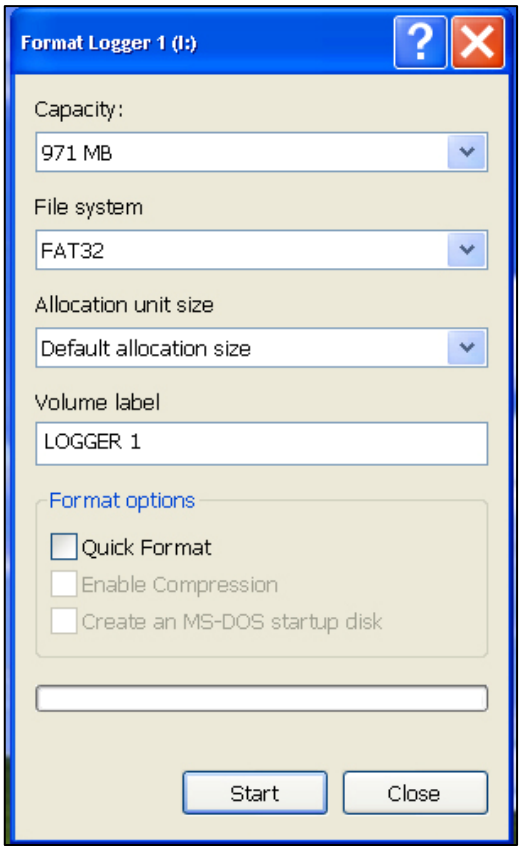


*Fig.4.Format Pop Up Box for Logger x.*


*Fig.5.Format Warning Box.*

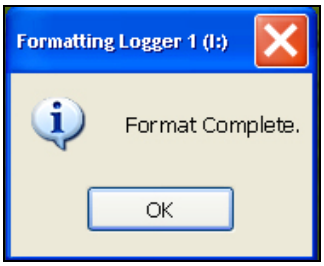


*Fig.6.Format Complete Box.*

- Click *Start*
- Click *OK* to the warning box that appears, in Fig 5
    - **Note: All data from the previous recording session will now be deleted**
- After a period of time the popup box in Fig 6 will appear. Click *OK*.
- Remove the micro-SD card from your PC
- You may now proceed to the next step.

# Recharge the monitor to full capacity.

***Important Notes***:

**As the data is stored on a micro-SD card it will not be lost if the battery is completely discharged.**

The monitor contains a 2000maH lithium polymer battery, at full capacity the battery will allow the device to record for 8.5 days. After this time the monitor will go into a sleep mode and data will no longer be recorded.

The ***Battery Status LED*** indicates the status of the battery.

This led indicates when the battery has reached both a low and a critically low level

When the battery has reached a low level this led will flash on and off slowly. The monitor will continue to record data. When the battery has reached a critically low level this led will stay on continuously. The monitor will cease recording data and enter a sleep mode. The monitor will stay in this mode until it is recharged or the battery completely discharges at which point no led will light.

***Instructions (See Fig. 7):***

- To recharge the battery plug the power adapter into the power socket on the monitor.
- The ***Charge Status LED*** indicates the status of the charging process.
- When this led is **red** the battery is still being charged.
- When this led is **green** the battery is 90% charged.
- The time to recharge the monitor is approximately 5 hours. However, this may vary as the capacity and recharge prosperities of every battery is unique.

**To enable the monitor to run for 8 days the battery must be charged to its full capacity, therefore to ensure this an extra step has been programmed into the charging phase.**

- Remove the power connector from the monitor, the Charge Status LED will turn off.
- Using an appropriate tool (ie. needle) gently press the reset button on the monitor, Fig. 8.
- **Do not repeatedly press this reset button.**
- ***If the battery has not been charged to its full capacity then all other leds will turn on.***
- You must plug the power adapter back into the monitor and allow it to charge for another hour.
- ***If the battery has been charged to its full capacity then all other leds will flash three times and you may proceed to the next step.***


*Fig.7.Recharging the monitor.*


*Fig.8.Reset the monitor.*

# Insert the micro-sd card & reset the monitor

***Important Notes***

The embedded reset button will restore the monitor to its original settings and initiates a new recording session.

The embedded reset button is very sensitive and unnecessary or excessive force should not be used.

***Instructions :***

- Using an appropriate tool (ie. needle) gently push the micro-sd card into the connector on the monitor until you hear a “click” indicating the card has been correctly inserted.
- **Do not use excessive force**
- Using an appropriate tool (ie. needle) gently press the reset button on the monitor.
- **Do not repeatedly press this reset button.**
- The monitor will flash the LEDs three times indicating the battery is at its maximum charge.
- The mobility monitor will then automatically go through an initiation phase. This is indicated by all LEDs being turned on. Once the monitor has completed this phase the SD-Card Status LED will flash slowly, approximately once every 5 seconds. This indicates the recording session has begun and the monitor will continue to run in this fashion for 8.5 days.

# Calibrate the monitor

***Important Notes***

As the monitor uses a triaxial accelerometer it must be calibrated prior to being attached to a subject. For the most part the monitor automatically performs self-calibration. However, to enable it to do so it must be orientated through 6 different positions.

***Instructions:***

- Place the monitor on a flat surface as in Fig 9a.
- Leave the monitor in this position for approximately 30 seconds.
- Repeat the above steps for the positions depicted in Fig 9b – 9f.
- The ***SD-Card Status LED*** should flash throughout this process.
- The monitor is now ready to be attached to a subject.


*Fig. 9a*


*Fia. 9b*


*Fig. 9c*


*Fig 9d*


*Fig. 9e*

*Fig. 9f*

# Downloading data from the monitor

***Important Notes***

At the end of a recording session the data must be downloaded from the monitor for post processing. The ***Battery Status LED*** will indicate the status of the battery, see section: *Recharge the monitor to its full capacity.*

***Instructions:***

- Data can be copied from the monitor in 2 ways, over USB or directly from the micro-SD card.

**Mirco-SD Card**

- Remove the micro-SD card from the monitor.
- Insert the micro-SD card into the standard SD holder and insert this into the SD slot on your PC.
- Double click *My Computer* and you will be see a new drive, *Logger x.*
- Double Click on *Logger x.*
- The file(s) stored on the micro-SD card will be displayed, as in Fig 10.

- **If the embedded reset button was pressed during the recording session this event will have been time stamped and a new log file will have been generated.**
- Copy the file(s) on the micro-SD card to your PC.
- **The file(s) will be significantly large, approximately 1GB in size. This is a reflection on the depth of data the monitor records while attached to the subject. As a result it will take a substantial amount of time to copy the file(s) across.**

**USB Connection**

- Data can also be downloaded using the mini-USB connection on the monitor.
- Connect the monitor to a PC using the mini-USB cable, as in Fog 12.
- Data can now be downloaded in a similar manner to above my going to *My Computer.*
- The speed of communication from micro-SD to USB is quite slow. Therefore, downloading the file(s) over USB will take a considerably longer period of time, several hours for a full download.

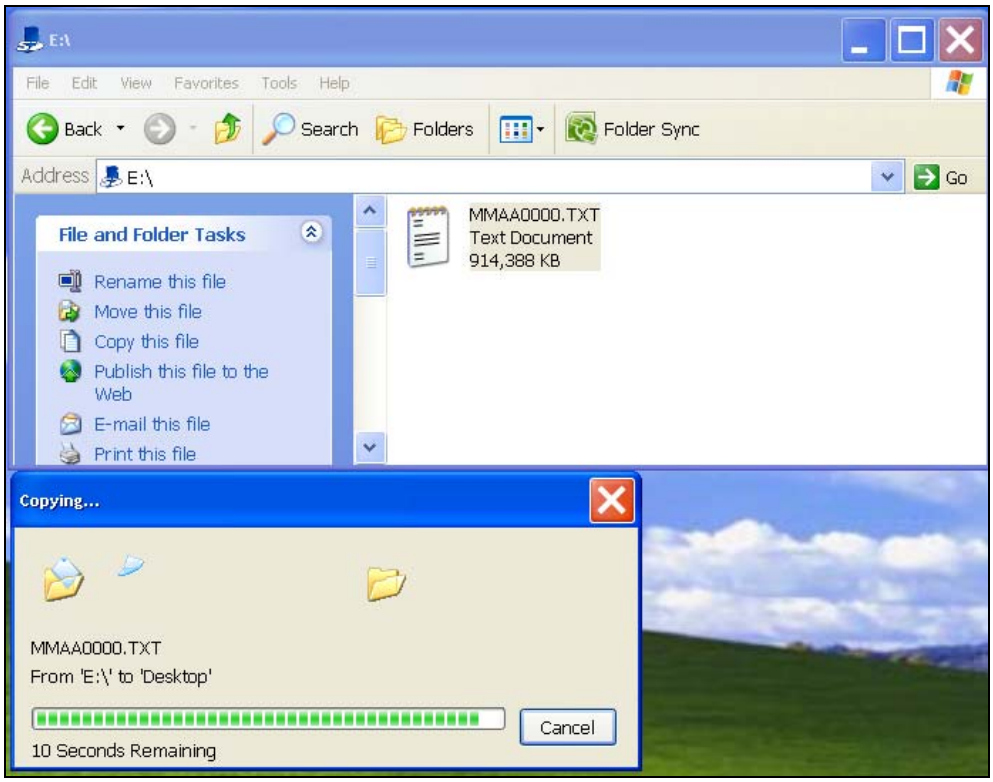


*Fig.10. Downloading data from the monitor*


*Fig. 10. Connecting a mini USB cable to the monitor*

# Uploading data for post processing

***Important Notes***

- The monitor encrypts and encodes the data as it is recorded.

***Instructions:***

- Open the following address in your browser, see Fig 11:
  - ***http://dropbox.yousendit.com/AnthonyDalton11699122***

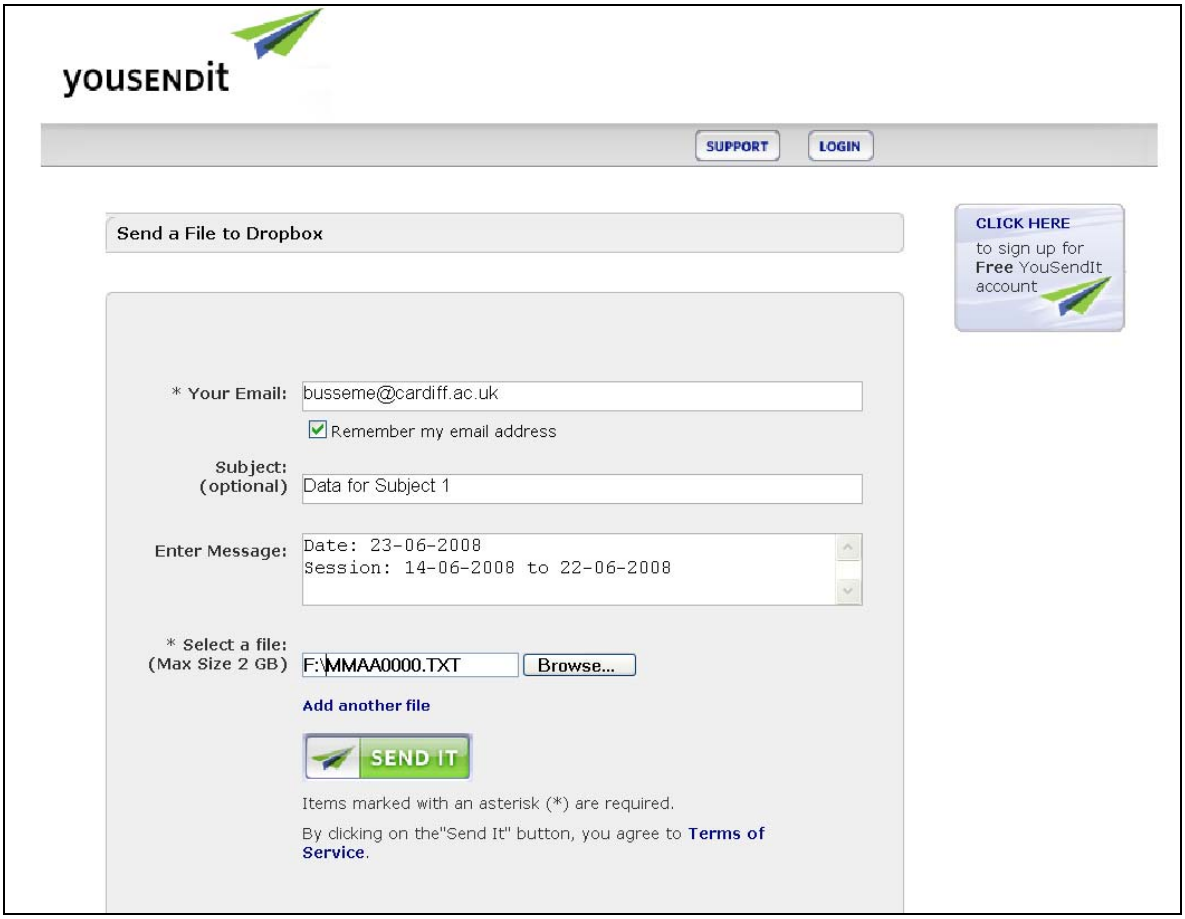


*Fig 11. DropBox for Uploading File(s)*

- Enter the appropriate details and upload the file.
- Click *Send it* and you will be presented with a screen similar to Fig 12

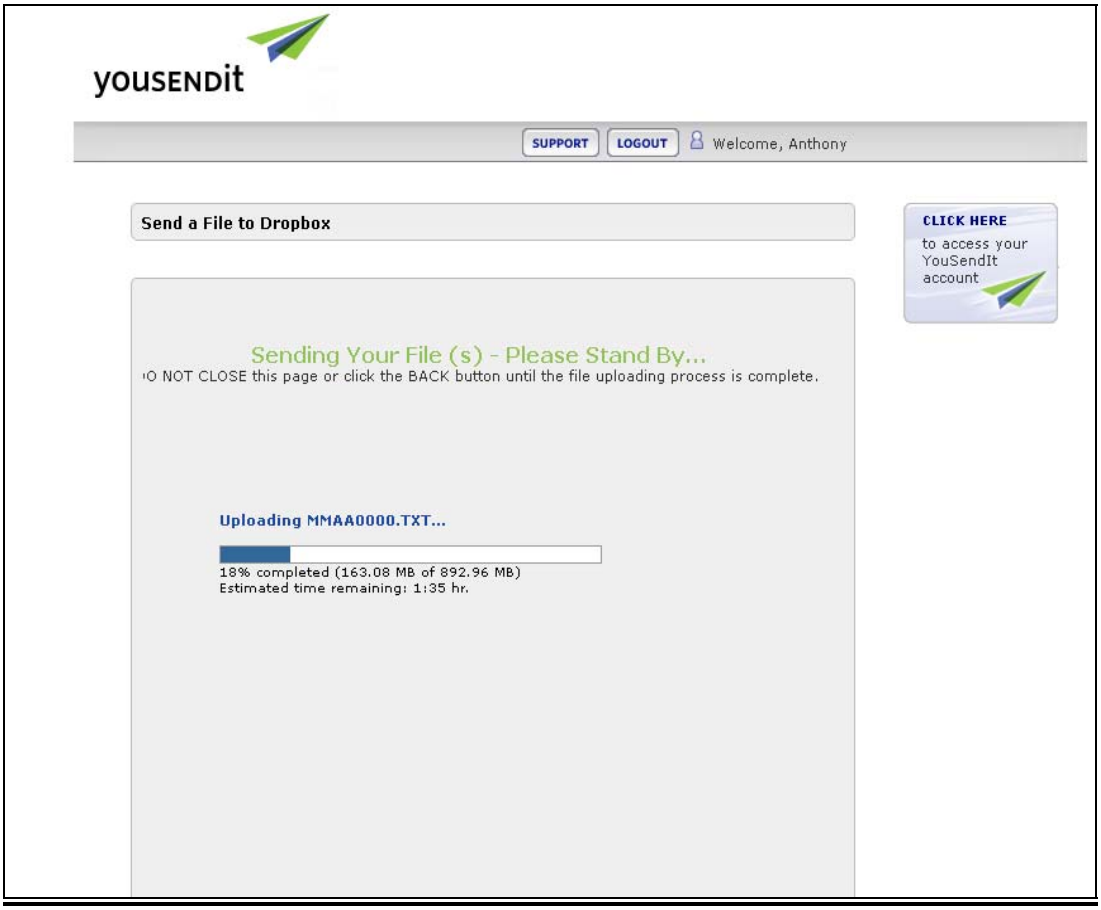


*Fig. 12 File being Uploaded*

- The time to upload the file will depend on your internet connection speed and available bandwidth.
- Once completed you will be given a confirmation screen and email.

# Appendix A

# Requirements Specification

## A.1 System Personnel


System End Users: Subjects participating in the clinical trials

System Developers: Mr. Anthony Dalton, Prof. Gearóid Ó Laighin, Dr. Fearghal Morgan.

Contact Details: anthony.f.dalton@gmail.com

gearoid.olaighin@nuigalway.ie

fearghal.morgan@nuigalway.ie

System Analysts: Dr. Monica Busse, Mr. Justin McCarthy

Contact Details: busseme@Cardiff.ac.uk

Justin.McCarthy@CardiffandVale.wales.nhs.uk


## A.2 Operational Setting

The AD-BRC Mobility Monitor will be capable of gathering data in the subjects own residence. The subject will not interact with the sensor in any way. At the end of a recording period the sensor will be removed from the subject and connected to a Laptop / PC to download stored data.

## A.3 Impact Analysis

The AD-BRC Mobility Monitor will be optimized for size, weight and subject comfort. Therefore only minor interference with everyday living is expected.

Parameters:

- Size: 70cm x 55cm x 5cm
- Weight: 95g
- Battery Life: 8 days

## A.4 Formal Hardware Specification

The AD-BRC Mobility Monitor consists of the following electronic components

- Transflash MicroSD Card
- MSP430F1611 MicroProcessor
- MMA7261Q Freescale Triaxial Accelerometer
- AT90USB162 USB IC
- 3.7V 2000mAh Lithium Ion Battery
- Mini-USB Female Connector
- Mini-Power Connector
- Lithium ion charger using the BQ2412x IC.
- Crystal, Decoupling Capacitors and Auxiliary Components.
- 4 status LEDs

## A.5 Formal Software Specification

- The file system used on the AD-BRC Mobility Monitor is Fat32.
- The USB IC used is AT90USB162
- The AD-BRC Mobility Monitor uses a convention similar to the unix system for timekeeping, it counts seconds since powerup based on crystal clock ticks.
- The name of the logfile is generated from the current time and has the format "mmaXhhhh.txt" where "X" is a letter and "hhhh" represents the initiation hour.

## A.6 Security

- All data is encrypted during logging of the data and the data can only be decrypted with a predefined key.

## A.7 Privacy

- All data will be stored on external hard drives with strict access available only to researchers involved in this study.

## A.8 Safety

- The AD-BRC Mobility Monitor falls under a Class 1 (low risk) device

## A.9 Modifiability and extensibility

- The AD-BRC Mobility Monitor may in the future incorporate a wireless architecture.